ISSN 2463-6029 (Print)
ISSN 2350-3432 (Online)

Waikato Shallow Lakes Modelling

2017

ERI Report 94

Client report prepared for DairyNZ, Waikato River Authority, Waikato Regional Council, DOC/Fonterra Living Waters Partnership and Waipa District Council

By Moritz K. Lehmann, David P. Hamilton, Kohji Muraoka, Grant W. Tempero, Kevin J Collier and Brendan J Hicks

Environmental Research Institute
University of Waikato, Private Bag 3105
Hamilton 3240, New Zealand

THE UNIVERSITY OF WAIKATO
Te Whare Wānanga o Waikato

Environmental Research Institute
Te Pūtahi Rangahau Taiao
THE UNIVERSITY OF WAIKATO

Cite report as:
Lehmann, M. K., Hamilton, D. P., Muraoka, K., Tempero, G. W., Collier, K. J., Hicks, B. J. 2017. Waikato Shallow Lakes Modelling. ERI Report 94. Environmental Research Institute, University of Waikato, Hamilton, New Zealand. 223 pp.

Cover photo:

Lake Ngāroto on a calm day in November 2015.

Disclaimer:

The information and opinions provided in this Report have been prepared for the Client and its specified purposes. Accordingly, any person other than the Client, who uses the information and opinions in this report, does so entirely at their own risk. The Report has been provided in good faith and on the basis that reasonable endeavours have been made to be accurate, not mislead in any way, and to exercise reasonable care, skill and judgment in providing information and opinions contained therein.

Neither the University of Waikato, nor any of its employees, officers, contractors, agents or other persons acting in its behalf or under its control, accepts any responsibility or liability to third parties in respect of any information or opinions provided in the Report.

Report reviewed by:

Marnie Campbell
University of Waikato

Approved for release by:

John Tyrrell
University of Waikato

Executive Summary

The principal aim of this study is to apply a modelling approach to identify, evaluate and prioritise specific in-lake and catchment restoration options which could be applied to improve the water quality and ecological health of peat and riverine lake types across the Waikato Region. Four representative lakes have been selected as case studies for this work based on their social, cultural and ecological significance, as well as the availability of historical monitoring data and the potential transferability of the study findings to similar lake systems. The lakes include Rotomānuka, Ngāroto, Waahi and Waikare.

This study comprises the following six objectives for each lake:

1. Define baseline water quality and ecological health based on existing monitoring data and knowledge.
2. Determine the key pressures, drivers and processes governing lake water quality and ecological health.
3. Define, evaluate and rank the likely effectiveness of a range of in-lake and catchment management strategies to improve existing water quality and biodiversity values.
4. Evaluate the level of certainty around the suggested restoration strategies that meet the desired outcomes, as well as the timeframes implementation and longevity.
5. Identify an achievable end state for water quality and ecological health, taking into consideration existing trophic state, legacies and catchment land use.
6. Provide an expert assessment on whether the strategies identified are also likely to be effective when applied to other similar Waikato lake types.

Process-based dynamic modelling was chosen for this study because it can be used to test the plausibility of conceptual models of lake ecosystem function, to shed light on the importance of various processes contributing to observed system behaviour, and to extrapolate to future scenarios that fall outside the range of historical observations. This report consists of a main body of text with an Extended Conclusions section that goes into detail about processes in the lakes that are relevant to understanding management, as well as 7 appendices.

For modelling of one-dimensional (1-D) lake hydrodynamics and ecological processes, we chose the one-dimensional, coupled hydrodynamic-ecological model DYRESM-CAEDYM as the tool for

assessing effects of altered hydrology, nutrient and sediment loads, and climate on physical and biogeochemical processes in Lakes Ngāroto, Waahi and Rotomānuka. Modelling of three-dimensional (3-D) hydrodynamics of Lake Waikare was initiated using Delft3D-FLOW but not progressed to the point of presenting simulations given the time constraints of the present study.

Catchment boundary conditions consisting of time series of discharges and contaminant loads for each of the lakes were generated using either the process-based INtegrated CAtchments model (INCA), the TopNet hydrological model or mass-balance calculations from known water level and outflow data, with measured data used to check the veracity of assumptions and model outputs.

Multiple lake management scenarios were conceptualised with a project working group and these were simulated using a DYRESM-CAEDYM model calibrated to each lake application (Ngāroto, Waahi and Rotomānuka). The management approaches assessed can be broadly considered as belonging to three categories:

1. External nutrient load reduction: associated with land use change or other nutrient loss reductions from improved management practices and/or targeted interventions, e.g., erosion control, denitrification beds;
2. Hydrological modifications: diversion of inflows away from the lake or increasing the water level to alter wind-driven resuspension of sediments;
3. Geochemical engineering: by using sediment capping to reduce internal loading and/or continuous low-dosage alum treatment to reduce dissolved P and increase flocculation in the water column.

The base model and each scenario simulation are presented and compared using metrics which describe the water quality in terms of summary statistics, for example, attribute bands (A, B, C or D) from the National Objectives Framework (NOF) of the National Policy Statement for Freshwater Management (NPS-FM, MfE 2015a).

Lake Ngāroto

Lake Ngāroto is the largest of the Waipa peat lakes (surface area of 108 ha) and is important for its cultural history and for recreational activities. Its current mean depth is c. 2 m and maximum depth 4 m. The Lake Ngāroto catchment is predominantly dairy pasture, resulting in high external nutrient loads to the lake. The high nutrient load, shallow depth, loss of submerged macrophytes and reduced lake volume (compared with historical levels) have collectively led to resuspension of bottom sediments, high water column turbidity and high levels of internal nutrient loading. Lake Ngāroto has recurrent algal blooms, hosts large populations of invasive fish including catfish, rudd,

gambusia, goldfish and koi carp, but also has valuable native fish populations including common bullies, shortfin eels and common smelt. Isotope data from this study indicate that the food base is dominated by organic matter, most likely primarily of terrestrial origin but with some seasonal variability, and large eels are at the top of the food web but with potential for some overlap of diet with catfish and koi carp.

The lake model for Ngāroto showed an acceptable match to observations of temperature, surface and bottom dissolved oxygen (DO), total nitrogen (TN), total phosphorus (TP), total suspended solids (TSS) and chlorophyll *a*, though observed data were quite sparse for deriving input data to the lake model and for comparisons with model outputs. In-lake data were repeated over a five-year period from one year of measured data for the purpose of model comparisons. There was also limited data on inflow composition to derive a daily inflow file consisting of discharges and concentrations of TSS and nutrient species. The model was most sensitive to parameters relating to the density of particulate organic matter, reinforcing that it would be useful to quantify the size and nature of suspended material in the water column of Lake Ngāroto, as well as establishing setting velocities. Parameters affecting the dynamics of cyanobacteria and temperature responses were also particularly sensitive.

Fourteen simulations were carried out for Lake Ngāroto to examine water quality effects of changes in external (catchment) loads, internal (bottom-sediment) loads, water level changes and an inflow (Ngārotoiti) diversion. Despite reductions in internal and external nutrient loads of up to 50%, no scenario resulted in NOF status of the lake improving from the D band. The scenario most effective at reducing median total phosphorus (TP), total nitrogen (TN) and chlorophyll *a* (TCHLA) was N14 (50% external reduction for P and 50% anoxic release reduction for P). This simulation might equate to some land use change and improved land management practices, as well as geochemical engineering to reduce the internal (bottom-sediment) nutrient load. Comparisons between scenarios which combine internal and external load reductions in N and P in various combinations (e.g., N3, N7, N13 and N14) suggest that chlorophyll *a* concentration is driven reasonably evenly by external and internal nutrient loading, with much of the internal loading occurring during summer when phytoplankton growing conditions are most suitable (i.e., warmer water temperature and higher irradiance). For Lake Ngāroto to meet the bottom line in the NOF within the next 3-4 decades will require intensive catchment actions that will ultimately reduce the level of nutrient enrichment in the bottom sediments. Perhaps more importantly, however, and with a much higher risk in terms of achievability, geochemical engineering to remove nutrient directly from the lake water column

and/or bottom sediments, and concerted control measures on the large pest fish populations (e.g., koi carp, catfish) are needed to shorten timelines for meeting the NOF bottom line.

Lake Waahi

Lake Waahi is a shallow (mean depth 2 m), turbid riverine lake formed as part originally as part of the Waikato River floodplain. The lake has received diffuse and direct discharge from coal mining, contributing large quantities of sediment and altering the turbidity of the lake, but the catchment has large areas used for pastoral grazing of dairy cows and dry stock. Like Lake Ngāroto, submerged macrophyte beds in the lake have collapsed some decades ago, and there are high rates of wind-induced sediment resuspension with high levels of suspended sediments and phytoplankton biomass.

Comparison of simulated data with measurements for Lake Waahi were deemed good relative to other water quality model applications and were assisted by relatively complete data to allow for synthesis of inflow, outflow and meteorological input data over the entire five-year simulation period. Sensitivity analysis revealed that the most sensitive parameters related to temperature dependence of sediment fluxes as well as phytoplankton growth and respiration, similar to Lake Ngāroto.

Nine model management scenarios were carried out for Lake Waahi. Several state variables improved markedly with the imposed management scenarios (e.g., changes in water level and different combinations of nitrogen and phosphorus reduction from both external and internal sources). The simulated improvements in water quality were not sufficient, however, for TN, TP or chlorophyll *a* to meet the bottom line in the NOF. Scenarios WH8 and WH9 showed the greatest improvement in water quality, driven primarily by a large reduction in the internal nutrient load (hypothetically through geochemical engineering). A combination of actions (e.g., internal and external nutrient load reductions, water level increase) is likely to be necessary for water quality in Lake Waahi to improve sufficiently to meet the NOF bottom line within 2-3 decades.

Lake Rotomānuka

Lake Rotomānuka has a south and north basin which were once likely to have been a single lake prior to extensive land drainage for pastoral grazing. The area between the lakes is now a wetland where water is exchanged between south and north basins. The focus of the current model application was on Rotomānuka North, which has a surface area of 17.1 ha and a maximum depth of 8.7 m. Lake Rotomānuka North has abundant native fish species and invasive rudd and goldfish have

been found in previous surveys. The hydrology of Lake Rotomānuka is complex and several assumptions were made as part of the derivation of a lake water balance that relies on measured water level and precipitation data, as well as calculated evaporation rates and outflow. The complex groundwater-surface water connections in the area mean that several assumptions also needed to be made about nutrient concentrations in the inflows to Lake Rotomānuka North, using a limited number of measurements for guidance. For example, nutrient attenuation in the wetland area between Rotomānuka North and Rotomānuka South was estimated to remove 40% of the nitrogen and 20% of the phosphorus as water flows from the south to north basin, though the veracity of this assumption was explored through a sensitivity analysis using different nutrient attenuation rates.

A regular record of water quality samples and vertical profiles of temperature and dissolved oxygen in Lake Rotomānuka provided a good basis for verification of model simulation outputs. A good match was obtained between surface and bottom observations for most variables. The assigned sediment nutrient release rate parameter (for N and P) had a high degree of uncertainty, however, as there was limited ability to define it accurately. Sensitivity analysis again revealed that parameters related to phytoplankton growth rates (mostly the cyanobacteria group) and sediment nutrient release rates most influenced model output, with the latter suggesting that there should be a focus on sediment nutrient releases in any subsequent studies. The sensitivity of the model output to sediment nutrient releases reinforces the need for more detailed studies of the bottom sediments in this lake.

Nine scenarios were simulated with the calibrated model for Lake Rotomānuka, two of which involved testing different rates of nutrient attenuation in the adjoining wetland, assuming no attenuation or a two-fold increase over the baseline simulation values. The simulations suggested not only improvements in water quality but that strong management activities may be transition this lake out of the NOF D band.

Conclusion

Peat lakes and riverine lakes are quite different systems; many riverine lakes have large sediment and phosphorus legacies and high levels of internal loading but low levels of inorganic phosphorus due to adsorption. This adsorbed P is stripped off when there is high demand, which supports high algal productivity. Peat lakes may be naturally slightly acidic, somewhat coloured and potentially have a natural resilience to high catchment loads, at least if they are deeper and therefore less subject to sediment resuspension. Because Ngāroto is shallower it represents an intermediate case (i.e., somewhat riverine and peat in character).

The modelling presented in this report provides a mechanism to synthesise available data, identify shortfalls in the data and to ensure that there is a logical process for the monitoring to document the effects of remediation actions (i.e., measuring the right things at the time frequency and in the right places). The scenario simulations have shown that modest changes related to managing the current levels of diffuse pollution will not be sufficient to lift these lakes out of the NOF D band now or in the future. Restoration goals pertain not just to water quality, however, and there may be tangible outcomes in the terrestrial environment from catchment restoration actions.

Generally, however, consideration is needed about whether to directly manage internal loads (i.e., through geochemical engineering) while concurrently making large reductions in external loads.

Several native fauna (keystone species; shortfin eels) are remarkably resilient to water quality pressures and have responded to high rates of productivity in these systems by also being productive. Isotope results suggest that invasive benthivorous fish species (koi carp and catfish) may occupy a similar niche to shortfin eels. Controlling invasive fish species therefore has the potential to increase eel populations and improve water quality through reducing disturbance of bottom sediments. While many of the lakes have abundant shortfin eels, populations may be close to their upper temperature tolerance limits, while koi carp and catfish are probably not. We identified that there is a high sensitivity of several model outputs to water temperature, mostly associated with a decline in water quality with increases in temperature. This means that there could be some uncertainty of our model predictions in a temperature regime (e.g., warming climate) that might be outside of the climate corresponding to the current modelled period but also that there might be a high potential that climate change will lead to changes in the lakes that will hinder remediation actions. The implication is that climate change should be built into future scenarios for the shallow lakes.

Three of the lakes have gone beyond ‘tipping points’, i.e., to a regime of no submerged plants, high levels of turbidity and high phytoplankton biomass. Continued high nutrient loading means these lakes may be subject to unpredictable outcomes (e.g., Lake Waikare ‘turning red’ with the alga *Monoraphidium*). The challenges for restoration are immense in dealing with some of the most eutrophic lakes in the world, and extraordinary measures and efforts will be required to not obviate responsibility in leaving a legacy for future generations to deal with.

Acknowledgements

We thank a large number of people who provided assistance and dedicated significant amounts of time to this project. We sincerely thank Keri Nielsen (Waikato River Authority/Envirostrat) and David Burger (DairyNZ) for their advice and assistance in coordinating this project. Deniz Özkundakci (Waikato Regional Council) provided valuable guidance on model selection and performance in addition to sourcing relevant monitoring data. Tracie Dean-Speirs and Natasha Grainger (Department of Conservation) provided valuable advice and data for fish community assessment and modelling of Lake Rotomānuka. Piet Verburg (NIWA) provided assistance with calculations of nutrient loads from the CLUES model. John Quinn (NIWA), Erina Rawiri-Watene (Waikato-Tainui), Paula Reeves (Waikato Regional Council), Aareka Hopkins (AM^2), Ian Duggan (University of Waikato) and Julian Williams (Waikato-Tainui) are thanked for their contributions and support as part of the wider project advisory group. Warrick Powrie (UoW) provided assistance with field sampling of Lake Rotomānuka and Lake Ngāroto. Ron Ram and Vanessa Cotterill (UoW) provided assistance in the processing and analysis of field samples, and Chris McBride (UoW) with processing buoy data. We thank the Department of Conservation staff who carried out gill netting in Lake Rotomānuka and Mike Holmes for fyke netting in Lake Ngāroto under contract to the Waipa District Council through Paula Reeves. Lena Schallenberg (UoW), Theo Kpodonu (UoW), Eunju Cho (UoW) and Uyen Nguyen (UoW) provided assistance with sourcing of data, working with models and documents. Richard Lamont (UoW) and Liancong Luo (NIGLAS) assisted with the application of the global sensitivity analysis. We also thank Marc Weeber (Deltares via DairyNZ) for his assistance in the experimental model set up.

Table of Contents

Executive Summary 3
Acknowledgements 9
Table of Contents 10
Introduction 14
Background 14
Study objectives 16
Methods 18
Modelling approach 18
The DYRESM-CAEDYM lake water quality model 19
The INCA catchment model 22
Scenario modelling 23
DYRESM-CAEDYM calibration and validation 25
DYRESM-CAEDYM sensitivity analysis 26
Sensitivity to input data 26
Sensitivity to key parameters: Uncertainty analysis 27
Meteorology 28
Hamilton AWS 29
Ruakura 2 EWS 30
Study sites and model assumptions 32
Lake Ngāroto 32
Lake Waahi 46
Lake Rotomānuka 54
Lake Waikare 70
Fish community 80
Scenarios 81

Results and Discussion 83
Lake Ngāroto 83
Calibration-validation process 83
Key characteristics of modelled and observed data 83
Sensitivity to key parameters: uncertainty analysis 96
Scenario simulation results 99
Validation of aggregation approach 103
Summary 104
Lake Waahi 107
Calibration-validation process 107
Key characteristics based on models and observations 107
Sensitivity to key parameters: uncertainty analysis 121
Scenario simulation results 122
Summary 125
Lake Rotomānuka 128
Calibration-validation process 128
Key characteristics based on models and observations 128
Sensitivity to key parameters: uncertainty analysis 139
Scenario simulation results 141
Summary 144
Extended conclusions 148
Overview of key processes and modelling of the study lakes 148
Nutrient dynamics and cyanobacteria responses 151
Insights from parameter sensitivity analysis 152
Lag times in response to restoration 153
Considerations of model spatial scales and relationships with field programmes 154
Resilience to global environmental change 155
Geochemical engineering 156

Food webs and effects of coarse fish 157
Achieving successful restoration 159
References 161
Appendix A: DYRESM-CAEDYM parameters used 168
Appendix B: Parameter sensitivity results 171
Ngāroto 171
Waahi 174
Rotomānuka 177
Appendix C: Waikare catchment model parameters and results 180
Appendix D: Field study 186
Methods 186
Results 187
Appendix E: Food-web analyses 193
Appendix F: Fish study 199
Introduction 199
Summary of results 199
Fish abundance estimates 199
Estimating sediment and nutrient yields from fish 201
Detailed estimates of fish abundance in Lake Ngāroto 202
Fishing effort 202
Results 203
Conclusion 204
Detailed estimates of fish abundance in Lake Waahi 209
Fishing effort 209
Results 209
Detailed estimates of fish abundance in Lake Rotomānuka 212
Fishing effort 212
Results 212

Detailed estimates of fish abundance in Lake Waikare 216
Fishing effort 216
Discussion 217
Lessons from Ohinewai 217
Key discussion points from a fish perspective 218
Acknowledgements 221
Appendix G: Sediment core incubations for phosphorus release 222

Introduction

Background

The lakes and rivers of the lower Waikato region present a significant challenge to management goals to restore their water quality and biodiversity. Many of the lowland lakes of the Waikato River floodplain have been heavily influenced by agricultural development in their catchments. Clearing of native riparian vegetation for pastoral grazing, horticulture and cropping have resulted in substantial increases in nutrient and sediment loads to these lakes (Hamilton *et al.* 2010). Water levels and the seasonal regimes of water level in these lakes have also been extensively modified through drainage schemes or flood control programmes, as well as through direct encroachment to support agricultural development. Decreased water levels have reduced lake water volumes that act to buffer external (catchment) and internal (bottom-sediment) sediment and nutrient fluxes, as well as increasing the potential for resuspension of particulate material from the lakebed bottom sediments (Hamilton *et al.* 2010). One manifestation of these pressures is that the lakes have switched from macrophyte dominated states to phytoplankton dominated states, with associated decreases in water clarity, biodiversity, aesthetics and recreational values (Schallenberg and Sorrell 2009).

Almost all of the lower Waikato's shallow lake systems have become devoid of submerged aquatic vegetation, exacerbating wind-driven sediment resuspension and nutrient release (Edwards *et al.* 2010). Many of these systems have also been invaded by exotic fish species such as koi carp (*Cyprinus carpio*) and brown bullhead catfish (*Ameiurus nebulosus*), contributing to declines in water quality and biodiversity (Collier & Grainger 2015). These pressures have resulted in 75% of monitored shallow lakes in the Waikato region being categorised as being very highly or extremely highly nutrient-enriched, with mean Trophic Level Index (TLI) values (see Burns *et al.* 1999 for details of TLI) of 5.0 or greater (i.e., "supertrophic") between 2008-12 (Dean-Speirs & Neilson 2014). Secchi depth (i.e., water clarity) for these lakes is typically <1 m, below the standard considered suitable for bathing and aesthetic considerations (Dean-Speirs & Neilson 2014; Smith & Davies-Colley 1992). In addition, many of these lakes have persistent phytoplankton blooms and health authorities commonly recommend extended recreational closures of lakes such as Rotoroa and Ngāroto due to potential for toxic cyanobacteria blooms (Hamilton *et al.* 2010).

More broadly, the challenges with managing the lowland shallow lakes in the Waikato region are symptomatic of those faced globally due to the characteristic regime shifts that occur in shallow lakes with external pressures of increased sediment and nutrient loading (Scheffer *et al.* 1994).

While there are examples of lakes overseas (Zimmer *et al.* 2009) and in New Zealand (Mitchell et al. 1989) where there have been regime shifts from a turbid state with little or no submerged vegetation to a clear-water state with productivity dominated by submerged macrophytes, there are no examples in the Waikato region in recent decades where lakes devoid of submerged vegetation have undergone such a regime shift. Lake Waikare, however, has been reported to have shifted from a devegated to a vegetated state some decades ago (Reeves et al. 2002). Some lakes still support significant beds of native submerged macrophytes (e.g., Lake Rotoroa, the Rotopiko lake complex) but with a general decline in the health of these beds (assessed via LakeSPI) in recent years. At Lake Ohinewai, fish exclusion cages resulted in establishment of exotic parrot's feather (*Myriophyllum aquaticum*) in shallow areas.

Restoration of the Waikato River and connected aquatic ecosystems is being driven, in part, through a partnership between DairyNZ, the Waikato River Authority (WRA) and the Waikato Regional Council (WRC). The Waikato and Waipa River Restoration Strategy has been developed to guide restoration work by identifying specific, achievable, and prioritised activities in consultation with catchment stakeholders. Once complete, the Strategy will provide and direct a staged 5 to 15 year action plan for restoring the Waikato and Waipa rivers for all organisations involved in catchment restoration activities. Aligned to the Restoration Strategy is a component of the Living Water Programme; a partnership between the Department of Conservation and Fonterra to improve biodiversity and water quality by showcasing achievements in five sensitive catchments from around New Zealand. Peat lakes in the Waikato region are included as one of these five sensitive catchments, with specific focus on lakes Areare, Ruatuna and Rotomānuka.

The Restoration Strategy will consist of four core units; Waipa, Upper Waikato, Central and Lower Waikato and Shallow Lakes. A fifth unit considering wetland restoration priorities is being developed by NIWA and once completed will be incorporated into the Restoration Strategy. The aim is to have strategies developed for all units by August 2017. The shallow lakes component of the Strategy is focused on developing a restoration framework to improve the water quality and health of shallow lakes in the Waikato and Waipa River catchments. There are 62 shallow lakes in these catchments, representing a combination of riverine, peat, dune and volcanic lake types. Many lakes are considered to have poor water quality or ecological state, which impacts upon their recreational, cultural and ecosystem values and uses. Despite existing research there is still considerable uncertainty around the key drivers of water quality across the different lake types, and in turn, which catchment or in-lake management strategies are most likely to be effective for restoration. As it is not possible to undertake a process-based experimental approach to answer these questions

within the timeframes of strategy development, a lake and catchment modelling approach is proposed.

Environmental decision making requires an in-depth understanding of how systems are directly or indirectly affected by anthropogenic activities. In this regard empirical approaches provide an opportunity to develop statistically significant relationships between dependent variables (e.g., phytoplankton biomass) and independent variables (e.g., nutrients) but they can have limitations as relationships are not necessarily causal (i.e., only statistical), and it can be difficult to include interactions amongst a wider range of variables (e.g., light, temperature). By contrast ecological models are based on attempts to include functional relationships amongst different variables (Schmolke *et al.* 2010). In aquatic sciences, ecological models have long been used to help understand and analyse physical, chemical and/or trophic dynamics (Norberg & DeAngelis 1997) and also for water quality management and forecasting purposes (Friedman *et al.* 1984, Arhonditsis & Brett 2005). Some of the disadvantages of ecological models are that they are deterministic (i.e., each model run provides only one possible solution unless a statistical approach such as Monte Carlo is invoked) and that their complexity can make it difficult to identify cause-effect relationships that managers often seek to assist with implementation of environmental management methods. Bayesian Belief Networks and Artificial Neural Networks are other modelling systems that may invoke expert knowledge and may attempt to weight the relative importance of independent variables towards the model outcome. We deal only with process-based deterministic models in the Waikato shallow lakes applications described in this report, primarily because they can be used to test the plausibility of conceptual models of lake ecosystem function, to shed light on the importance of various processes contributing to observed system behaviour, and to extrapolate to scenarios that fall outside the range of historical observations.

Study objectives

The principal aim of this study is to apply a modelling approach to identify, evaluate and prioritise specific in-lake and catchment restoration options which could be applied to improve the water quality and ecological health of peat and riverine lake types across the Waikato Region. Four representative lakes have been selected as case studies for this work based on their social, cultural and ecological significance, as well as the availability of historical monitoring data and the potential transferability of the study findings to similar lake systems. The lakes include:

- Rotomānuka,
- Ngāroto,

- Waahi, and
- Waikare.

This study is comprised of the following six objectives for each lake:

1. Define baseline water quality and ecological health based on existing monitoring data and knowledge.
2. Determine the key pressures, drivers and processes governing lake water quality and ecological health.
3. Define, evaluate and rank the likely effectiveness of a range of in-lake and catchment management strategies to improve existing water quality and biodiversity values.
4. Evaluate the level of certainty around the suggested restoration strategies that meet the desired outcomes, as well as the timeframes implementation and longevity.
5. Identify an achievable end state for water quality and ecological health, taking into consideration existing trophic state, legacies and catchment land use.
6. Provide an expert assessment on whether the strategies identified are also likely to be effective when applied to other similar Waikato lake types.

To support the modelling required to contribute to the above objectives, three field-based investigations have taken place which are reported in Appendices D to F. The main findings of these studies are summarised in lake-specific results sections. First, sampling of water quality and vertical profiles of temperature and dissolved oxygen were conducted over about three months in Lake Rotomānuka and Lake Ngāroto. Second, analyses of the flow of energy through the food webs of Lake Rotomānuka and Lake Ngāroto were conducted. Such analyses can give insights into trophic inter-relationships among species and their reliance on particular food resources. These analyses can also highlight the potential for trophic interactions between native and non-indigenous species, and key energy pathways that need to be maintained to promote of productivity of aquatic species of interest. Third, a fish study was carried out to estimate the potential for improvement of water quality that might be associated with removal of invasive fish. To do this, we aimed to predict the amount of sediment that could be resuspended by koi carp compared to other processes, e.g., wind turbulence, and we produced estimates of nutrient release and sediment resuspension.

Methods

Modelling approach

Our process-based lake water quality modelling approach is driven by interactions of external drivers operating as boundary-condition inputs to the model (inputs of water, nutrients and other contaminants; meteorological data) and internal processes operating within the lake waterbody itself (Figure 1).

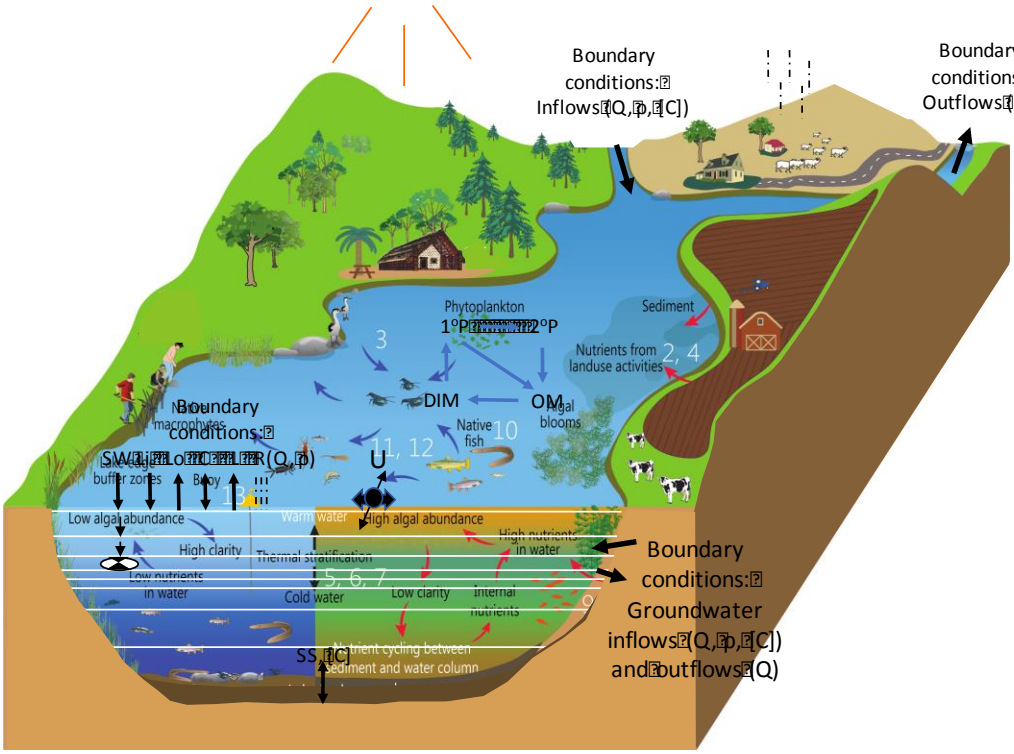

Figure 1: One-dimensional representation of a lake. The white lines in the lake represent model layers. Boundary conditions include discharge (Q), density (ρ) and composition [C] for inflows, Q for outflows, and shortwave radiation (SW), longwave input (Li), longwave emission (Lo), conductive (C) and latent (L) heat exchanges, rainfall (R) for which Q, ρ and [C] can be defined. Note that shortwave radiation is represented to penetrate below the water-atmosphere boundary layer. SS represents suspended sediment (e.g., from sediment resuspension). Biogeochemical processes are represented in very simple terms in the diagram in the middle of the lake, showing relationships amongst primary producers (1˚P: phytoplankton taking up dissolved inorganic matter, i.e., nutrients), secondary producers (2˚P: zooplankton consuming phytoplankton) and organic matter (OM: nutrients in organic form) and inorganic nutrients (DIM) that take place at each time step. Boundary fluxes would include atmospheric exchanges if the layer was at the surface or sediment-water fluxes if the layer was at the bottom (e.g., sedimentation of nutrients out of the water column, sediment resuspension and/or dissolved nutrient exchanges).

The model requires daily data for stream inflow discharge, and nutrient and sediment concentrations. Usually, field data are not available at sufficient temporal resolution, making it necessary to model these components. We used different approaches for modelling catchment discharges and contaminant loads for each of the lakes due to their individual complexities and availability of data. Broadly, three approaches have been used to generate daily time series of inflow and outflow discharge volumes:

1. Process-based modelling of inflow using the INtegrated CAtchments model (INCA) (Whitehead *et al.* 1998a)
2. Inflow time series from the TopNet hydrological model; and
3. Calculation using mass-balance approach to derive inflow discharge from known water level and outflow data.

Likewise, the concentrations of nutrients, suspended sediments and other state variables for inflows, required as input for the lake model, were determined using different approaches:

1. Process-based modelling of inflow using INCA-N and INCA-P validated against field observations;
2. Monitoring of inflow concentrations together with interpolation to provide values for days not monitored; and
3. CLUES output of annual loads disaggregated to daily values.

For Lakes Ngāroto, Waahi and Rotomānuka, a one-dimensional (1-D) modelling approach was chosen in order to generate multi-year simulations, with no attempt made to capture horizontal variability (i.e., horizontal variability is averaged out by using vertically-differentiated horizontal layers in a computationally efficient manner). For Lake Waikare, the 3-D model Delft3d was chosen to resolve horizontal and vertical processes in the lake. Only a catchment model and lake hydrodynamics were simulated for this lake due to time constraints.

The DYRESM-CAEDYM lake water quality model

For modelling of 1-D lake hydrodynamics and ecological processes, we chose the one-dimensional, coupled hydrodynamic-ecological model DYRESM-CAEDYM as the tool for assessing effects of altered hydrology, nutrient and sediment loads, and climate on physical and biogeochemical processes in Lakes Ngāroto, Waahi and Rotomānuka. This model was developed at the Centre for Water Research, University of Western Australia and has previously been applied in New Zealand

and overseas for the purpose of assisting with lake management decisions (e.g., Burger *et al.* 2008; Özkundakci *et al.* 2011; Trolle *et al.* 2008). DYRESM-CAEDYM is the most widely used and cited aquatic ecosystem model documented in the scientific literature (Trolle *et al.* 2011).

DYRESM (version 3.1.0-03) was coupled with the aquatic ecological model CAEDYM (version 3.1.0-06) to simulate water quality. DYRESM resolves the vertical distribution of temperature, salinity, and density taking account of vertical mixing processes. CAEDYM simulates time-varying fluxes of biogeochemical variables (e.g. nutrient species, phytoplankton biomass). The model includes cycles for carbon (C), nitrogen (N), phosphorus (P), and dissolved oxygen (DO), and inorganic suspended solids and the interactions in the N and P cycles are illustrated in Figure 2. Several applications have been made of DYRESM-CAEDYM to different lakes (e.g., Burger *et al.* 2008; Gal *et al.* 2009; Özkundakci *et al.* 2011; Trolle *et al.* 2011) and detailed descriptions of the model equations can be found in (Gal *et al.* 2003; Romero *et al.* 2004). It is important to note that the one-dimensional set-up of DYRESM-CAEDYM precludes ability to explicitly represent horizontal variations in water quality. This simplification is made to reduce model run times, allow intensive parameter calibration through repeated model runs, and ultimately to allow multi-year simulations that are important for long-term management considerations. It means that specific features of shallow lakes such as horizontal variations in suspended sediments or cyanobacteria populations from wind resuspension or wind-driven accumulations of buoyant cells, respectively, are not captured explicitly.

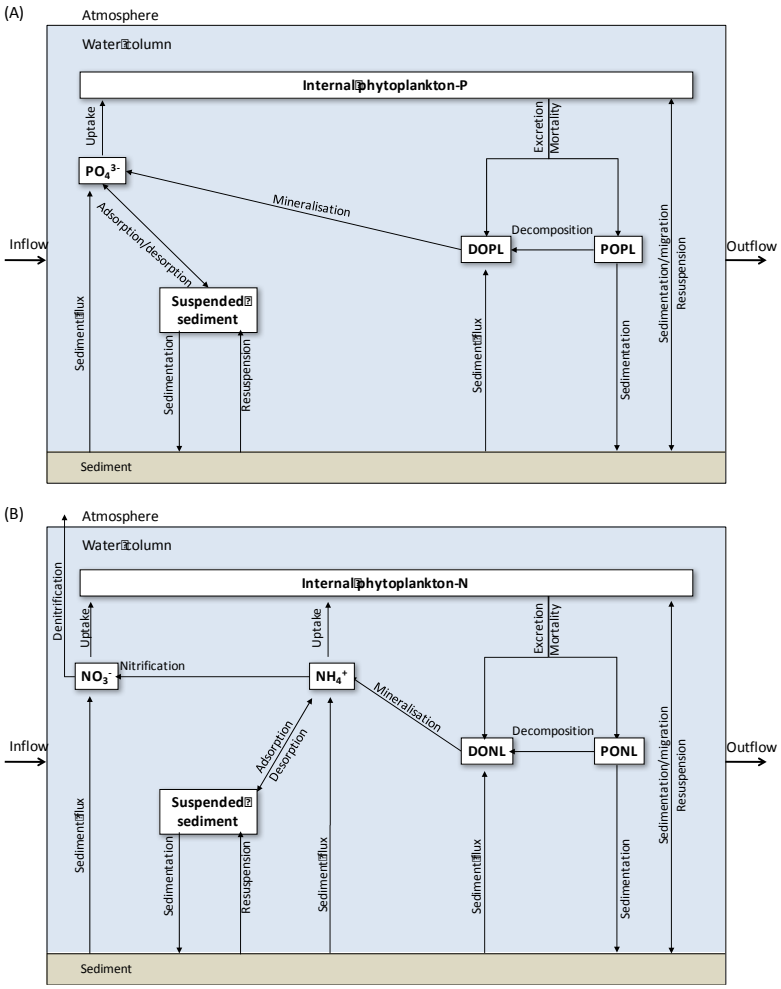

Figure 2: Conceptual model of the (A) phosphorus and (B) nitrogen cycles represented in DYRESM-CAEDYM for the present study. POPL, PONL, DOPL and DONL represent particulate labile organic phosphorus and nitrogen, and dissolved labile organic phosphorus and nitrogen, respectively. Adapted from Hamilton et al. (2012).

The biogeochemical variables in CAEDYM are generally configured according to the goals of the model application and availability of data. For each of the three shallow lakes in this study we configured two groups of phytoplankton in CAEDYM. These groups corresponded to cyanobacteria which are positively buoyant, but did not fix nitrogen, and other groups represented generically by diatoms, based on observations from sampling carried out by the Waikato Regional Council that indicated the dominance of these two groups. The interactions between phytoplankton growth and losses, sediment mineralisation and decomposition of particulate organic matter influence N and P cycling in the model. Fluxes of dissolved inorganic and organic nutrients from the bottom sediments are dependent on temperature and concentrations of nitrate and dissolved oxygen (DO) of the water layer immediately above the sediment surface. Humic compounds (i.e., associated with chromophoric dissolved organic matter) and pH of inflowing water were not modelled. The humic complex typically contains metal cations (Fe and Al) that can sorb phosphate and effectively

compete with phytoplankton for P in the water. The effect of pH may be related mostly to ligand exchange of P and OH^- associated with clay minerals (the dominant binding constituent for P in natural waters). High (or low) pH, for example, results in ligand exchange, in which P is substituted by OH- in the Fe and Al (hydr)oxides in these clay minerals. The net result is that the P is desorbed and becomes available to phytoplankton. The current modelling approach of not including these details was considered to be a reasonable compromise between model complexity, data availability and conceptualisation of the key processes.

Wherever possible, parameters in the model were set to be identical amongst the three lakes but some calibration was specific for the lake under consideration (e.g., to reflect different bottom-sediment composition and therefore different rates of sediment-water exchange). Parameter values were derived using a combination of literature values (e.g., from an extensive parameter library available from the large number of studies undertaken with DYRESM-CAEDYM), calibration within literature ranges based on repeated model runs, or fixed values on the basis of stoichiometry or lack of sensitivity of model output to the parameter under consideration. Parameters used in this study are given in Appendix A.

For all three lakes, DYRESM-CAEDYM was run for approximately five years at hourly time steps between 1 July 2010 and 20 May 2016. Input data (for meteorology, inflows and outflows) were provided as daily averages and output was also recorded as a daily average value.

The INCA catchment model

We chose the The INtegrated CAtchments model for Phosphorus and Nitrogen (INCA-P version 0.1.31 and INCA-N version 1.11.10), respectively, to simulate catchment discharges and nutrient concentrations into Lakes Rotomānuka, Waikare and Ngāroto. The INCA model was developed over 12 years as part of two EU-funded projects and is freely available. INCA is a process-based dynamic model which represents plant-soil system dynamics and in-stream biogeochemical and hydrological dynamics. It has been used to assess a wide range of environmental issues in catchments including land use change, climate change and point and diffuse source pollution (Jin *et al.* 2013; Wade *et al.* 2002; Wade *et al.* 2004; Whitehead *et al.* 1998a).

INCA-P and N are run as separate models. INCA-P is a process-based, mass balance model describing the water, sediment and TP transport in both the land and in-stream components of river catchments (Wade *et al.* 2002). Multiple sources of P are considered by the model (Whitehead *et al.* 2009). In modelling catchment hydrology, a simple two-box approach is used in which major stores in the reactive zone and deep groundwater zone are used and their controlling factor of residence

time is accounted for (Rankinen *et al.* 2002). Base Flow Index (BI) is used to divide the total volume of water stored between the soil and the groundwater (Wade *et al.* 2002). Calculation of river flow is based on mass balance of flow and on a multi-reach description of the river system (Whitehead *et al.* 1998a; Whitehead *et al.* 1998b). The model simulates spatial variation in P export from different land use types within a river system using a semi-distributed representation, thereby accounting for the impacts of different land management practices.

The dynamic INCA-N (Integrated Nutrients in Catchments–Nitrogen) model integrates hydrology and N processes (Whitehead *et al.* 1998a, Wade *et al.* 2002; Wade *et al.* 2004). The model is semi-distributed, meaning the land surface is not described in detail, but rather by the land-use classes in sub-basins. The sources of N include atmospheric deposition, leaching from the terrestrial environment and direct discharges. The terrestrial N fluxes are calculated in up to six user-defined land use classes. The hydrologically effective rainfall (HER) is used to drive the N through the catchment system so that the N can enter the river system by lateral flow through the surface soil layers or by vertical movement and transport through the groundwater zone. The hydrology within the subcatchments is modelled using a simple two-box approach, with reservoirs of water in the reactive soil zone and in the deeper groundwater zone. The mass balance equations for NO_3-N and NH_4-N in the soil and groundwater zones are solved simultaneously with the flow equations. The key N processes that are simulated in the soil water zone are nitrification, denitrification, mineralization, immobilisation, N fixation and plant uptake of inorganic N in six land use classes. It is assumed that no biochemical reactions occur in the groundwater zone. In the rivers the key N processes are nitrification and denitrification. Mineral fertilizers are assumed to decay at a rate of 0.15 d^{-1} (default value in INCA). Application of manure is assumed to increase the pool of NH_4-N. This pool is assumed to nitrify rapidly (70% within 5 days). Further, manure was assumed to increase mineralization potential on those fields where it was applied.

Scenario modelling

Multiple lake management scenarios were conceptualised with a project working group[1] and modelled using a DYRESM-CAEDYM model calibrated to each lake application. The management approaches assessed can be broadly considered as belonging to three categories:

[1] The main project working group included the researchers who were authors on this report, Waikato River Authority/Envirostrat (Keri Nielsen), DairyNZ (David Burger), Waikato Regional Council (Deniz Özkundakci, Paula Reeves), Waikato-Tainui (Erina Rawiri-Watene), Department of Conservation (Tracie Dean-Spiers,

1. External nutrient load reduction: associated with land use change or nutrient loss mitigation by improved management practices and/or targeted interventions, e.g., erosion mitigation, denitrification beds;
2. Hydrological modifications: diversion of inflows away from the lake or increasing the water level to alter wind-driven resuspension of sediments;
3. Geochemical engineering: by sediment capping to reduce internal loading and/or continuous low-dosage alum treatment to reduce dissolved P and increase flocculation in the water column.

The final set of scenario simulations was derived in a series of meetings between the University of Waikato and the project working group in an adaptive fashion. The first set of model scenarios to be run was decided upon during a meeting of the working group on 17 October 2016 at which the results of the calibrated base models were presented. The scenario results were presented to the same group on 30 November 2016 and further scenarios were decided upon to investigate in more detail the effectiveness of various mitigation strategies. The final set of scenarios was developed following a working group meeting on 17 January 2017.

Each management scenario is implemented by a specific modification of the model set-up as illustrated in Figure 3. The base model and each scenario simulation is summarised using metrics which describe the water quality in terms of attribute bands (A, B, C or D) from the National Objectives Framework (NOF) of the National Policy Statement for Freshwater Management (NPS-FM, MfE 2015). Reporting against the NOF is based on annual median values of water quality attributes (Burns *et al.* 2000). Properties useful for environmental management are given in Table 1. NOF bands for the three water quality attributes considered in this study are shown in Table 2.

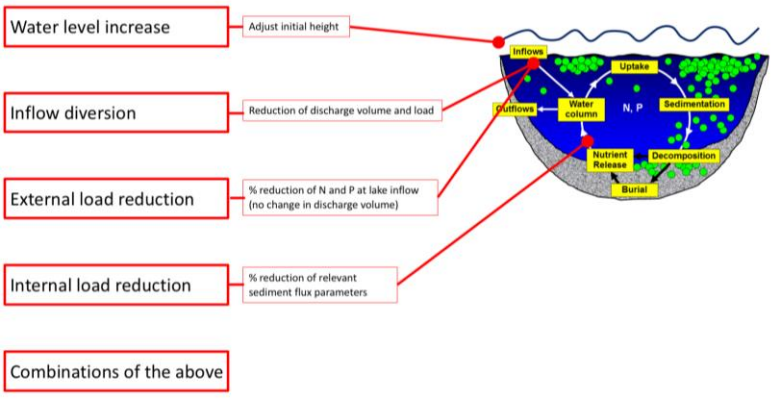

Figure **3**: Illustration of management scenarios and their corresponding model modifications.

Natasha Grainger), NIWA (John Quinn, Piet Verburg), Aareka Hopkins (AM^2). Julian Williams (Waikato-Tainui) was also part of the wider project advisory group.

Table 1: Metrics calculated for each model scenario.

Metric	Method	Variables
Medians	Arithmetic mean of five annual medians calculated on daily values for each variable.	TCHLA, TN, TSS, TP, SD
Surface mean	Arithmetic mean of daily values of variables in surface 0.5 m of the lake.	TCHLA, TN, TP, DO, DRP, NO_3-N, NH_4-N
Bottom mean	Arithmetic mean of daily values of variables in bottom layer of the model grid.	TCHLA, TN, TP, DO, DRP, NO_3-N, NH_4-N
Summer means	Arithmetic mean of variables calculated between 1 December to 30 March.	TCHLA, Cyanobacteria chlorophyll *a* (CYANO)
Number of low-oxygen days	Number of days of bottom oxygen (DO) concentration below 2 mg L^{-1}	DO
Number of cyanobacteria bloom days	Number of days during which cyanobacteria chlorophyll *a* exceeds 15 mg m^{-3}*	
Number of stratified days	Number of days in a year in which temperature difference between surface and bottom is greater than 0.5˚C	

*15 mg m^{-3} of cyanobacterial chlorophyll *a* is assumed to be equivalent to the recreational health limit of 15,000 cells mL^{-1} assuming a carbon-to-chlorophyll ratio of 50:1 and a biovolume of 100 μm^3 $cell^{-1}$ (average volume of a small cell of *Anabaena* or large cell of *Microcystis*).

Table 2: Summary of NOF bands of three water quality attributes (MfE 2015a).

	Chlorophyll *a* (mg m^{-3})		**TN (g m^{-3})**		**TP (g m^{-3})**
Bands	**Annual median**	**Annual maximum**	**Annual median (monomictic / brackish)**	**Annual median (polymictic)**	**Annual median**
A	<2	<10	<0.160	<0.300	<0.010
B	2 — <5	10 — <25	0.160 — <0.350	0.300 — <0.500	0.010 — <0.020
C	5 — <12	25 — <60	0.350 — <0.750	0.500 — <0.800	0.020 — <0.050
D	> 12	> 60	> 0.750	> 0.800	> 0.050

DYRESM-CAEDYM calibration and validation

Selected parameters in DYRESM-CAEDYM were calibrated using comparisons of model output observations for variables of temperature, salinity, dissolved oxygen (DO), chlorophyll *a* (TCHLA), dissolved reactive phosphorus (DRP), total phosphorus TP, ammonia-nitrogen (NH_4-N), nitrate-

nitrogen (NO_3-N), total nitrogen (TN) and total suspended sediments (TSS). The two simulated generic phytoplankton groups (i.e., cyanophytes and diatoms) collectively contributed to a total simulated chlorophyll *a* concentration, for which a surface value was calibrated against measured surface chlorophyll *a*. Model parameters were adjusted manually using a trial and error approach with values set to within literature ranges (e.g., Schladow & Hamilton 1997; Trolle *et al.* 2012). For lakes Rotomānuka and Waahi, observations for comparisons with model output were taken from field data collected by WRC from their central sampling station in each lake over the five-year simulation period from July 2010 to June 2015. For Lake Ngāroto only DO and temperature were available during the simulation period and the model was calibrated against a combination of these two variables and monthly median values of the other variables calculated from observations before the simulation period, as described in the Ngāroto section of the Methods. The approach of calibrating the model against an aggregate monthly cycle was validated using the model for Lake Waahi. Key parameter performances are shown as root mean square error (RMSE) and coefficient of variation of RMSE (CV(RMSE)), derived as follows:

$$RMSE = \sqrt{\sum_{t=1}^{n} (\hat{y}_t - y_t)^2}$$

$$CV(RMSE) = RMSE / \bar{y}$$

where $\hat{y}_t$ is the observation at time t, y_t is the model results at time t, $\bar{y}$ is the average of the observation.

Other methods of validation, for example, splitting the observations into unique sets for calibration and validation, respectively, have not been performed. We believe that the small number of observations and the limited duration of the simulation rendered this technique obsolete and would not have produced statistically meaningful results.

DYRESM-CAEDYM sensitivity analysis

Sensitivity to input data

The results of the simulations are aggregated into means of the five annual medians or overall means for the simulation period (Table 1) in order to assess the effectiveness of management strategies. The sensitivity of these metrics to input data is therefore quantified as the variability around the five-year mean. These results are shown in the bar charts which compare the metrics

derived from the different scenario simulations in the section *Scenario simulation results* in the Results section for each individual lake.

Sensitivity to key parameters: Uncertainty analysis

Sensitivity of the lake simulation output to the model parameters was carried out to provide insights into how robust the model conclusions were with respect to uncertainty in the values of the model parameters. Two approaches were chosen; a local sensitivity analysis in which one parameter at a time was changed, and a Monte Carlo approach involving random simultaneous perturbations to several different parameters.

The local sensitivity analysis was conducted on selected model parameters using a one-factor-at-a-time method (Morris 1991). Parameter selection for the sensitivity analysis was based initially on considerations of Schladow and Hamilton (1997), but the ability to automate the running of simulations and subsequent analysis of results allowed the inclusion of more parameters than considered in previous efforts (e.g., Hamilton *et al.* 2012). Therefore, we changed 65 parameters by ± 10% of their calibrated values for the local sensitivity analysis. The sensitivity of the model output to changed values of the model parameters was assessed and quantified by calculating the relative difference (in percent) of the summary metrics used to report the simulations (Table 1).

The Monte Carlo procedure involves the creation of an arbitrary number of parameter sets by adjusting a subset of the model parameters simultaneously by a small random perturbation from the calibrated value. Based on considerations of Schladow & Hamilton (1997) and experience gained during model calibration, we chose 65 parameters for the Monte Carlo procedure (Appendix A). The perturbations were of random magnitude drawn from a uniform distribution within 5% of the calibrated value. Because all parameters are changed simultaneously, the 5% range was chosen as opposed to the 10% range of the one-factor-at-a-time method. The number of simulations performed during this sensitivity analysis varied from hundreds to thousands. However, not all parameter combinations generated by this method produce a system in which all components stay within realistic bounds and several simulations 'crashed'. The simulations which did not crash are reported as probability density functions and medians over the duration of the simulation period.

Results of the Monte Carlo parameter sensitivity analysis are presented in the form of ensemble simulation plots and summary statistics for the metrics shown in Table 1. The ensemble simulation plots show time series of the median of all simulations surrounded by colour shaded probability density functions which show the statistical distribution of the entire ensemble of simulations at every point in time. The metrics from Table 1 were calculated for each iteration of the simulation in

the same way as for the base simulation, i.e., by calculating annual medians and averaging these over the five years of the simulation. An overall (ensemble) median was then calculated. The uncertainty due to parameter perturbations was quantified as the 25% and 75% percentiles of the ensemble of medians.

Meteorology

Meteorological data required for the simulation period for Lakes Rotomānuka and Ngāroto was obtained from the climate station at Hamilton Airport (Hamilton AWS, 37.865˚ S, 175.336˚ E). Meteorological data for the model of Lake Waahi was obtained from the Ruakura 2 EWS in Hamilton (37.776 S, 175.305 E). The meteorological forcing data sets used in the lake models of Lake Ngāroto and Lake Rotomānuka are shown in Figure 4 and for Waahi in Figure 5.

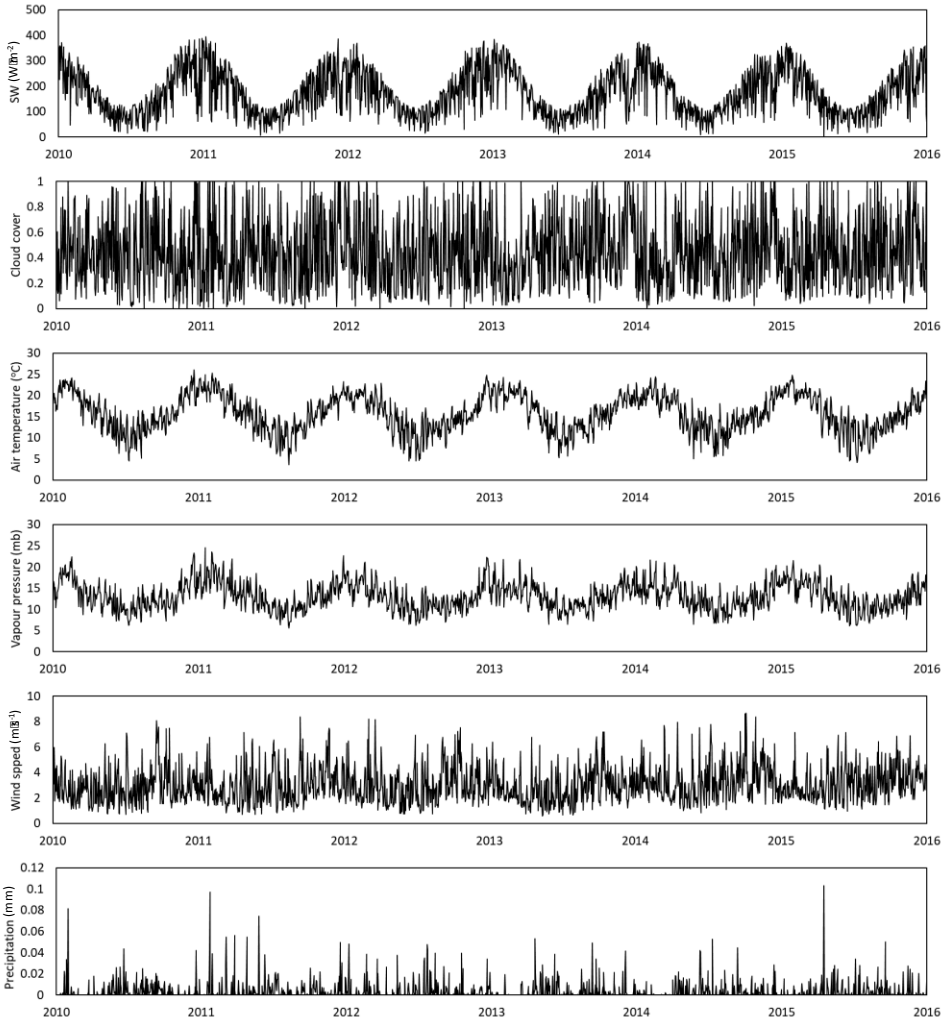

Figure 4: Meteorological forcing for Lakes Ngāroto and Rotomānuka from Hamilton airport.

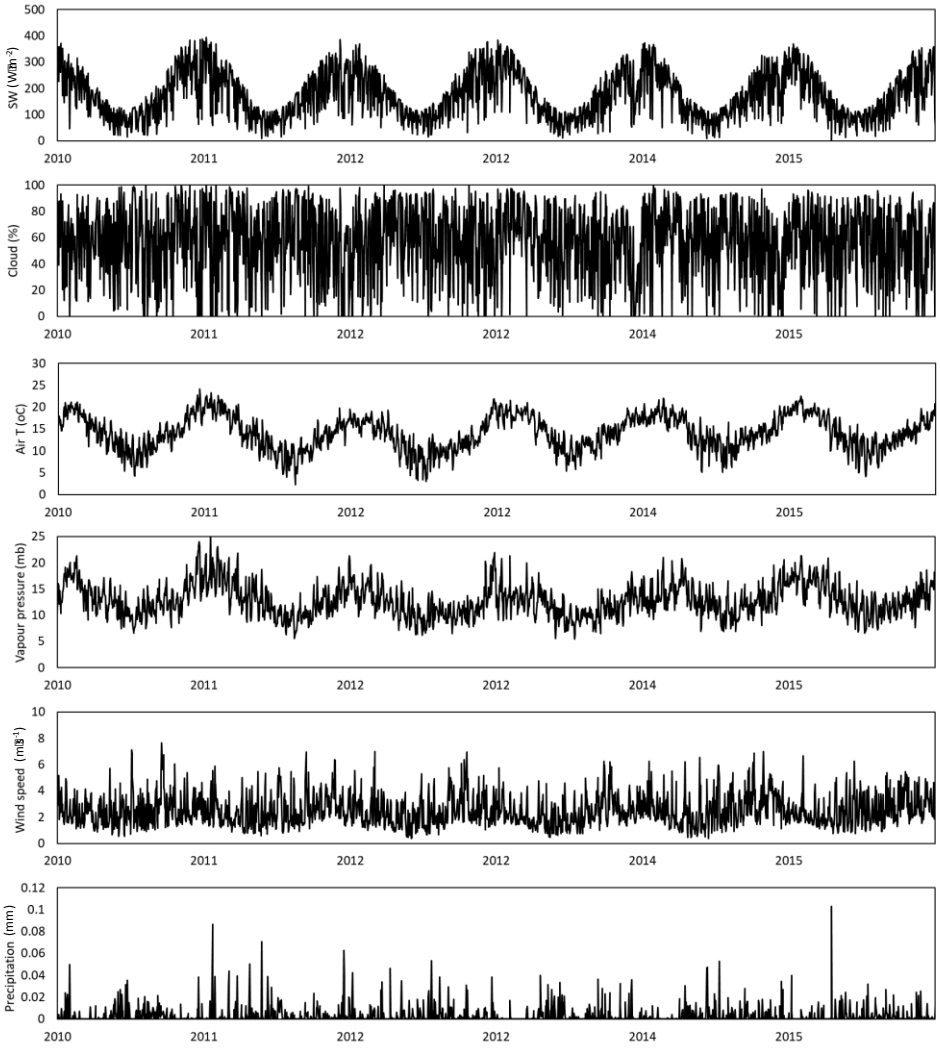

Figure 5: Meteorological forcing for Lake Waahi from Ruakura met station.

Hamilton AWS

Hourly meteorological data for years 2003 - 2013 for station Hamilton AWS (-37.865°S; 175.336°E) were downloaded from the NIWA Cliflo database. Data from this station for the years 2013 - 2016 were provided by the MetService directly (Robert Hamilton, pers. comm.). The data included atmospheric pressure (*P*, hPa), air temperature (*Tair*, ˚C), wet bulb temperature (*Twet*, ˚C), dew point temperature (*Tdew*, ˚C), relative humidity (*RH*, %), precipitation (*precip*, mm), wind speed (*U*, m s^{-1}), and wind direction (*Udir*, degrees). Gaps in the data set were either linearly interpolated or filled with data from the Ruakura 2 EWS site.

The meteorological forcing data necessary for the model (cloud cover fraction, *Tair*, *Pv*, *U*, *precip*) were generated in daily frequency by averaging or summation, as appropriate. Shortwave radiation (*SW*, W m^{-2}) was obtained from Ruakura 2 EWS, as it was not contained in the Hamilton AWS data set.

Air temperature measurements also exist from the Lake Ngāroto observation buoy between 2009 and 2016. These data was used to adjust air temperature measurements from Hamilton AWS using the empirical relationship between two air temperature observations (Figure 6). The adjusted air temperature was used for modelling in favour of using the buoy observations in order to provide consistency between the lake models and to minimise gaps in the data set.

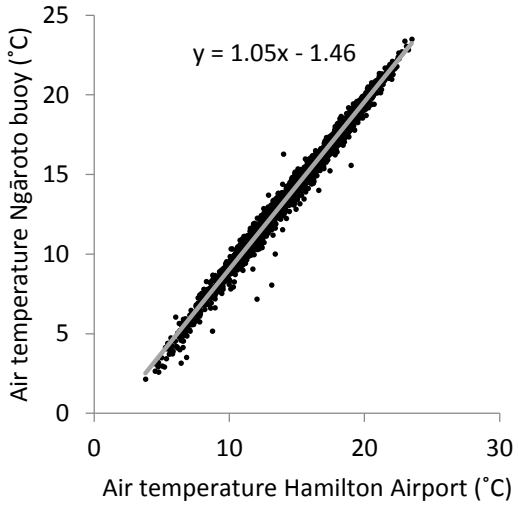

Figure 6: Relationship between air temperature measurements at Hamilton AWS and the monitoring buoy in Lake Ngāroto.

Ruakura 2 EWS

Hourly meteorological data for years 2006 - 2016 for station Ruakura EWS (-37.776°S; 175.305°E) were downloaded from the NIWA Cliflo database. The data included air temperature (*Tair*, ˚C), wet bulb temperature (*Twet*, ˚C), dew point temperature (*Tdew*, ˚C), relative humidity (*RH*, %), precipitation (*precip*, mm), wind speed (*U*, m s^{-1}), shortwave radiation (*SW*, W m^{-2}) and wind direction (*Udir*, degrees). Gaps in this data set were either linearly interpolated or filled with data from the Hamilton AWS site.

The cloud cover fraction (*CLOUD*) is required by the model to calculate long wave radiation, but is not provided in the meteorological data. It was derived from the relationship between observed SW and clear-sky shortwave radiation (SW_{clear}) and shortwave radiation under 100% cloud cover (SW_{cloudy}) as follows:

For $SW > SW_{cloudy}$

$$CLOUD = 1 - \frac{SW - SW_{cloudy}}{SW_{clear} - SW_{cloudy}}$$

and for $SW < SW_{cloudy}$

$$CLOUD = 1$$

SW_{clear} was modelled as a sine function through the maxima (i.e., clear-sky) of all available SW observations by day of year (T) using the equation

$$SW_{clear} = a\ sin\left(\frac{2\pi T}{365.33} + 2\pi c\right) + d$$

The coefficients a, b and c were fitted using Matlab's fminsearch function. SW_{cloudy} was modelled the same way, but fitted through the minima of all available SW observations and then adjusting d so that 5% of all SW observations were below SW_{cloudy}. Figure 7 shows the upper and lower levels of shortwave radiation used to define the cloud cover.

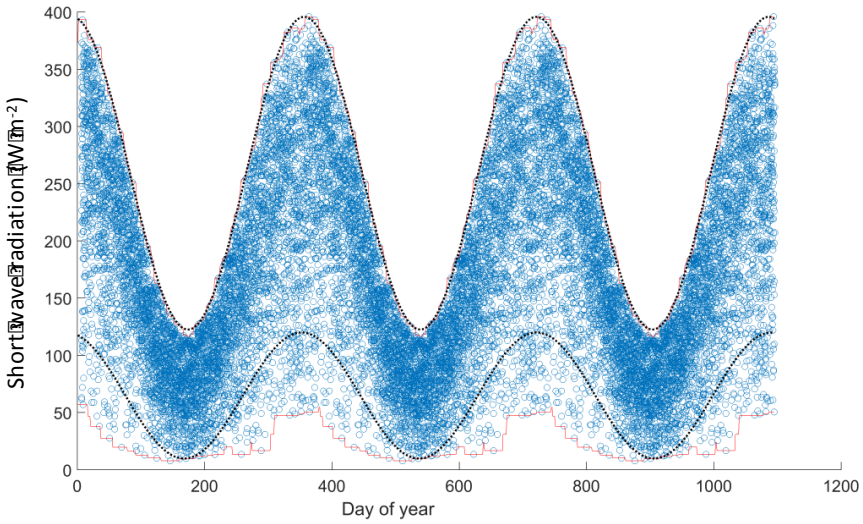

Figure 7: All observations of shortwave radiation from Hamilton AWS plotted by day of year (and repeated for three years). The upper and lower dotted sine waves represent SW_{clear} and SW_{cloudy}, respectively. The red lines show the envelope given by the maxima and minima of SW observations through which the sine waves were fitted.

Air temperature measurements also exist from the Lake Waahi observation buoy. These data were used to adjust air temperature measurements from the Ruakura met station using the empirical relationship between two air temperature observations (Figure 8). The adjusted air temperature was used for modelling in favour of using the buoy observations in order to provide consistency between the lake models and to minimise gaps in the data set.

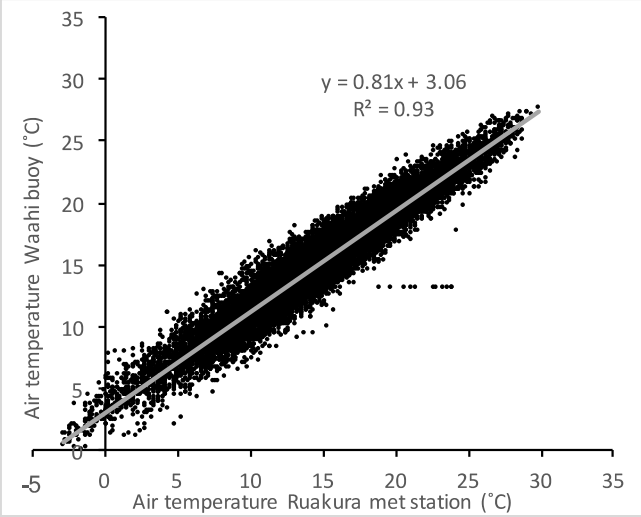

Figure 8: Relationship between air temperature measurements at Ruakura met station and the monitoring buoy in Lake Waahi.

Study sites and model assumptions

Lake Ngāroto

Lake Ngāroto is located 19 km south of Hamilton City and 8 km northwest of Te Awamutu and is the largest of the Waipa peat lakes with a surface area of 108 ha and a catchment area of 1846 ha (Dean-Speirs & Neilson 2014) (Figure 9). Peat surrounding Lake Ngāroto extends to about 0.5 m deep at the lake margin and down to 2.5 m approximately 600 m from the lake edge. Most of the peat is lake-based material deposited when the lake area was larger with large area of surrounding sedges (Thompson 1994). The current mean depth is ca. 2 m and maximum depth 4 m; however, the lake was deeper prior to European settlement and even at the turn of the 20th century was thought to encompass 220 ha of open water. Following European settlement the surrounding peat soils and swampland were drained for agriculture, likely lowering the lake by several metres (Faithfull *et al.* 2005; MfE 2001). The lake has several inlets and one outlet controlled by an adjustable weir gate to allow for recreational activities and season controls of lake levels (MfE 2001). The largest surface inflow enters Lake Ngāroto via Lake Ngāroto-iti, which provides approximately one-third of the inflows to the lake and the highest relative nutrient inputs (BCD 2014).

Figure 9: Photo of Lake Ngāroto viewed from the north end of the lake.

Lake Ngāroto has existed in a highly degraded state since the early 1990s and is currently classified as hypertrophic (Dean-Speirs & Neilson 2014). Although monitoring data is sporadic, the data indicate the lake is likely to be within the NOF D-band for TN, TP and chlorophyll *a* (Figure 10). The decline in lake water quality can be attributed to a number of factors including historical lowering of the lake level through drainage activities, thereby increasing wind driven sediment resuspension, increasing agricultural development within the greater catchment leading to nutrient and sediment loading, and the subsequent loss of submerged macrophytes (Dean-Speirs & Neilson 2014).

The Lake Ngāroto catchment is predominantly dairy pasture, resulting in high external nutrient loads to the lake. The high nutrient load, shallow depth and reduced mean lake volume, together with resuspension of bottom sediments, contribute to high water column turbidity and internal nutrient loading (MfE 2001). Prior to the 1990s water quality sampling was intermittent but a significant decline in mean Secchi depth occurred between 1977 (1.2 m) and 1988 (0.48 m) (Dean-Speirs & Neilson 2014). Lake Ngāroto was determined to be hypertrophic based on monthly water quality sampling between 1988 and 1994 (Hamill & Lew 2006). More recently, there has been no evidence of improvement in lake water quality and the lake remains classified as hypertrophic (Dean-Speirs & Neilson 2014).

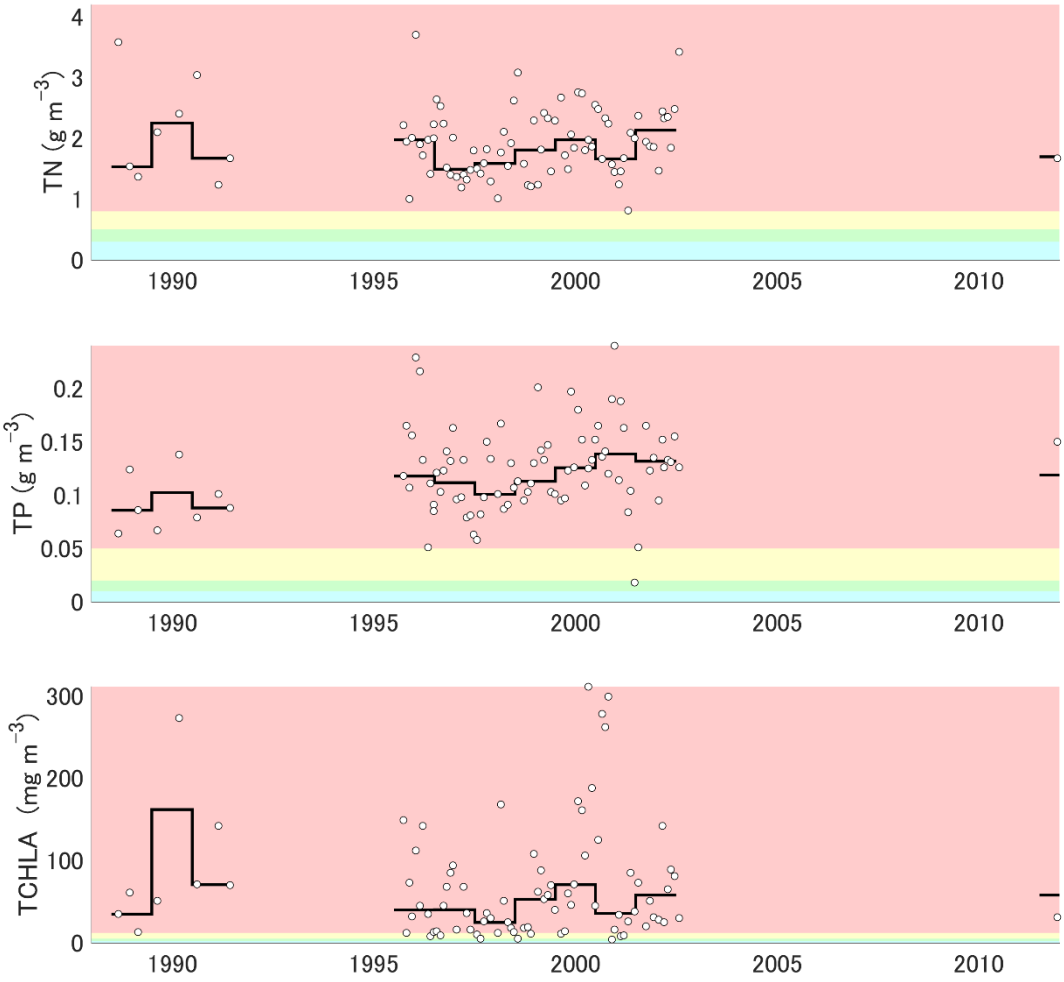

Figure 10: Time series of TP, TN and TCHLA used for calibration of the model (white scatter plots) and annual median values for Lake Ngāroto. The coloured areas show National Objectives Framework (NOF) bands A (light blue), B (light green), C (yellow) and D (red).

In its current state, Lake Ngāroto has recurrent algal blooms, which are dominated by the cyanobacteria (blue-green algae) species *Microcystis* sp. (Paul *et al.* 2008) but with *Anabaena* sp. also common. Several species and/or strains of *Microcystis* produce the hepatotoxin microcystin and *Anabaena* sp. can produce the neurotoxin anatoxin. The Public Health Unit of the Waikato District Health Board or the Waikato Regional Council may issue a health alert to the public to avoid contact recreation when cyanobacteria blooms occur.

Lake Ngāroto hosts large populations of invasive fish including brown bullhead catfish (*Ameiurus nebulosus*), rudd (*Scardinius erythrophthalmus*), gambusia (*Gambusia affinis*), goldfish (*Carassius auratus*) and koi carp (*Cyprinus carpio*). Native fish in the lake include common bullies (*Gobiomorphus cotidianus*), shortfin eels (*Anguilla australis*), and common smelt (*Retropinna retropinna*). Exotic submerged macrophytes such as oxygen weeds (*Lagarosiphon* and *Egeria*) and hornwort (*Ceratophyllum demersum*) were first identified in the lake in 1968-69, and expanded

rapidly before collapse of these populations around 1992 (Edwards *et al.* 2010). No submerged plants have since persisted in the lake under the prevailing conditions of high turbidity.

Table 3: Data for Lake Ngāroto obtained for this study.

Measurement type	Detail	Variables	Time period	Frequency	Number of measurements
Profiles		DO and Temperature	Dec 2011 - May 2013	Dec, March and May	60 each
Water Level	By Waipa District Council at the jetty by the boat ramp	Water Level (m)	Nov 2003 - Sep 2015	Irregular, usually 15-30mins	357398
Temperature	By Waipa District Council at the jetty by the boat ramp	Temperature (deg C)	Oct 2007 - Sep 2015	Irregular, usually 15-30mins	280333
Water quality samples	Waipa DCWRC	TCHLA, NH4-N, NO3-N, DRP, TSS, TN, TP, Secchi depth, pH	1996 - 2003	Monthly samples	
	CBER 54				
	CBER 91				
Inflows		Where available: NO3-N, NH4-N, DRP, TN, TP, PONL, POPL, DONL, DOPL	2006-2007		
		Flow (m3/day)	Dec 2006 - Sep 2007	Irregular, c. monthly	21
High-frequency buoy		Wind speed, wind dir, air temp, water temp, turb, rel humidity, DO, TCHLA etc.	March 2009 - April 2016	15 mins	
Fish		Number of fish	10 days in Dec		

Summary of model setup and assumptions

The model is run using realistic meteorological forcing from 1 July 2010 to 30 May 2016. Outflow measurements and water level observations are used to derive surface water inflow. The most significant difference of the Lake Ngāroto model setup in comparison to the other lake models is that its biogeochemical component is calibrated to periodic idealised annual cycles.

The general parameterisation of the DYRESM-CAEDYM model common to all lake models in this study is in the section *The DYRESM-CAEDYM lake water quality model* and can be summarised as:

- Vertical processes of biogeochemical variables dominate over horizontal processes such that a 1-D model is sufficiently representative of the whole lake; for example:

    - Horizontal variations in suspended sediments or cyanobacteria populations from wind resuspension or wind-driven accumulations of buoyant cells, respectively, are not captured explicitly.
- Two groups of phytoplankton (parameterised as cyanobacteria and diatoms) are used to capture the seasonal dynamics of primary producers and to broadly represent phytoplankton that float and sink, respectively;
- Nitrogen fixation by cyanobacteria does not contribute significantly;
- Humic compounds (i.e., associated with chromophoric dissolved organic matter) are not modelled;
- pH of the water from catchment discharge is neglected as well as within the lake
- There is no atmospheric deposition of nutrients;
- Adsorption and desorption of phosphorus to suspended sediments is not modelled explicitly.

Assumptions specific to Lake Ngāroto are:

1. Groundwater inflows are not considered (the water balance is closed by calculating inflow from observed outflow and water levels);
2. The annual inflow nutrient loads are based on CLUES;
3. Daily variation of nutrient concentrations in the inflow are driven by dynamic catchment processes (as modelled by INCA-N and INCA-P);
4. Hamilton airport weather, i.e., meteorological forcing, is applicable to Lake Ngāroto (except air temperature);
5. Air temperature forcing is based on an empirical fit between Hamilton airport observations and lake buoy observations;
6. Temperature of the inflowing water is similar to lake surface water temperature;
7. Calibration to real-time oxygen measurements and representative seasonal cycles of nutrients and chlorophyll produces a useful model to project the outcome of management scenarios through annual indicators.

In-lake data for model calibration

Field observations of water quality constituents for Lake Ngāroto are sparse during the model period (2010-2015, Table 4) and do not provide sufficient information for a robust calibration of the biogeochemical lake model (Figure 10). However, a number of observations exist between 1996 and 2006. High frequency observations of temperature profiles and dissolved oxygen at the bottom of

the lake are also available from an observation buoy from 2009 to present (Figure 12) and water level observations are available from November 2002 (Figure 14). The lack of water quality observations in recent years when water level and high-frequency measurements are available posed a major challenge to setting up a calibrated model for this lake.

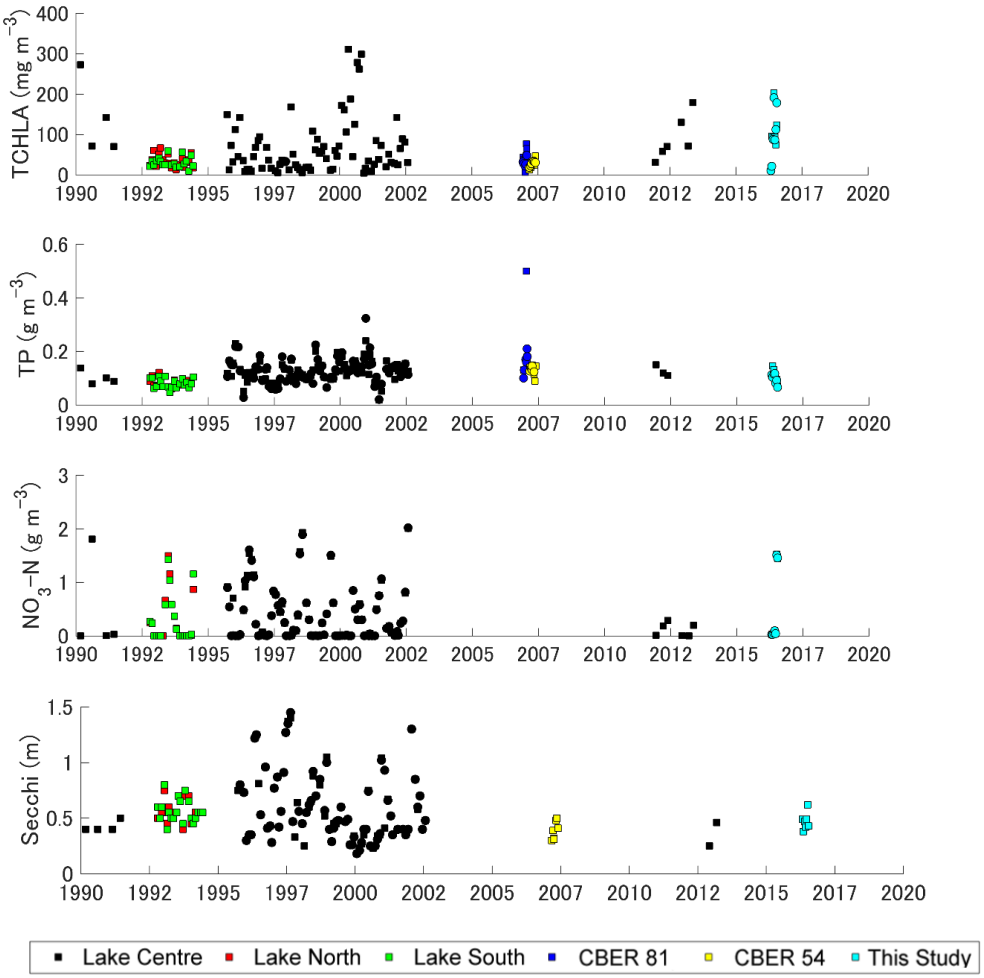

Figure 11: Time series of available field observations from various sources (see legend) for chlorophyll *a*, TP, NNN (nitrate-N plus nitrite-N) and Secchi depth for Lake Ngāroto. CBER 54 refers to Beaton et al. (2007) and CBER 81 refers to Paul *et al.* (2008).

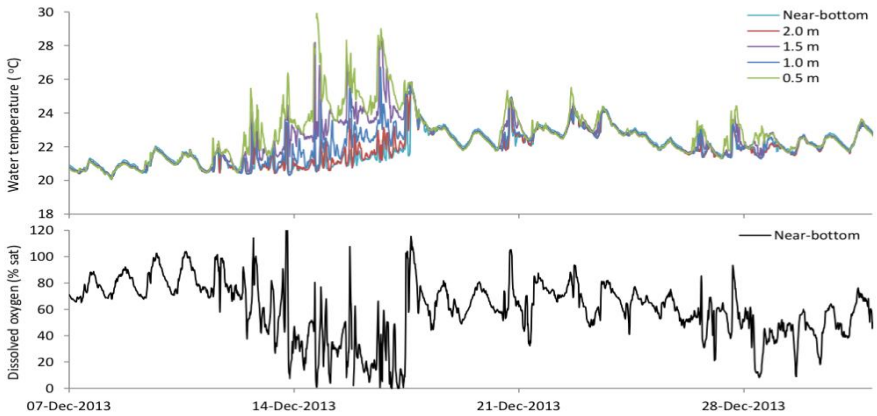

Figure 12: Excerpts of the high-frequency time series of temperature and dissolved oxygen from the Lake Ngāroto observation buoy. Top: temperature at four selected depths. Bottom: dissolved oxygen from a sensor positioned immediately above the bottom of the lake.

Due to the availability of good temperature, DO and water level observations, the model was set up for the time period of 2010 to 2015 and not for the time period when biogeochemical data was available. As a result, a reliable physical model is available to drive the ecosystem model, but the water quality simulation cannot be both calibrated and validated. In order to generate information to calibrate the biogeochemical model, we calculated the monthly medians from all available observations (Figure 13). Thus, the model simulations use realistic forcing data between 2010 and 2015 and are calibrated to temperature and dissolved oxygen concentrations from the same period. The results of the biogeochemical model are compared (and calibrated) to an aggregated annual cycle. Calibration of the model involved adjusting physical and biogeochemical parameters to reproduce the characteristic repeated annual cycle of the data.

As a consequence of this approach, the model for Lake Ngāroto is not calibrated to the interannual variability of timing and magnitude of the biogeochemical state variables, in contrast to the other lake models which are calibrated to observations taken monthly or every two months over the simulation period. By aggregating the available observations into monthly medians, the information content of the time series changes such that information at time scales shorter than monthly and longer than one year is lost. The model is therefore capable of predicting seasonal patterns as long as these are stationary, i.e. there are no long-term trends on top of the seasonal cycles (Wei 1979). Assuming stationarity, this method is consistent with the general approach of this study to predict the future state of the system in terms of representative annual properties calculated as annual medians and averaged over the five-year simulation period. Violation of this assumption, i.e., if there was a trend in water quality, means that the current calibrated model would over- or underestimate water quality parameters. It is noted that this also applies to some extent the models for Lake Waahi and Lake Rotomānuka, because long-term trends in the calibration set of biogeochemical variables

may be masked by interannual variability in a five-year model simulation period. We have not been able to find examples in the scientific literature for our approach and have therefore performed a proof-of-concept test using a model for Lake Waahi where physical and biogeochemical variables are available from 1995 to present (see Figure 23). The results of this test are presented in the section *Validation of aggregation approach*.

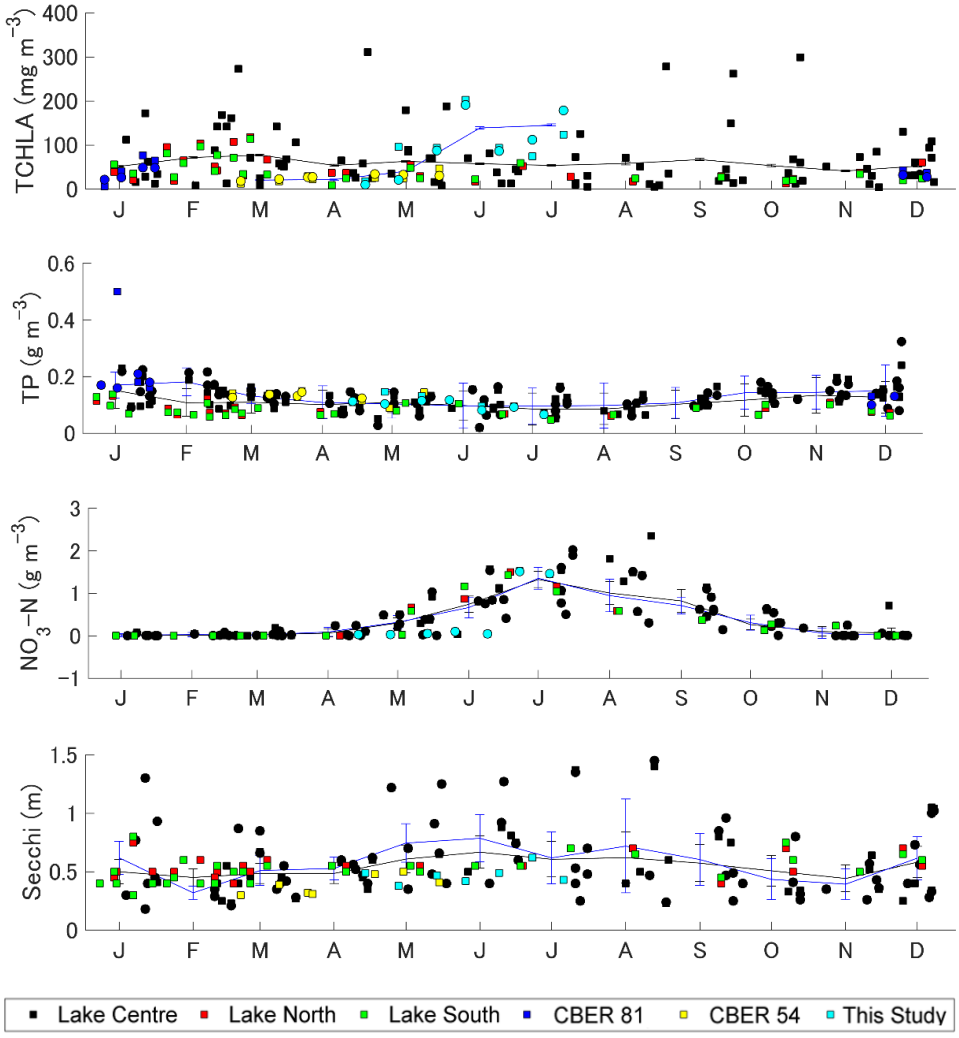

Figure 13: Available field observations for Lake Ngāroto plotted by day of year. The lines through the data connect the monthly medians from surface (black) and deep (blue) samples, respectively. The differences in colour are different sources of the sample, namely from Council data (Lake Centre, Lake North, Lake South), two CBER reports (Beaton *et al.* 2007, Paul *et al.* 2008), and samples taken for this report.

Hydrology

There are no detailed measurements of bathymetry of Lake Ngāroto and so the maximum depth of the lake was determined using the following lines of evidence. The WRC Shallow Lakes management plan (Dean-Speirs & Neilson 2014) cites lake maximum depth at 4 m and according to reports by technicians, the Ngāroto observation buoy was anchored in approximately 3 m of water on 19

March 2015, but not in the deepest part of the lake (Chris McBride, pers. comm.). Water level data shows that the average water level on that day was 33.7424 m (relative to Moturiki datum), which is very low relative to the average (Figure 14). In the absence of accurate measurements, it is assumed that the maximum depth of the lake is 4 m. Subtracting 4 m from the mean elevation of the lake water level results in a geodetic elevation of the deepest part of the lake of 30.3851 m above MSL.

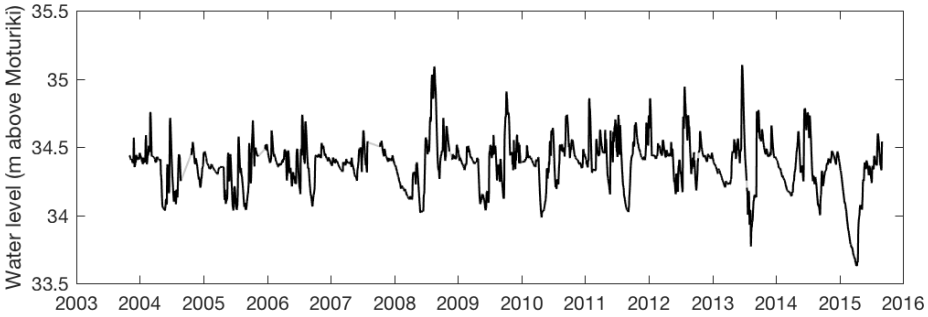

Figure 14: Water level observations from Lake Ngāroto; gaps in the time series are filled using linear interpolation (grey sections).

A hypsographic curve (Figure 15) was taken from a hydrological modelling report produced by HVC Consulting Ltd (Vink 2014). This areal data is extended from 36 m to 33 m relative to Moturiki Datum, therefore a linear assumption was made for deriving area between 33 m and 30.38 m where the bottom area was set as 0 m^2.

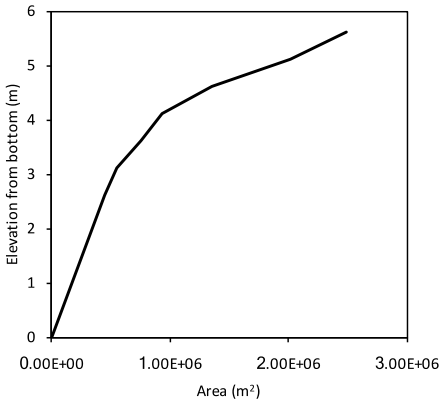

Figure 15: Hypsographic curve used in the Lake Ngāroto model.

High frequency observations of lake surface water level and withdrawal volume from the lake were provided by the Waikato Regional Council. Lake Ngāroto daily inflow volume was calculated by closing the water balance of the lake. This involved estimation of daily surface area and corresponding evaporation volume, precipitation to the lake, daily discharge measurements, and daily fluctuation of the lake heights. Once the DYRESM-CAEDYM model was set up, inflow volume

was re-calibrated iteratively so that water level was estimated accurately (Figure 16). CLUES model estimates of annual inflow volume for Lake Ngāroto (13 million m^3) were referred to as a check on the water balance and inflow and outflow discharges (Figure 17).

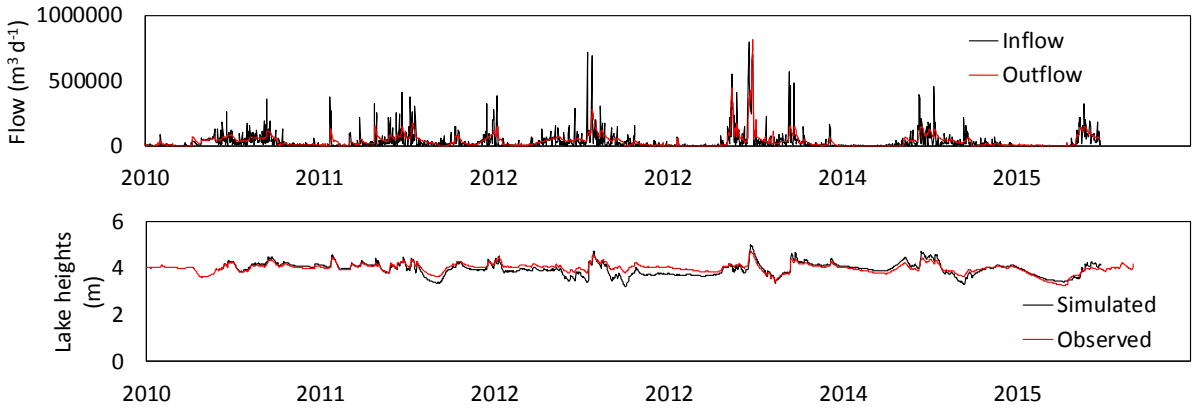

Figure 16. Top: time series plots of Lake Ngāroto total inflow (black line, "VOL") and outflow (red line) volume. Middle: time series plot of temperature assigned to the Lake Ngāroto inflow. Bottom: time series plot of Lake Ngāroto simulated water level (black line) and observed water level (red line).

Inflow water temperature was assumed to be similar to the lake surface temperature. Daily averaged lake surface temperature (0.5 m deep, observed from the lake monitoring buoy) was compared with 9 daily average air temperatures observed at Hamilton airport. The resultant linear fit equation was used to estimate inflow water temperature using meteorological station air temperature observations.

Figure 17. Estimated annual inflow to Lake Ngāroto for the modelling period (dots) and approximate CLUES annual load estimates (red line).

Inflow nutrient concentrations

There are fifteen water quality observations for inflows to Lake Ngāroto. These were taken between December 2006 and September 2007 (Figure 18). The observed variables include nitrate (NO_3-N), dissolved reactive phosphorus (DRP), ammonium (NH_4-N), TN, TP, labile particulate organic nitrogen (PONL), labile particulate organic phosphorus (POPL), labile dissolved organic nitrogen (DONL), and labile dissolved organic nitrogen (DOPL). As these data are limited to less than one year, they are not sufficient to provide a reliable seasonal cycle of concentrations in the inflow. No significant relationships have been established between inflow constituent concentrations and daily discharge volumes (Figure 18).

The inflow nutrient concentration was calculated as follows:

1. The time series of water discharge into the lake was determined by closing the water balance given outflow, precipitation-evaporation and water level boundary conditions;
2. An INCA model was set up for the Ngāroto catchment to estimate daily concentration of TN and TP in the discharge into the lake. This INCA model was calibrated to the observations shown in Figure 18.
3. The other nutrient species were calculated using observed stoichiometry (Table 4).

The resulting time series of nutrient loads and concentrations in the inflow are shown in Figure 20 and Figure 21, respectively. Reasonable matches with the observed average values from the 2006-2007 period were found.

Table 4: Observed mean concentrations of nitrogen and phosphorus compounds in the inflow to Lake Ngāroto. The mean ratio of the phosphorus and nitrogen compounds is calculated relative to TP and TN, respectively; it is used to derive the concentrations of the compounds based on TP and TN concentrations provided by CLUES.

	NO_3-N	**DRP**	**NH_4-N**	**TN**	**TP**	**PONL**	**POPL**	**DOPL**	**DONL**
Observed mean ($g\ m^{-3}$)	0.664	0.022	0.081	2.033	0.111	0.661	0.052	0.050	0.486
Mean ratio	0.281	0.210	0.055	1.000	1.000	0.340	0.443	0.429	0.293

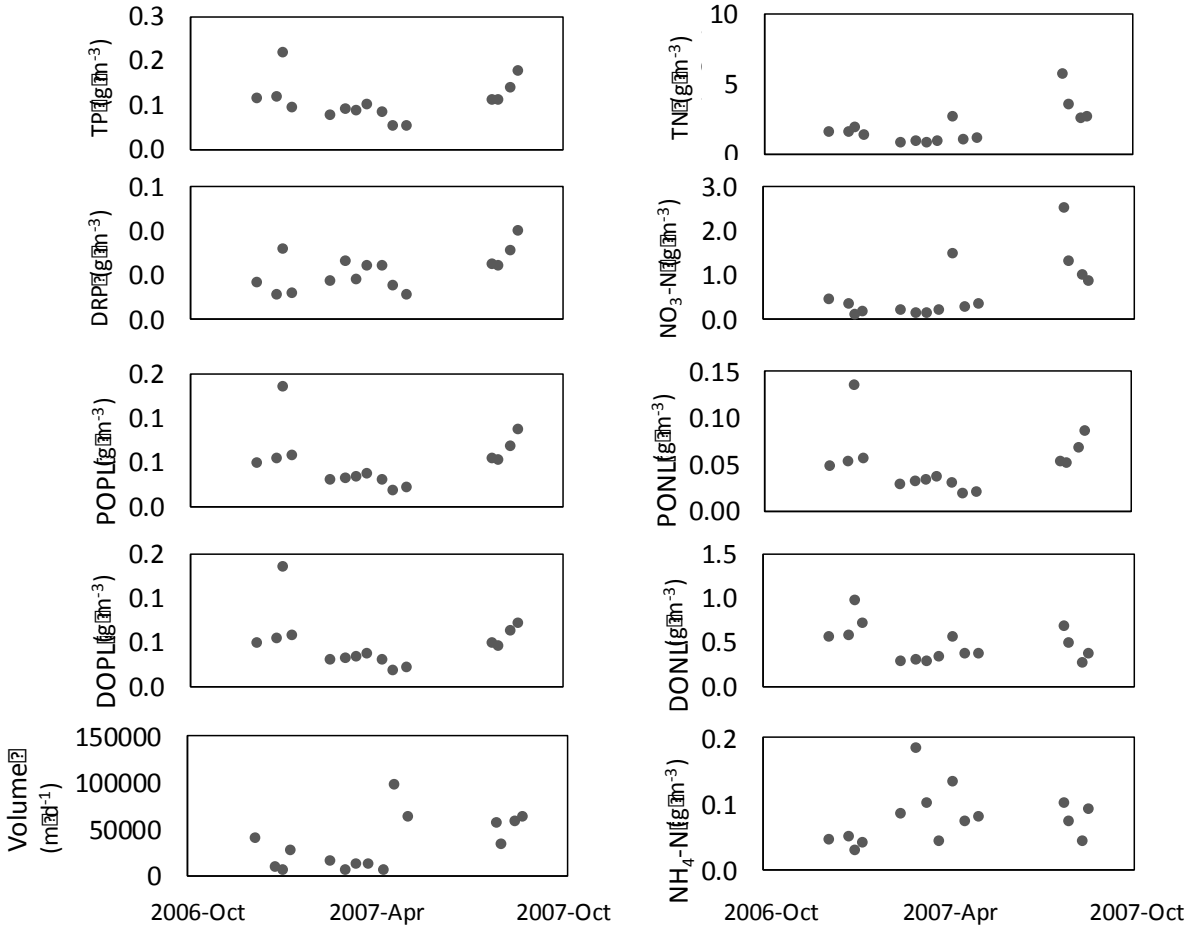

Figure 18: Average inflow nutrient concentrations (observed) and inflow volume (water balance model). Concentrations are given as NO_3-N, DRP and NH_3-N.

Catchment nutrient load

The annual loads of nitrogen and phosphorus to the Lake Ngāroto were derived using CLUES by summing the loads of three reach systems entering the lake (Figure 19) and accounting for the component of the load which is modified by nutrient attenuation by the lake (see catchment model for Lake Rotomānuka). Furthermore, contributions to the lake load from a small portion of the subcatchment associated with the outflow (catchment A in Figure 19, left panel) were also included by pro-rating the load of subcatchment B according to surface area. The total nutrient load to Lake Ngāroto based on this analysis is given in Table 5. The resulting time series of nutrient loads and concentrations in the inflow are shown in Figure 20 and Figure 21, respectively. Reasonable matches with the observed average values from 2006-2007 period (Figure 18) were found.

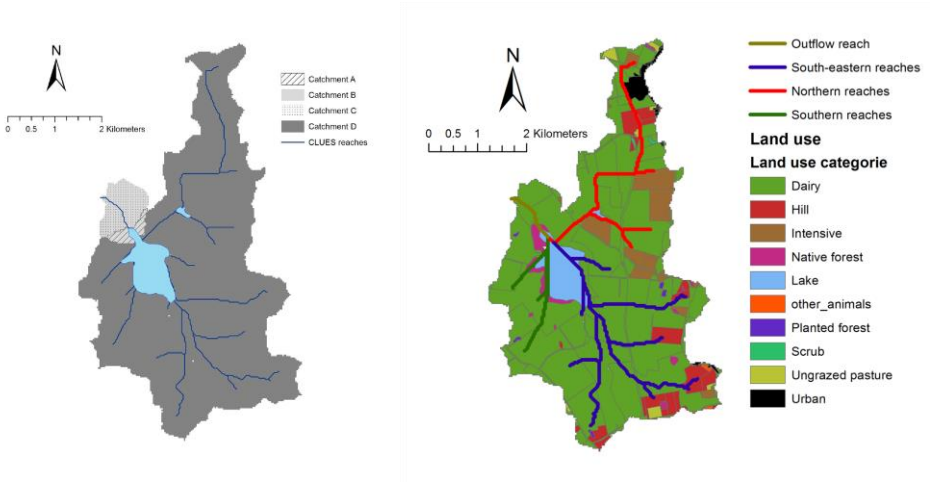

Figure 19: Left: Catchment and reach system of Lake Ngāroto as defined in CLUES. The subcatchment including the outflow (B) is divided into portions A and C. Right: Land use in the catchment of Lake Ngāroto.

Table 5: Lake Ngāroto annual total nitrogen, total phosphorus and suspended sediment (kg ha^{-1} y^{-1}) catchment loads determined from CLUES, with area normalised to lake surface area (88.3 ha).

	Annual load ($kg\ y^{-1}$)	**Area specific annual load** ($kg\ ha^{-1}\ y^{-1}$)
Phosphorus	1,538	17
Nitrogen	26,492	300
Sediments	499,714	5,659

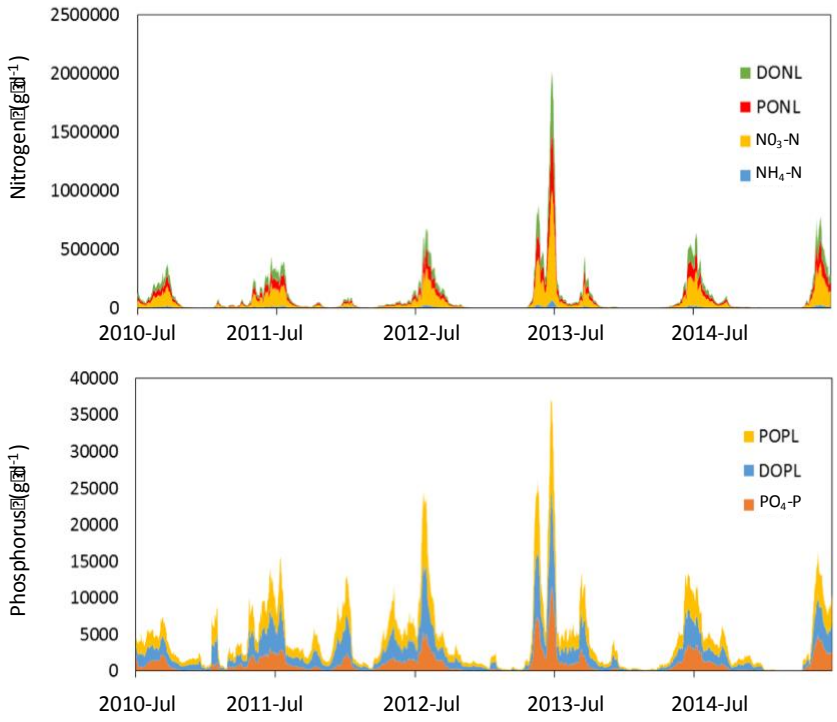

Figure 20: Daily loads of total nutrients in the inflow to Lake Ngāroto modelled using INCA.

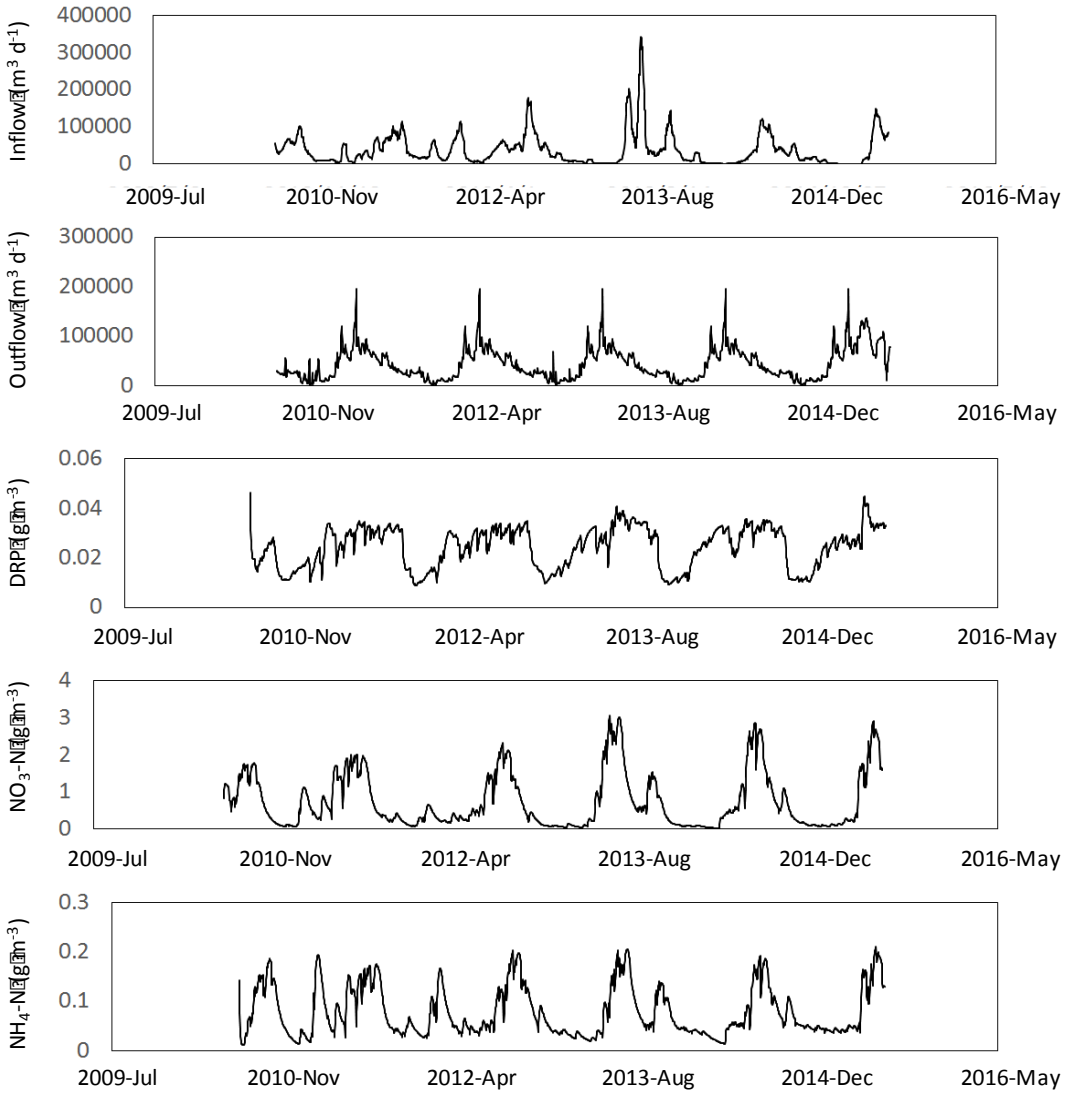

Figure 21: Inflow and outflow water volumes and inflow nutrient concentrations for Lake Ngāroto.

Lake Waahi

Lake Waahi is a shallow (mean depth 2 m), turbid riverine lake associated with the Waikato River and west of Huntly township (Figure 22). The surface area is 522 ha and the catchment area is 9221 ha (Dean-Speirs & Neilson 2014). Lake Waahi was formed within the past 1800 years from deposition of Taupo Pumice Alluvium following the Taupo eruption c. 180 AD (Hamilton *et al.* 2010). The lake receives inflows from a number of sources, the most significant being the Awaroa Stream to the south-east and the Waikokowai Stream to the north-west (Kingett 1984). Discharge is via a single controlled outlet to the Waikato River (Barnes 2002a). A coal haulage road built in 1977 crosses the north-west arm of the lake, and water transfer between the arm and the main body of the lake is restricted (Dean-Speirs & Neilson 2014). Historically, the lake has received diffuse and direct discharge from coal mining, contributing large quantities of sediment and altering the clarity and colour of the lake (Kingett 1984). Land use in the catchment is predominantly dairy and drystock (64%) and is a major contributor to the external load of sediment and nutrients to the lake (Jenkins & Vant 2007).

Lake Waahi supported dense populations of native submerged macrophytes, which were subsequently dominated by invasive exotics such as *Elodea canadensis* by the 1950s. However, following an increase in turbidity during the 1970s and 1980s, likely due to a number of stressors including coal mine discharges, pollution and water level variations, the macrophyte beds collapsed (Ward *et al.* 1987). Elevated inputs of sediment and nutrients from the catchment, as well as wind-induced sediment resuspension, have resulted in high suspended sediment concentrations and phytoplankton biomass in the water column of the lake. These conditions have largely prevented the re-establishment of submerged macrophytes, due to severe light limitation. Recent (i.e., 2008 to 2013) bimonthly monitoring by Waikato Regional Council has shown Secchi depth of between 0.05 m and 1.1 m (average 0.36 m) and chlorophyll *a* concentrations on occasion exceeding 100 mg m^{-3}.

The water quality of Lake Waahi has declined since the collapse of the submerged macrophyte beds in the late 1970s. Current estimated TLI levels indicate that the lake is hypertrophic (Dean-Speirs & Neilson 2014) and within the NOF D-band for TN and chlorophyll *a* and within the C and D-Bands for TP (Figure 23). Lake Waahi has a significant legacy of mining related discharge, particularly with regard to suspended sediment (Dean-Speirs & Neilson 2014) which appears to regularly resuspended due to wind-driven wave action leading to low water clarity and light penetration (Kingett 1984). In addition, the greater catchment of Lake Waahi has been largely developed for agricultural land-use, increasing sediment and nutrient loads to the lake (Hamilton et al. 2010).

Figure 22: Lake Puketirini and Lake Waahi from (a) the northern side (photo: Deniz Özkundakci) and (b) the eastern side, soon after filling of Lake Puketirini. Note the difference in clarity between the two lakes.

Based on Trophic Level Index values (>5.0) and high levels of suspended sediment Lake Waahi is considered supertrophic and highly degraded (Dean-Speirs & Neilson 2014). However, it contains large populations of native fish species, including īnanga (*Galaxias maculatus*), longfin eel (*Anguilla dieffenbachii*), shortfin eel (*Anguilla australis*), common smelt (*Retropinna retropinna*), common bully (*Gobiomorphus cotiadianus*) and grey mullet (*Mugil cephalus*) (Hayes & Rutledge 1991; West *et al.* 2000). Lake Waahi also contains a number of introduced pest fish, such as gambusia (*Gambusia affinis*), catfish (*Ameiurus nebulosus*), koi carp (*Cyprinus carpio*), perch (*Perca fluviatilis*) and goldfish (*Carassius auratus*), which likely contribute to lake degradation through bioturbation and resuspension of bottom sediments, and altering the food web, and may hinder restoration efforts (Collier & Grainger 2015).

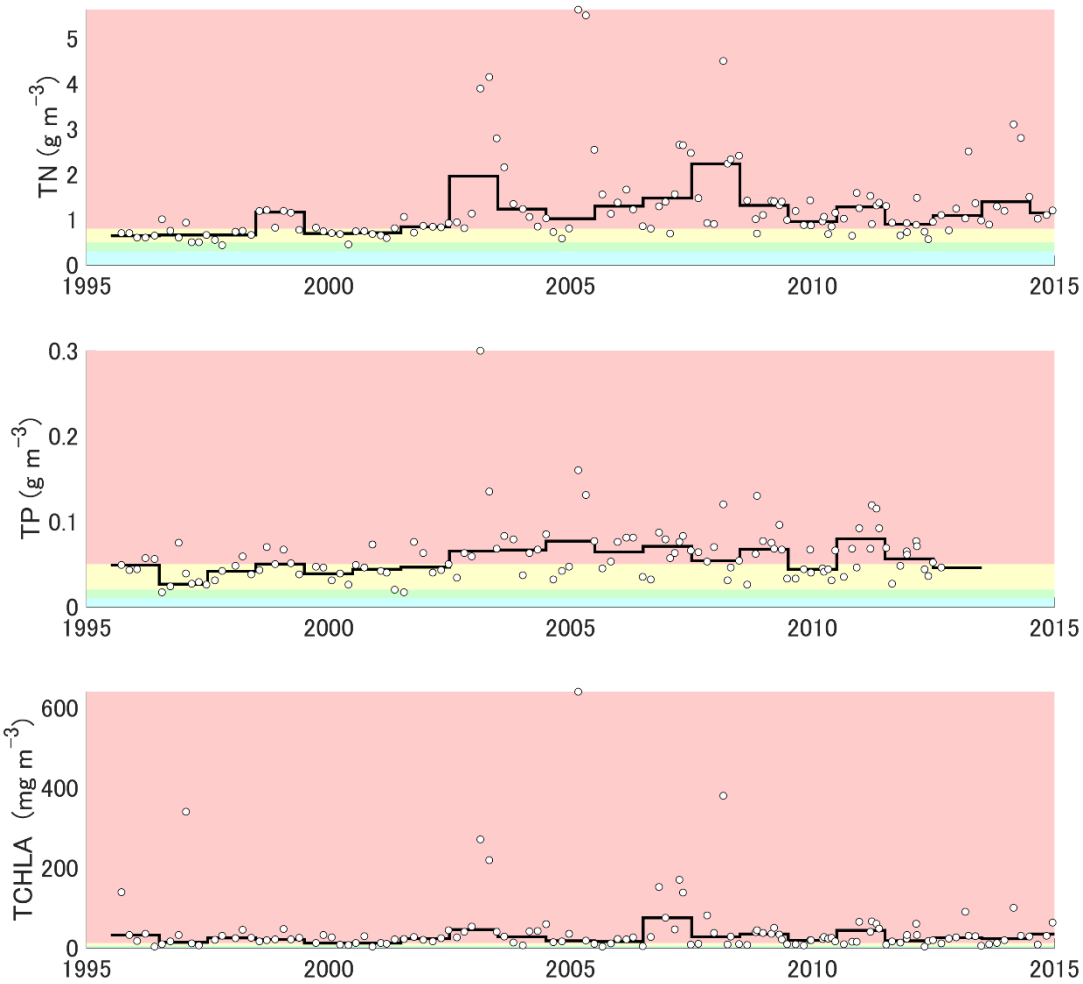

Figure 23: Time series of TP, TN and TCHLA used for calibration of the lake model (white scatter plots) and annual median values in Lake Waahi. The coloured areas show National Objectives Framework (NOF) bands A (light blue), B (light green), C (yellow) and D (red).

Summary of model setup and assumptions

The lake model was run using meteorological forcing from 1 July 2010 to 30 May 2016; water quality observations were available throughout the model simulation period and have been used for calibration. Inflow from a hydrological model and water level observations have been used to close the water balance. The general parameterisation of the DYRESM-CAEDYM model, conceptually common to all lake models in this study, is given in the section *The DYRESM-CAEDYM lake water quality model* and summarised in the (unnumbered) bullets below:

- Vertical processes of biogeochemical variables dominate over horizontal processes such that a 1-D model is sufficiently representative of the whole lake; for example:
    - Horizontal variations in suspended sediments or cyanobacteria populations from wind resuspension or wind-driven accumulations of buoyant cells, respectively, are not captured explicitly.

- Two groups of phytoplankton (parameterised as cyanobacteria and diatoms) are used to capture the seasonal dynamics of planktonic primary producers and to broadly represent phytoplankton that float and sink, respectively;
- Nitrogen fixation by cyanobacteria does not contribute significantly to nitrogen budgets or cyanobacteria dominance;
- Humic compounds (i.e., associated with chromophoric dissolved organic matter) are not modelled;
- pH of the water from catchment discharge is neglected as well as within the lake
- There is no atmospheric deposition of nutrients as this source is considered to be very small compared with catchment inputs;
- Adsorption and desorption of phosphorus to suspended sediments is not modelled explicitly.

Assumptions specific to Lake Waahi are:

1. Water balance derived from TopNet hydrological model and water level requires an additional water inflow which is assumed to have the same nutrient load as stream discharge;
2. There is no backflow from the Waikato River into Lake Waahi;
3. Nutrient loads in inflows are based on observed concentrations;
4. Ruakura met station weather data is applicable (except air temperature);
5. Air temperature forcing is based on an empirical fit between Ruakura met station observations and Waahi lake buoy observations;
6. Temperature of the inflowing water is similar to lake surface water temperature;

In lake observations and model calibration

Bimonthly surface water quality observations (chlorophyll *a* concentration, dissolved reactive phosphorus, ammonium, nitrate-nitrogen, Secchi disk depth, suspended solids, total phosphorus and total nitrogen) were provided by the Waikato Regional Council for the entire modelling period (Figure 23). However, bottom water quality observations were not available for the modelling period. Lake physical observations were rarely available for the earlier modelling period, but high-frequency monitoring buoy observations for surface temperature and dissolved oxygen were available for the calibration from December 2013. The model was calibrated manually using the available data, and results have been plotted against observations for visual assessment.

Hydrology

Lake Waahi discharges via Waahi Stream to the Waikato River. Two rock weirs at each end of the outlet prevent backflow from the river into the lake when river levels are high. In addition, floodgates near the Waahi marae prevent river inflow to the lake during flood events. These gates are regularly maintained and cleared of debris which otherwise might prevent their closure. The only log-jam preventing their closure occurred in 2013 and lasted for less than a day (Philip Ecclestone, WRC, pers. comm., 11 Nov 2016). The flood gate has a 30-cm hole for fish passage, which allows a choke on river water entering Lake Waahi during flood conditions.

Lake surface elevation and discharge are monitored by Waikato Regional Council. Lake hypsography information was adopted from Jones and Hamilton (2014) (Figure 24). Inflow data for Lake Waahi was limited (n=5, green dots in the bottom panel of Figure 26), so time series estimates were sourced from a calibrated TopNet model for Lake Waahi (Zammit 2015). The TopNet discharge was not sufficient to close the water balance while matching the water level. Therefore, TopNet results were increased by the addition of a constant factor on discharge to match CLUES estimates of the average annual inflow (Figure 25). The observed and simulated water levels are shown in the top panel of Figure 26 and the time series of daily in- and outflows used in the model are shown in the bottom panel of Figure 26.

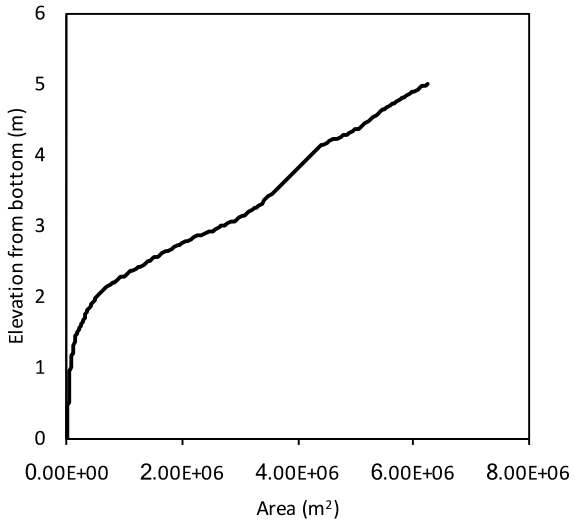

Figure 24: Lake Waahi hypsographic curve (Jones & Hamilton 2014).

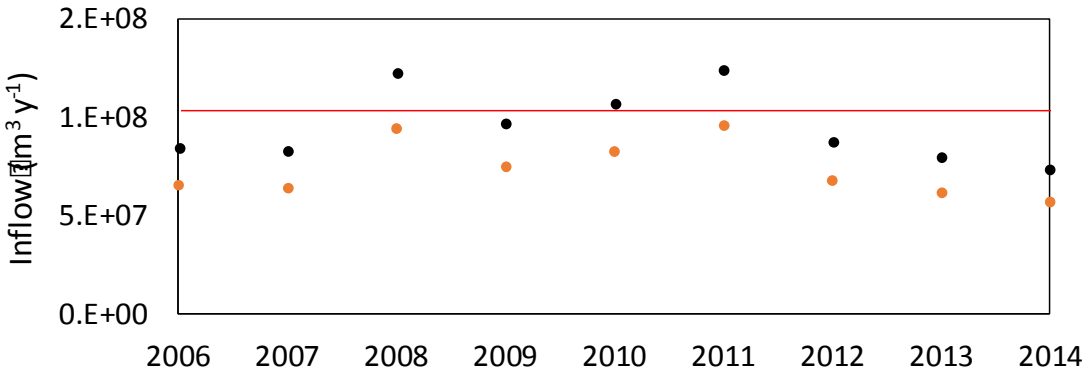

Figure 25: TopNet estimate of the annual inflow volume (orange), adjusted annual loads (black) and CLUES annual load (red) for Lake Waahi.

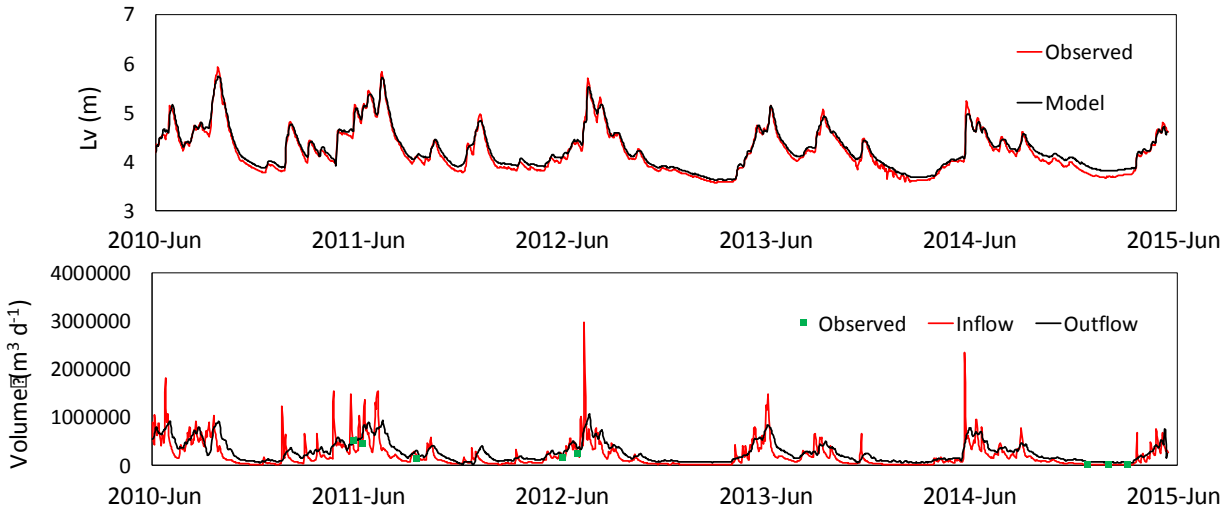

Figure 26: Top: Water level (Lv, m) as observed (red) and DYRESM-CAEDYM model results (black). Bottom: time series of inflow (red) and outflow (black) volumes used to force the model. Green dots represent observed inflow values.

Inflow nutrient concentrations

Air temperature measured at the Ruakura meteorological station was adjusted to Lake Waahi air temperature on the buoy, and used to determine lake surface water temperature, which was then used to define the inflow temperature. The adjustment was based on the relationship between air temperature measured at the Lake Waahi high frequency monitoring buoy and the Ruakura meteorological station data (Figure 27).

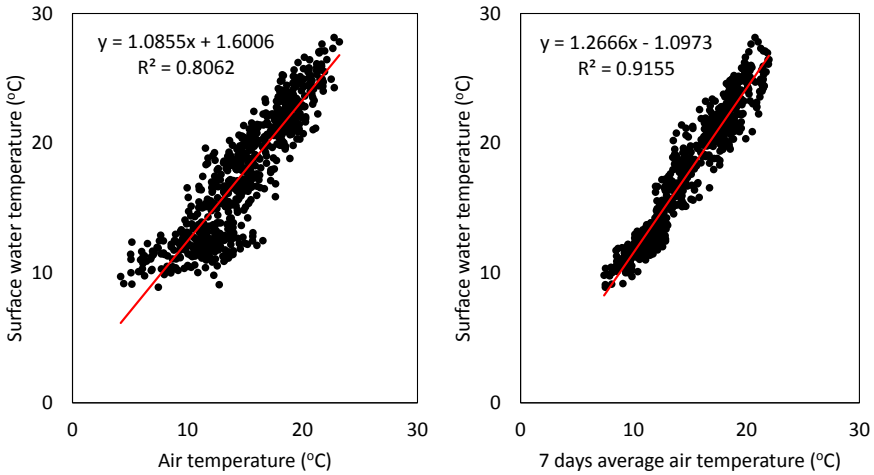

Figure 27: Lake Waahi surface observed temperature and adjusted air temperature at site. This relationship was used to define Lake Waahi inflow water temperature.

Inflow water quality forcing data was primarily taken from the Awaroa Stream monthly monitoring program (Figure 28) but with two exceptions, (1) high frequency inflow water temperatures were estimated using the relationship between the air temperature and lake water surface temperature, and (2) inflow suspended solids concentrations were estimated from monthly inflow black disc observations using the following relationship (West & Scott, 2016):

$$\mathrm{TSS} = \left(\frac{\mathrm{BD}}{4.3}\right)^{\frac{1}{-0.71}}$$

It is noted that the estimated TSS discharge may be biased by the fact that the Awaroa stream contains sediment from mining operations upstream and thus may not be representative of the other discharges to the lake. This may lead to an overestimate of TSS discharge.

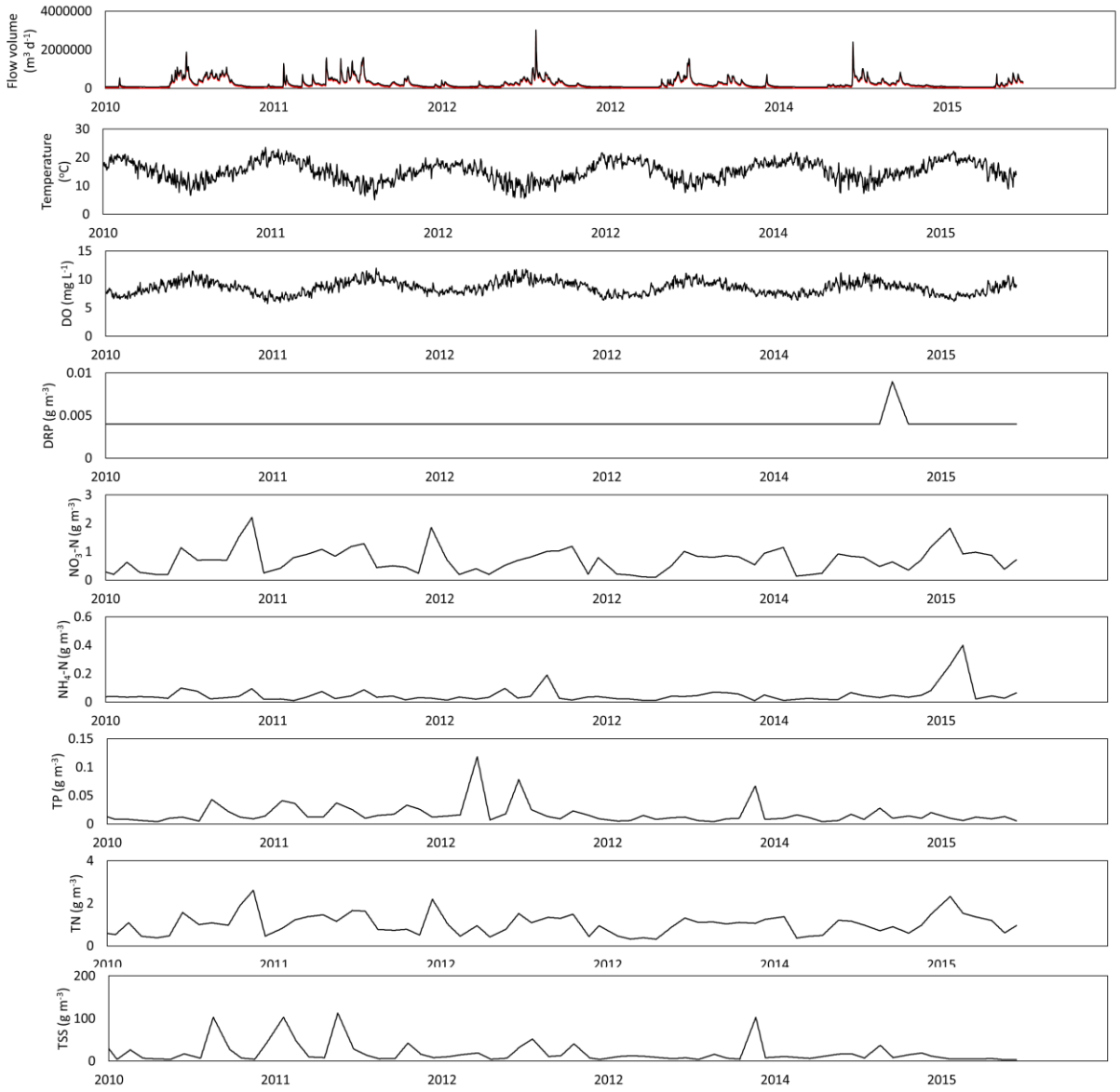

Figure 28: Lake Waahi inflow volume and concentrations of nutrients in the inflow (expressed as concentrations of DRP, NO_3-N and NH_4-N), and outflow.

Lake Rotomānuka

Lake Rotomānuka is 12 km north of Te Awamutu. It has a catchment area of 479 ha which is dominated by pasture for dairy farming. Due to drainage in the eastern and northern catchments, as well as lowering of an outlet channel in 1972, the larger pre-existing lake is now split into two and connected by 41 ha the of marginal wetland (Dean 2015). Rotomānuka North has a surface area of 17.1 ha and a maximum depth of 8.7 m while Rotomānuka South has a surface area of 6.8 ha and a maximum depth of 4.8 m (Figure 29). To the south of Lake Rotomānuka lies the Rotopiko (Serpentine) lake complex, which has been artificially linked to Rotomānuka South (Dean 2015). The wetland therefore forms a hydrological connection of Lake Rotomānuka North to the Rotopiko lakes via Rotomānuka South. The outlet of Rotomānuka North drains this entire system to the northeast (Figure 30).

Figure 29: Photo of Lake Rotomānuka taken from the western side of the lake.

Lake Rotomānuka North is considered to be eutrophic and Lake Rotomānuka South is considered to be hypertrophic by Waikato Regional Council. Historical data suggest that water clarity declined in Lake Rotomānuka North prior to 1998, but there appears to have been little change in the intervening period. One potential cause is a large die-off of oxygen weed (*Egeria densa*) that populated large areas of the lake during the summer of 1996/1997. This die-off resulted in massive plant decomposition and may have contributed to the decline in water quality. In contrast, the more degraded state of Lake Rotomānuka South is likely to be a direct result of contaminants entering the lake from pastoral areas adjacent to the lake. In addition, a major drain that flows into the lake used to receive treated effluent from neighbouring dairy farms (Dean 2015).

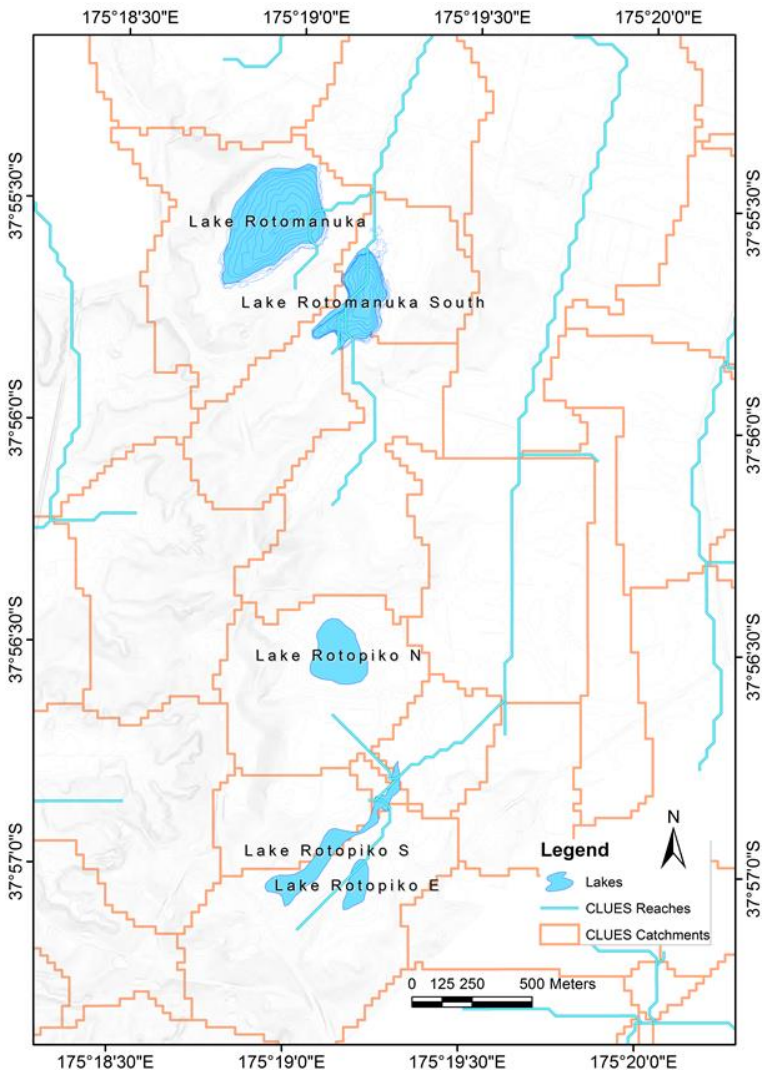

Figure 30: Map of the Rotomānuka-Rotopiko lake system with catchment delineations and stream connections according to CLUES.

Drainage of the peat land surrounding the Rotomānuka and Rotopiko lake complex has resulted in compaction of the peat soils and lowering of lake levels (Stockdale 1995). Historically, Rotomānuka North was contiguous with Rotomānuka South, however lower lake levels have resulted in the formation of an isthmus between the two lakes which is over-topped annually during the winter during heavy rainfall. The isthmus appears to form a natural wetland, possibly reducing sediment and nutrient loads to Rotomānuka North from Rotomānuka South. Rotomānuka North is currently classified as eutrophic and while monitoring data for Rotomānuka South is fragmented, it was assessed as hypertrophic when it was last assessed in 2001 (Dean-Spears and Neilson 2014). Assessment of NOF limits indicate that Rotomānuka North is within the D-band for TN and C-Band for TP and chlorophyll *a* (Figure 31). In addition, the local catchment for Rotomānuka North is comparatively small (<60 ha) for the size of the lake, and the catchment land-use is low-intensity agriculture or urban. When coupled with the depth of the lake (8.2 m) and the protective hills to the

west, sheltering the lake from the prevailing westerly winds the lake bed is unlikely to be subject to substantial sediment resuspension, unlike the other lakes described in this study but is much more likely to become thermally stratified for periods during summer.

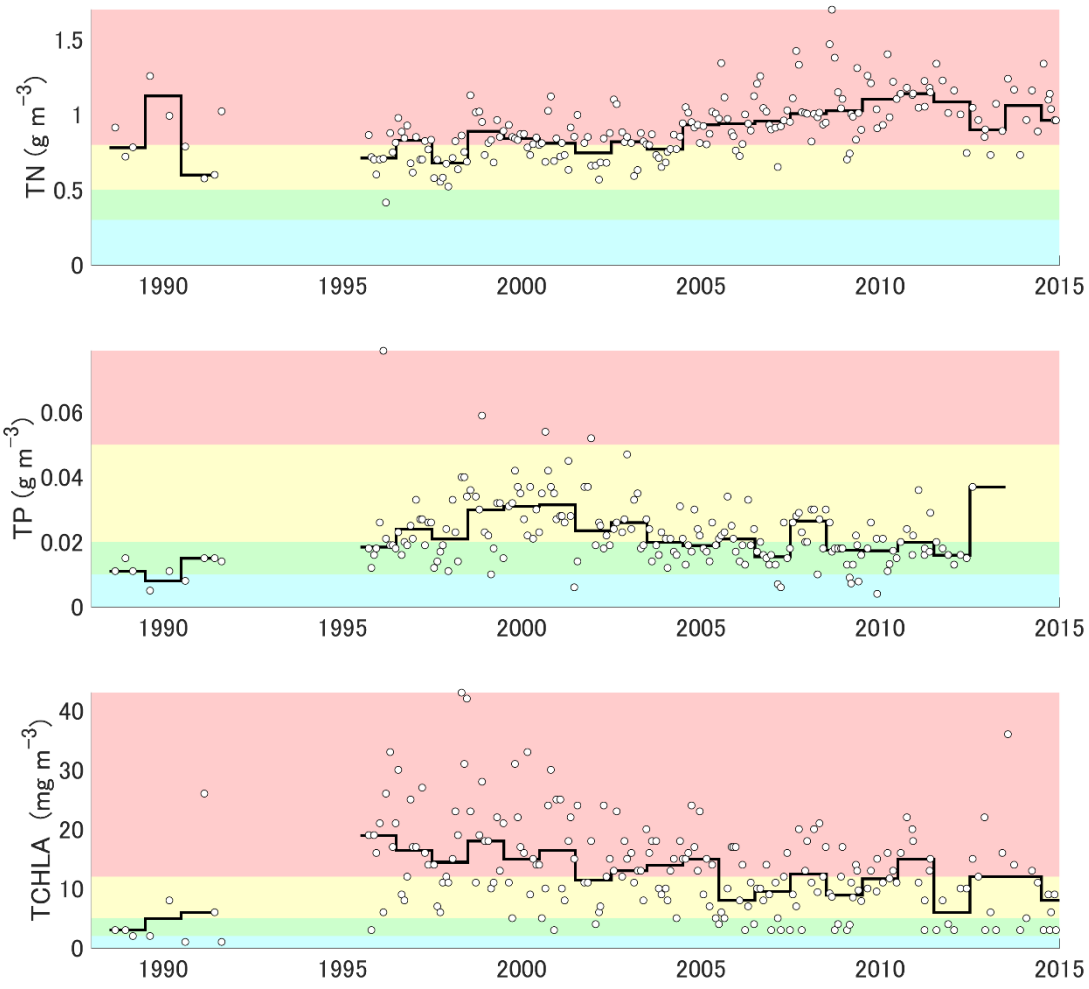

Figure 31: Time series of TP, TN and TCHLA used for calibration of the Lake Rotomānuka model. The coloured areas show National Objectives Framework (NOF) bands A (light blue), B (light green), C (yellow) and D (red).

A fish survey of Lake Rotomānuka in 2001 found that there were 21 native and four invasive fish species (Speirs & Barnes 2002). Goldfish (*Carassius auratus*) were not found during the 2001 fish survey but were present in 1983, indicating that they may be present in low numbers or absent from the lake. The 2001 survey found rudd (*Scardinius erythrophthalmus*), which are known for their detrimental impact on native submerged macrophytes. Lake Rotomānuka contains healthy populations of common smelt that are genetically distinct from the Waikato River smelt, likely due to the landlocked nature of the lake.

This study considers water quality in Rotomānuka North. Inflow into Rotomānuka North from Rotomānuka South and the connection to the Rotopiko lakes are parameterised as described in the section Catchment model, below.

Summary of model setup and assumptions

The model is run using meteorological forcing from 1 July 2010 to 30 May 2016; water quality observations are available throughout the model simulation period and are used for model calibration. The water balance in this system is complicated and relies on a number of assumptions regarding the volume of flows into the lake and the source of the inflows. Most of these assumptions are not supported by observations.

The general parameterisation of the DYRESM-CAEDYM model common to all lake models in this study is given in the section *The DYRESM-CAEDYM lake water quality model* and summarised in the (unnumbered) bullets below:

- Vertical processes of biogeochemical variables dominate over horizontal processes such that a 1-D model is sufficiently representative of the whole lake; for example:
    - Horizontal variations in suspended sediments or cyanobacteria populations from wind resuspension or wind-driven accumulations of buoyant cells, respectively, are not captured explicitly.
- Two groups of phytoplankton (parameterised as cyanobacteria and diatoms) are used to capture the seasonal dynamics of primary producers and to broadly represent phytoplankton that float and sink, respectively;
- Nitrogen fixation by cyanobacteria does not contribute significantly to whole-lake nitrogen or cyanobacteria dominance;
- Humic compounds (i.e., associated with chromophoric dissolved organic matter) are not modelled;
- pH of the water from catchment discharge is neglected as well as within the lake
- There is no atmospheric deposition of nutrients as this source will be very small in relation to the catchment inputs;
- Adsorption and desorption of phosphorus to suspended sediments is not modelled explicitly.

Assumptions specific to Lake Rotomānuka are:

1. The water level record of Lake Rotomānuka contains gaps which are filled using a statistical relationship with water level records in Lake Rotopiko East;
2. Two types of inflows exist: runoff from the small catchment immediately surrounding the lake and seepage through the wetland between Rotomānuka North to Rotomānuka South;
    - The catchment directly surrounding Lake Rotomānuka North is small and it discharges into the lake only via ephemeral drainage ditches and perhaps surface water runoff;
    - The catchment of Rotomānuka South is connected to the Rotopiko lakes catchment and thus, a hydrological connection exists between Rotomānuka North and the Rotopiko lakes.
3. The flow volume through the wetland is determined as the residual of the water balance calculated from outflow volume and water level of Lake Rotomānuka North;
4. The wetland removes 20% of total phosphorus and 40% of total nitrogen from the discharge to it and ultimately into Lake Rotomānuka;
5. All nutrient concentrations in the inflows are derived from CLUES and have been disaggregated into daily values using INCA;
6. Hamilton airport weather, i.e., meteorological forcing, is applicable to Lake Ngāroto (except air temperature);
7. Air temperature forcing is based on an empirical fit between Hamilton airport observations and lake buoy observations;
8. Temperature of the inflowing water is similar to lake surface water temperature;
9. Sediment resuspension is not included in the model due to the depth of the lake, which would preclude this process from occurring.

In-lake data for model calibration

Water quality samples and vertical profiles of temperature and DO have been collected at regular intervals of 1-2 months by WRC. Data obtained for this study are listed in Table 6, and time series of TP, TN and TCHLA used in the calibration of the Rotomānuka model are presented in Figure 31.

Table 6: Data for Lake Rotomānuka obtained for this study.

Measurement type	**Detail**	**Variables**	**Time period**	**Frequency**	**No. measurements**
Discharges	WRC outflow temperature	Temperature (°C)	Sep 2011 - Dec 2015	On average 15 minutes (2-20 minutes)	325037
	WRC outflow rating curve	Discharge ($m^3 s^{-1}$) at water level elevation (m)	n/a	n/a	n/a
Water Level	Water Level at outlet	Water Level (m)	Jul/Aug 2006 Sept 2011 - Dec 2015 (6 data gaps)	5 minutes	292248
Vertical profiles	WRC water quality monitoring	DO (mg L^{-1}) and Temperature	Jan 2005 - Jan 2016	Approx. monthly	1598 each (DO and Temp)
	CTD casts as part of this study	Temp, DO, Conductivity, Fluorescence, Beam attenuation, PAR	March - July 2016	9 bi-weekly samples	9 High-res profiles
Water quality samples	WRC water quality monitoring	TCHLA, NH_4-N, NO_3-N, DRP, TSS, TN, TP, Secchi depth, pH	Jan 2005 - Jan 2016	Approx. one sample per month from at least one depth	
	Water samples as part of this study	TCHLA, NH_4-N, NO_3-N, DRP, TN, TP, TSS, Secchi	March - July 2016	9 bi-weekly samples	Samples from 0.5 m and 8 m from surface
Inflow monitoring	As part of this study	Discharge, NH_4-N, NO_3-N, DRP, TN, TP, TSS	March - July 2016	5 samples, when inflow observed	
Fish		Fish catch data	3/11/2015	Single-day set net	
Bathymetry		Contour shapefiles			

Hydrology

The hypsographic curve for the lake model is shown in Figure 32. A water level gauge installed in Lake Rotomānuka provides useful data for calculating the water balance used to derive volumetric inputs to the lake model. The level gauge is installed at 49.760 m Moturiki datum. Discharge from Lake Rotomānuka was calculated using the flow rating curve presented in Figure 33. However, the water level time series contains a number of gaps when the level gauge was above the water level (Figure 34).

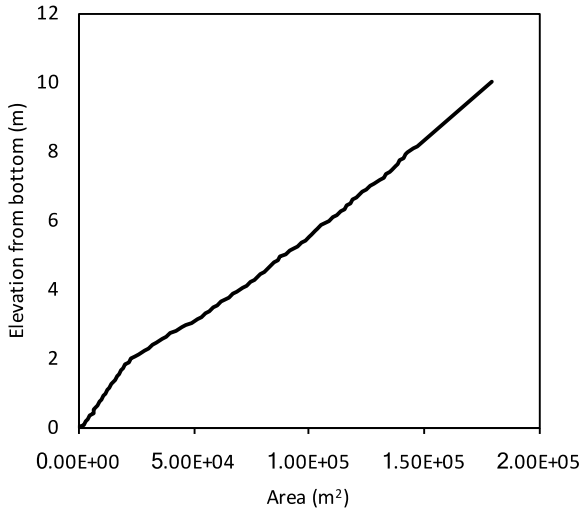

Figure 32: Hypsographic curve for Lake Rotomānuka.

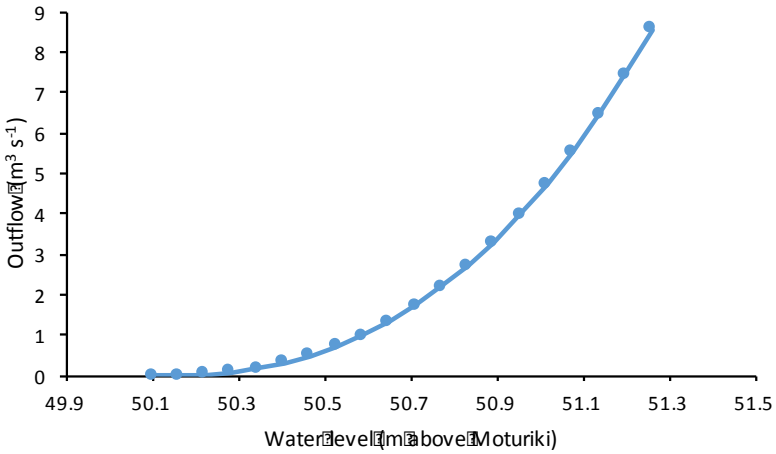

Figure 33: Flow rating curve for Lake Rotomānuka.

Water level observations also exist for the three Rotopiko lakes, and these provide a semi-continuous record over the simulation period (Figure 34). The relationship between Rotopiko East and Rotomānuka water levels was described statistically using a piecewise linear regression with three segments (Figure 35). This model is used to predict the water level in Rotomānuka during times of missing observations (Figure 36).

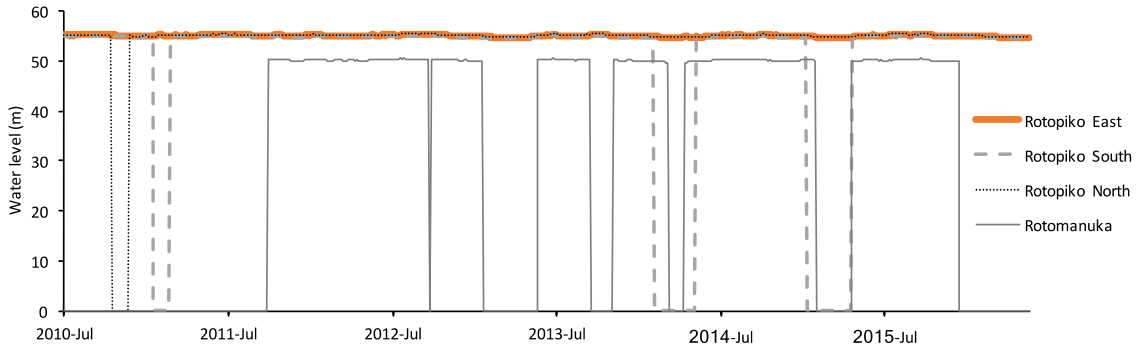

Figure 34: Water levels relative to Moturiki datum of Lake Rotomānuka and three Rotopiko lakes. Gaps in the time series are shown as zero values.

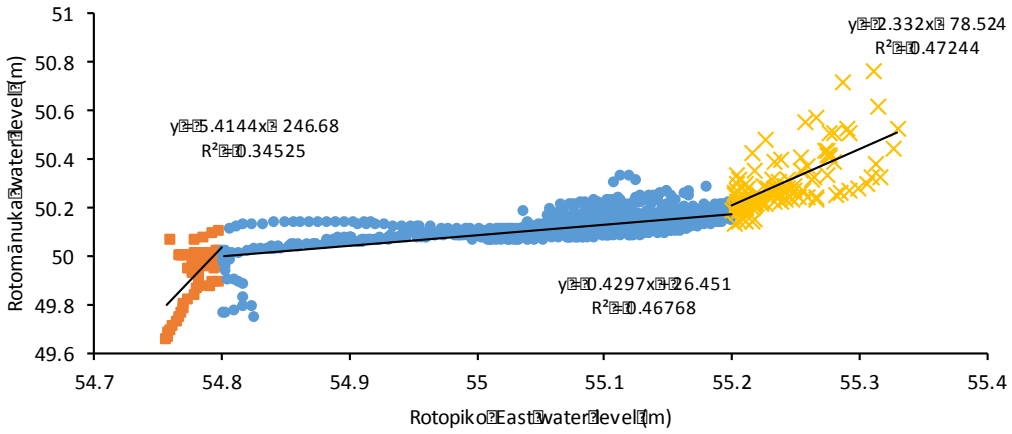

Figure 35: Scatterplot of water levels observed in lakes Rotopiko East and Rotomānuka showing a piecewise linear regression model applied to three segments of the water levels.

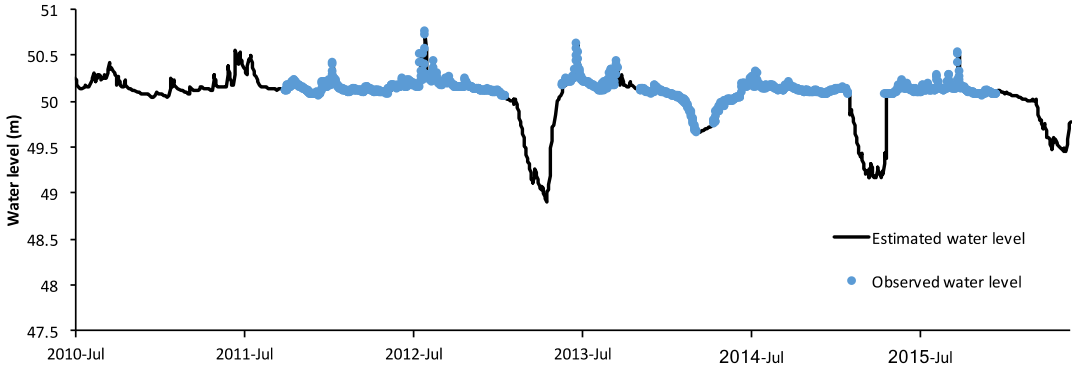

Figure 36: Observed water level in Lake Rotomānuka, with gaps filled using the piecewise linear model of Lake Rotopiko East.

Rotomānuka maximum depth and vertical datum

A bathymetric survey was conducted in lakes Rotomānuka North and South on 28 Feb 2014 (de Winton *et al.* 2014). The bathymetry in this survey is provided as depths from the water surface only. On that, day there was no data from the water level logger and thus the depth measurements cannot be tied to a vertical datum. The depth gauge was not recording, presumably because the water level was below the operational limit for the instrument.

The survey found a maximum depth of 8.31 m in the central basin of Lake Rotomānuka. The lake has been previously reported to have a maximum depth of 8.7 m. According to our water level model (based on a regression relationship with water levels in Rotopiko East), the water level elevation on the day of the survey was 49.741 m (above Moturiki datum). This level was used to tie the bathymetric measurements into the vertical datum. We set the elevation of the deepest point of the lake at 49.741 - 8.31 m = 41.431 m (above Moturiki datum).

Inflow nutrient concentrations

To the best of our knowledge, there are no observations of discharges or nutrient loads into Lake Rotomānuka so CLUES was used to provide estimates of nutrient loads to the lake. In CLUES, the Rotomānuka and Rotopiko catchment complexes are not hydrologically linked and therefore, a recalculation of the CLUES loads was conducted to estimate the nutrients entering Rotomānuka North the Rotopiko region.

The approach and assumptions for catchment modelling of Lake Rotomānuka is as follows:

1. Total discharge into Lake Rotomānuka was made up of two components which were determined independently:
    a. Discharge from the catchment immediately surrounding Rotomānuka, but excluding the wetland between Rotomānuka North and Rotomānuka South, was determined using INCA; and
    b. Discharge through the wetland between Rotomānuka North and Rotomānuka South, was determined through water-balance closure calculations.
2. Nutrient loads in both discharges into Lake Rotomānuka were determined from CLUES annual loads which were disaggregated to daily loads using the discharges from the INCA model, i.e., the INCA model was used to distribute annual loads to daily loads which are the unit of input for the lake water quality model.
3. The flow into Rotomānuka North through the wetland was from Rotomānuka South only and the wetland is assumed to be the only hydrological connection between the two lakes.

4. The entire discharge from the Rotopiko Lakes (denoted by B in Figure 37) and a third subcatchment (denoted C) was routed to Rotomānuka South.
5. Nutrient attenuation by the Rotopiko lakes was calculated adequately within CLUES.
6. Nutrient loads from B+C in Figure 37 were reduced by attenuation in Rotomānuka South according to CLUES methodology (P. Verburg, pers. comm.).
7. Nutrient loads to the wetland from Rotomānuka South were calculated in the same proportion as the ratio of total discharge; (A+B+C)/wetland discharge = 0.283.
8. The wetland attenuates nutrients flowing into Rotomānuka from Rotomānuka South by 40% for nitrogen and 20% for phosphorus. Sensitivity of the model simulation output to uncertainty in wetland attenuation is addressed by simulating two other scenarios:
    a. 0% N and 0% P; and
    b. 80% N and 40% P.
9. The catchment delineations used for this study were taken from CLUES.

The approach used for to connect the components of the Lake Rotomānuka North system is illustrated in Figure 38.

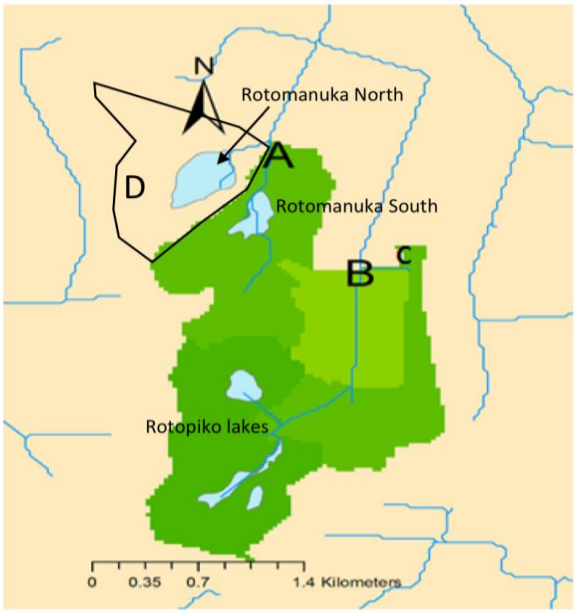

Figure 37: Catchments of the Rotomānuka and Serpentine lakes as implemented in CLUES.

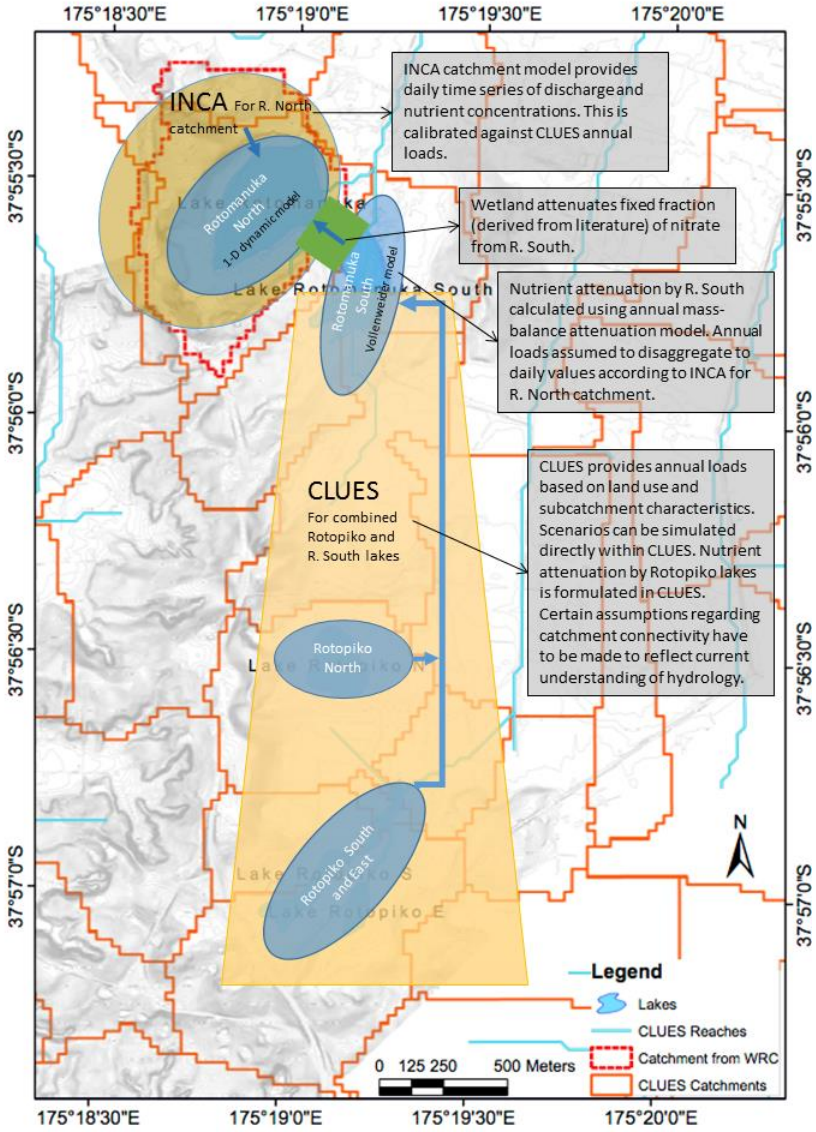

Figure 38: Diagram illustrating the components of the Lake Rotomānuka catchment diagram.

Nutrient load from Lake Rotomānuka South

We used CLUES results to calculate total nutrient loads out of Lake Rotomānuka South. A fraction of this load goes to Lake Rotomānuka North via the wetland and the remaining fraction flows directly to the discharge (away from the system).

Due to the CLUES' catchment setup, the real Lake Rotomānuka South outlet load is a combination of CLUES Lake Rotomānuka South outlet values (Catchment A) and CLUES Rotopiko Lakes catchment outlet values (Catchments B & C) as illustrated in Figure 37.

Catchment A loads: CLUES was used to define Rotomānuka South catchment outflow, including in-lake nutrient attenuation in Rotomānuka South.

Catchments B & C loads: Lake Rotopiko catchment loads do not include Lake Rotomānuka South in-lake attenuation. This attenuation was applied according to CLUES methodology as outlined below (P. Verburg, pers. comm.).

Lake attenuation calculation:
external load = outflow load*(1+KRES/RESLOAD)

where KRES is a settling parameter (P: 36.1 m y^{-1}; N: 7.46 m y^{-1}) * and RESLOAD is the lake hydraulic overflow rate, i.e., the discharge rate divided by the lake area (m y^{-1}).

RESLOAD = [Discharges A + B + C] (m^3/y) / 61165.4 (m^2)

Therefore,
Rotomānuka South outflow load

= [(Lake South Catchment Load B+C) / (1+KRES/RESLOAD)] + (Catchment A load)

Nutrient load from Rotomānuka South to the wetland

Part of the nutrient load exiting Rotomānuka South flows into Rotomānuka North (through the wetland) and the remainder is considered to be outside of the system of interest. This section describes the method used to determine the fraction of the total nutrient load from Rotomānuka South to the wetland.

Example for nitrogen species

(1) Calculate the proportion of the seepage discharge relative to the total discharge from Lake Rotomānuka South:

Annual seepage [2] / Annual total discharge from Rotomānuka South (i.e., CLUES annual discharge from Catchments A, B and C)

= 28.3%

(2) Total N load for simulation period (2151 days = 5.89 yr) via seepage

= 0.283 x TN load from CLUES Catchments ABC x 5.89
= 3.85 t / 5.89 yr

Disaggregating annual loads to daily loads

The daily concentration of nutrients in the flow to the wetland ($TN^{wetl}(i)$) before wetland attenuation is calculated by disaggregating the total load determined in [4] to a daily load. The daily variability is provided by the INCA simulation for the Rotomānuka North catchment. Details of the method using total nitrogen as an example are shown below:

p: ratio between INCA concentration and residual inflow concentration

TN^t : Total TN load into the wetland for simulated period (t): 3.85 t

$TN^{INCA}(i)$: concentration of TN on day *i* (g/m^3) for INCA flow

Ratio(*i*): concentration ratio of TN on day *i* (dimensionless) for INCA flow

$$Ratio(i) = \frac{TN^{INCA}(i)}{\sum_{i=1}^{2151\ days} TN^{INCA}(i)}$$

$TN^d(i)$: daily load to the wetland of TN on day *i* (g/d)

$TN^{wetl}(i)$: concentration of TN on day *i* (g/m^3) for residual flow

Q(*i*): Daily residual flow rate (m^3/d)

$$TN^{wetl}(i) = p \times TN^{INCA}(i)$$

$$TN^{INCA}(i) = Ratio(i) \times \sum_{i=1}^{2151\ days} TN^{INCA}(i) = Ratio(i) \times 2684.45$$

$$TN^{wetl}(i) = p \times TN^{INCA}(i) = p \times Ratio(i) \times 2684.45$$

$$TN^t = \sum_{i=1}^{2151 days} TN^d(i) = 3.85\ t$$

$$TN^d(i) = TN^{wetl}(i) \times Q(i) = \{p \times Ratio(i) \times 2684.45\} \times Q(i)$$

$$TN^t = \sum_{i=1}^{2151 days} TN^d(i) = \sum_{i=1}^{2151 days} \{p \times Ratio(i) \times 2684.45 \times Q(i)\}$$

$$= p \times 2684.45 \sum_{i=1}^{2151 days} \{Ratio(i) \times Q(i)\}$$

$$\sum_{i=1}^{2151 days} \{Ratio(i) \times Q(i)\} = 0.002745$$

$$TN^t = 3.85\ t = p \times 2684.45 \times 0.002745$$

$$p = 0.5218$$

The resultant inflow and outflow are shown in Figure 39.

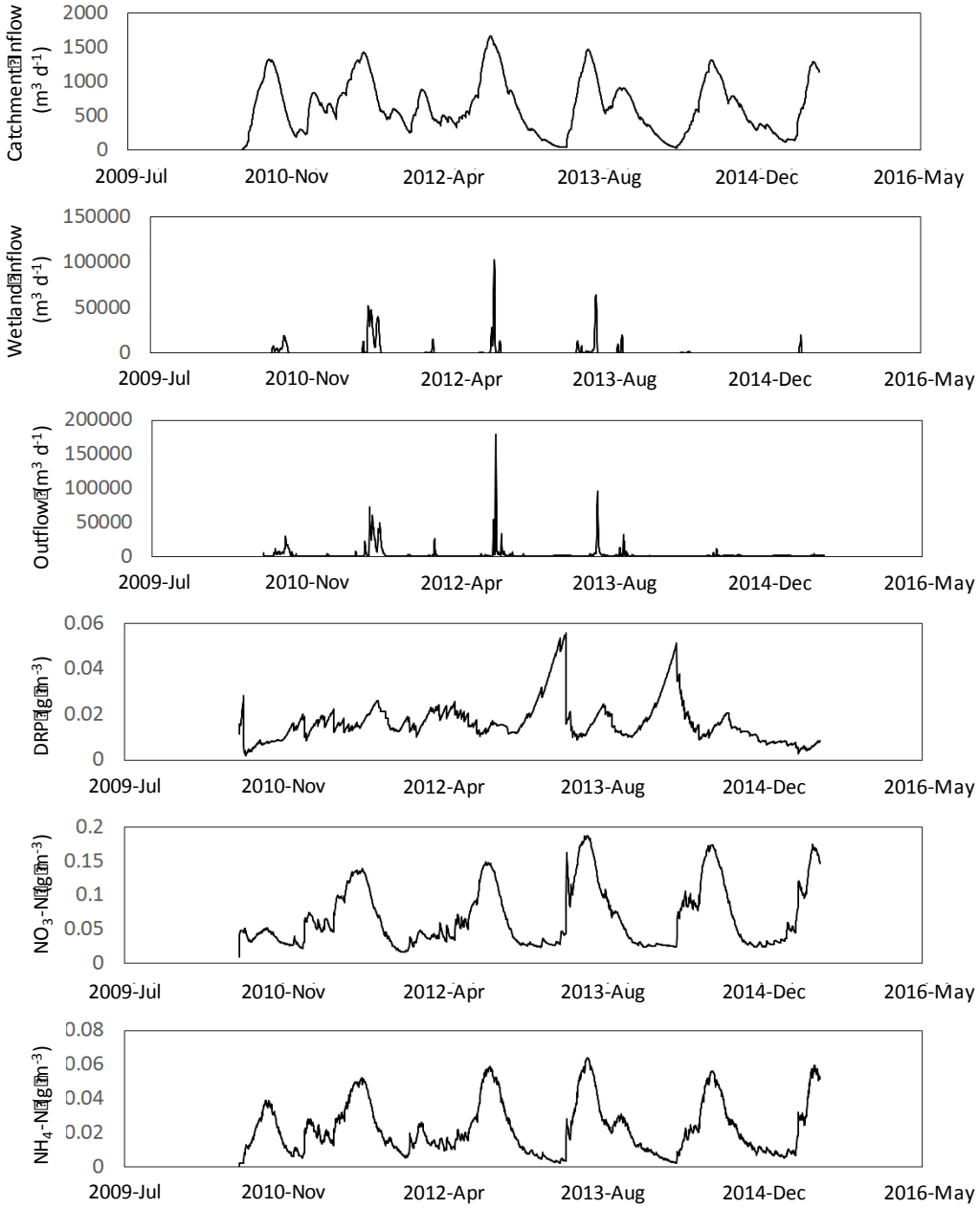

Figure 39: Inflows and outflows for Lake Rotomānuka. Nutrient concentrations are given as DRP, NO_3-N and NH_4-N.

Wetland nutrient attenuation scenarios

The modelling team and the steering committee agreed on the following wetland attenuation scenarios:

Base scenario

TP reduction due to wetland: 20%

TN reduction due to wetland: 40%

No removal scenario

TP reduction due to wetland: 0%

TN reduction due to wetland: 0%

High removal scenario

TP reduction due to wetland: 40%

TN reduction due to wetland: 80%

Catchment D: INCA

We established INCA-N and INCA-P models for the catchment immediately surrounding Lake Rotomānuka (catchment D in Figure 37) for the period from 1 July 2010 to 30 May 2016 using daily time steps. Catchment boundaries, land use percentages and reach characteristics were taken from CLUES version 10 (Table 7).

No validation of the INCA model application to Lake Rotomānuka was possible due to the absence of monitoring data. The year 2010 was considered as a 'warm up' period to eliminate initial bias caused by estimation errors in initial conditions. Inflows were assumed to be predominantly sub-surface. Model parameters were adjusted manually using a trial and error approach with values set to within literature ranges. The model was driven by meteorological variables consisting of air temperature, actual precipitation, soil moisture deficit, evapotranspiration and hydraulic effective rainfall (HER) as shown in Figure 4. Air temperature, actual precipitation, soil moisture deficit and evapotranspiration were sourced from www.niwa.co.nz/cliflo, and hydrologically effective rainfall (HER) was calculated based on (Rankinen *et al.* 2002) as

$$HER = (P + M) – ET – \Delta S$$

where P is precipitation, M is snowmelt (not applicable), ET is evapotranspiration and S is soil water storage. These are direct output variables from www.niwa.co.nz/cliflo . The INCA model was set up

for subsurface flows only to reflect observations of lack of surface streams and the presence of only low flow rates in drains, even during wet periods.

Table 7: Land use in Rotomānuka catchment D from CLUES.

Land use type	**Area (ha)**	**Proportion of total**
Dry stock	29.16	0.61
Dairy	15.98	0.29
Urban	5.44	0.10

Lake Waikare

Lake Waikare is south-east of Te Kauwhata Township and is the largest lake in the lower Waikato catchment, with 3442 ha of open water. It has an average depth of 1.5 m and a maximum depth of 1.8 m. The lake receives inflows from a number of sources including the Waikato River via the Te Onetea Stream which acts as a flood storage reservoir within the Lower Waikato Waipa Flood Control Scheme. As part of this scheme the lake level was lowered by 1 m in 1965 and water now discharges from the lake into the Whangamarino River via the Pungarehu Canal (Dean-Speirs & Neilson 2014). Another major inflow is the Matahuru Stream which drains a large sub-catchment known to generate high amounts of sediment. This sediment is likely to be resuspended in the extensive shallow areas of the lake. The suspended sediment also represents a major issue in contributing to high rates of sedimentation in the Whangamarino wetland. Lake Waikare has poor water quality, high levels of inorganic suspended solids and is classified as hypertrophic.

In early botanical surveys of the 1870s, Lake Waikare appears to have had native aquatic plants (Hamilton *et al.* 2010) but an aerial photograph suggests that lake water was turbid by the 1940s, likely due to effects of clearance and development in the catchment. However, soon after there is some suggestion of cycling between collapse and recovery of the macrophyte beds (aided by more robust invasive species such as *Ceratophyllum demersum*) until complete loss of the submerged macrophytes in 1977/78 (Reeves et al. 2002). In 1965, lowering the water level by 1 m for flood control resulted in a major loss of the surrounding wetland habitat. Council has measured lake water quality (TN, TP and Chlorophyll *a*) with annual median values shown in Figure 40.

Apart from Lake Ellesmere (Te Waihora), Lake Waikare is the most heavily degraded large lake in New Zealand (Verburg et al. 2010). The current trophic status for Lake Waikare is hypertrophic (Dean-Spears and Neilson, 2014) and TN, TP and chlorophyll *a* levels are all within the NOF D-band (Figure 36). Algal blooms now persist throughout the year, which in association with high turbidity levels, restricts light penetration to the bottom of the lake and prevents submerged macrophyte establishment. In addition, the shallow water level (1.8 m) and large wind fetch distance exacerbates wind resuspension of sediment, adding to suspended sediment and nutrient loads contributed from the catchment. Lake Waikare also contains significant populations of catfish, koi, carp and goldfish which have been shown to contribute to sediment resuspension and nutrient cycling (Collier & Grainger 2015).

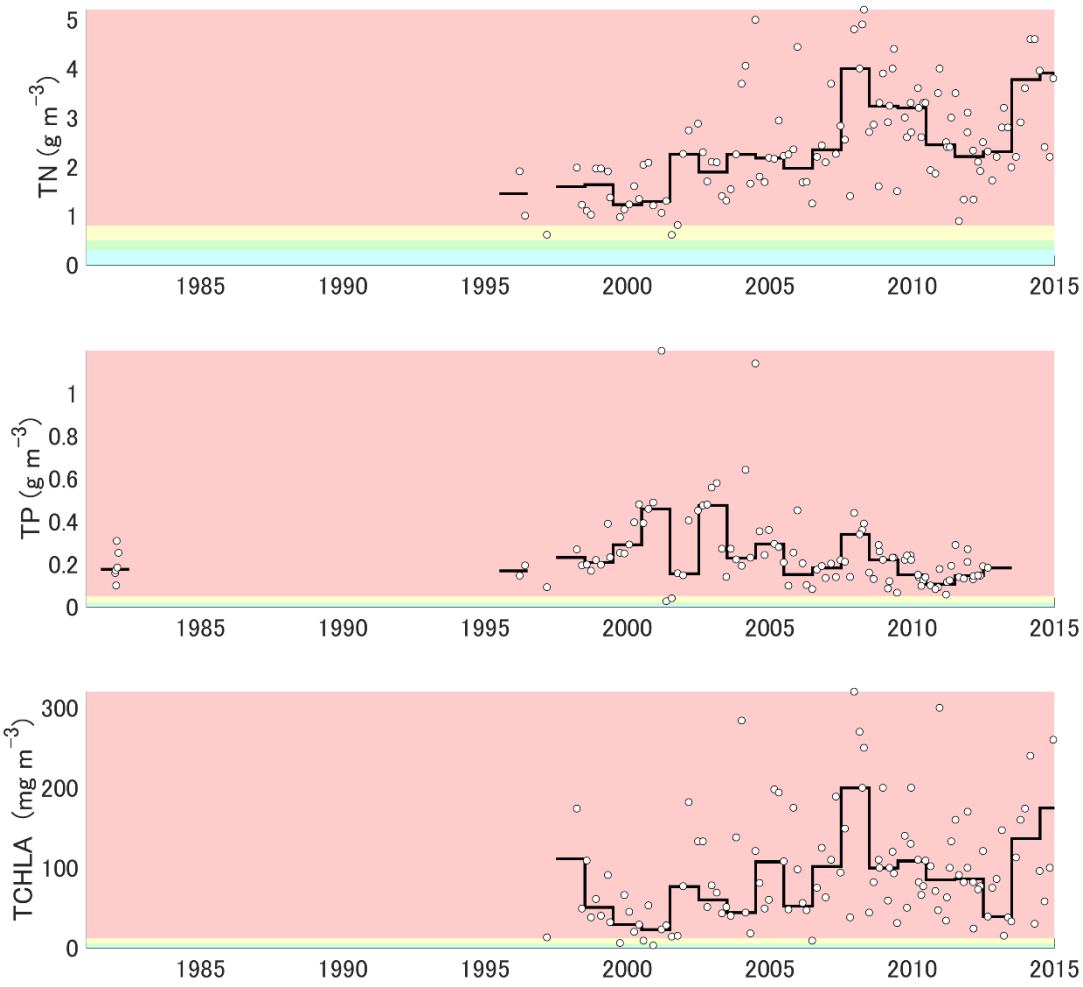

Figure 40: Time series of TP, TN and TCHLA observed in the lake (white scatter plots) and annual median values in Lake Waikare. The coloured areas show National Objectives Framework (NOF) bands A (light blue), B (light green), C (yellow) and D (red).

Inflow nutrient concentrations

An INCA model was established and calibrated for the entire catchment of Lake Waikare for the period 1 July 2012 to 20 May 2016 using a daily time step. Meteorological inputs were obtained from the Virtual Climate Network (NIWA; obtained by license thorough the Waikato River Authority) and are shown in Figure 41. Hydraulically effective rainfall (*HER*) was calculated based on (Rankinen *et al.* 2002) as $HER = (P + M) - ET - \Delta S$ where P is liquid precipitation, M is snowmelt (not applicable), ET is evapotranspiration and ΔS is soil water storage.

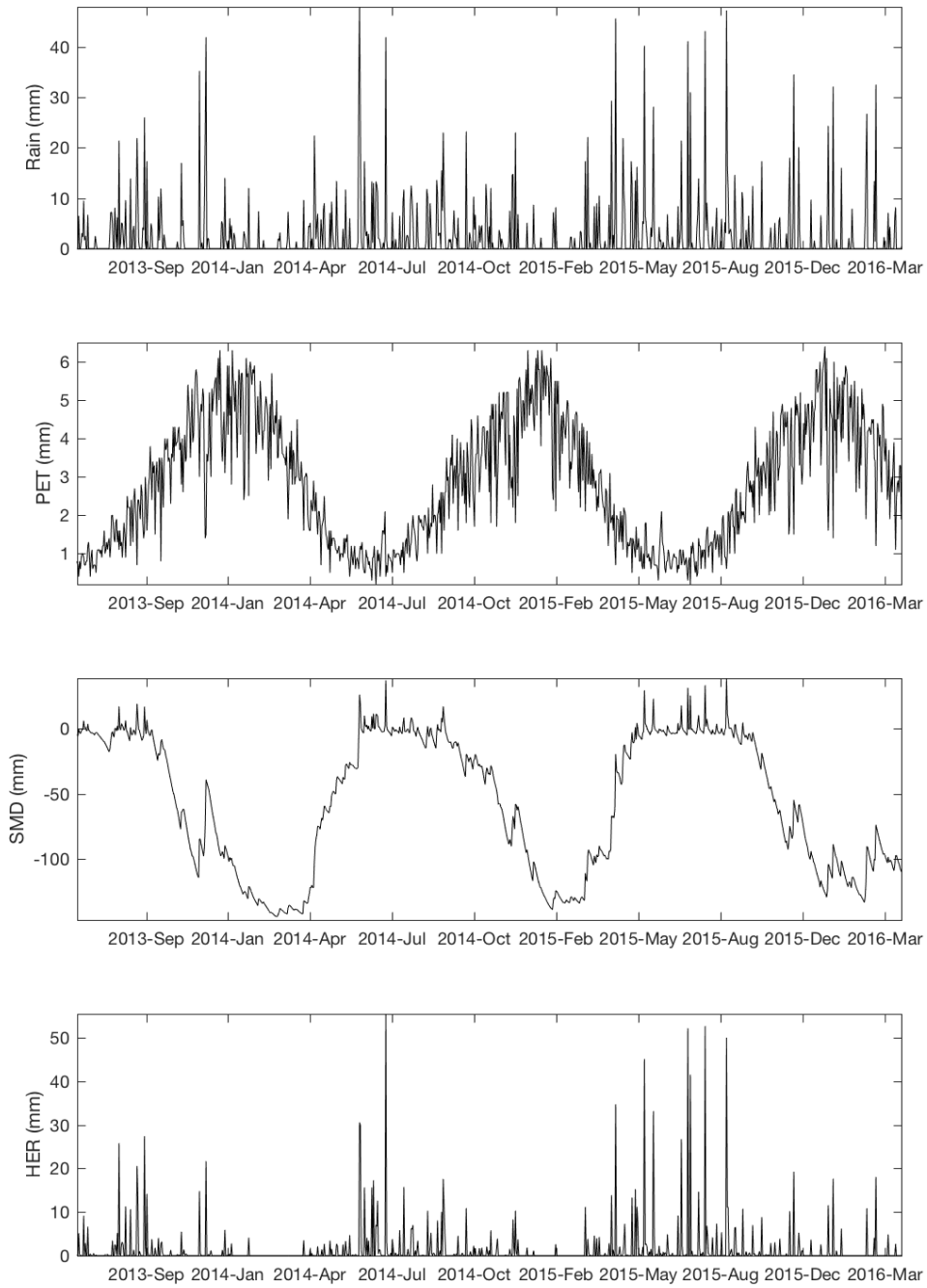

Figure 41: Virtual Climate Station Network data for Lake Waikare. PET: Potential evapotranspiration, SMD: Soil moisture deficit, HER: Hydraulically effective rainfall.

The delineations of the catchment and subcatchments of Lake Waikare used in this study are based on CLUES. According to CLUES output, the total catchment is 16,148 ha with 25 streams flowing directly into the lake (Figure 42). The inflows and their respective subcatchments were aggregated into ten groups for simulation with INCA-N and INCA-P. The grouping is shown by colour coded stream IDs in Figure 42 and are listed in Table 8.

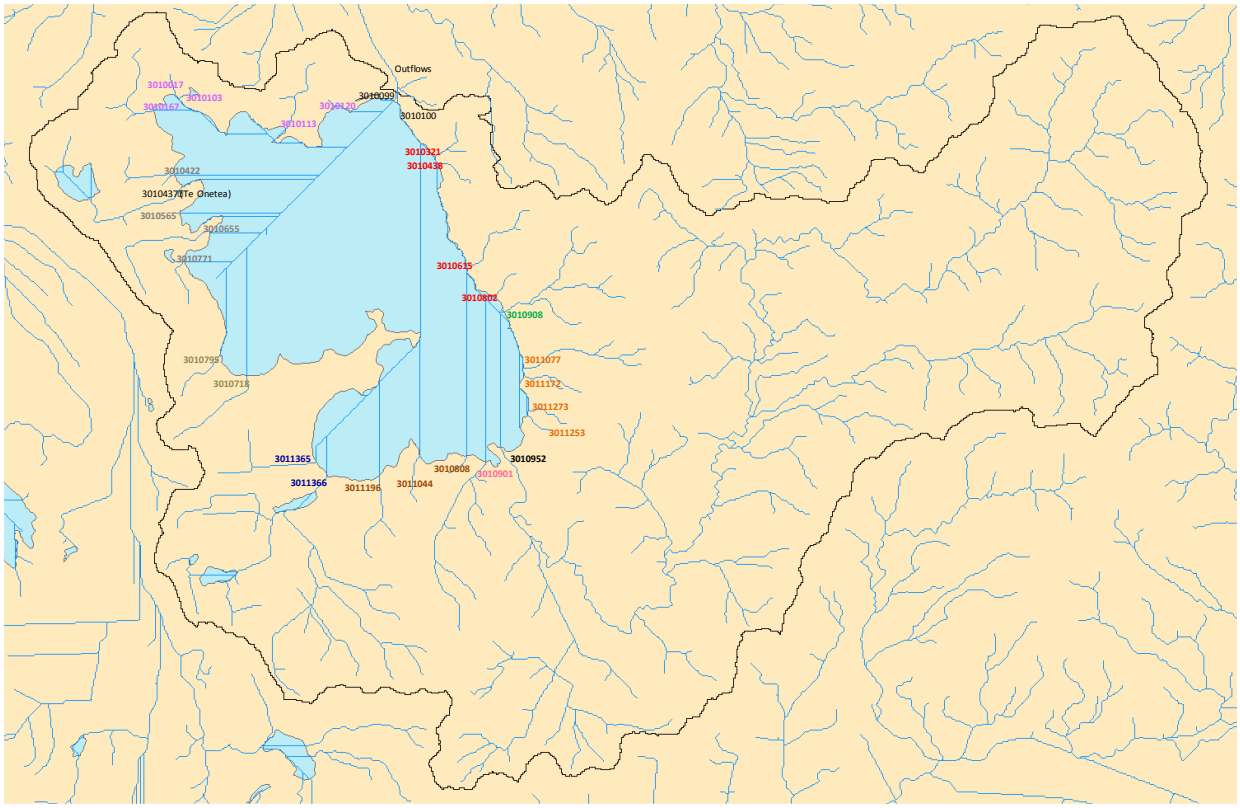

Figure 42: Catchment of Lake Waikare with stream network according to CLUES. CLUES IDs of streams discharging into the lake are provided; their colour coding identifies pooling into individual INCA simulations.

Table 8: Lake Waikare stream aggregation for INCA simulations. Stream 3010437 (Te Onetea) was not modelled in INCA (see text for details).

Colour	Letter code	Aggregated reach numbers
	A	3010321, 3010438, 3010615, 3010802
	B	3010908
	C	3011077,3011172, 3011273, 3011253
	D	3010952 (Matahuru)
	E	3010901
	F	3011196, 3011044, 3010808
	G	3011366, 3011365
	H	3010718, 3010795
	I	3010422, 3010437, 3010565, 3010655, 3010771
	J	3018167, 3010017, 3010103, 3010113, 3010120
Outflows		3010099, 3010100 (Pungarehu weir)

Land use in CLUES is divided into 19 categories. These were aggregated into six land use classes for the INCA model: native forest, exotic forest, scrub, deer/drystock, dairy, urban as shown in Table 9. The area of the aggregated subcatchments A to J and their respective land use cover areas are provided in Table 10.

Table 9: Land use classes used in the INCA catchment model and corresponding CLUES land use classes.

INCA land use class	CLUES land use class*
Native forest	LC_NATIVE
Exotic forest	LC_EXOTIC
Scrub	LC_SCRUB
Deer/drystock	INTENSIV + HILL + HIGH + DEER (Matahuru)
Dairy	DAIRY
Urban	URBAN

*Land use classes given in CLUES which do not occur in the Lake Waikare catchment are not shown (e.g., TUSS_DAIRY).

Table 10: Size and land use of aggregated subcatchments of Lake Waikare.

Catchment	Area (ha)						
aggregate	Total	Native forest	Exotic forest	Scrub	Deer/Drystock	Dairy	Urban
A	421.2	47.0	5.6	38.4	261.7	68.6	0.0
B	500.4	55.6	5.6	0.6	354.1	84.5	0.0
C	516.6	36.0	87.2	17.4	294.4	81.6	0.0
D	10617.9	609.7	336.1	177.2	6533.0	2961.9	0.0
E	562.3	4.4	1.1	0.0	225.8	331.0	0.0
F	314.6	0.1	0.0	0.0	148.2	166.3	0.0
G	1895.3	95.7	4.4	12.3	1034.2	747.0	1.7
H	258.2	47.0	5.6	38.4	98.6	68.6	0.0
I	646.0	1.6	1.4	0.0	292.8	349.1	1.1
J	415.3	13.8	3.9	0.1	188.3	117.0	92.2
Total	**16147.7**	**911.0**	**451.0**	**284.3**	**9431.2**	**4975.4**	**95.0**

Stream flow observations are available from a gauge at the Myjers farm bridge on the Matahuru Stream (Figure 43) since July 2006 and suspended sediment concentrations have been monitored during a number of discharge events (Figure 44). An additional site exists further downstream at the Waiterimu Road confluence (Figure 43) at which monthly samples of water quality variables have been measured since April 2004 in addition to continuous measurements flow and event-driven sampling of suspended sediments (Figure 45). Flow at the Waiterimu site is influenced by Lake

Waikare water during high lake levels and therefore, observations from the Myjers Farm site were used to calibrate the flow predicted by INCA. However, no water quality measurements were available from that site, so Waiterimu Road samples were used to calibrate the nutrient concentrations predicted by INCA.

INCA model parameters were adjusted manually to obtain a satisfactory fit with observations using a trial-and-error approach from values set to within literature values (Wade et al. 2002). During model calibration, model error was quantified using root-mean-square-error and mean absolute error for each output variable after the adjustment of model coefficients. Calibration continued until there was negligible improvement in these metrics with repeated model simulations. Satisfactory model performance was achieved for INCA-N and INCA-P, including discharge time series, but not for suspended sediment concentration. Suspended sediment concentration was derived empirically using the relationship between flow and suspended sediment concentration from observations at both locations as described below.

Figure 43: Satellite image of part of the Matahuru Stream and the southeast corner of Lake Waikare showing the locations of two stream monitoring sites. Air photo taken from Apple Maps from an unknown source and date.

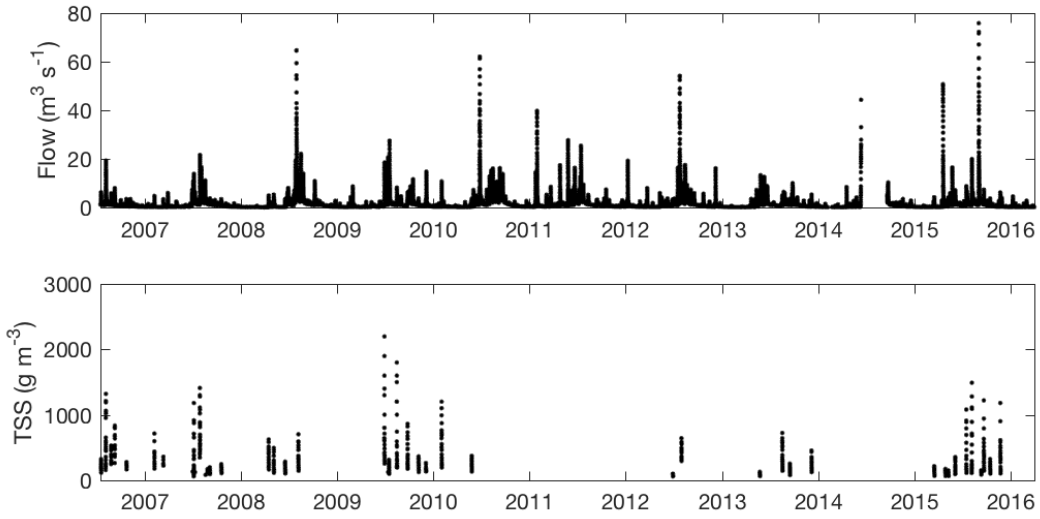

Figure 44: Flow and suspended sediments observed at the Myjers Bridge site on the Matahuru Stream.

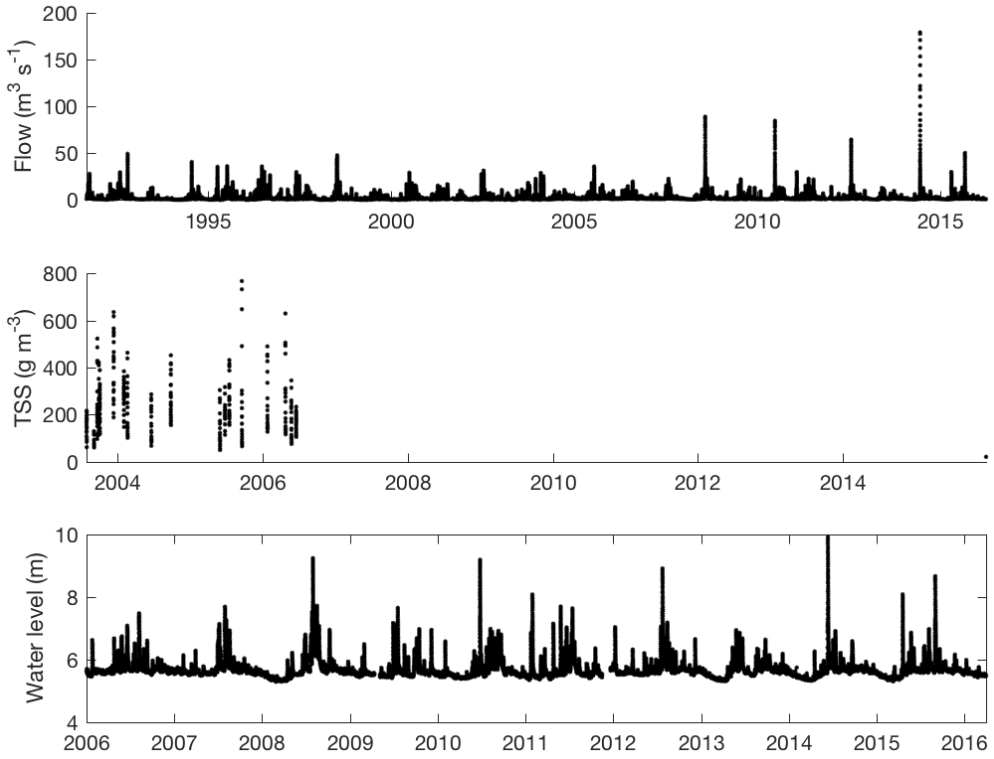

Figure 45: Flow, suspended sediments and water level observed at the Waiterimu Road confluence sampling site on the Matahuru Stream.

The calibrated model parameters for the Matahuru Stream observations are listed in Table 31 in Appendix C. The calibration time series plots of discharge and nutrient concentrations at the Matahuru Stream and from the calibrated INCA simulation are shown in Figure 126 to Figure 129 (Appendix C). These parameters were then transferred to INCA set ups for the nine other aggregated catchments to generate discharge and nutrient concentration time series. Modelled time series of

discharge and nutrient concentration for all streams are shown in Figure 130 and Figure 131 (Appendix C), respectively. Averages of annual discharges and loads of total nitrogen and total phosphorus derived from the INCA simulations are shown in Table 11 and plotted in Figure 46. Table 12 shows a summary of the loads to Lake Waikare normalised to the surface area of the lake for comparison with the other lakes of this study (Table 21, Table 25 and Table 29).

Table 11: Average annual discharge and nutrient loads from each aggregated subcatchment of Lake Waikare from INCA simulation. Loads derived from CLUES are shown for comparison.

Catchment aggregate	Discharge (m^3 y^{-1})	TN (kg y^{-1})	TP (kg y^{-1})	CLUES TN (kg y^{-1})	CLUES TP (kg y^{-1})
A	1,915,126.9	1,481.8	118.9	2,681.0	679.0
B	14,081,646.4	5,517.5	676.4	2,759.6	1,644.0
C	8,116,933.3	5,133.6	371.0	4,327.1	719.0
D (Matahuru)	33,694,006.6	70,979.7	4,247.0	96,188.8	18,864.0
E	21,542,045.9	9,796.7	1,054.5	7,600.4	668.0
F	4,353,451.8	3,689.1	243.5	4,811.5	185.0
G	28,767,933.2	32,561.2	1,521.4	14,813.6	1,819.0
H	3,303,205.3	2,277.7	186.1	7,386.3	135.0
I	18,430,046.5	5,239.8	1,018.3	11,261.5	371.0
J	3,155,043.7	5,819.8	174.9	4,547.1	260.0
Total	**137,359,439.6**	**142,496.8**	**9,612.1**	**156,376.9**	**25,344.0**

Table 12: Lake Waikare annual mean total nitrogen, total phosphorus and suspended sediment (kg ha^{-1} y^{-1}) contributed from external (catchment) loads. Area normalisation is to lake surface (3442 ha).

		External
Phosphorus (kg ha^{-1} y^{-1})	Mean	2.79
	Range	2.0 – 3.5
Nitrogen (kg ha^{-1} y^{-1})	Mean	41.4
	Range	31.9 – 77.7
Sediments* (kg ha^{-1} y^{-1})	Mean	165
	Range	13 – 457

*Sediment load for Matahuru Stream only.

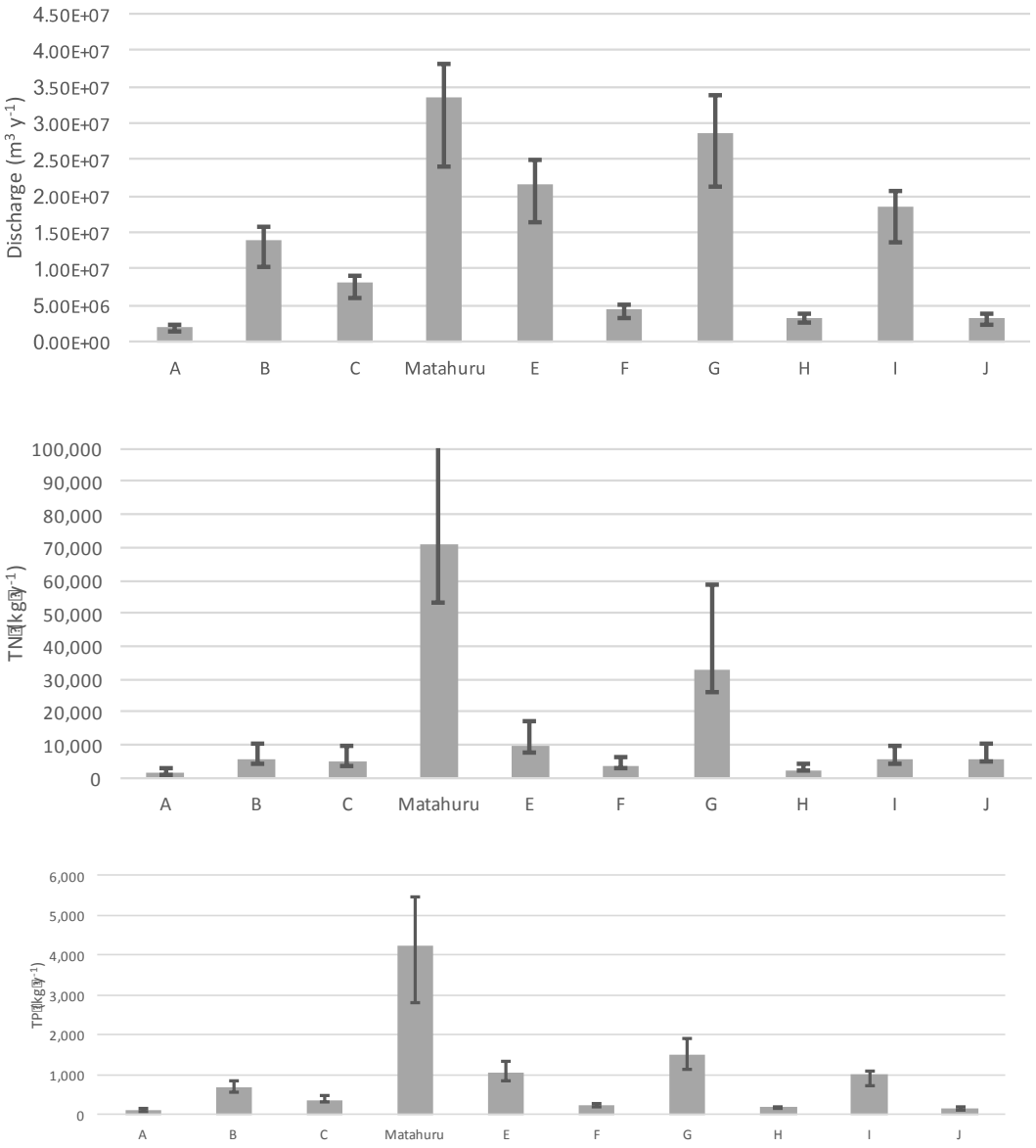

Figure 46: Annual water discharge (top graph), TN loads and TP loads from the Matahuru Stream and aggregated catchment inputs into Lake Waikare as modelled by INCA. The bar height represents the median of four annual values and the error bars show the minima and maxima of the four annual values. The error bar for TN load of the Matahuru Stream extends to 137,915 kg y^{-1}, but the y-axis was scaled to show the height of the smaller bars.

Suspended sediment discharge

Suspended sediment concentration in the Matahuru Stream was derived empirically using the relationship between flow and suspended sediment concentration from observations at both locations. The fit was determined on hourly averaged data using a type-2 linear fit approach on the log-transformed data by computing the first empirical orthogonal function using principal component analysis (Figure 47). In linear space, the fit becomes a power function of the form $y = a\,x^b$ where y is TSS concentration (g m^{-3}), and x is flow rate (m^3 s^{-1}). The equation for the TSS versus flow relationship at each of the locations are:

Myjers: $y = 30.8\ x^{1.4}$

Waiterimu: $y = 2.4\ x^{1.86}$

Median annual TSS discharges were calculated using the hourly flow time series and the flow versus TSS relationships at each respective location (Table 13).

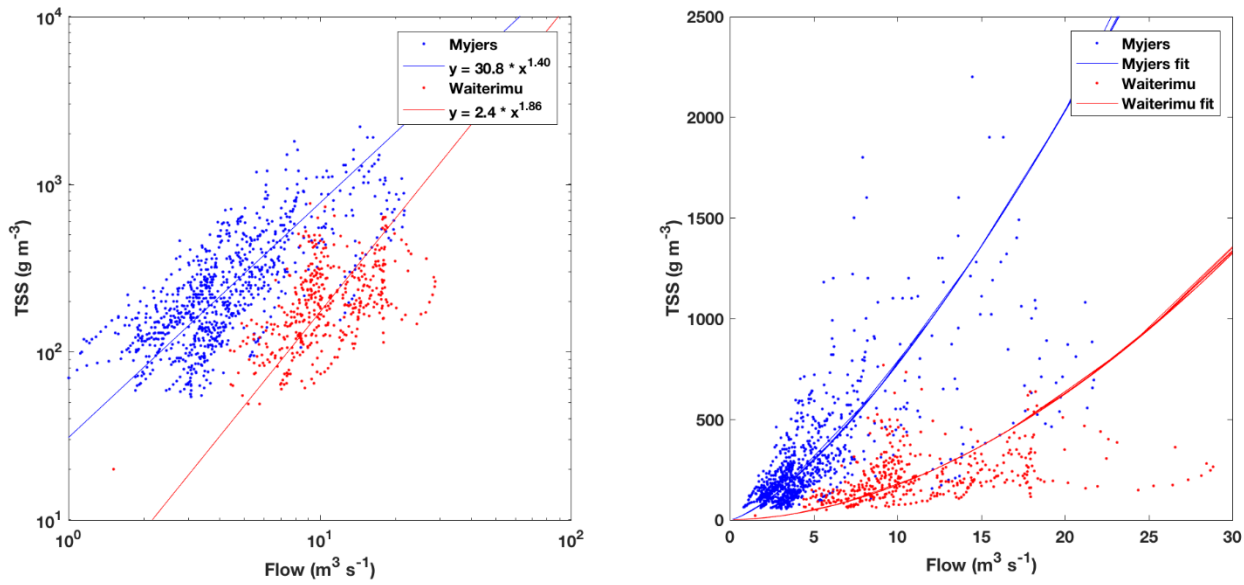

Figure 47: Empirical relationships between flow and suspended sediment concentrations in the Matahuru Stream at Waiterimu Road and Myjers Bridge sampling sites, respectively.

Table 13: Median, minimum and maximum annual TSS discharges at Myjers Bridge and Waiterimu Road in the Matahuru Stream. Medians calculated from the annual loads between 2006 and 2015 for Myjers and 1991 to 2015 for Waiterimu Road.

	TSS load (kg y^{-1})	
	Waiterimu Road	**Myjers Bridge**
Median	566,594	1,843,519
Minimum	46,418	1,011,172
Maximum	1,574,115	3,534,120

Te Onetea Stream discharge

Gauging of inflows also exist for the Te Onetea stream which connects the lake to the Waikato River and usually is an inflow to Lake Waikare. Hourly flow gauging record for Te Onetea was provided by the Waikato Regional Council with the cautionary note that the flows are indicative only are not to be used for flow analysis (Debbie Eastwood, 9 Nov 2016, pers. comm.). The most obvious problems

with the time series provided were that their maxima and minima were 'capped' at 6.41 and -6.41 $m^3 s^{-1}$, respectively, and that fluctuations between large positive and negative values often appear between adjacent time steps. Therefore, the hourly data has been averaged to daily flow values (Figure 48).

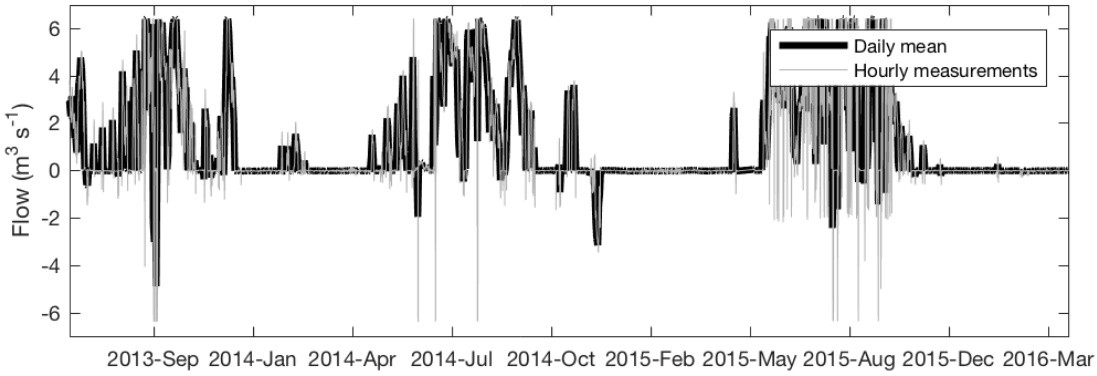

Figure 48: Te Onetea flow time series. Hourly measurements (thin grey line) are averaged into daily means (thick black line). Positive values denote flows into Lake Waikare.

Fish community

The fish community of Lake Waikare is known only from two rather old records of boat electrofishing. Fishing in 2003 was shortly after launch of the electrofishing boat and was before a protocol of 10 shots per lake had been established. Similarly, the 2008 fishing did not employ our established protocol and comprised only six shoreline sites, with one wading electrofishing shot on the margins that caught only gambusia. Nevertheless, we can establish the likely koi carp biomass in Lake Waikare from this fishing, from which we projected sediment and nutrient contributions from koi carp. Koi carp biomass in Lake Waikare was the highest of any of the four lakes in this study (131-217 kg ha^{-1}), and from this we conclude that koi carp could contribute 12-20% of the observed suspended sediment in the lake. Goldfish were numerically similar to koi carp in abundance, and shortfin eels were also abundant in Lake Waikare (6-17% of the fish community). Boat electrofishing almost certainly underestimated the abundance of eels, so a study with fyke nets would be useful adjunct. We did not find catfish or rudd in Lake Waikare, but they are almost certainly present. Common smelt were abundant in 2003, but were not found in 2008, which could be interpreted as a fish passage problem for recruitment from the river.

Scenarios

Table 14, Table 15 and Table 16 summarise the individual scenarios simulated for Lake Ngāroto, Lake Waahi and Lake Rotomānuka, respectively. These scenarios were developed through consultation with the main project working group[2].

Table 14: Lake Ngāroto scenario list identifying showing acronym (ID) and relevant description.

ID	Description
N1	10% reduction in external TN and TP load
N2	25% reduction in external TN and TP load
N3	50% reduction in external TN and TP load
N4	25% reduction in internal TN and TP load
N5	50% internal load reduction load
N6	Ngārotoiti diversion
N7	25% reduction in external TN and TP load + 50% reduction in internal load + Ngārotoiti diversion (= N2+N5+N6)
N8	25% reduction in internal TN and TP load + 50% internal load reduction load + 0.5 m increase in water level
N9	25% reduction in external TN load
N10	25% reduction in external TP load
N11	50% reduction in internal TN and TP load associated with sediment resuspension
N12	50% reduction in internal TN and TP load associated with anoxic release
N13	50% reduction in external TP load
N14	50% reduction in external TP load and 50% TP load reduction associated with anoxic release

[2] The main project working group included the researchers who were authors on this report, Waikato River Authority/Envirostrat (Keri Nielsen), DairyNZ (David Burger), Waikato Regional Council (Deniz Ozkundakci, Paula Reeves), Erina Rawiri-Watene (Waikato-Tainui), Tracie Dean-Spiers (Department of Conservation), NIWA (John Quinn, Piet Verburg), Aareka Hopkins (AM^2)

Table 15: Lake Waahi scenario list identifying showing acronym (ID) and relevant description.

ID	Description
WH1	25% reduction in external TN load
WH2	25% reduction in external TP load
WH3	25% reduction in external TN and TP (=WH1+WH2)
WH4	50% reduction in external TP load
WH5	1 m increase in water level
WH6	25% reduction in external TN load + 1 m increase in water level (=WH1 + WH3)
WH7	25% reduction in external TP load + 1 m increase in water level (=WH2 + WH3)
WH8	1 m increase in water level, 25% reduction in external TP load, 25% reduction in internal TP load
WH9	50% reduction in internal TN and TP load

Table 16: Lake Rotomānuka scenario list identifying showing acronym (ID) and relevant description.

ID	Description
R1	Wetland scenario - no attenuation
R2	Wetland scenario – high attenuation (80% N, 40% P)
R3	25% reduction in external TN load (total catchment areas A-B-C-D)
R4	25% reduction in external TP load (total catchment areas A-B-C-D)
R5	25% reduction in external TN and TP load (total catchment areas A-B-C-D)
R6	50% reduction in external TN load (total catchment areas A-B-C-D)
R7	50% reduction in external TP load (total catchment areas A-B-C-D)
R8	50% reduction in external TN and TP load (total catchment areas A-B-C-D)
R9	Rotomānuka South inflow diversion + 25% reduction in external TN and TP load (catchment D only)

Results and Discussion

Lake Ngāroto

Calibration-validation process

The calibration process ended when an acceptable match was reproduced of the simulation output to the observed data. The main focus was on temperature, surface and bottom DO, TN, TP, TSS and chlorophyll *a* which was represented as a total value (i.e., the sum of the two constituent phytoplankton groups in the model). The statistical comparison (Table 17) was deemed reasonable by comparison with other modelling applications. It should be kept in mind that some major simplifications were inherent in the model input data (primarily the sparse nature of the inflow monitoring and limited duration, i.e., only one year) and in the in-lake data, which were repeated over a five-year period from one year of data.

Table 17: Model performance using root mean square error (RMSE) and coefficient of variation of root mean square deviation CV(RMSE) for high frequency buoy observations (n > 1500; surface temperature: Tsrf, bottom temperature: Tbtm, surface dissolved oxygen: DOsrf, bottom dissolved oxygen: Dobtm) and repeated observations (n = 61; total nitrogen: TN, total phosphorus: TP, total suspended solids: TSS, total chlorophyll *a*: TCHLA).

	Tsrf (^oC)	**Tbtm (^oC)**	**DOsrf (mg L^{-1})**	**DObtm (mg L^{-1})**	**TN (g m^{-3})**	**TP (g m^{-3})**	**TSS (g m^{-3})**	**TCHLA (mg m^{-3})**
RMSE	1.05	1.95	2.60	N/A	0.56	0.04	9.51	24.0
CV(RMSE)	0.06	0.11	0.33	N/A	0.30	0.32	0.47	0.51

Key characteristics based on models and observed data

A logical sequence of calibration and presentation of results generally involves physical variables first, followed by biogeochemical variables. This sequence is useful because a smaller number of model parameters control the physical variables (e.g., water temperature) and reliable simulations of biogeochemical variables can generally only follow once transport and mixing processes are reasonably well resolved (as indicated indirectly by good fit of observed and modelling water temperatures). Figure 49 shows observed and simulated water temperatures at the surface and near the bottom of Lake Ngāroto. Annual extremes in water temperature at both depths range from approximately 8^{o}C in winter to 26^{o}C in summer. The model simulations reproduce observations well

but show a slight tendency to be too low in winter. This discrepancy may be related to the remote location of the meteorological station (i.e., Hamilton DWS) although corrections were made for air temperature based on measurements from the buoy on the lake.

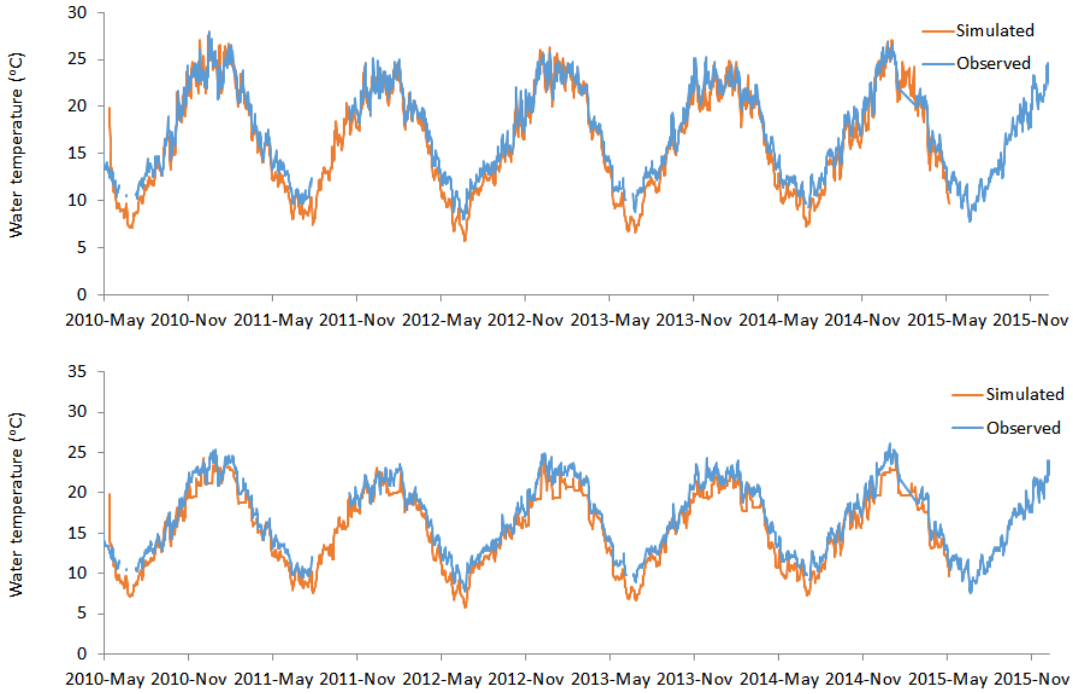

Figure 49: Top: Surface water temperature for Lake Ngāroto. Bottom: near-bottom water temperature at in Lake Ngāroto. Orange line is the simulated data, and blue line is the high-frequency buoy observations.

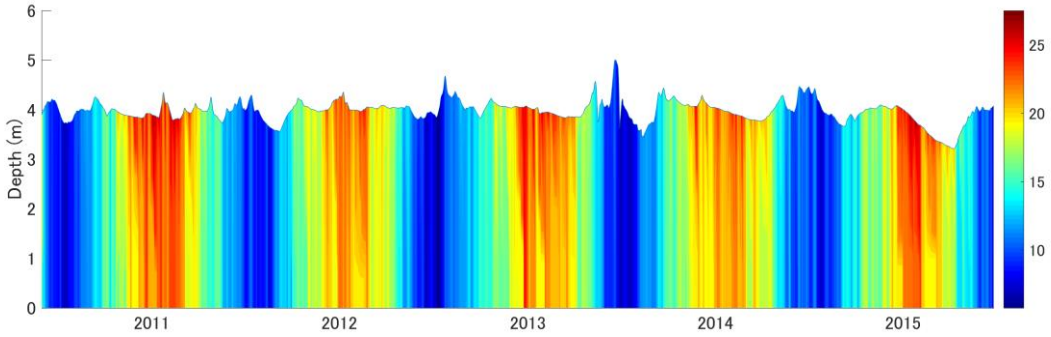

Figure 50: Temperature through the water column of Lake Ngāroto for the five-year simulation period. Colours represent water temperature with a scale (°C) given on the right-hand side.

Simulated temperature values have been represented over the entire lake depth in Figure 50. This figure includes water level variations, with high water levels occurring in winter 2013 and a progressive reduction in water level through summer 2015. The wide range of the colour scale in this figure tends to hide important differences in temperature between the surface and near-bottom depths. These differences are revealed in more detail in Figure 51 which shows a 15-month subset of the 5-year simulation period. Here the model tended to over-predict the 'strength' of stratification

(i.e., given by the temperature difference) during summer and this may have also resulted in slight over-estimation of the duration of stratification events, shown over the whole simulation period in Figure 52. Nevertheless, we consider that the model provides a good representation of an important feature of lake stratification which has potential to affect a number of other biogeochemical variables. It is notable that large temperature differences occur through the 4-m depth of Lake Ngāroto and periods of stratification can sometimes extend to two or more weeks.

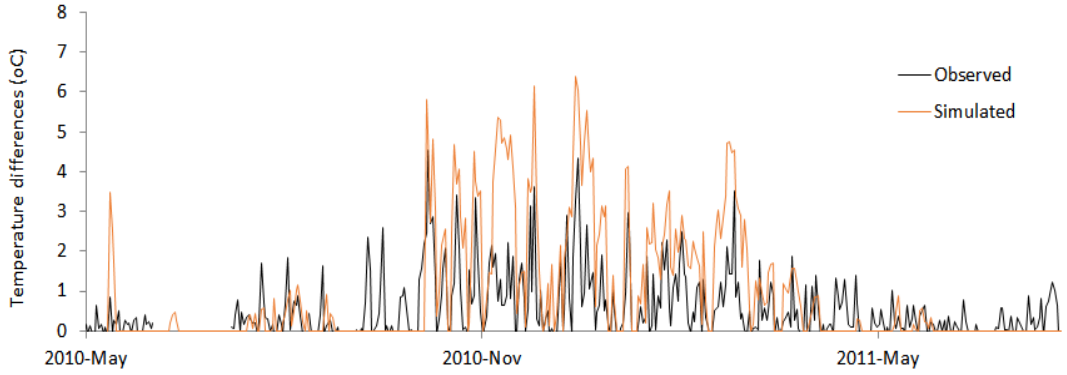

Figure 51: Observed (black) and simulated (orange) differences in water temperature between the surface and bottom for the five-year simulation period for Lake Ngāroto.

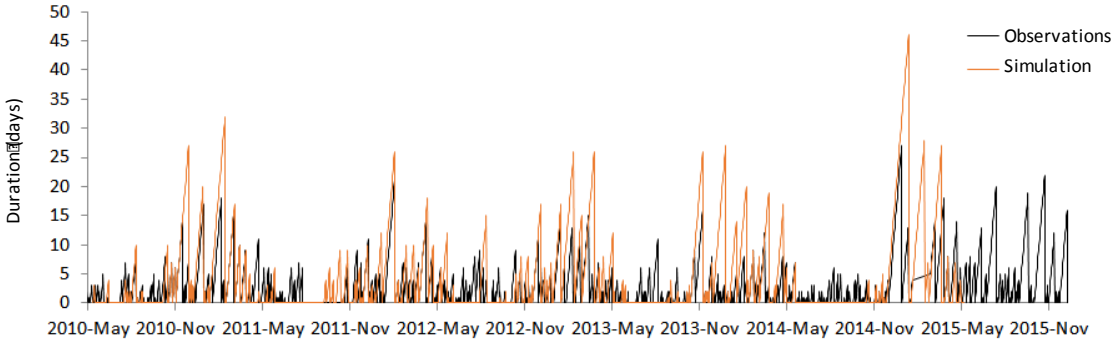

Figure 52: Observed (Obs_daily; black) and simulated (orange) duration of stratification events (as defined in Table 1) for the five-year simulation period for Lake Ngāroto.

In contrast to water temperature, DO was measured only at the near-bottom location and not at the water surface. The surface DO plot in Figure 53 therefore shows only simulated data. It reveals an expected seasonal cycling of DO from high in winter to low in summer. This cycle is expected because of the annual pattern of DO concentrations for water at saturation. However, the annual range in DO is very large, from around 2 mg L^{-1} in summer to c. 11 mg L^{-1} in winter. These values correspond to severe undersaturation of DO in summer to slight supersaturation of DO in winter. We have no way of validating this model output in the absence of DO measurements at the surface as opposed to the model comparison enabled by near-bottom DO measurements.

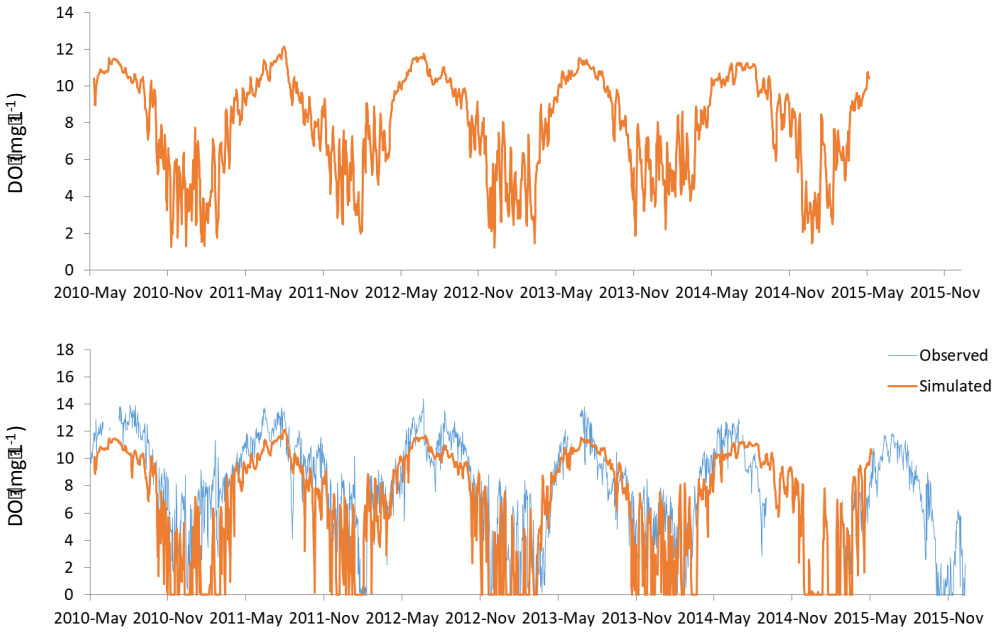

Figure 53: Simulated (orange) time series of dissolved oxygen at the surface (top panel) and the bottom (bottom panel) for the five-year simulation period for Lake Ngāroto. Monitoring buoy observations are available at the bottom only (blue line).

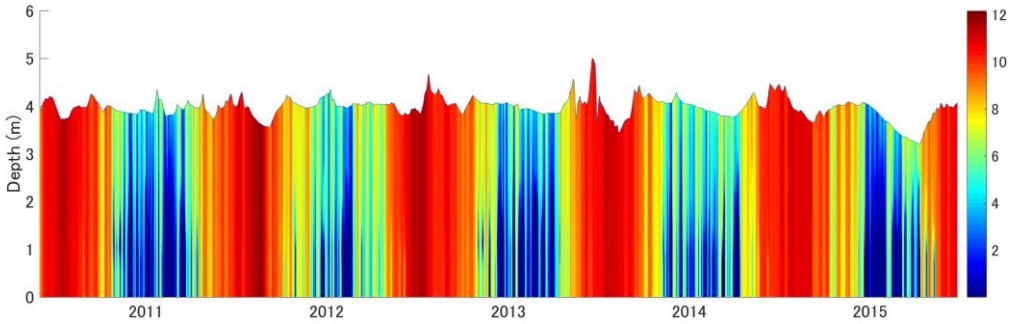

Figure 54: Simulated dissolved oxygen through the water column of Lake Ngāroto for the five-year simulation period. Colours represent dissolved oxygen with a scale (mg L^{-1}) given on the right-hand side.

The high frequency near-bottom measurements of DO can be compared directly with model simulations of DO at the corresponding depth (Figure 53). In this case the seasonal DO cycle is reproduced well in the simulations. There was a slight tendency to under-predict dissolved oxygen in winter (by c. 1 mg L^{-1}) but concentrations in summer were generally well reproduced (see also the statistical comparison in Table 17). It is important to recognize that any discrepancies between the simulation output and the observations may be only partly related to model parameter settings for DO (e.g., sediment oxygen demand) and that many other interacting factors (e.g., stratification, phytoplankton production) also have an effect on water column DO concentrations. Both measurements and model simulations reveal that bottom waters in Lake Ngāroto can be devoid of DO for several days in summer and that anoxia (here arbitrarily taken to be DO < 2 mg L^{-1}) is a

common occurrence. Figure 54 shows simulated DO through the entire water column. In this figure, there are rapid fluctuations in DO during summer (i.e., frequent changes in colour through time) and correspond to alternation of stratification events (that result in rapid depletion of DO through much of the water column) with mixing events (that provide a limited amount of replenishment of DO through the water column).

Nutrient concentrations (TN, TP, NO_3-N, NH_4-N and DRP) were examined by comparison of observed and simulated data for the water surface and bottom water (Figure 55 to Figure 60). The observations are represented as a representative annual cycle and are therefore repeated to provide comparison with model outputs over the five-year period. Model parameters were calibrated so that state variables were of similar magnitude to the observed variables capturing their seasonality. It is easy to over-interpret the results and infer a process understanding in the observed data, but a few generalisations are possible.

Total nitrogen concentrations varied mostly with changes in concentrations of nitrate. Nitrate concentrations tended to be higher in winter and this may reflect (1) increased inputs of nitrate when soils in the catchment are more likely to be saturated and discharge is therefore elevated in association with reduced levels of evapotranspiration, and (2) alleviation of low oxygen levels (i.e., low water oxidation state) through the water column, which may support higher rates of nitrification. Reduced levels of ammonium in mid to late winter also lend support to nitrification being an important driver for the increased nitrate and reduced ammonium concentrations at this time. Ammonium concentrations were generally high through summer, on occasion close to 0.2 g m^{-3} (Figure 57 and Figure 58). The presence of such elevated levels of ammonium likely reflects a poorly oxidized water column, with this theory also supported by model simulations which show low levels of dissolved oxygen through the entire water column in summer. Ammonium is likely being regenerated in large amounts from the bottom sediments; part of a cycle of high rates of organic matter production (i.e., high phytoplankton biomass) in the water column leading to high rates of organic matter sedimentation, mineralization of this material in the bottom sediments and release back to the water column as ammonium under the prevailing low-oxygen environment. The model simulations suggest that these release events are magnified by anoxia during stratification events. Observations of ammonium concentrations in bottom waters might be expected to capture only a small number of these events because of their intermittent nature. The model simulations indicate that the ammonium release through this mechanism is likely to be substantial and adds to the heterotrophic (i.e., oxygen deficit) nature of the water column.

Observed (and simulated) nitrate and ammonium concentrations decrease substantially in summer, remaining relatively low for about eight months of the year. Of particular note is that nitrate-N concentrations are reduced to, or close to, detection limits (0.05 g m^{-3}), while ammonium-N concentrations tend to be somewhat higher at around 0.03 g m^{-3}. This situation is somewhat unusual in the surface waters of natural lakes and reflects the low oxidation state through the water column.

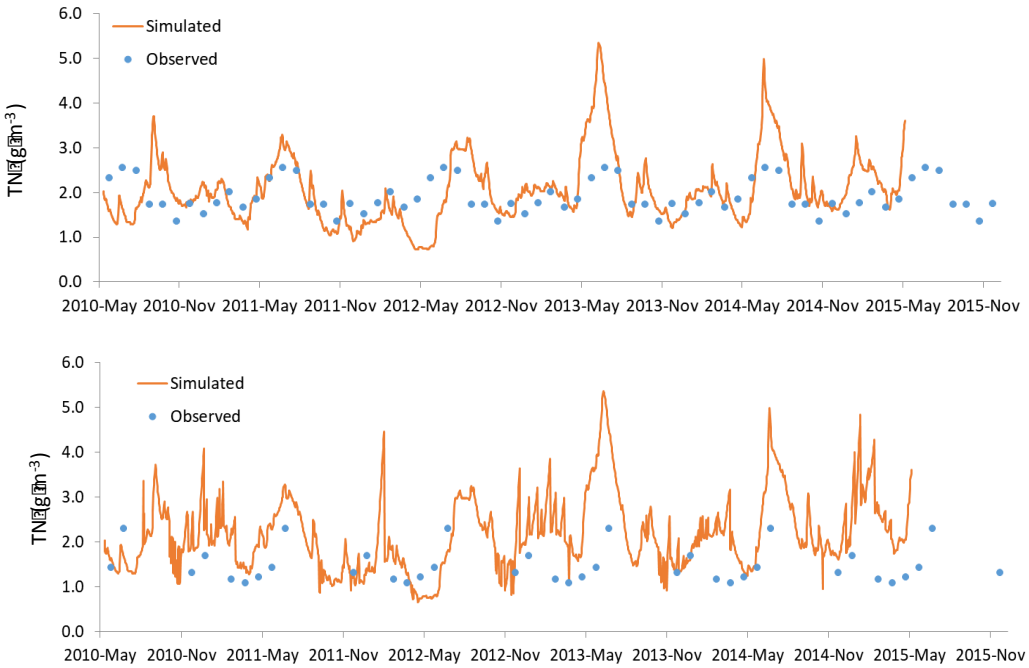

Figure 55: Observations (blue dots) and simulated values (orange) of total nitrogen concentration at (top) the surface and (bottom) a bottom-water location for the five-year simulation period for Lake Ngāroto. Observations are monthly medians of available observations, repeated annually (see text for detail).

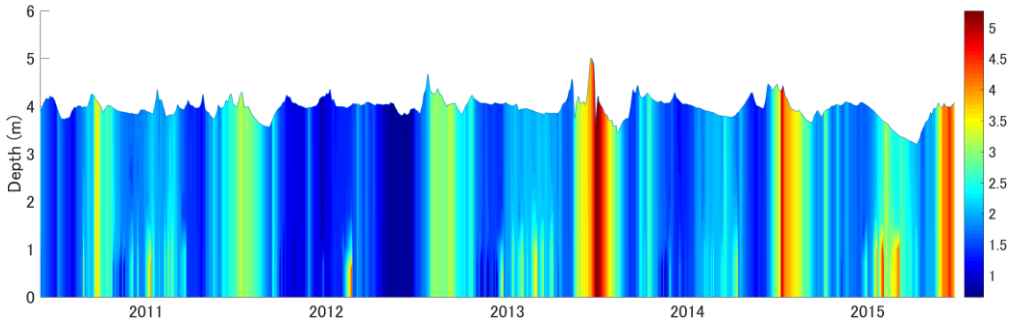

Figure 56: Simulated total nitrogen concentration through the water column of Lake Ngāroto for the five-year simulation period. Colours represent total nitrogen with a scale (g m^{-3}) given on the right-hand side.

The model simulations indicate that there is considerable inter-annual variability in nitrogen concentrations. This variability is contributed by different catchment nitrogen loads amongst years, mostly reflecting differences in discharge, and by different rates of internal nitrogen loading, largely

reflecting meteorological factors of wind and air temperature, that alter the timing and duration of stratification and anoxia. A monitoring programme should capture (1) interannual variability by developing good time series data extending over multiple years, (2) seasonal variability that reflects different levels of catchment nitrogen loads between winter and summer, and (3) short-term variability in water column nitrogen concentrations driven by intermittent releases of ammonium from bottom sediments and possibly also resuspension of particulate nitrogen from the bottom sediments (see below). Thought should be given to how best to stage this monitoring so that it is both practical and comprehensive, while addressing the three time scales mentioned above.

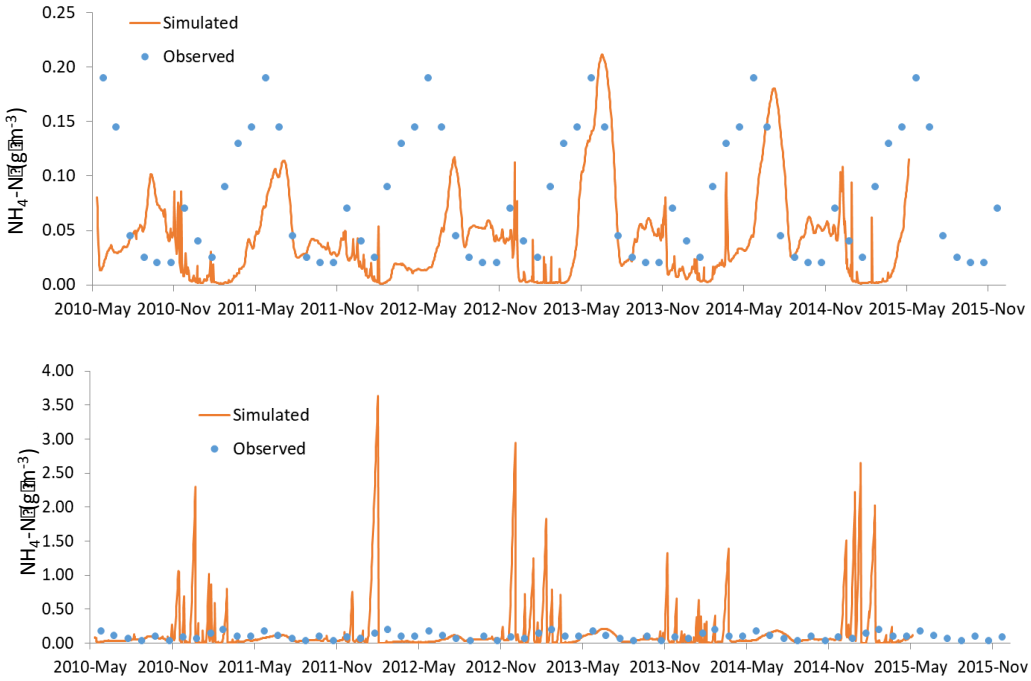

Figure 57: Observations (blue dots) and simulated values (orange) of ammonium-N concentration at (top) the surface and (bottom) a bottom-water location for the five-year simulation period for Lake Ngāroto. Observations are monthly medians of available observations, repeated annually.

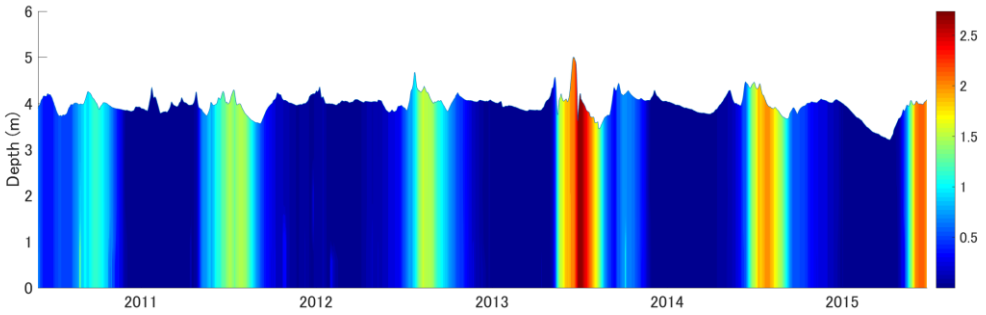

Figure 58: Simulated ammonium concentration through the water column of Lake Ngāroto for the five-year simulation period. Colours represent ammonium with a scale (g m^{-3}) given on the right-hand side.

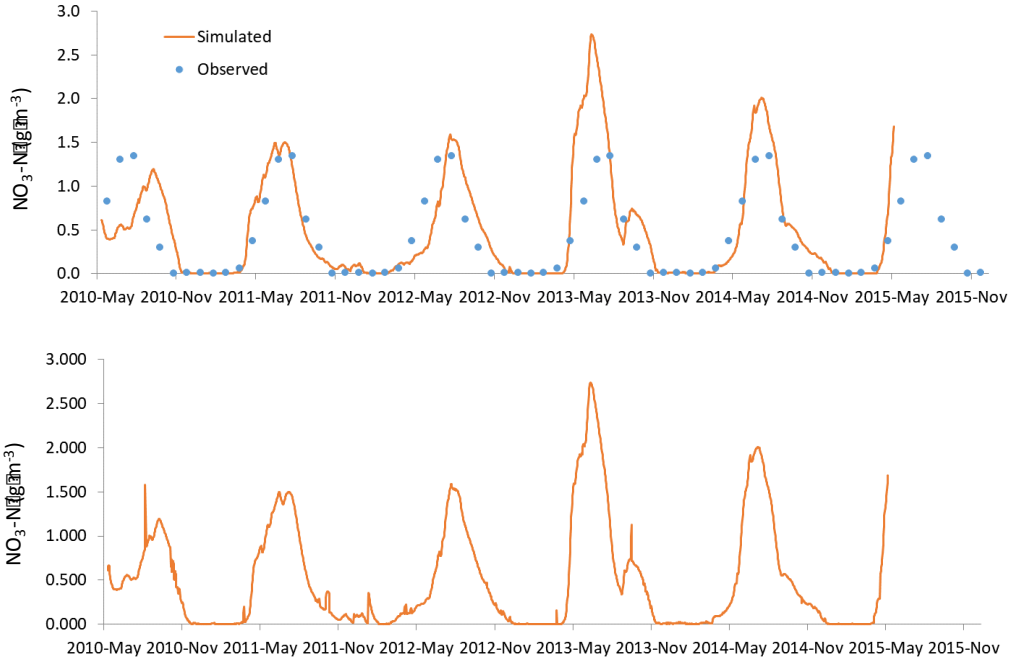

Figure 59: Observations (blue dots) and simulated values (orange) of nitrate-N concentration at (top) the surface and (bottom) a bottom-water location for the five-year simulation period for Lake Ngāroto. Observations (top) are monthly medians of available observations, repeated annually.

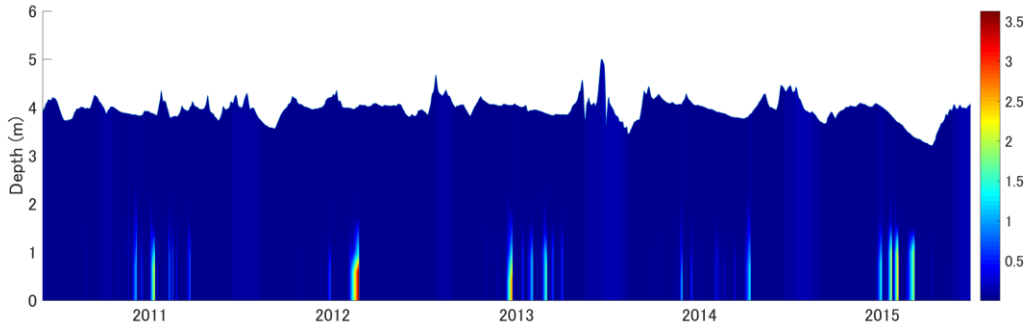

Figure 60: Simulated nitrate-N concentration through the water column of Lake Ngāroto for the five-year simulation period. Colours represent nitrate-N with a scale (g m^{-3}) given on the right-hand side.

Total phosphorus concentrations (Figure 61) do not show the same degree of variability as total nitrogen concentrations. For the single year of sampling, concentrations tended to be higher in summer than in winter, which may reflect higher algal biomass in summer (Figure 65), with more phosphorus tied up in the biomass, as well as less seasonal variability of phosphorus in inflows compared with nitrogen. It is possible that the model simulations overestimate the extent of anoxic release events driven by water column stratification, as evidenced by observed TP and DRP being lower in bottom waters in three summers, but for two of the summers the model provided a good representation of TP. Again, it is worth noting that the observations represent a median annual cycle repeated for the five years and we do not know the actual interannual variability of phosphorus over the simulation period.

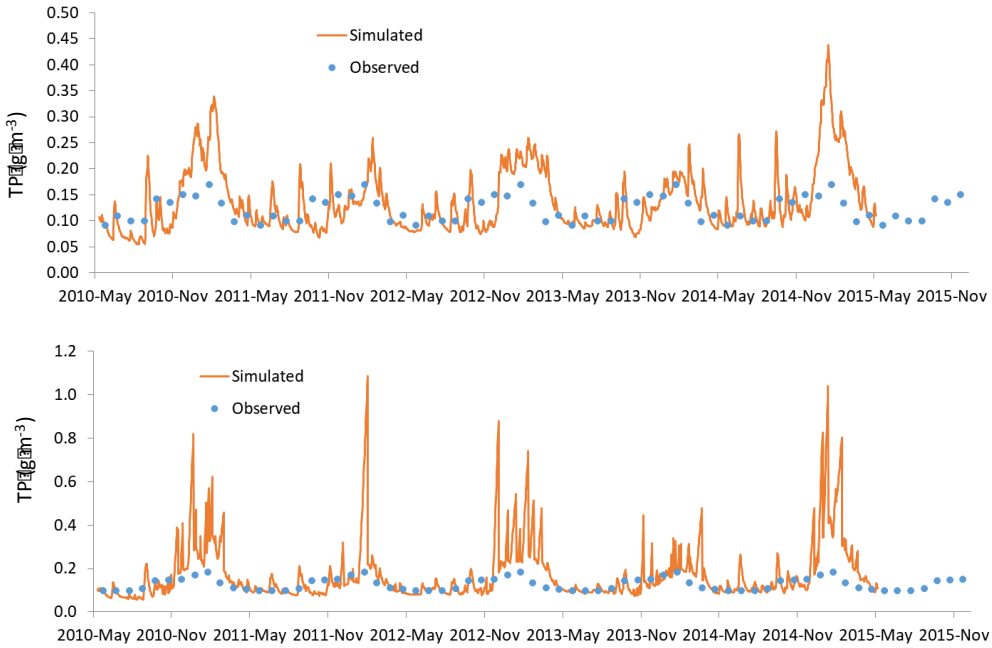

Figure 61: Observations (blue dots) and simulated values (orange) of total phosphorus concentration at (top) the surface and (bottom) a bottom-water location for the five-year simulation period for Lake Ngāroto. Observations are monthly medians of available observations, repeated annually.

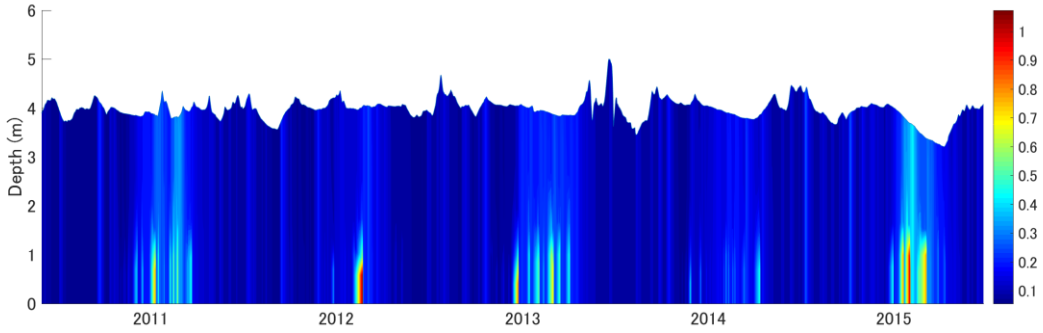

Figure 62: Simulated total phosphorus concentration through the water column of Lake Ngāroto for the five-year simulation period. Colours represent total phosphorus with a scale (g m^{-3}) given on the right-hand side.

Concentrations of DRP are very close to, or below, detection limits (0.08 g m^{-3}) (Figure 63, Figure 64). The ratio of DRP to TP is very low and probably reflects P in particulate form that is associated both with inorganic sediments and organic material, mostly as phytoplankton biomass. It is likely that these two constituents effectively compete with each other so that any DRP in the water column is rapidly scavenged and either taken up by phytoplankton or sorbed to inorganic sediments. Thus when there is strong demand for P by phytoplankton (e.g., during summer blooms) some of the particulate inorganic P may either be scavenged by phytoplankton or desorbed as a result of readjustment of the sorption kinetics (i.e., release from inorganic particles when DRP concentrations are very low). Any future phosphorus monitoring programme should consider the different time

scales of monitoring but also to address the large number of non-detects associated with the relatively high analytical detection limits.

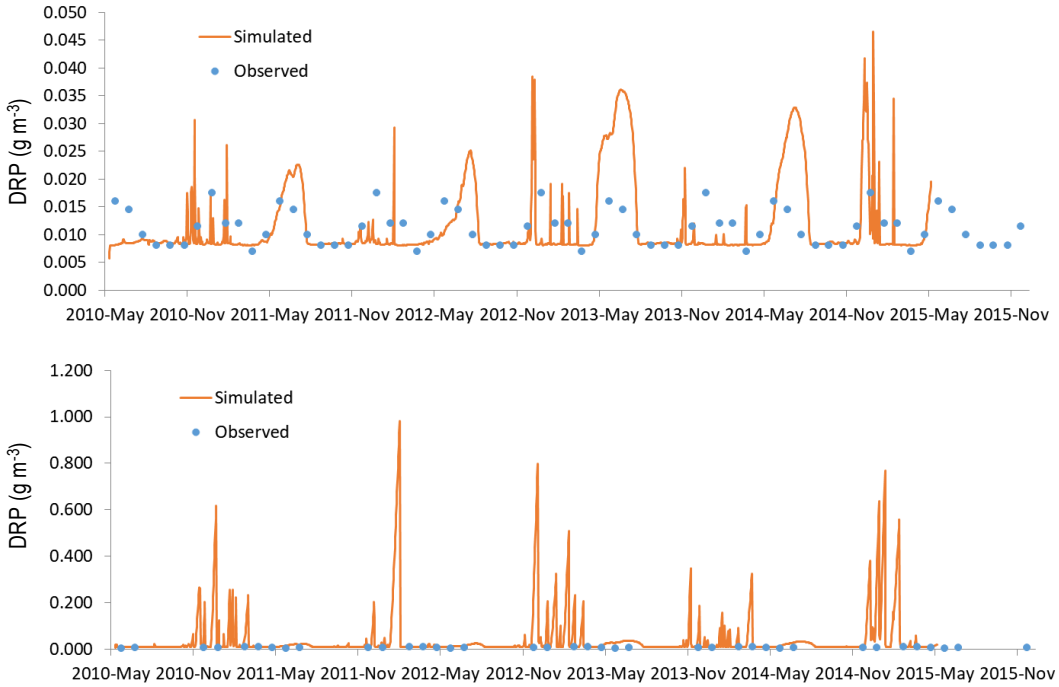

Figure 63: Observations (blue dots) and simulated values (orange) of dissolved reactive phosphorus (DRP) concentration at (top) the surface and (bottom) a bottom-water location for the five-year simulation period for Lake Ngāroto. Observations are monthly medians of available observations, repeated annually.

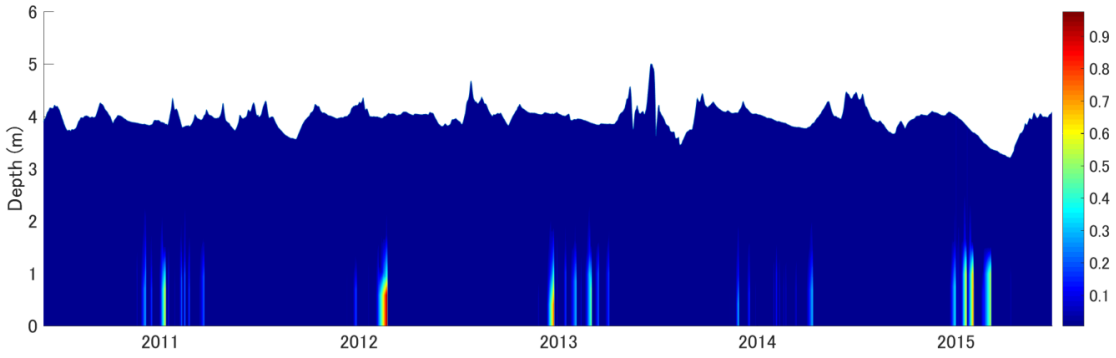

Figure 64: Simulated dissolved reactive phosphorus (DRP) concentration through the water column of Lake Ngāroto for the five-year simulation period. Colours represent DRP with a scale (g m^{-3}) given on the right-hand side.

The median cycle of observed chlorophyll *a* concentrations were in the range of 20 to 100 µg L^{-1} (Figure 65). The highest concentrations occurred in late summer and the lowest concentrations in mid winter (Figure 66), likely associated with higher irradiance and temperature in summer. The model generally represented this seasonal variability adequately but may have over-estimated concentrations in summer and under-estimated concentrations in winter. Without having observed data spanning the entire five-year period of the simulations, it is difficult to know how representative these discrepancies are. Phytoplankton biomass was strongly dominated by cyanobacteria for most of the time in the model simulations, except for intermittent periods in winter, and this corresponds anecdotally with visual observations as well as shoreline assessments for cyanobacteria recreational health monitoring. Marked vertical variations in chlorophyll *a* concentrations reflect stratification events when cyanobacteria floated towards the surface under the quiescent conditions in the water column (Figure 66). Some of these events would have been associated with observations of dense blooms of cyanobacteria.

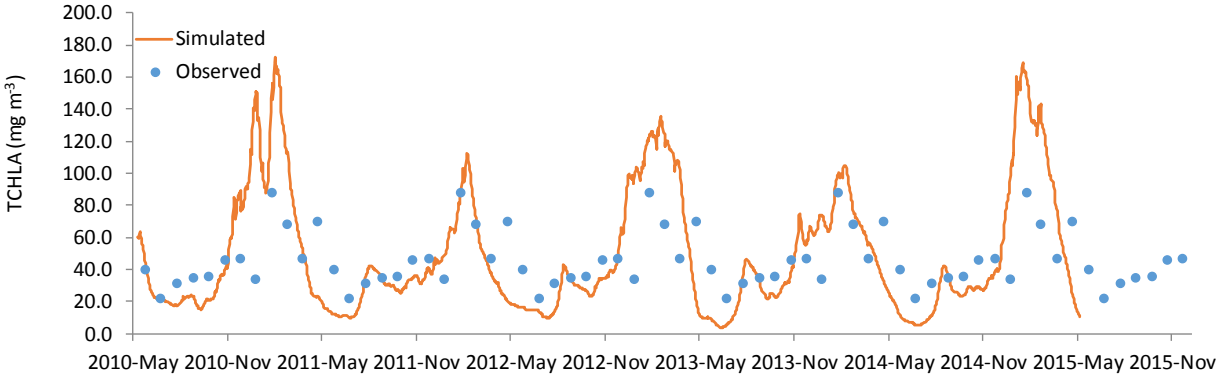

Figure 65: Observations (blue dots) and simulated values (orange) of chlorophyll *a* concentration at the surface for the five-year simulation period for Lake Ngāroto. Observations are monthly medians of available observations, repeated annually.

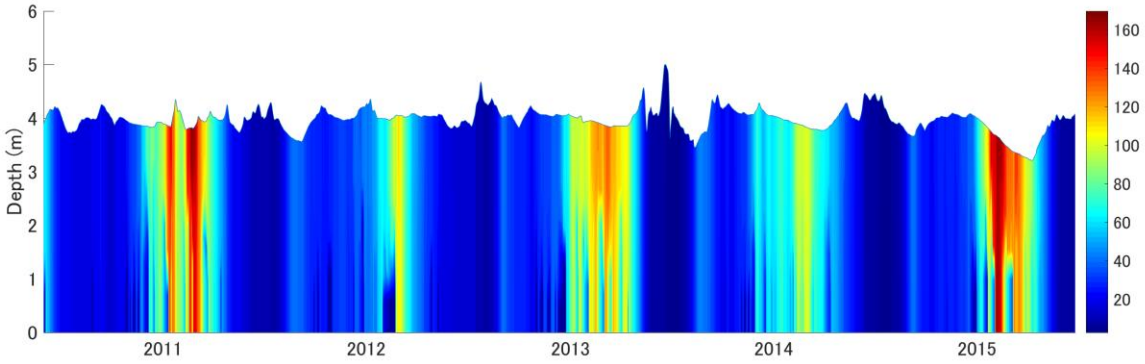

Figure 66: Simulated chlorophyll *a* concentration through the water column of Lake Ngāroto for the five-year simulation period. Colours represent chlorophyll *a* with a scale (µg L^{-1}) given on the right-hand side.

Figure 67 shows the limitation functions for cyanobacteria over the course of the simulation. Temperature is a simple multiplier on the growth rate and varies about a value of one (corresponding to 20°C). Values of the temperature function increase above one in summer when temperature exceeds 20°C and less than one for the remainder of the year. A minimum function is used to describe the effect of nitrogen, phosphorus and light on phytoplankton growth. The value of whichever of these functions is lowest (i.e. "Liebig's law of the minimum") is multiplied by the maximum growth rate. Light varies strongly over the course of each day and so values of the limitation term for light should be interpreted carefully; the main value in the output in Figure 67 is to compare the duration of periods of nitrogen and phosphorus limitation; phosphorus limitation is highly persistent but there are periods when limitation is very closely matched between nitrogen limitation and phosphorus limitation, and very occasional periods of nitrogen limitation.

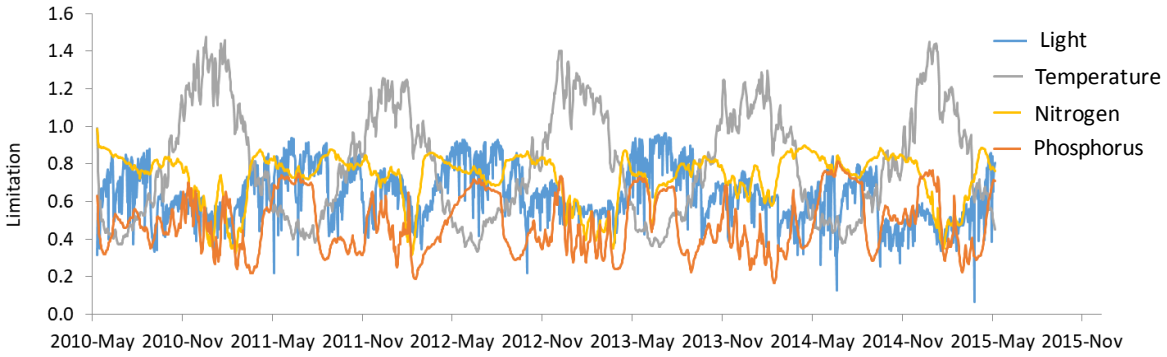

Figure 67: Time series of limitation factors for cyanobacteria in Lake Ngāroto. The temperature function extends above one as it is referenced as one for 20˚C); the model multiplies the temperature function by the minimum of the light, nitrogen or phosphorus functions.

Like other variables, it is difficult to judge how representative the median cycle of observations of suspended solids is with respect to the model simulations of this variable. The simulations appear to show greater variability of inorganic suspended solids (Figure 68), which may be interpreted as a steep ascending limb when concentrations increase rapidly in response to sediment resuspension events, and a flatter descending limb when sedimentation predominates. Quantifying the size and density of organic and inorganic particles in the water column would increase confidence about the time scales of these sedimentation events, which for most resuspension events result in resuspended sediments persisting for a month or so (Figure 69). Accurate simulations of suspended solids are important because of their importance to the light climate in Lake Ngāroto. Over the year of observations, Secchi depths varied from about 0.35 to 0.75 m. Therefore little light would reach bottom sediments in the lake, assuming the euphotic depth (1% of surface radiation) is about 2.5 times the Secchi depth, and it would therefore be difficult to re-establish macrophytes. The model

captured the seasonal variability of Secchi depth for the one year of observations (Figure 70); clarity was lowest in early winter and highest in early to mid summer. A comparison of time series of suspended solids (Figure 68) and Secchi depth (Figure 70) shows that the two variables can behave somewhat independently. In other words, water clarity is influenced by both the fine inorganic sediment particles as well as organic material most likely associated with phytoplankton.

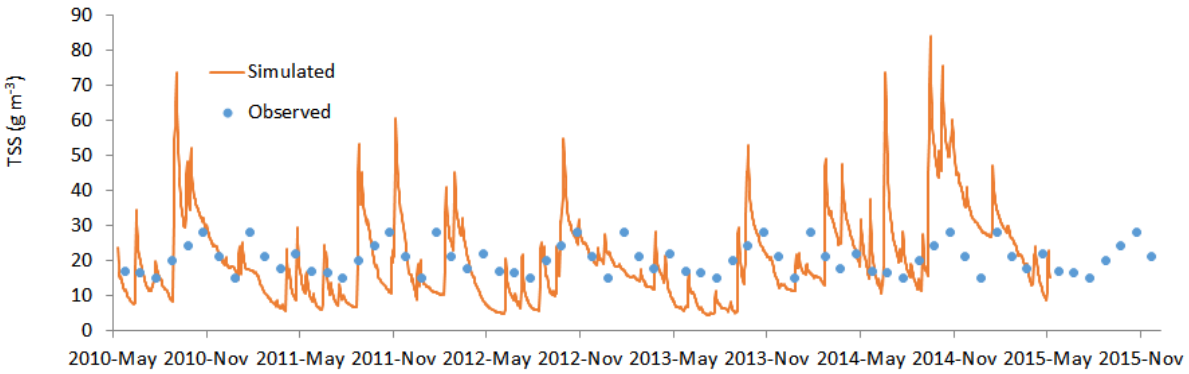

Figure 68: Observations (blue dots) and simulated (orange) total suspended solids concentrations at the surface. Observations are monthly medians of available observations, repeated annually.

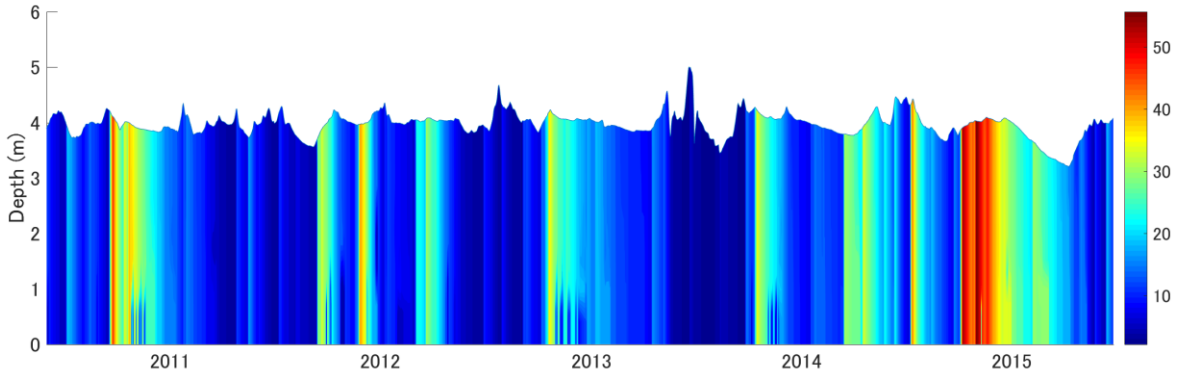

Figure 69: Simulated suspended solids concentration through the water column of Lake Ngāroto for the five-year simulation period. Colours represent suspended solids with the scale (g m^{-3}) on the right-hand side.

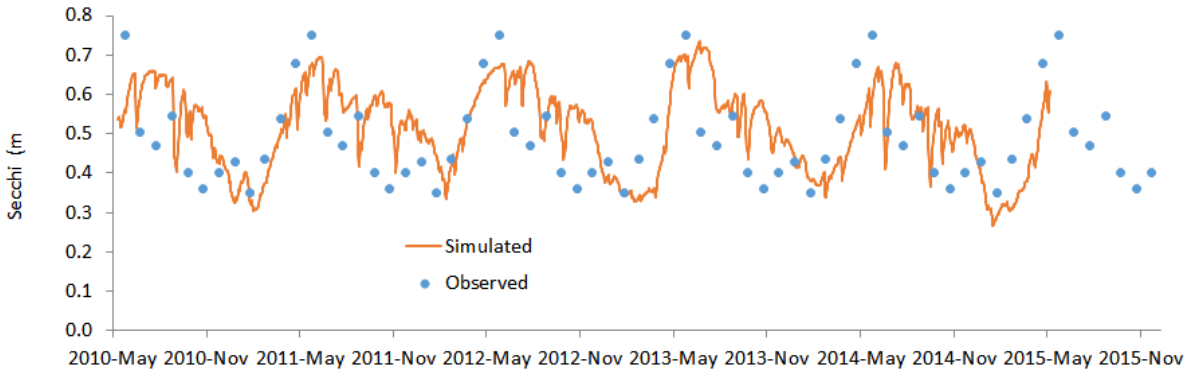

Figure 70: Observations (blue dots) and simulated (orange) Secchi disk depth. Observations are monthly medians of available observations, repeated annually.

Sensitivity to key parameters: uncertainty analysis

A sensitivity analysis was carried out with the calibrated Lake Ngāroto model. The sensitivity analysis involved 65 simulations with one-at-a-time (OAT) adjustment of the parameters to values ±10% of their calibrated value. The list of 65 parameters used for the OAT analysis is shown in Appendix A. Table 18 summarises these results by showing output metrics for any change in a state variable that are >±10% of the value in the calibrated model. The state variables chosen for this purpose were TP (surface and bottom), TN (surface and bottom), and chlorophyll *a* (surface and bottom). Only five parameters, when altered by ±10%, resulted in > ±10% change in any of these state variables. For Lake Ngāroto, the model simulation output is most sensitive to the density of particulate organic matter. This finding reinforces that it would be useful to quantify the size and nature of suspended material in the water column of Lake Ngāroto, as well as establishing setting velocities for it. Somewhat surprisingly, given that phytoplankton biomass in the simulations is dominated by cyanobacteria, a parameter which controls the temperature dependence of diatom growth was found to strongly influence chlorophyll *a* concentrations. This may be related to the importance of diatom sedimentation for nutrient fluxes. Unsurprisingly, parameters affecting the dynamics of cyanobacteria; the temperature multiplier and the buoyancy, were amongst the sensitive parameters.

Table 18: Summary of one-factor-at-a-time sensitivity analysis for Lake Ngāroto DYRESM-CAEDYM model.

TP surface		TP bottom		TN bottom		TCHLA surface		TCHLA bottom	
Parameter	**δ%**	**Parameter**	**δ%**	**Parameter**	**δ%**	**Parameter**	**δ%**	**Parameter**	**δ%**
Density of POM particles (labile) -10%	346	Density of POM particles (labile) -10%	284	Density of POM particles (labile) -10%	149	Temperature multiplier for phytoplankton growth (FDIAT) -10%	101	Temperature multiplier for phytoplankton growth (FDIAT) -10%	96
Density of POM particles (labile) +10%	18	Density of POM particles (labile) +10%	17	Density of POM particles (labile) +10%	16			Temperature multiplier for phytoplankton respiration (FDIAT) +10%	48
Temperature multiplier of sediment fluxes +10%	13							Temperature multiplier for phytoplankton growth (FDIAT) +10%	20
								Constant settling velocity (CYANO) -10%	18
								Temperature multiplier for phytoplankton respiration (FDIAT) -10%	18
								Temperature multiplier for phytoplankton respiration (CYANO) +10%	14

δ%: Relative percent difference of simulation with changed parameter value relative to base simulation

Results of the Monte Carlo approach to parameter sensitivity are presented in the form of ensemble simulations and summary statistics for the metrics shown in Table 1. The 713 model simulations are

summarised in Figure 71 in the form of time series of the median of all simulations surrounded by colour shaded probability density functions which show the statistical distribution of the entire ensemble of simulations for each day in the simulation. These graphs show that the ensemble median closely matches the time series of the calibrated base model for TP, TN and chlorophyll *a* and that the probability density functions are approximately symmetric around the median. This suggests that the model results, specifically the values of the diagnostic statistics, are robust to small random perturbations of the parameter space. The width of the probability density functions at any given day shows the range of possible concentrations of the state variable. This width can exceed the median multiple times, especially at peak concentrations. This indicates that the concentrations of maxima are most uncertain and variable. In chlorophyll *a* concentrations (Figure 65) summer concentrations can be very low under some parameter sets, suggesting that summer blooms may not occur, however, these cases are relatively rare.

The behaviour of the ensemble simulations for chlorophyll *a* in winter and spring is interesting as the base model shows a different trajectory to the median of the ensemble simulations. This suggests a bimodal probability distribution in which the model predicts either high or low concentrations, but the median concentration is actually an unlikely model solution. This base model consistently predicts a small phytoplankton (cyanobacterial) bloom in early spring and many random parameter sets also show this behaviour, but in many other parameter sets, this bloom is absent. Therefore, the confidence in our model predictions chlorophyll concentrations between winter and spring is lower than at other times.

Table 19 summarises the results of the Monte Carlo sensitivity analysis in terms of uncertainty around the simulation metrics of Table 1. The medians of the variables in the ensemble simulations are within 8% of those in the base simulation and within the interquartile range of the ensemble simulations. This match supports the interpretation of the time series of probability density, that the model with the base parameter set is generally robust to small random perturbations.

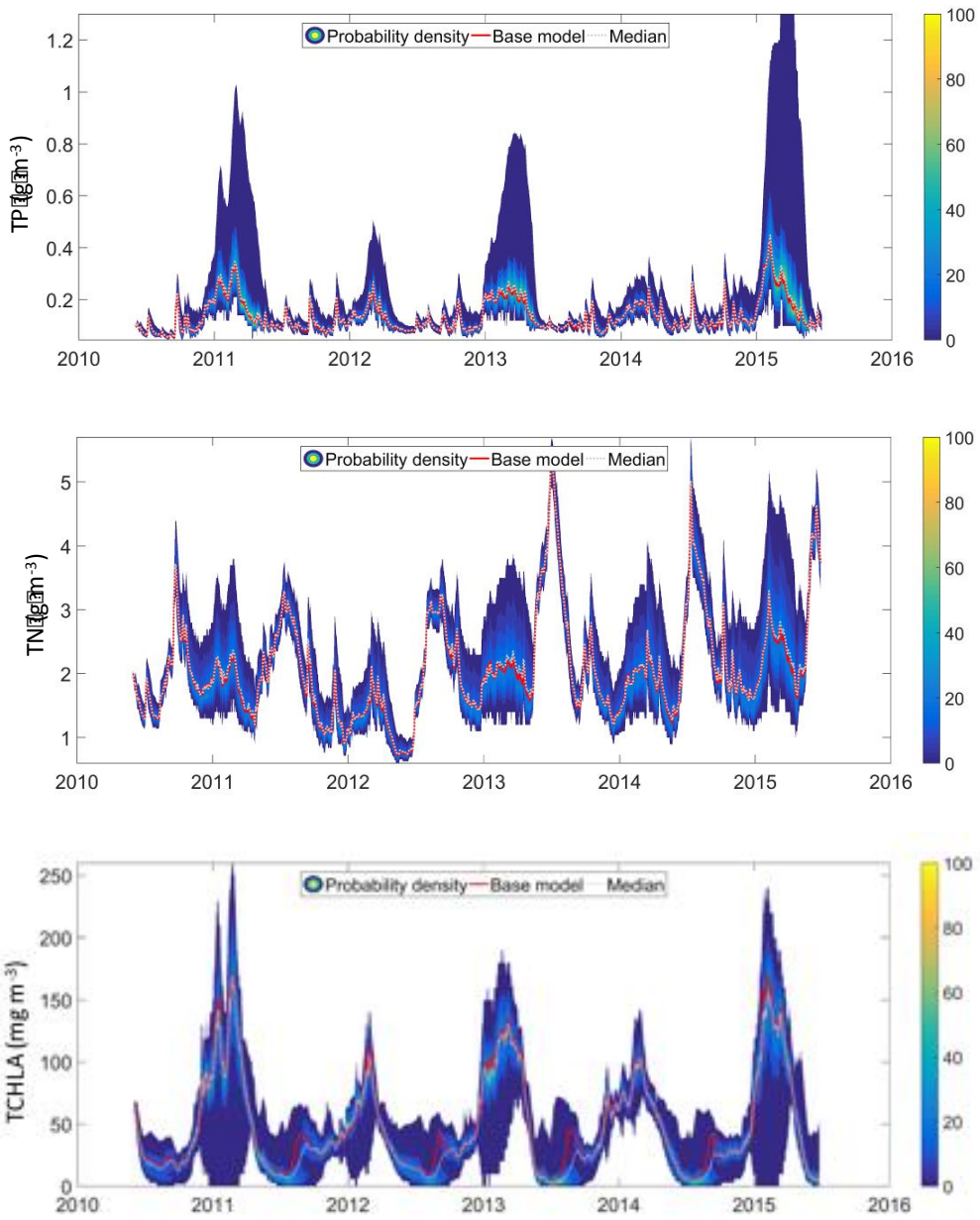

Figure 71: (a) Total phosphorus, (b) total nitrogen and (c) total chlorophyll *a* concentrations at the surface for the randomized parameter permutation results (N = 713) in Lake Ngāroto. The colour contour illustrates the empirical density estimates of the model results (in %), where the red and dotted grey lines show base model results and median value of the all model results respectively. The models which did not complete the simulation for various reasons have been removed from the analysis.

Table 19: Summary of the results of the Monte Carlo sensitivity analysis for Lake Ngāroto. See Table 2 for definition of 'Bloom'.

	TCHLA (mg m^{-3})	**TP (g m^{-3})**	**TN (g m^{-3})**	**SD (m)**	**dT>0.5 (^{o}C)**	**DO<2 mg L^{-1}**	**Bloom (mg m^{-3})**
75%	29.9	0.11	1.68	0.32	147.8	71.0	136.9
Ensemble medians	32.7	0.12	1.82	0.32	150.3	72.5	152.5
25%	37.3	0.13	2.05	0.33	153.3	74.5	179.3
Base simulation medians	34.2	0.11	1.81	0.33	151.5	72.0	165.0

Scenario simulation results

Fourteen simulations were carried out for Lake Ngāroto to examine the model response to the assigned scenarios (Figure 72). Despite reductions in internal and external nutrient loads of up to 50%, no scenario resulted in NOF status of the lake improving from the D band (Figure 73). The scenario most effective at reducing median TP, TN and TCHLA was N14 (50% external reduction for P and 50% anoxic release reduction for P) (Figure 72). Comparisons between scenarios which combine internal and external load reductions in N and P in various combinations (e.g., N3, N7, N13 and N14) suggest that chlorophyll *a* concentration is driven by a reasonably even combination of external and internal P loading, with much of the internal loading occurring during summer when phytoplankton growing conditions are most suitable (i.e., warmer water temperature and higher irradiance)

N7 (25% external reduction for N and P, 50% internal load reduction and diversion of inflow from Lake Ngārotoiti) achieved similar improvements in water quality to N14 (50% external reduction for P and 50% anoxic release reduction for P), but considering the results of all scenarios, it is clear that N7's improvements are largely due to internal and external P reduction only. Scenario N6 indicates that diverting water from Lake Ngārotoiti (N6) will have little effect on median water quality attributes in Lake Ngāroto. Figure 74 shows the percentage change of water quality attributes relative to the base simulation (N0). Summer chlorophyll and cyanobacteria concentrations can be quite strongly influenced by management actions in some of the scenarios (N4, N5, N7, N8 and N14), but temperature, days with DO < 2 mg L^{-1} and days with cyanobacteria chlorophyll > 15 mg m^{-3} were much less strongly influenced by the management actions exerted in these scenarios.

Increasing the water level by 0.5 m approximately doubles the median TSS concentration and therefore reduces Secchi depth by increasing the shallow area of the lake in which wind-driven turbulence can cause resuspension of sediments. This effect is a result of the topography of the lake

such that increasing water depth floods more shallow area than it deepens parts of the bottom beyond the reach of wind-driven turbulent wave action (Figure 75). This result is based on the assumption that the shallow sediment is devoid of emergent macrophyte vegetation, which, if present, could otherwise dampen turbulence and therefore reduce sediment resuspension. DYRESM-CAEDYM does not have a model specific to freshwater macrophytes.

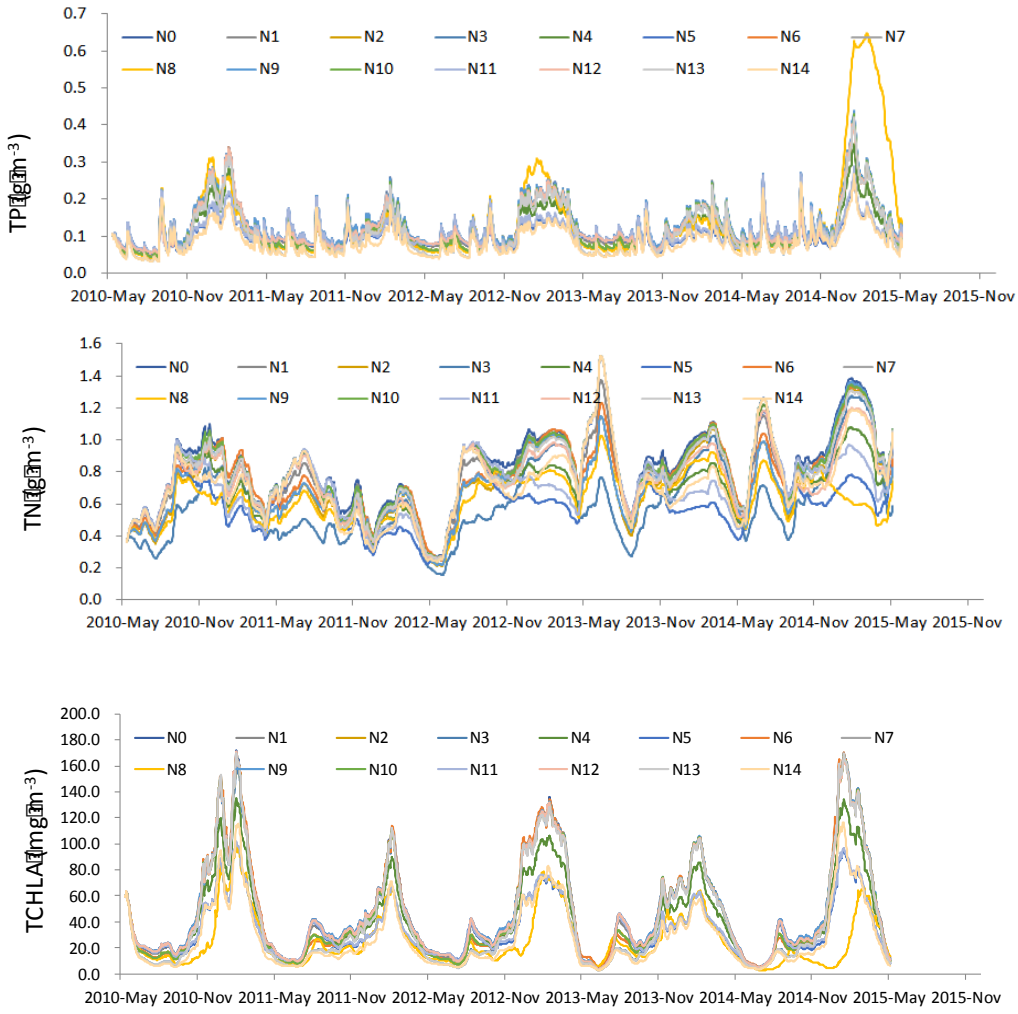

Figure 72: Simulated concentrations of total phosphorus, total nitrogen and total chlorophyll *a* concentrations at the surface for all the scenarios in Lake Ngāroto.

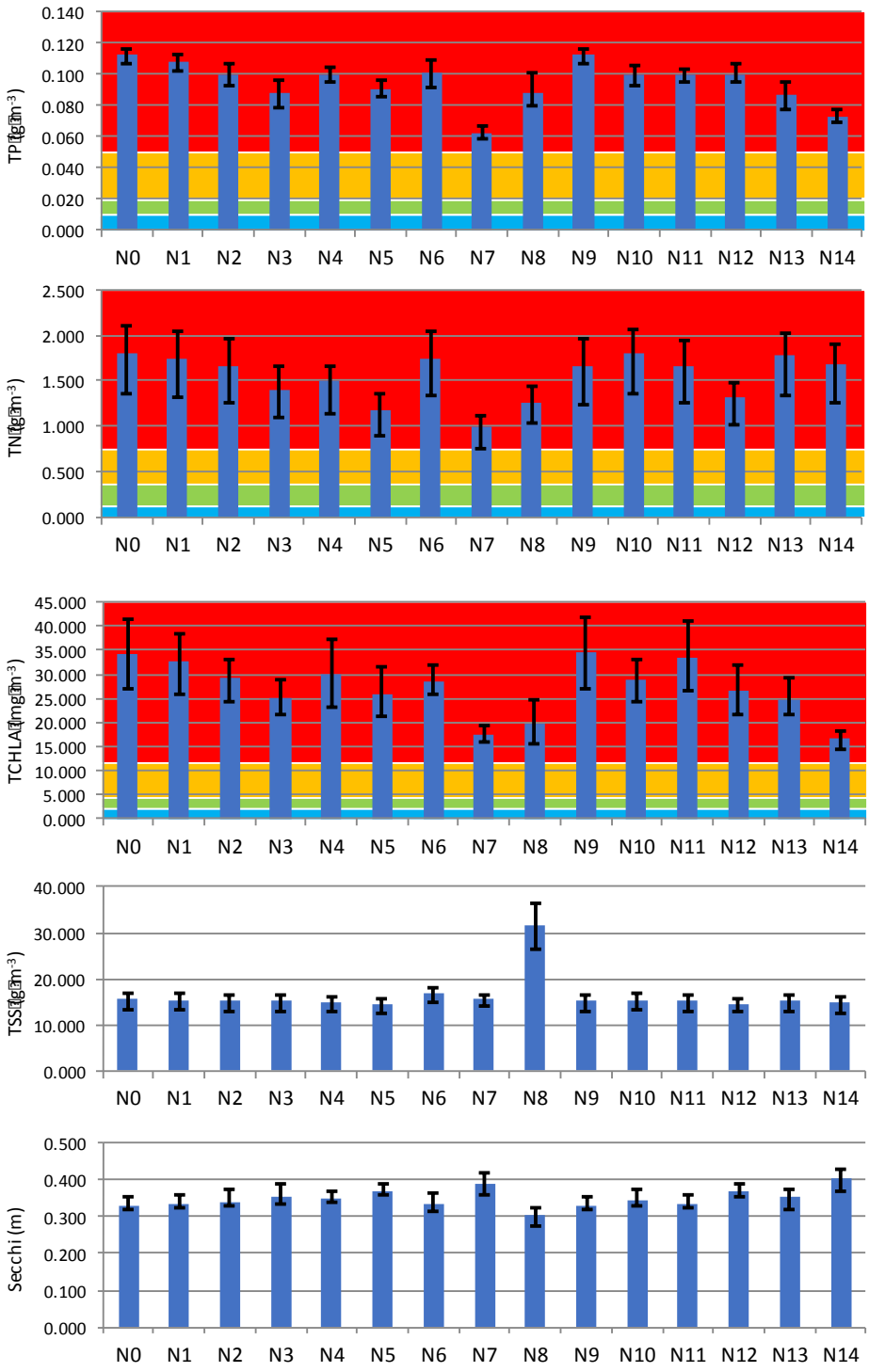

Figure 73: Bar charts of median water quality attributes for Ngāroto scenario simulations. Bar height is the average of five yearly medians, error bars are the minima and maxima of the five yearly medians. Coloured background in TP, TN and TCHLA charts indicate NOF bands (D: red, C: yellow, B: green, A: blue).

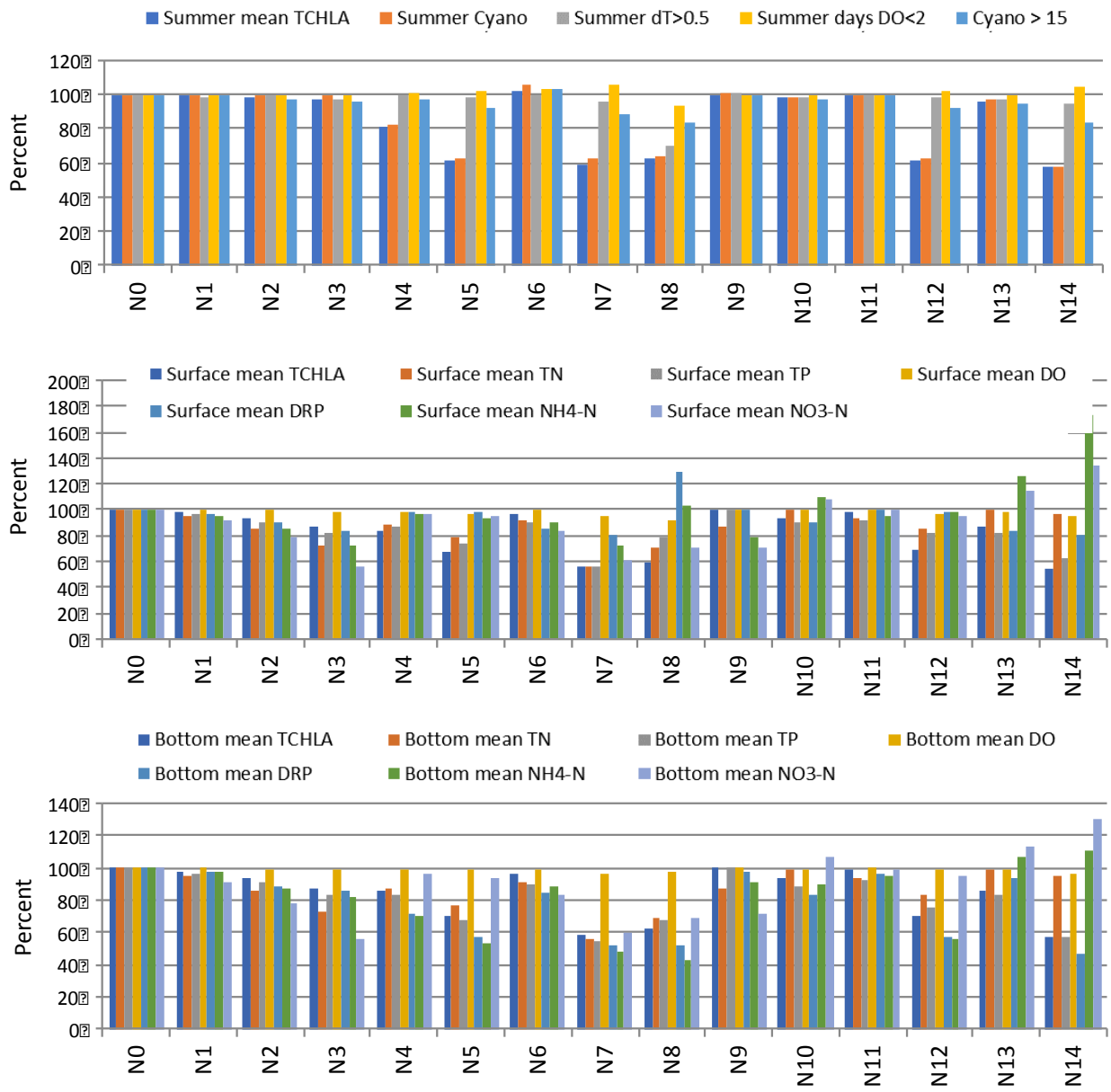

Figure 74: Bar graphs showing the percentage change of water quality attributes relative to the base simulation (N0) for Lake Ngāroto. The water quality attributes are defined in Table 1.

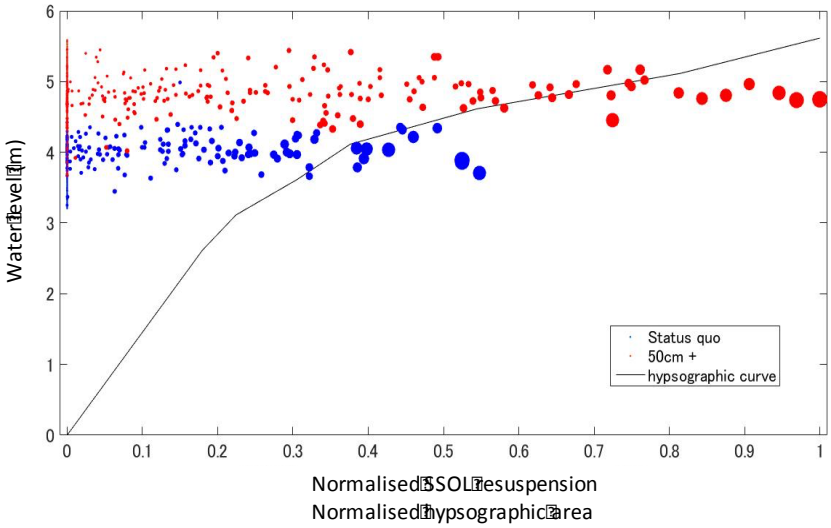

Figure 75: Suspended sediment concentration (SSOL, a fine fraction of sediments modelled with DYRESM-CAEDYM) where resuspension occurred divided by total area for the base simulation (Status quo) and scenario N8 (50 cm water level increase). The normalised hypsographic curve is provided to illustrate the increase in lake area with water level is increased. The size of the dots indicates wind speed (in relative units).

Validation of aggregation approach

The biogeochemical model of Lake Ngāroto was calibrated to an aggregated annual cycle derived from historic observations (see section *In-lake data for model calibration*). This section reports the results of a proof-of-concept experiment using a model for Lake Waahi where physical and biogeochemical variables are available from 1995 to present (see Figure 23 on page 48). In the same manner as for Lake Ngāroto: (1) We calculated a representative annual cycle for the biogeochemical variables from the monthly medians of all observations and calibrated; (2) the physical model was forced and calibrated using observations from 2010 – 2015; and (3) the biogeochemical model was calibrated to the annual cycle of monthly medians. The predictions of biogeochemical variables of this test model were compared to the actual observations from the model period (Figure 76) and the model fit was contrasted to that of the base model for Lake Waahi (Table 20). The comparison of the RMSE values from both models shows that, based on the RMSE, the base model is better only for some variables and that the model calibrated to a representative annual cycle outperforms the base model in the simulation of chlorophyll *a* and TN.

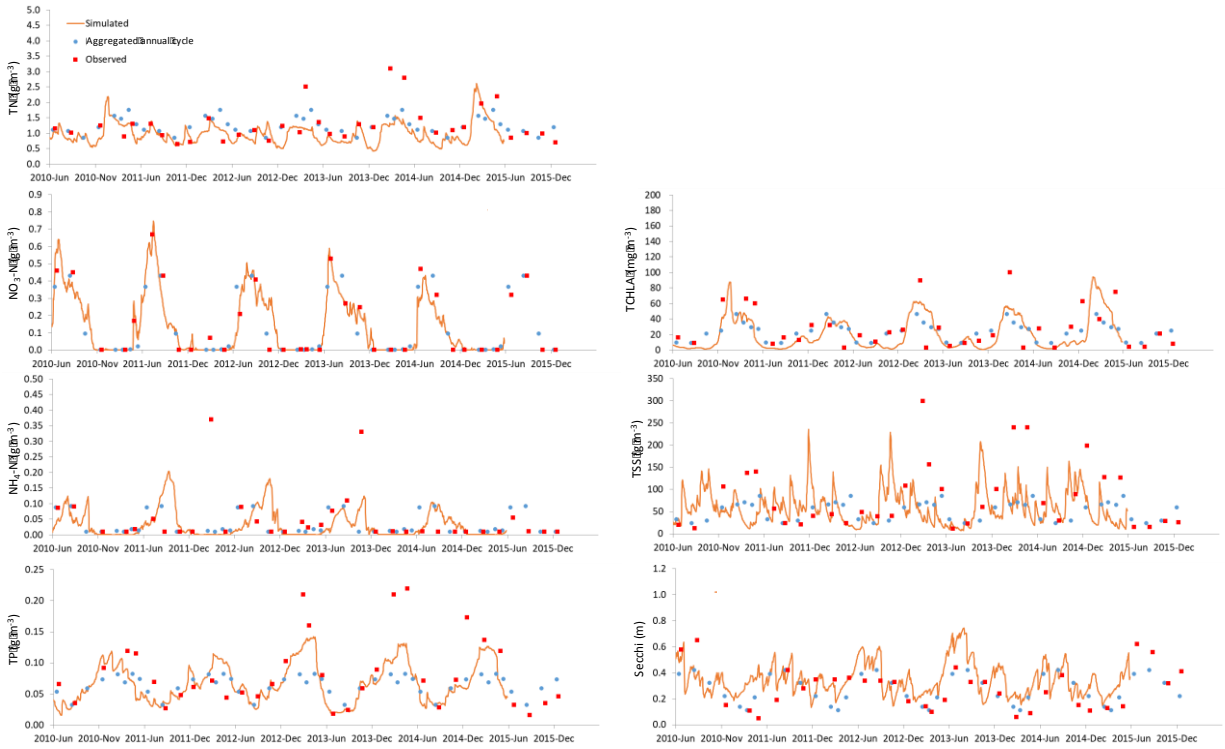

Figure 76: Results of the Lake Waahi model calibrated to a representative annual cycle of biogeochemical observations. The actual in situ observations are shown in red and the aggregated annual cycle of monthly median is shown as blue dots.

Table 20: Root-mean-square error of the base model against in situ observations and of the test model. Model fit statistics for the base model are taken from Table 23.

	TN ($g\ m^{-3}$)	TP ($g\ m^{-3}$)	TSS ($g\ m^{-3}$)	TCHLA ($mg\ m^{-3}$)
RMSE Base model	0.65	0.03	46.26	25.55
RMSE Test model	0.46	0.03	72.05	21.00

Summary

At a depth of four metres depth, Lake Ngāroto is a peat lake of intermediate depth compared with Lake Waahi (shallower) and Lake Rotomānuka (deeper). This intermediate depth allows occurrence of both internal drivers of nutrient dynamics — wind-driven sediment resuspension and low-oxygen-enhanced sediment release, albeit at different times of the year. Table 21 provides a comparison of the estimated amounts of the constituents that are contributed from external (catchment) discharge, in-lake sediment resuspension and release of dissolved nutrients from the bottom

sediments. This table shows that the external contribution of nitrogen is more important than for phosphorus and suspended sediment, because resuspension of bottom sediments has a major impact on the levels of sediment and phosphorus in the water column. By contrast, for nitrogen, which is contained almost entirely as particulate organic nitrogen within the bottom sediments, sediment resuspension represents only a fraction (~ 33%) of the catchment load.

Table 21: Lake Ngāroto annual mean total nitrogen, total phosphorus and suspended sediment (kg ha^{-1} y^{-1}) contributed from external (catchment) loads, sediment resuspension and release of dissolved nutrients from bottom sediments. Area normalisation to lake surface area as derived from the hypsographic curve used for the model (88.3 ha).

		External	Resuspension	Sediment release
Phosphorus (kg ha^{-1} y^{-1})	Mean	19	21	16
	Range	15 – 26	20 – 22	16 – 20
Nitrogen (kg ha^{-1} y^{-1})	Mean	446	150	139
	Range	217 – 841	14 – 163	123 – 162
Sediments (kg ha^{-1} y^{-1})	Mean	982	5,053	-
	Range	698 – 1,333	4,334 – 5,569	-

Table 22: Proportion (% Carp) of sediment, total phosphorus and total nitrogen inputs to Lake Ngāroto due to carp resuspension in relation to the total inputs (external + internal loads), proportion of external to total internal inputs (External/ Internal) and resuspension to sediment nutrient release ratio (Resuspension/ Sediment release) for Lake Ngāroto.

	% Carp	External / Internal	Resuspension / Sediment release
Phosphorus	3	0.53	1.33
Nitrogen	3	1.54	1.08
Sediments	16	0.19	-

Comparisons between scenarios which combine internal and external load reductions in N and P in various combinations (e.g., N3, N7, N13 and N14) suggest that chlorophyll concentration is driven by both external and internal P loading. The scenario most effective at reducing median TP, TN and TCHLA was a 50% external reduction for P and 50% anoxic release reduction for P (N14). Scenario N6 confirms that diverting water from Lake Ngārotoiti is not predicted to improve median water quality attributes in Lake Ngāroto. Despite reductions in internal and external nutrient loads of up to 50%, no scenario resulted in NOF status of the lake improving from the D band.

Lake Ngāroto has a diverse fish community and has been extensively fished between 2001 and 2015 with a combination of fyke netting, gill netting, and boat electrofishing. Considering this, the changes in fish community are probably the best known of the four lakes in this study. There is a relatively modest biomass of koi carp (about 72 kg ha^{-1}) but catfish are very abundant in this lake. Since 2001, however, catfish have declined from 73% to 36% of the fish population by number. Over the same period, shortfin eels have increased from 6% to 54% of the fish community, which is a nine-fold increase. Longfin eels have increased in abundance from 0.14% to 6% of the fish community (a 43-fold increase). This lake is closed to commercial eel fishing, which has probably allowed the increases in eel abundance. These changes in the fish community were determined with the same technique (fyke netting), so are reliable indicators of ecosystem changes. Despite the general improvements in the fish community towards greater proportion of native species, benthivorous fish still have the potential to make a significant contribution to suspended sediment and nutrient concentrations in lakes by resuspending bottom sediments. Carp contribute around 3% of the total (internal + external) nitrogen and phosphorus loads to Lake Ngāroto (Table 22) and about 16% of the total sediment load (but note that several caveats are applicable to these calculations in section *Overview of key processes and modelling of the study lakes* of the *Extended conclusions*).

The Lake Ngāroto food-web was well resolved using isotope biplots (Figure 136 in Appendix E). Isotope data indicate that the food base was dominated by organic matter most likely primarily of terrestrial origin although this appeared to vary seasonally with seston apparently more important in spring. Large eels (note short-fins only are presented in plots) were at the top of the food-web in both seasons with other fish/size classes generally closely grouped in biplot space. There was some suggestion of dietary overlap between catfish and small-medium sized eels in summer, confirmed by subsequent gut analyses (Collier et al. in prep.). This potential overlap in diet between catfish and eels suggests that management outcomes targeting an increase in eel biomass may simultaneously need to control catfish numbers. Common carp were similar to large catfish in the spring sample, presumably reflecting a similar benthic diet.

Lake Waahi

Calibration-validation process

The main focus of achieving an acceptable calibration for Lake Waahi was on reproducing temperature, surface and bottom DO, TN, TP, TSS, and chlorophyll *a* represented as a total value. The statistical comparison (Table 23) was deemed reasonable by comparison with other modelling applications. Lake Waahi represented a lake with a moderate amount of data for which it was possible to input variability in inflow data for the entire simulation period and have in-lake data for calibration for the simulation also. The high RMSE values for TSS and chlorophyll *a* in this model relative to the models for the other lakes reflect the extreme range of concentrations observed in Lake Waahi and their short-term variability. This lake also displays more interannual variability in the five-year time series than the other lakes.

Table 23: Model performance for Lake Waahi using root mean square error (RMSE) and coefficient of variation of root mean square deviation CV(RMSE) for high frequency buoy observations (n > 360; surface temperature: Tsrf, bottom temperature: Tbtm, surface dissolved oxygen: DOsrf, bottom dissolved oxygen: DObtm) and manual sampling results (n = 30; total nitrogen: TN, total phosphorus: TP, total suspended solids: TSS, total chlorophyll *a*: TCHLA).

	Tsrf (°C)	**Tbtm (°C)**	**DOsrf (mg L^{-1})**	**DObtm (mg L^{-1})**	**TN (g m^{-3})**	**TP (g m^{-3})**	**TSS (g m^{-3})**	**TCHLA (mg m^{-3})**
RMSE	0.93	1.16	1.02	1.11	0.65	0.03	46.26	25.55
CV(RMSE)	0.05	0.07	0.11	0.13	0.49	0.39	0.51	0.84

Key characteristics based on models and observations

Two measured sources of temperature were available to examine the accuracy of simulation outputs of this variable. One was measurements made manually at approximately bimonthly intervals (surface waters) or less frequently (bottom waters), and the other was automated measurements made from a lake buoy. As noted in Figure 77, the simulations provide an excellent match to automated observations over a period of one year (2014-15). By contrast, there are discrepancies between the simulated data and the manually measured data. Most of these discrepancies can be attributed to the observed data being considerably warmer in winter. The manual observations are also substantially warmer than the automated observations although overlapping years have not been examined. We are unsure of why water temperature is up to 3 to 4°C warmer in winter in the manual observations but we suggest that the buoy data and the model

simulations more accurately quantify the surface and bottom temperatures in Lake Waahi than the earlier manual data, as well as providing a semi-continuous record.

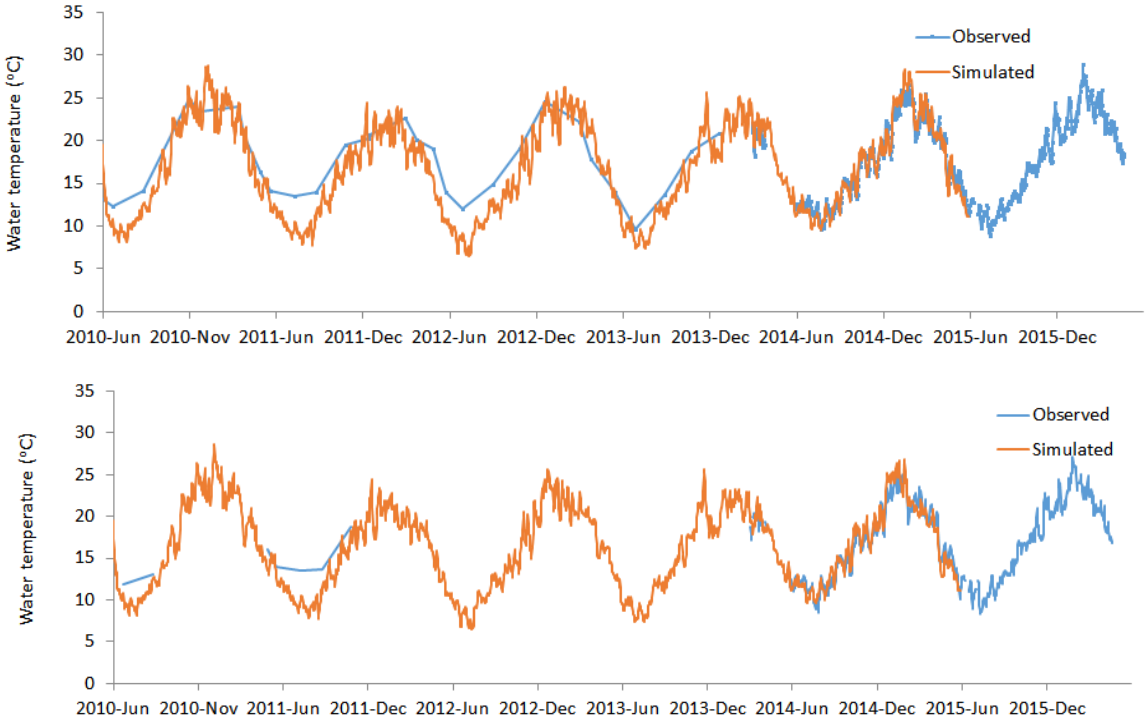

Figure 77: Surface (top) and (bottom) bottom (2 m) water temperature for Lake Waahi. Orange line is the simulated values, and blue line is observed values. Observations of temperature were from a high-frequency monitoring buoy.

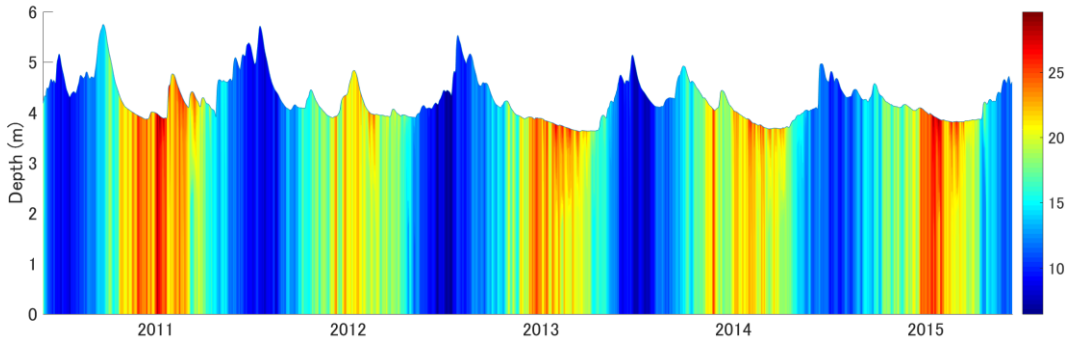

Figure 78: Temperature through the water column of Lake Waahi for the five-year simulation period. Colours represent water temperature with a scale (°C) given on the right-hand side.

Model temperature output over all depths can be visualized with heat maps based on elevation above the bottom of the lake (vertical axis) and time (horizontal axis) (Figure 78). Aside from showing the large water level fluctuations between summer and winter (> 1 m maximum) in Lake Waahi, the heat maps show periods of stratification which are most clearly evident in late summer when there is a warm surface layer of depth c. 1 m deep and temperature in this layer is commonly around 25°C.

The stratification intensity, indicated by the difference in temperature between surface and bottom waters (Figure 79), and the duration of stratification (Figure 80), indicated by the temperature gradient between surface and bottom waters, is well captured by the model simulations. Gradients of temperature >5°C occurred between surface and bottom waters in Lake Waahi and there were periods of continuous stratification of up to 20 days. There may have been a tendency for the model to under-predict stratification in winter when the buoy data suggest there was stratification for periods of a day or so, but it is likely that for this time of year the stratification would not persist (i.e., mixing would be expected to occur overnight) and so the inability of the model to pick up the winter stratification inconsequential in terms of its ecological consequences.

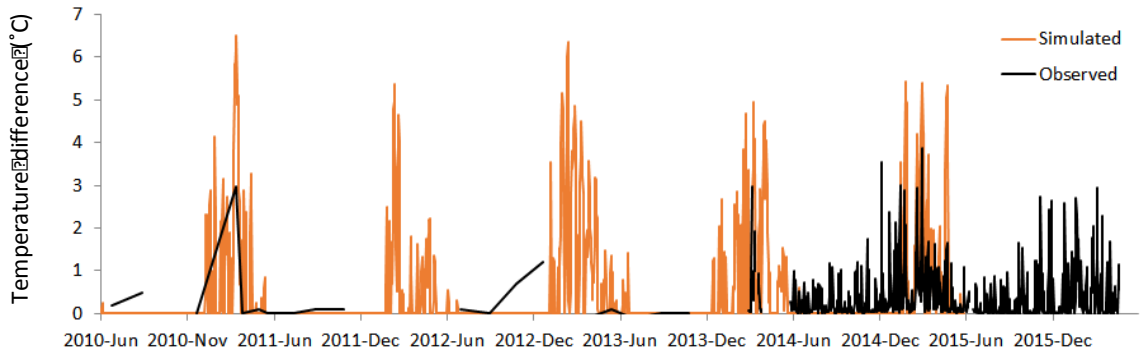

Figure 79: Observed (black line) and simulated (orange line) differences in water temperature between the surface and 2 m for Lake Waahi.

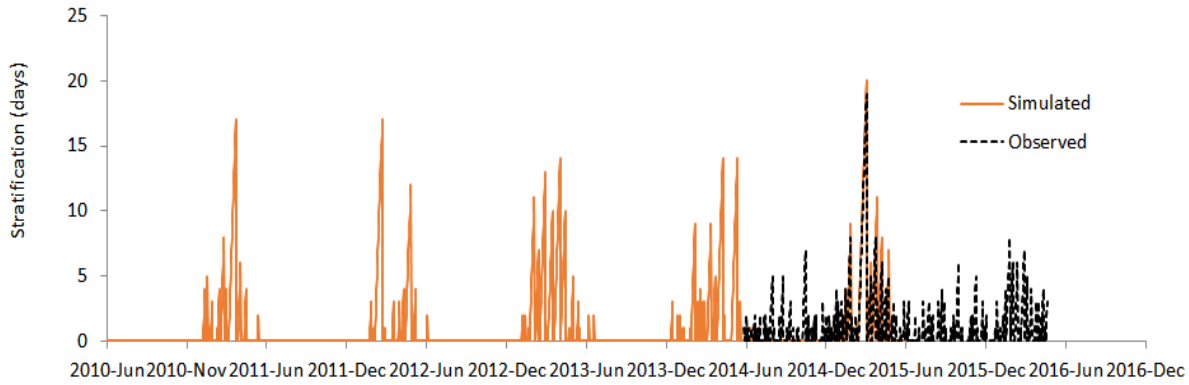

Figure 80: Top: Temperature difference between surface and bottom water temperature from observations (black line) and model simulation (orange line) in Lake Waahi. Bottom: Duration of stratification events (as defined in Table 1) for Lake Waahi.

Dissolved oxygen concentrations followed an expected seasonal pattern of higher in winter than summer (Figure 81), aligning with increased saturation capacity of cooler waters. The model simulations generally reproduced the observations of surface DO well but with a slight tendency for under-prediction in winter when observed DO was slightly super-saturated. An interesting feature of the observations was a prolonged and continuous decline at the lake buoy site beyond the duration of the simulations. Levels of DO at the end of the period shown in Figure 81 had declined to be just

above 50% of saturation values. This period corresponded to very warm water temperature. The model simulations of DO for bottom waters provided an excellent match with observations – both manual and automated. Simulated DO in bottom waters closely matched surface waters except during periods of stratification when anoxia (< 2 mg L^{-1}) occurred but there was not complete loss of DO from bottom waters (Figure 81). This is well illustrated in Figure 82 which shows simulated DO concentrations throughout the water column. The region of hypoxia commonly extended from the lake bed to as high as 1 m from the water surface during more prolonged periods of stratification. Incidences of seasonal hypoxia appeared to vary through the simulation period, being more severe in 2013 and 2015, but notably more common in the latter half of the study period.

The model simulations of TN provided a modest fit to observed data (Figure 83). The simulations through the entire water column indicated that concentrations tended to be reasonably homogenous with depth but were highly variable through time (Figure 84). Based on the difference between NH_4-N and NO_3-N, a considerable portion of the TN was in organic form, most as particulate material in detritus and phytoplankton biomass. The processes governing this constituent of N are likely to be less well quantified and have multiple governing fluxes than those for NH_4-N (Figure 85). For NH_4-N it was evident that anoxic releases from the lake bed, in combination with limited nitrification under the prevailing anoxic conditions, led to the buildup of NH_4-N during stratification events, with the NH_4-N rapidly transported through the entire water column during subsequent mixing events (Figure 86). By contrast, NO_3-N concentrations in model simulations, which very accurately matched observations (Figure 87), were highly seasonal, with a mid-winter (i.e. mid-year) peak, typically following by a gradual decline until the end of the year. For the remaining part of the year (i.e., Jan to May), NO_3-N concentrations were at or close to detection limits (Figure 88).

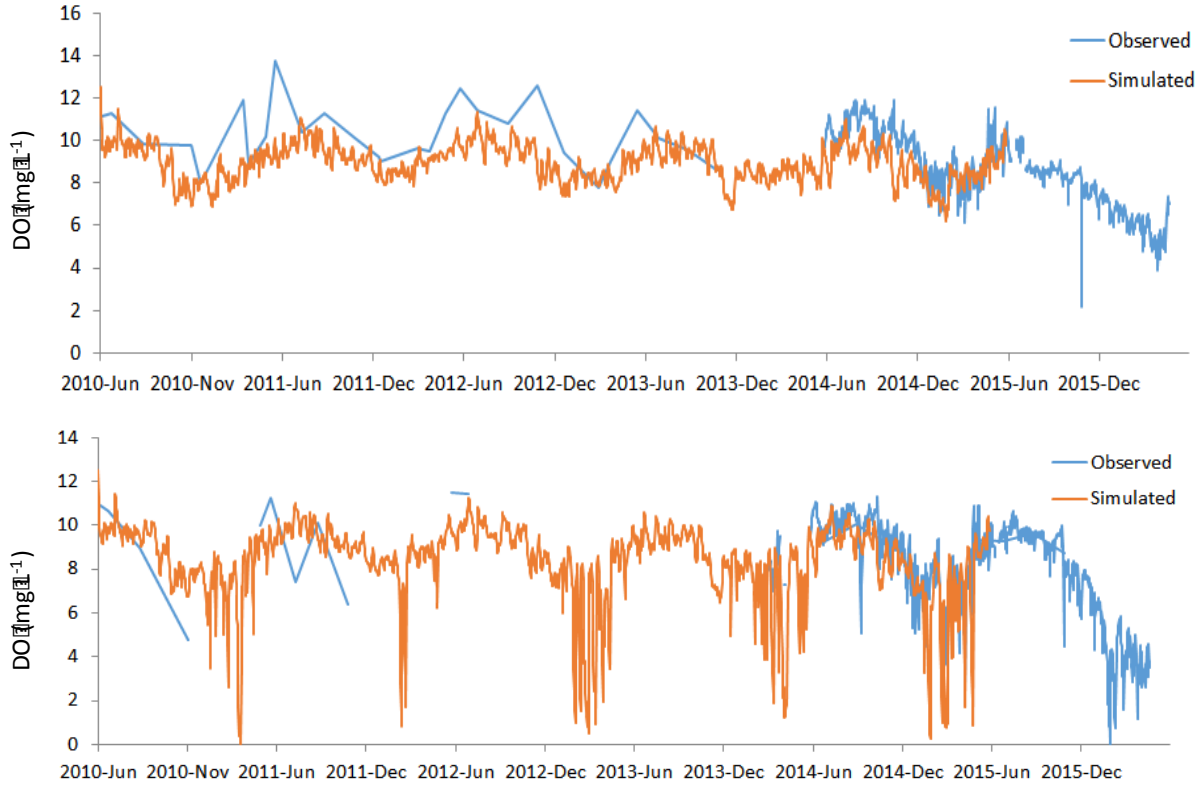

Figure 81: Top: surface dissolved oxygen for Lake Waahi; Bottom: dissolved oxygen at 2 m. Orange line is the simulated values, and blue line is observed values. Observations of temperature were from a high-frequency monitoring buoy.

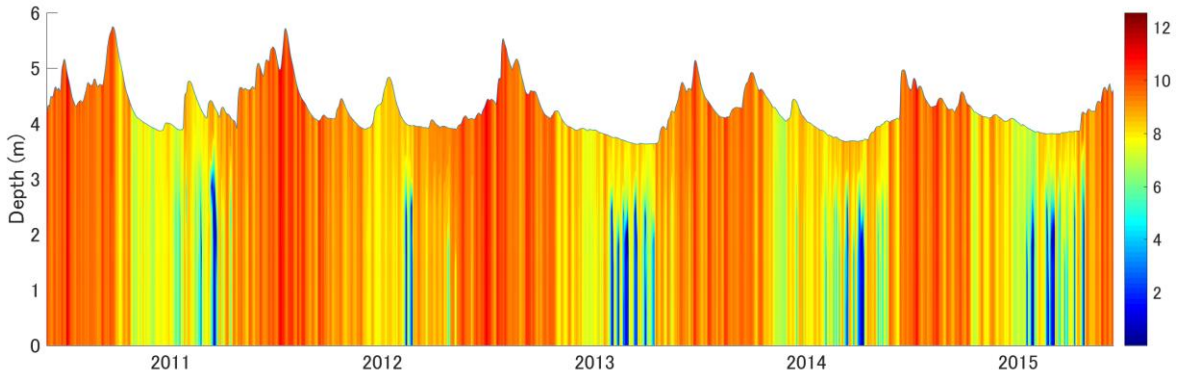

Figure 82: Dissolved oxygen through the water column of Lake Waahi for the five-year simulation period. Colours represent dissolved oxygen with a scale (mg L^{-1}) given on the right-hand side.

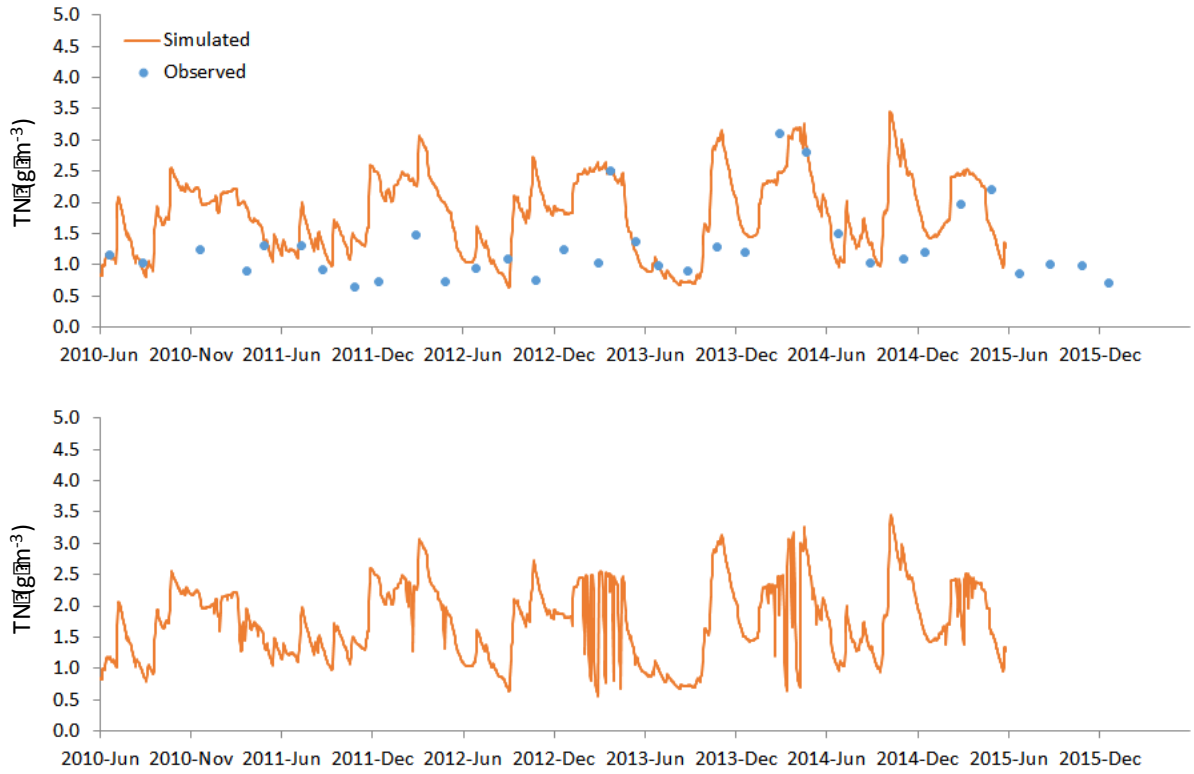

Figure 83: Observations (blue dots) and simulated values (orange line) of total nitrogen concentration at (top) the surface and (bottom) bottom-water location for the five-year simulation period for Lake Waahi.

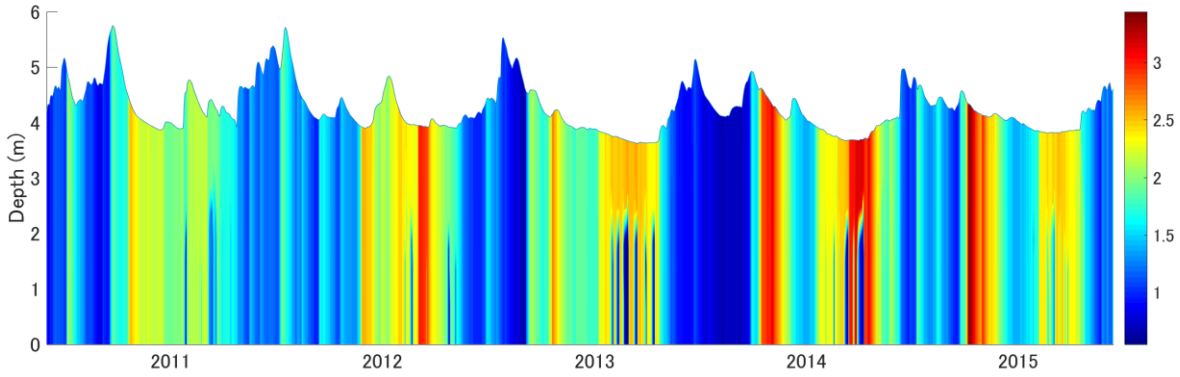

Figure 84: Total nitrogen through the water column of Lake Waahi for the five-year simulation period. Colours represent dissolved oxygen with a scale (mg L^{-1}) given on the right-hand side.

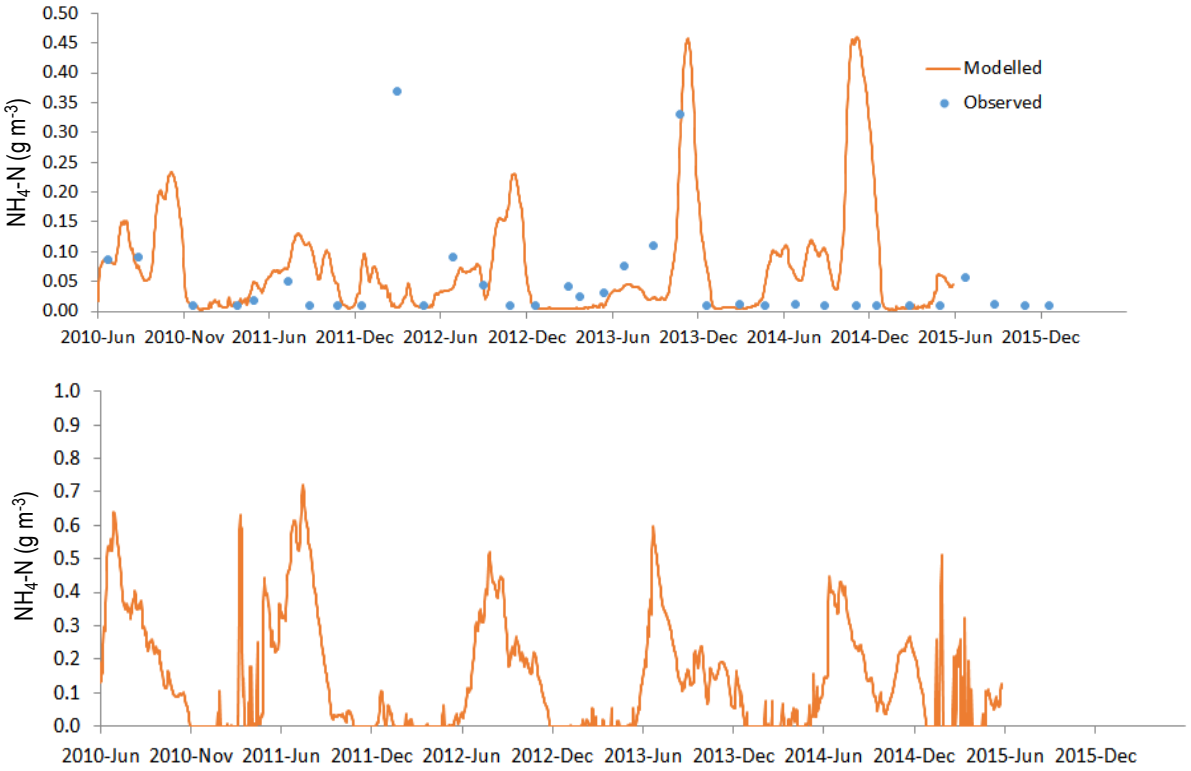

Figure 85: Observations (blue dots) and simulated values (orange line) of ammonium concentration at (top) the surface and (bottom) bottom-water location for the five-year simulation period for Lake Waahi.

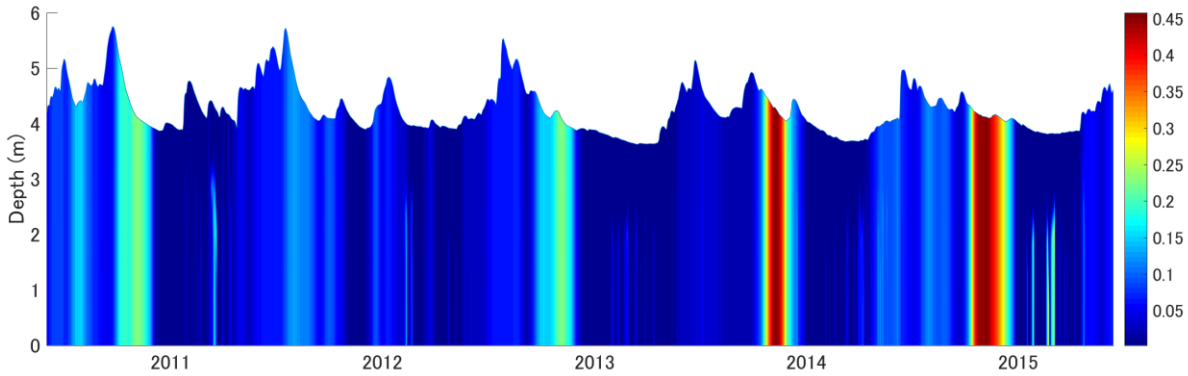

Figure 86: Ammonium (NH_4-N) concentrations through the water column of Lake Waahi for the five-year simulation period. Colours represent NH_4-N with a scale (mg L^{-1}) given on the right-hand side.

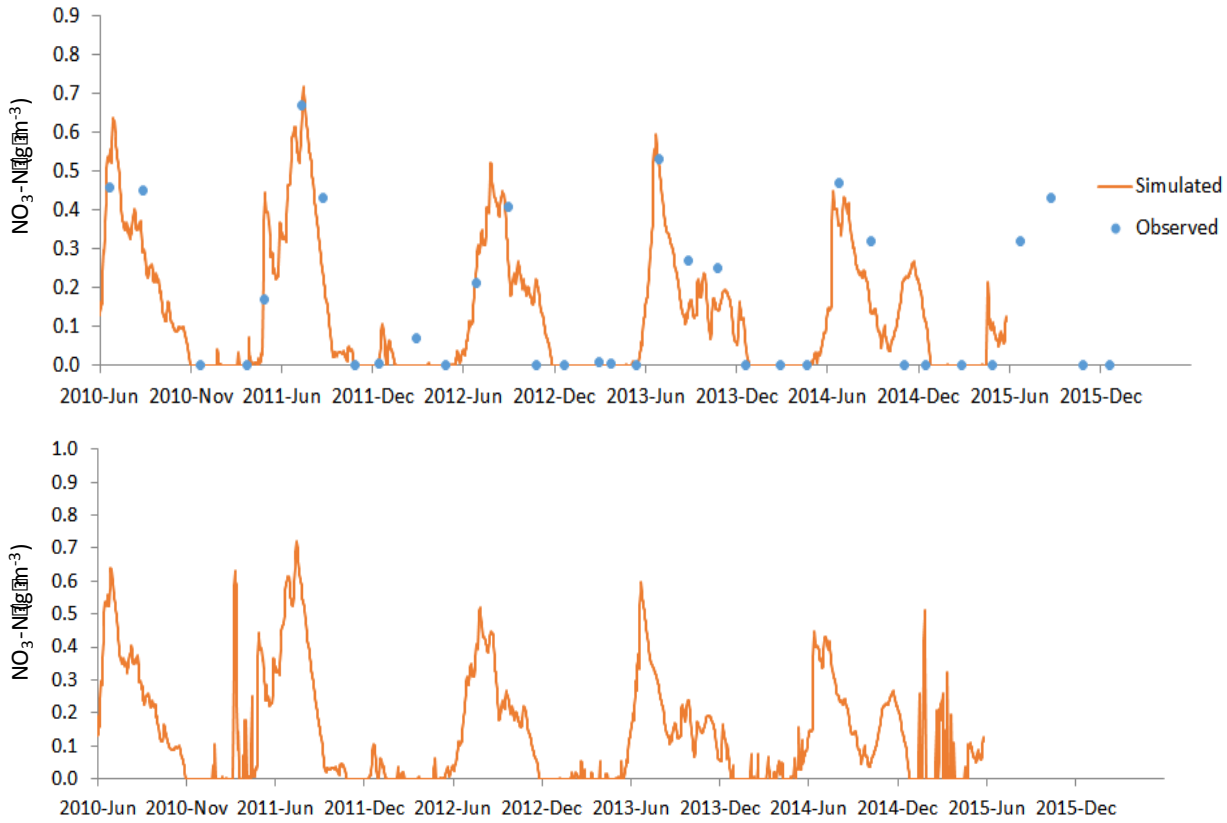

Figure 87: Observations (blue dots) and simulated values (orange line) of nitrate concentration at (top) the surface and (bottom) bottom-water location for the five-year simulation period for Lake Waahi.

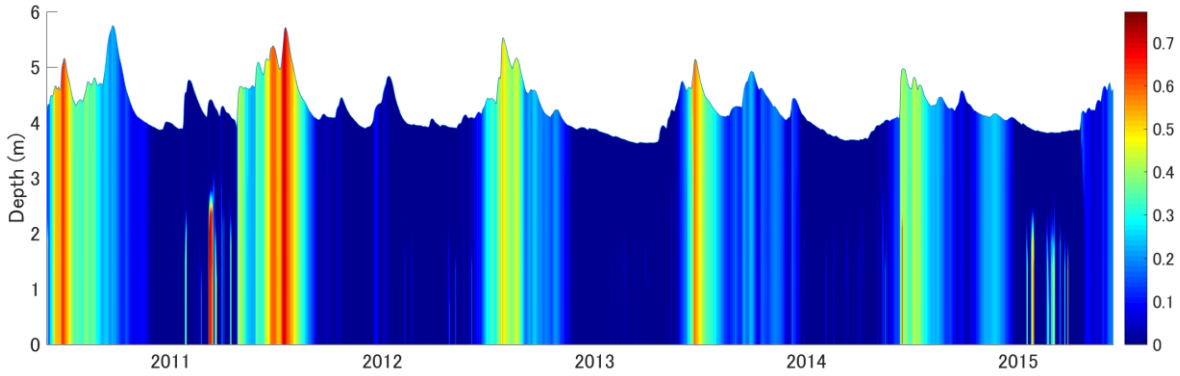

Figure 88: Nitrate (NO_3-N) through the water column of Lake Waahi for the five-year simulation period. Colours represent NO_3-N with a scale (g m^{-3}) given on the right-hand side.

Like nitrate, model simulations of total phosphorus captured the magnitude and seasonality of variation in observations (Figure 89). In the case of TP, however, concentrations were maximal in late summer-early autumn (in both observed and simulated data), as opposed to winter. There was generally little variation in concentration between surface and bottom waters (Figure 90). Concentrations were up to 0.25 g m^{-3} in surface waters which is well above the value of 0.05 g m^{-3} where a lake would fail to meet the bottom line in the NOF. Notably, however, concentrations declined to quite low values (c. 0.03 g m^{-3}) in late winter. On the basis of some stratification of TP through the water column in late summer (Figure 90), it appears that high values of TP are associated with periods of increased cyanobacteria biomass. This is reinforced by the simulated DRP concentration in bottom waters, which is a relatively small fraction of the TP except when there are 'spikes' associated with bottom-sediment resuspension (Figure 91, Figure 92). At other times the model simulates concentrations of DRP in surface and bottom waters that are close to detection limits, as observed in observed data. Unless detection limits are improved, there seems little point in continuing to monitor DRP when observations are almost all being recorded as non-detects. Like Lake Ngāroto, the low levels of DRP are probably due to strong sorption of this plant-available compound to the abundant fine inorganic suspended solids in the water column. This sorbed P should not necessarily be regarded as unavailable, however, and it may be desorbed when there is high biomass of P-starved cells (e.g., during a cyanobacterial bloom).

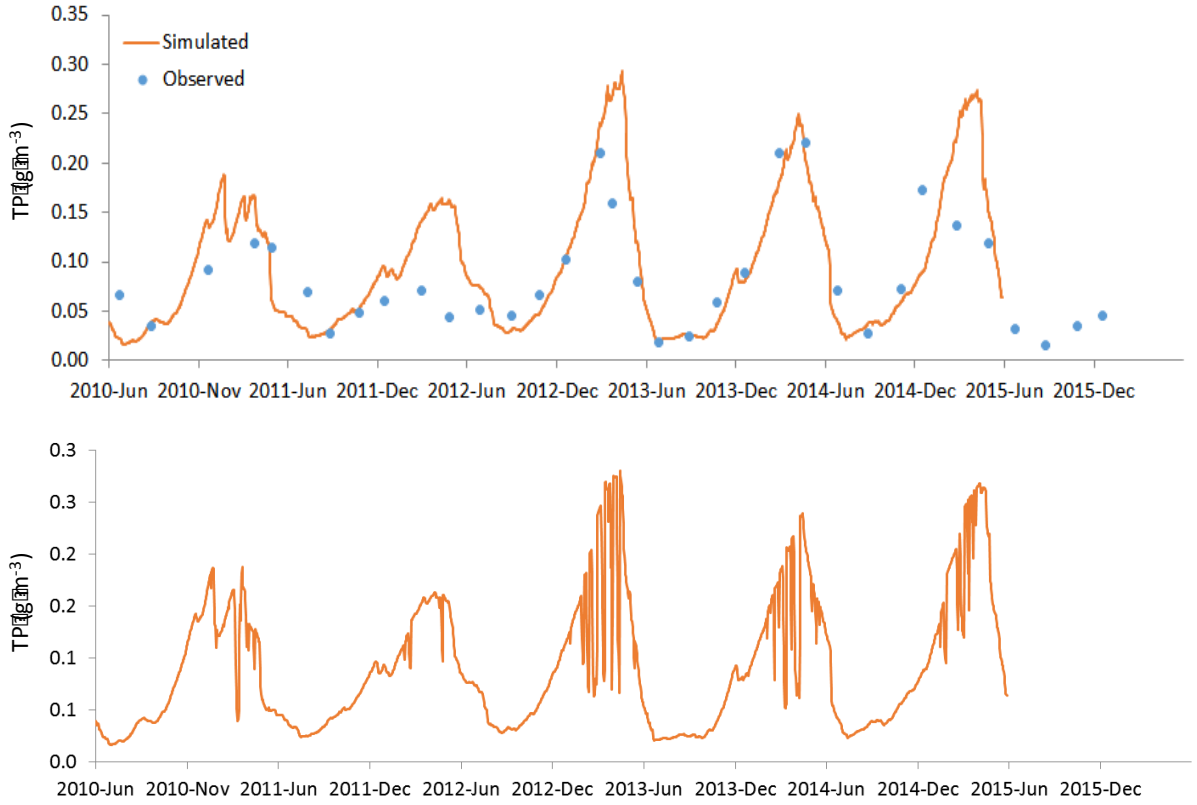

Figure 89: Observations (blue dots) and simulated values (orange line) of total phosphorus concentration at (top) the surface and (bottom) bottom-water location for the five-year simulation period for Lake Waahi.

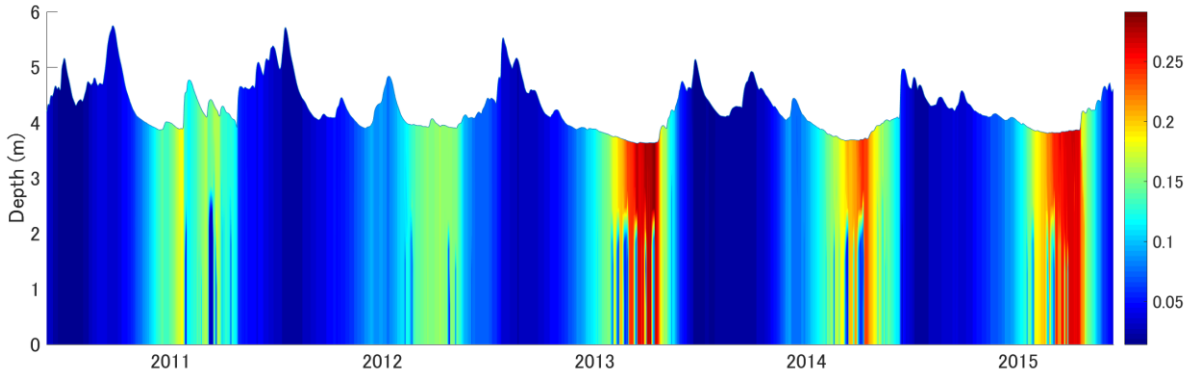

Figure 90: Total phosphorus through the water column of Lake Waahi for the five-year simulation period. Colours represent TP with a scale (g m^{-3}) given on the right-hand side.

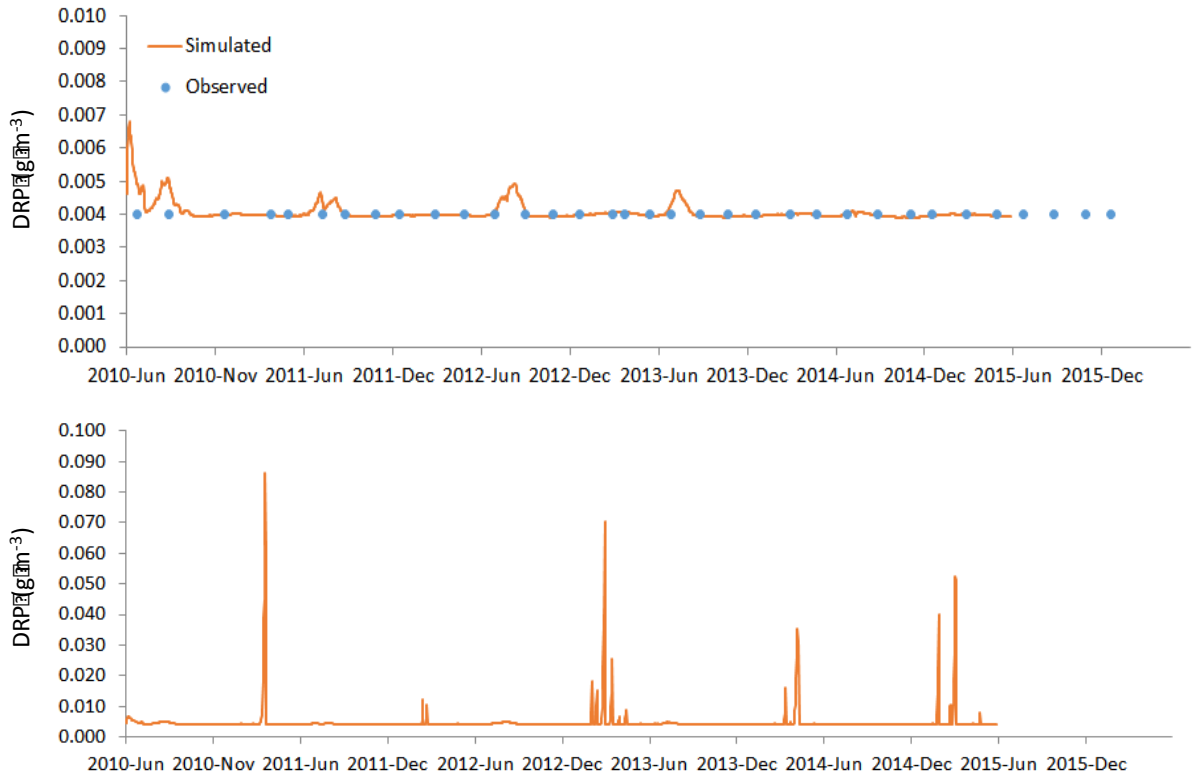

Figure 91: Observations (blue dots) and simulated values (orange) of DRP concentration at (top) the surface and (bottom) bottom-water location for the five-year simulation period for Lake Waahi.

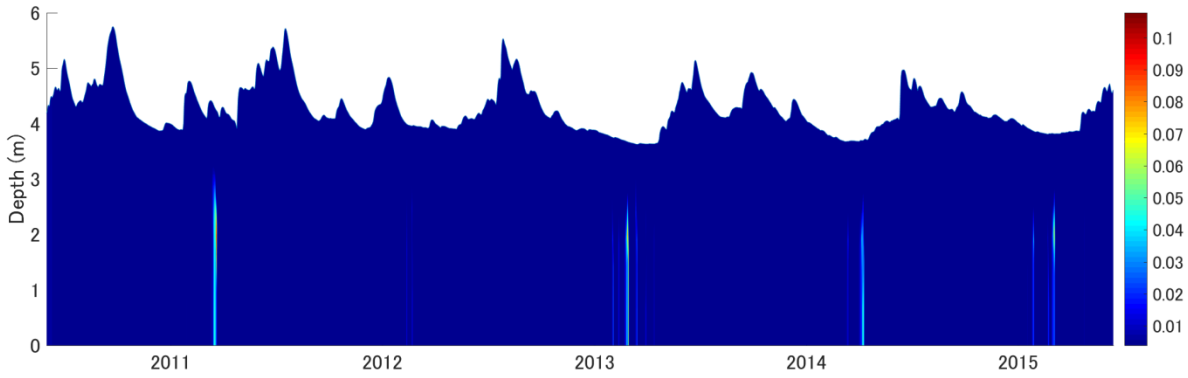

Figure 92: Dissolved reactive phosphorus (DRP) concentrations through the water column of Lake Waahi for the five-year simulation period. Colours represent TP with a scale (g m^{-3}) given on the right-hand side.

Observed concentrations of total chlorophyll *a* show strong seasonal and inter-annual variation (Figure 93). We consider the simulations of chlorophyll *a* replicate the observed data reasonably well, capturing the magnitude of the peaks and the general timing of the troughs (later winter). Water column concentrations of chlorophyll *a* are mostly homogeneous except when there is stratification in summer, which results in brief periods of low chlorophyll *a* in bottom waters and elevated concentrations in surface waters (Figure 94). Considering that cyanobacteria dominate the phytoplankton assemblage (both observed and simulated data), these periods correspond to surface cyanobacteria blooms.

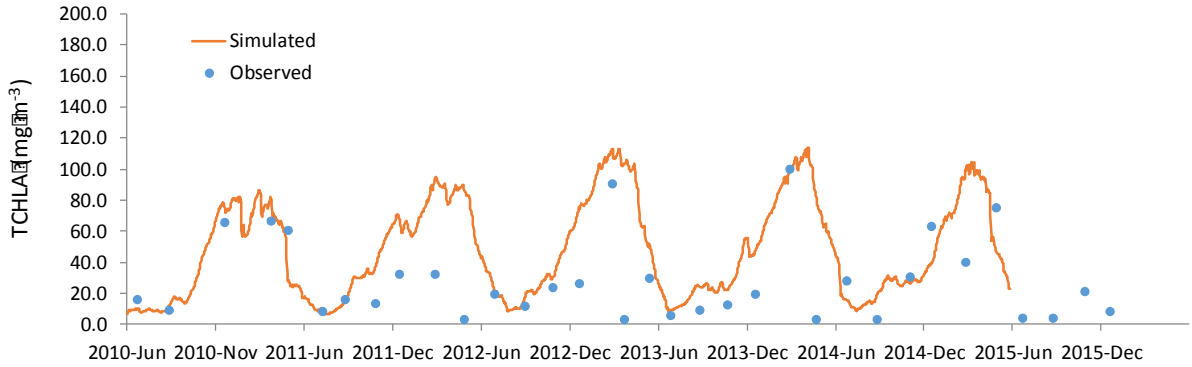

Figure 93: Observations (blue dots) and simulated values (orange) of chlorophyll *a* concentration at the surface water location for the five-year simulation period for Lake Waahi.

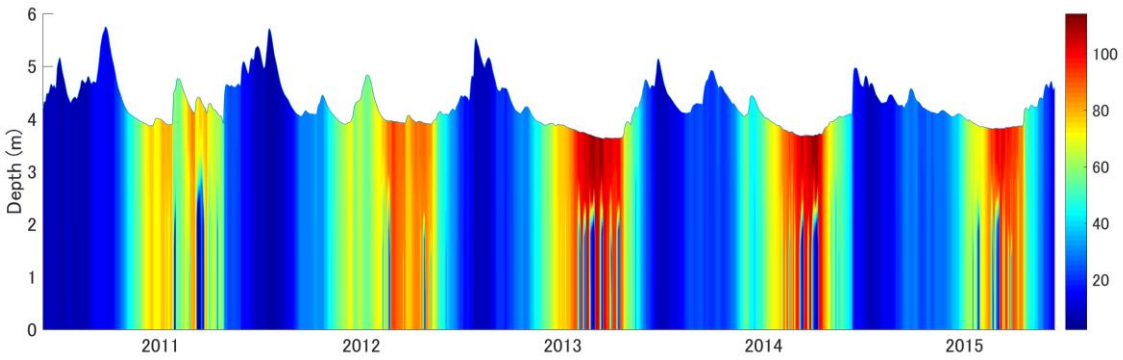

Figure 94: Chlorophyll *a* concentrations through the water column of Lake Waahi for the five-year simulation period. Colours represent chlorophyll *a* with a scale (µg L^{-1}) given on the right-hand side.

Figure 95 shows the limitation functions for cyanobacteria over the course of the simulation. Phosphorus limitation is most common but there are also periods of nitrogen limitation including when the limitation function for phosphorus is relatively elevated (i.e., indicating important on nitrogen control at these times, in order to constrain phytoplankton growth).

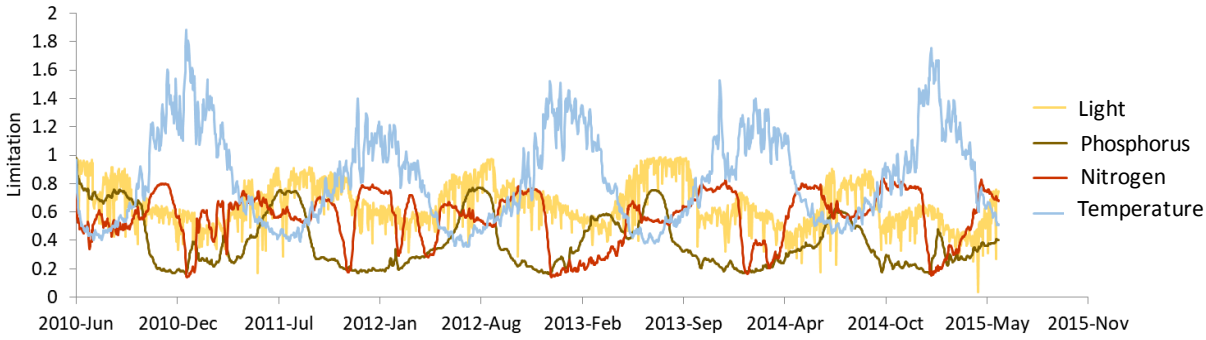

Figure 95: Time series of limitation factors for cyanobacteria in Lake Waahi. The temperature function extends above one as it is referenced as one for water temperature of 20˚C); the model multiplies the temperature function by the minimum of the light, nitrogen or phosphorus functions.

Observed concentrations of suspended solids were reasonably well replicated with the model which also captured a general tendency for suspended solids to increase over the five-year period (Figure 96, Figure 97), with concurrent reductions in Secchi disk depth (Figure 98). This suggests that internal processes may be highly important, i.e., the combination of sediment nutrient releases under anoxic conditions during calm summer-stratified periods and sediment resuspension during strong wind events. Slightly shallower water depth in 2014-2015 may have resulted in higher levels of sediment resuspension (Figure 99). In combination with relatively high temperature and higher frequency of stratification events, this could partly explain some recent general deterioration in water quality.

The relationship between suspended sediment and water level in Lake Waahi is not simple. In situ observations of TSS and high-frequency records of water level suggest a general trend of an inverse relationship between the two variables in a time series plot (Figure 99, left panel). A plot of TSS versus water level suggest that high TSS levels coincide with lake levels below 8 m relative to Moturiki datum (Figure 99, right panel), but the large scatter suggests that other factors, such as wind events and settling rates, need to be considered in detail.

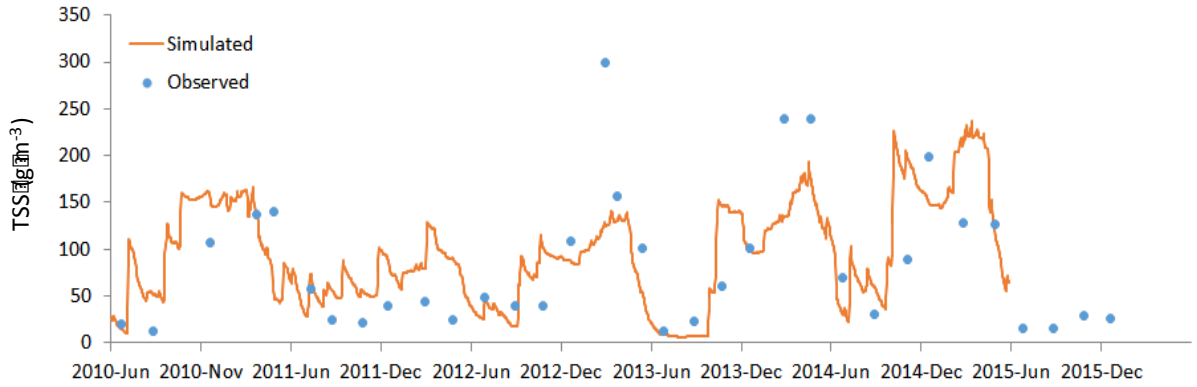

Figure 96: Observations (blue dots) and simulated values (orange) of suspended solids concentration at the surface water location for the five-year simulation period for Lake Waahi.

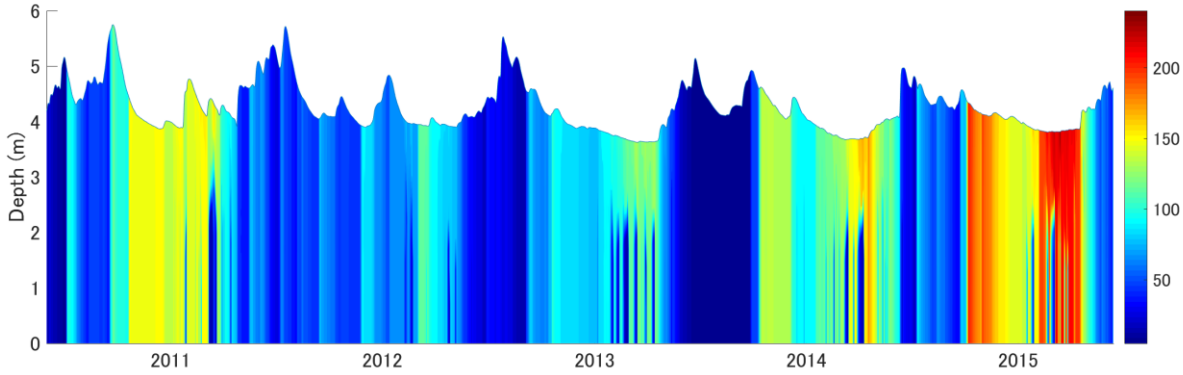

Figure 97: Suspended solids concentrations through the water column of Lake Waahi for the five-year simulation period. Colours represent suspended solids with a scale (g m^{-3}) given on the right-hand side.

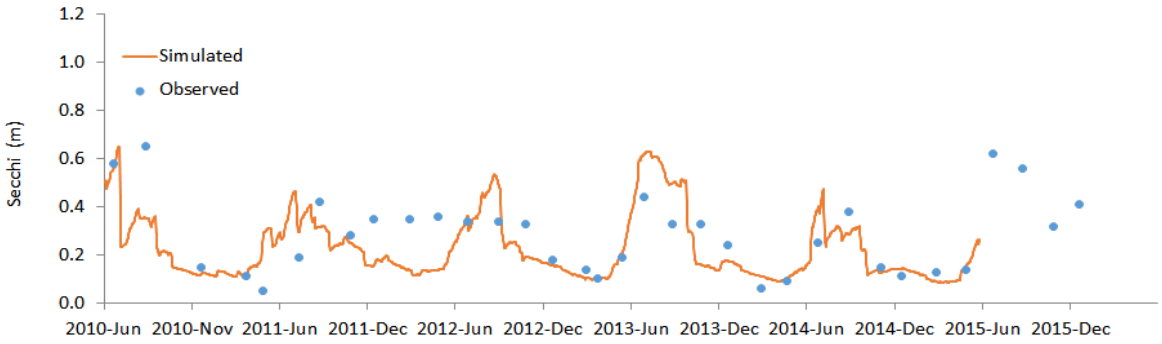

Figure 98: Observations (blue dots) and simulated values (orange lines) of Secchi disk depth at the surface water location for the five-year simulation period for Lake Waahi.

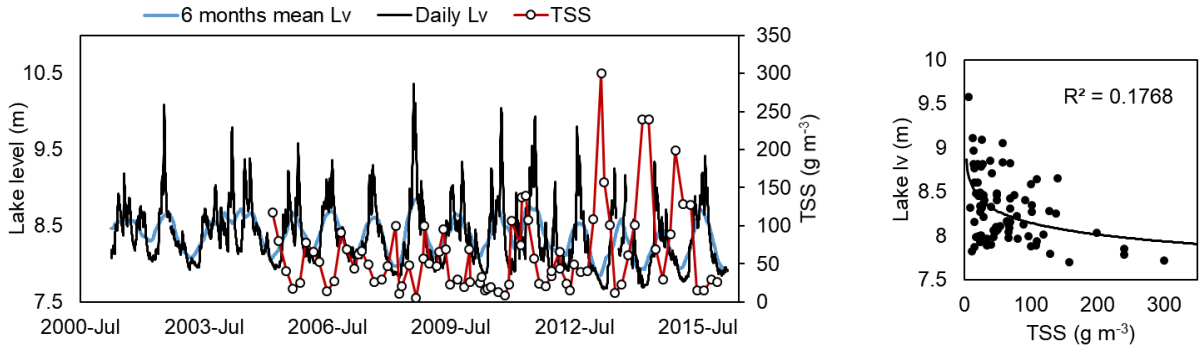

Figure 99: Observations of suspended sediment (TSS) and water level (Lv relative to Moturiki datum) in Lake Waahi.

Sensitivity to key parameters: uncertainty analysis

Sensitivity of the calibrated Lake Waahi model to 65 parameters is shown in Appendix B. Table 24 summarises results by showing those metrics (of Table 1) which were affected by a minimum of 10% (positive or negative). Only four parameters when altered by ±10%, result in an effect on simulation metrics > ±10%. These results suggest that the Lake Waahi model is especially sensitive to parameters which control the temperature dependence of sediment fluxes as well as phytoplankton growth respiration. Again, this result is not surprising given that sediment nutrient fluxes have already been shown to be important in the dynamics of this lake, and that phytoplankton appear to be sensitive to relatively small changes in temperature.

Table 24: Summary of local sensitivity analysis showing the most sensitive parameters. Full results are provided in Appendix B.

TP surface		TP bottom		TCHLA surface		TCHLA bottom	
Parameter	**δ%**	**Parameter**	**δ%**	**Parameter**	**δ%**	**Parameter**	**δ%**
Temperature multiplier of sediment fluxes -10%	48	Temperature multiplier of sediment fluxes -10%	49	Temperature multiplier of sediment fluxes -10%	47	Temperature multiplier of sediment fluxes -10%	47
				Temperature multiplier for phytoplankton respiration (CYANO) +10%	23	Temperature multiplier for phytoplankton respiration (CYANO) +10%	24
				Temperature multiplier of sediment fluxes +10%	19	Temperature multiplier of sediment fluxes +10%	19
				Temperature multiplier for phytoplankton growth -10%	11	Temperature multiplier for phytoplankton growth -10%	12
						Respiration rate coefficient (CYANO) -10%	10

δ%: Relative percent difference of simulation with changed parameter value relative to base simulation

Scenario simulation results

In an identical manner to Lake Ngāroto, there was no outstanding difference in key water quality variables in the model scenario simulations (Figure 100). Differences amongst scenarios were small in winter-spring, but considerably larger in summer-autumn. Two scenarios (WH8 and WH9) stood out in terms on their impact on TP, TN and TCHLA. The common feature of these scenarios was a reduction in the internal nutrient load. Scenario WH8 had both internal and external loads of TP reduced by 50%, while scenario WH9 had a 50% reduction in internal TN and TP load. In addition, scenario WH8 had a 1-m increase in water level. The 1-m increase in water level in WH8 resulted in the lowest levels of total suspended solids as a result of reduced levels of sediment resuspension. While scenario WH9 did not have a reduction in internal N load (cf. WH8), it had the largest reduction in TN (e.g., lower than TN in scenario WH9 for which there was a 50% reduction in internal TN load). This may seem surprising but was likely to be associated with the greatest reduction in chlorophyll *a* in WH9 and therefore less organic N in surface waters. Overall, even with the most severe reductions in nutrients and with 1-m increases in water level, there was still some gap between simulated TP, TN and chlorophyll *a,* and values in the NOF bottom line for these variables (Figure 101).

Figure 102 shows the percentage change of a number of water quality attributes in the nine scenarios relative to base case (WH0). The evaluation included derivations of variables (summer mean chlorophyll *a*, summer cyanobacteria chlorophyll *a*, summer days of stratification with temperature differences > 0.5^{o}C between surface and bottom waters, summer days with DO < 2 mg L^{-1} and 'bloom days' with cyanobacteria chlorophyll > 15 mg m^{-3}). Other state variable were direct model outputs and are given in Figure 102 including mean surface and bottom values of chlorophyll *a* and the five standard nutrient species (TN, TP, NO_3-N, NH_4-N and DRP). Several variables in some of the scenarios showed reductions of around 20-30% - an apparently good outcome – but still not enough to meet the bottom line in the NOF, which illustrates the magnitude of the degradation that has occurred in Lake Waahi.

The effect of the 1-m increase in water level is most evident in large increases in NH_4-N. This change is associated with greater stratification and an increase of nearly 100% in the number of days of anoxia (DO < 2 mg L^{-1}). Interestingly, the scenarios with water level increase produced only modest increases in DRP concentrations in bottom waters. Similar to Lake Ngāroto, it needs to be emphasised that there are large sources of uncertainty in this result. Some of this uncertainty may relate to the hydrodynamic model and the DO in bottom waters, as simulations were operating outside of the forcing data bounds under which they were tested. Other sources of uncertainty are

inherent in the prescribed values of sediment nutrient release (which is not measured directly) and knowledge of how emergent vegetation might affect resuspension by colonising the increased littoral region of scenarios where there was a deeper lake. However, given the good fit of the model to the observed data in the base simulation, the scenarios of water level increase at least provide some guidance on some of the issues that could arise with increased water levels.

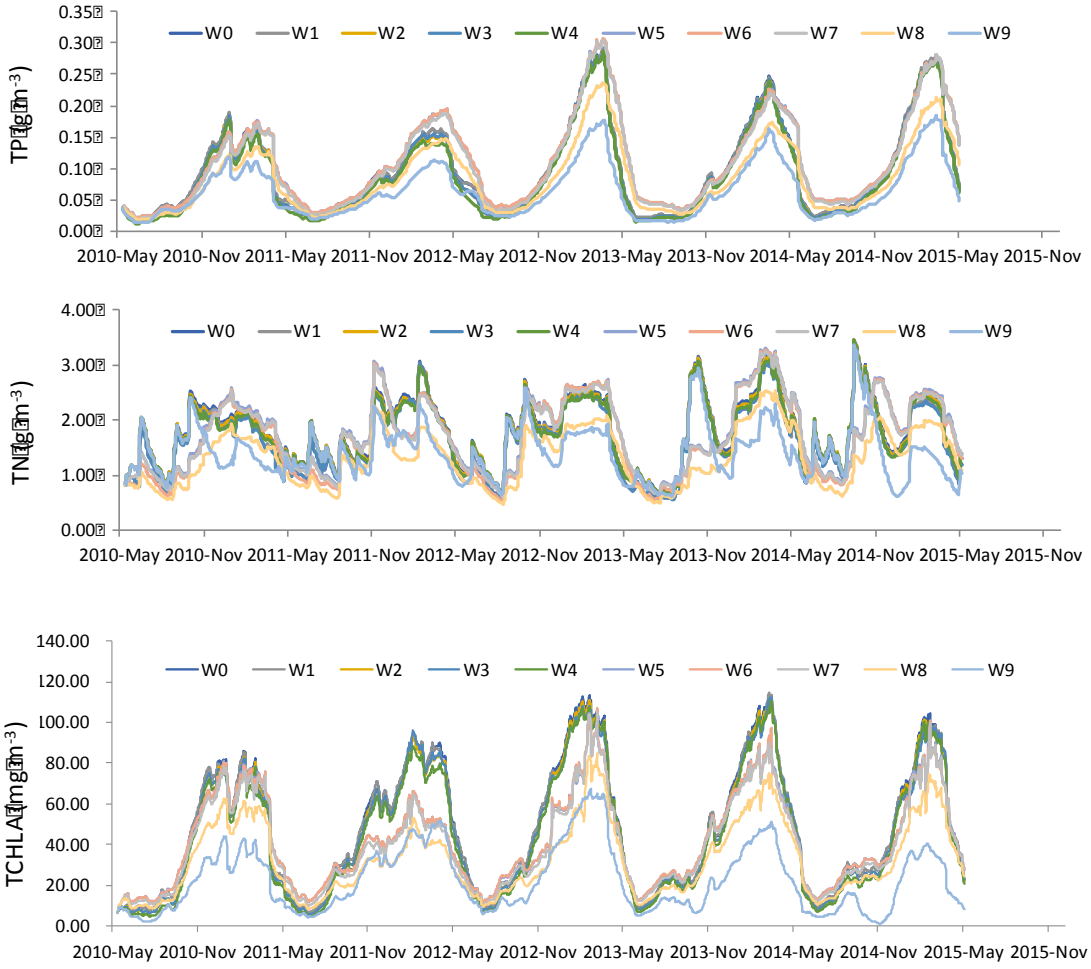

Figure 100: Simulated concentrations of total phosphorus, total nitrogen and total chlorophyll *a* at the surface for scenarios (W1-W9) and base case (W0) for Lake Waahi.

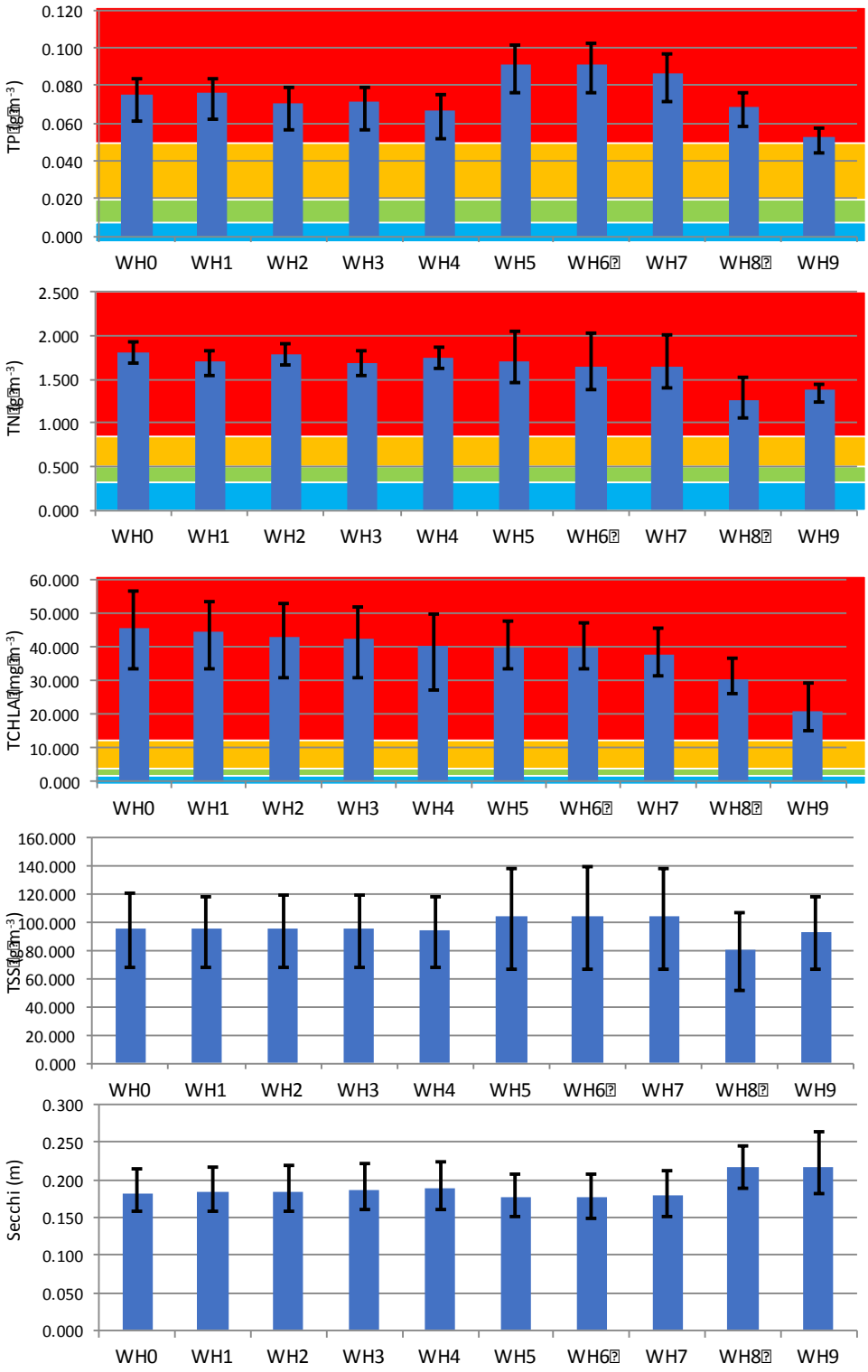

Figure 101: Bar charts of median water quality attributes for Waahi scenario simulations. Bar height is the average of five yearly medians, error bars are the minima and maxima of the five yearly medians. Coloured background in TP, TN and TCHLA charts indicate NOF bands (D: red, C: yellow, B: green, A: blue).

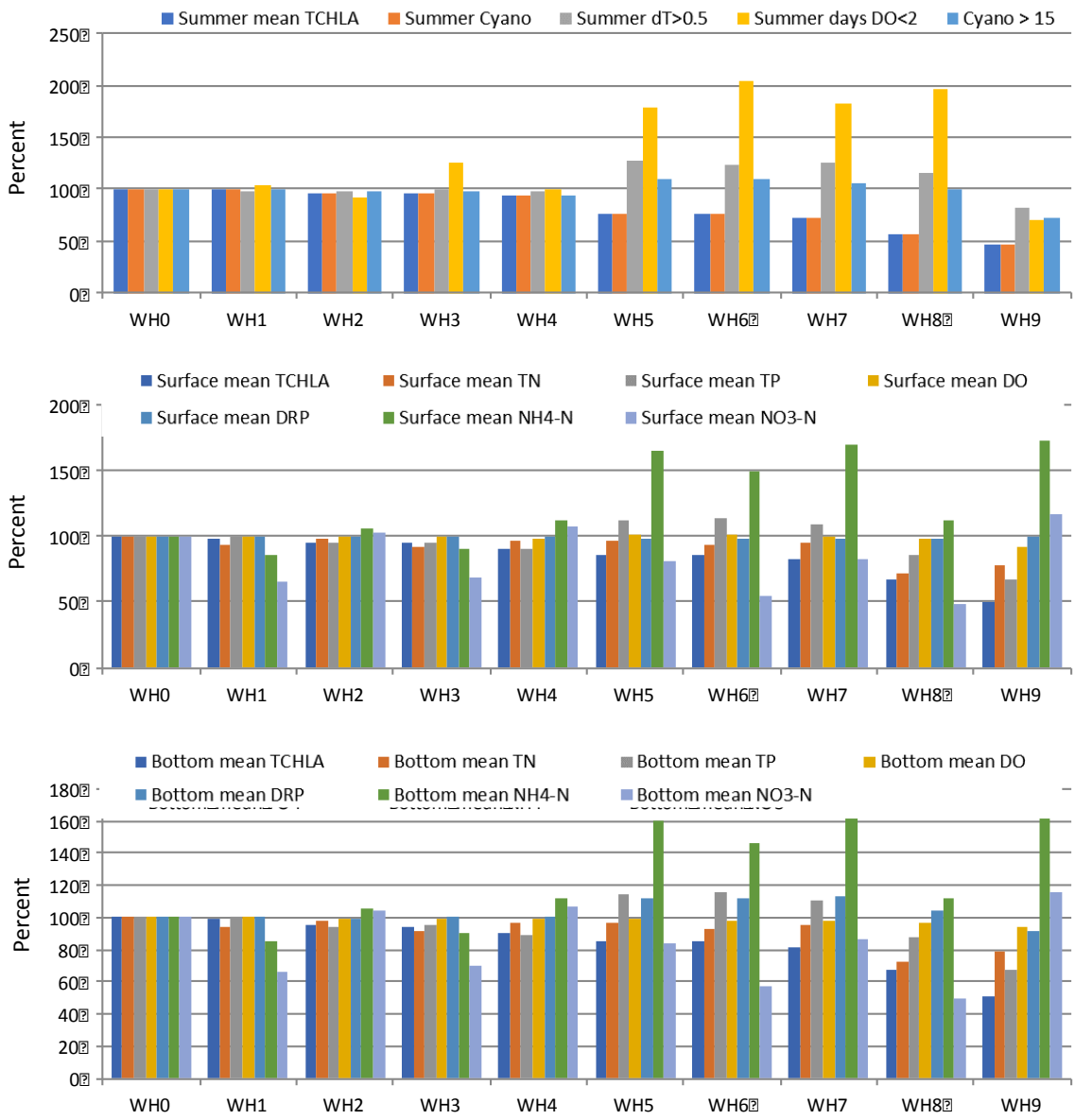

Figure 102: Bar graphs showing the percentage change of water quality attributes relative to the base simulation (N0) for Lake Waahi. The water quality attributes are defined in Table **1**.

Summary

The large size of the lake, its shallowness and the substantial legacy of historic sediment input suggest the dominance of internal drivers for water quality in Lake Waahi. Despite its shallowness, Waahi stratifies for short periods in lake summer and autumn which can cause low oxygen concentrations and anoxic release of NH_4-N from the lake bed. Table 25 provides a comparison of the estimated amounts of the constituents that are contributed from external (catchment) discharge, in-lake sediment resuspension and release of dissolved nutrients from the bottom sediments. This table shows that the external contribution of nitrogen is more important than for phosphorus and suspended sediment, because resuspension of bottom sediments has a major

impact on the levels of sediment and phosphorus in the water column. By contrast, for nitrogen, which is contained almost entirely as particulate organic nitrogen within the bottom sediments, sediment resuspension represents only a fraction (~ 17%) of the catchment load. Table 26 shows that sediment resuspension dominates over sediment nutrient release in Lake Waahi.

The scenarios in which the internal loads of nutrient are reduced stood out as the most effective at reducing lake median TP, TN, TCHLA and TSS (WH8 and WH9), and when TP reduction is combined with a water level increase (WH8). Overall, even with the most severe reductions in nutrients and with 1-m increases in water level, there was still some gap between simulated TP, TN and chlorophyll *a,* and values given in the NOF for these variables.

Table 25: Lake Waahi annual mean total nitrogen, total phosphorus and suspended sediment (kg ha^{-1} y^{-1}) contributed from external (catchment) loads, sediment resuspension and release of dissolved nutrients from bottom sediments. Area normalisation to lake surface area as derived from the hypsographic curve used in the model (476 ha).

		External	Resuspension	Sediment release
Phosphorus (kg ha^{-1} y^{-1})	Mean	4	2	5
	Range	2 – 7	2 – 3	5 – 6
Nitrogen (kg ha^{-1} y^{-1})	Mean	231	41	77
	Range	161 – 343	29 – 56	73 – 89
Sediments (kg ha^{-1} y^{-1})	Mean	5,768	16,298	-
	Range	2,255 – 13,588	13,152 – 20, 479	-

Table 26: Proportion (% Carp) of sediment, total phosphorus and total nitrogen inputs to Lake Waahi due to carp resuspension in relation to the total inputs (external + internal loads), proportion of external to total internal inputs (External/ Internal) and resuspension to sediment nutrient release ratio (Resuspension/ Sediment release).

	% Carp	External / Internal	Resuspension / Sediment release
Phosphorus	3	0.54	0.45
Nitrogen	3	1.95	0.53
Sediments	16	0.35	-

Geochemical engineering to address the legacy load of nutrients and sediments in the bottom of the lake is a possible management option. Comments on this option are presented in the Extended conclusions: *Geochemical engineering*. It is noted that Alum (aluminium sulphate) dosing for lake restoration is highly dependent on lake pH and buffering capacity both in terms of phosphorus

binding capability and potential toxic effects. Detailed studies and a duly conservative approach (Tempero 2015) are recommended should alum dosing be selected as a restoration tool for Lake Waahi.

Lake Waahi has been fished twice by boat electrofishing (2007 and 2011) and has shown remarkable consistency in the fish population. Goldfish dominate numerically, comprising 27 to 44% of the fish community, whereas koi carp comprised 5 to 8%. Shortfin eels comprised 31% of fish community, and given that boat electrofishing is biased against eels (see Appendix F) they are most likely more abundant than this estimate suggests. Koi carp, however, are larger fish so comprise 33-65 kg ha^{-1}. The apparent decline in koi carp biomass between 2007 and 2011 was probably more likely a reflection of the fishing conditions in 2011 than a real decrease. Benthivorous fish have the potential to make a significant contribution to suspended sediment and nutrient concentrations in lakes by resuspending bottom sediments. Carp contribute around 3% of the total (internal + external) nitrogen and phosphorus loads to Lake Waahi (Table 26) and about 16% of the total sediment load (but note that several caveats are applicable to these calculations in the section *Overview of key processes and modelling of the study lakes*).

Lake Rotomānuka

Calibration-validation process

Rotomānuka showed large variation between surface and bottom observations, as well as seasonally, in selected output variables. This variation provided an opportunity for good fit to the observed data, but data for other variables and at depth tended to be somewhat sparse and sporadic (with respect to consistency of depth sampled), which meant some uncertainties in the model parameters, particularly those related to sediment nutrient releases. The main focus of the calibration was again on temperature, surface and bottom DO, TN, TP, TSS and chlorophyll *a*, which was represented as a total value. The statistical comparison (Table 27) was deemed reasonable to good by comparison with other modelling applications. Again, it should be emphasized that some fairly gross assumptions needed to be made to be able to generate the daily discharge and composition data required for input as input to the lake model. One of these assumptions involved nutrient attenuation in the wetland area where water was designated to flow from Rotomānuka South to Rotomānuka North. The attenuation assigned in input to the model was 40% for nitrogen and 20% for phosphorus. Sensitivity analysis was used to test the variations in wetland nutrient attenuation affected model output, in order to better inform the calibration and range of model outputs, but detailed knowledge of the hydrology and biogeochemical dynamics of this area are lacking.

Table 27: Model performance of Lake Rotomānuka using root mean square error (RMSE) and coefficient of variation of root mean square deviation CV(RMSE) for high frequency buoy observations (n > 36; surface temperature: Tsrf, bottom temperature: Tbtm, surface dissolved oxygen: DOsrf, bottom dissolved oxygen: DObtm) and manual sampling results (n = 46; total nitrogen: TN, total phosphorus: TP, total suspended solids: TSS, total chlorophyll *a*: TCHLA).

	Tsrf (°C)	**Tbtm (°C)**	**DOsrf (mg L^{-1})**	**DObtm (mg L^{-1})**	**TN (g m^{-3})**	**TP (g m^{-3})**	**TSS (g m^{-3})**	**TCHLA (mg m^{-3})**
RMSE	1.42	1.30	0.83	1.62	0.22	0.01	2.02	7.62
CV(RMSE)	0.08	0.09	0.09	0.37	0.21	0.40	0.43	0.73

Key characteristics based on models and observations

The individual time series of temperature at the water surface and at a near-bottom location (c. 8 m) show clearly the large difference in summer temperatures corresponding to seasonal thermal stratification (Figure 103). Water temperature at the surface exceeded 25°C at times during summer but for bottom waters the temperature did not exceed 20°C. The coloured nature of the water

column could partly explain the relatively high surface water temperatures, due to increased heat trapping, in addition to the prolonged seasonal stratification (Figure 104). The heat map of water column temperature distributions shows a period of persistent thermal stratification for about 3 to 4 months each year. Prolonged thermal stratification also has a pronounced effect on the DO regime in bottom waters. The bottom waters quickly (in a few days) went anoxic (Figure 105) with the onset of thermal stratification, but there were periods when stratification was first setting up, of establishment of anoxic conditions followed by mixing and replenishment of DO to levels similar to surface waters (Figure 105). This sequence produced a 'jagged' profile of DO, often alternating rapidly between levels close to saturation and anoxia over a window time just outside of the occurrence of persistent thermal stratification. By contrast, DO in surface waters fluctuated reasonably predictably with temperature, with levels close to saturation throughout the year.

The contour plot of dissolved oxygen through the water column (Figure 106) revealed a substantial fraction of the water column that was anoxic. This 'dead zone' intruded high into the water column, and combined with decreasing water levels (2013, 14 and 15 in particular), meant that only a shallow surface layer (2-3 m) of the entire water column contained oxygen (Figure 106).

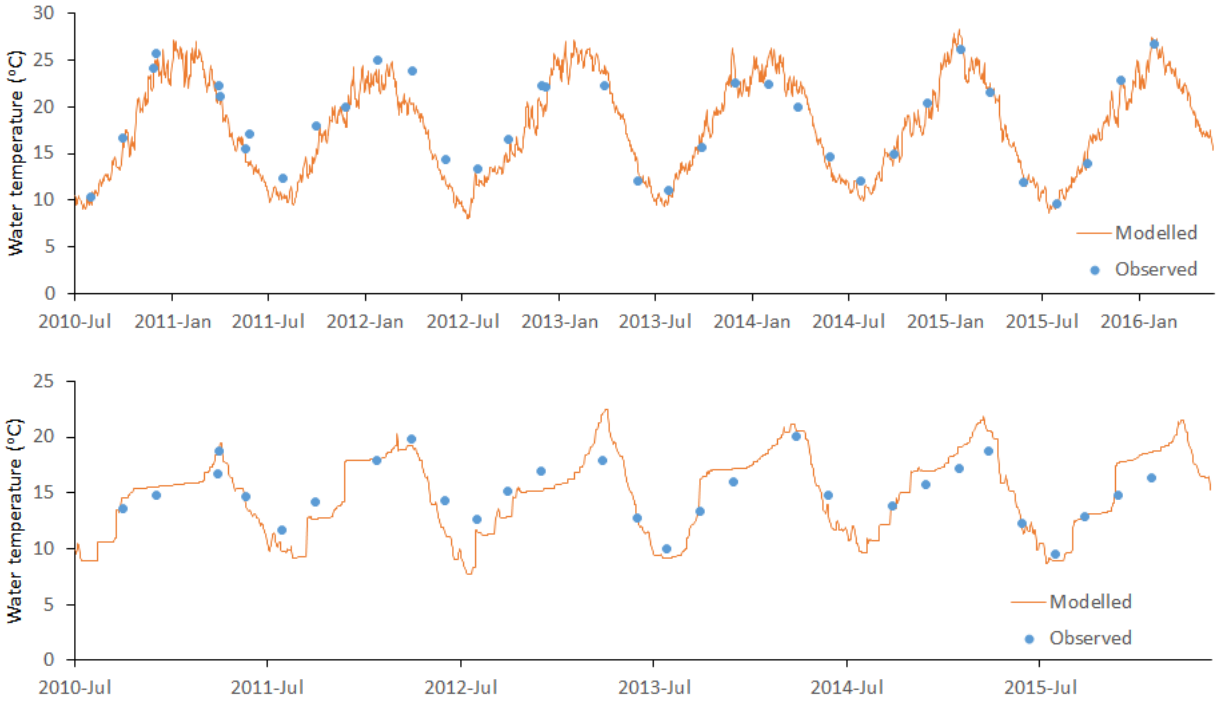

Figure 103: Surface (top) and (bottom) near-bottom water temperature for Lake Rotomānuka. Orange line is the simulated values and blue dots are observed values.

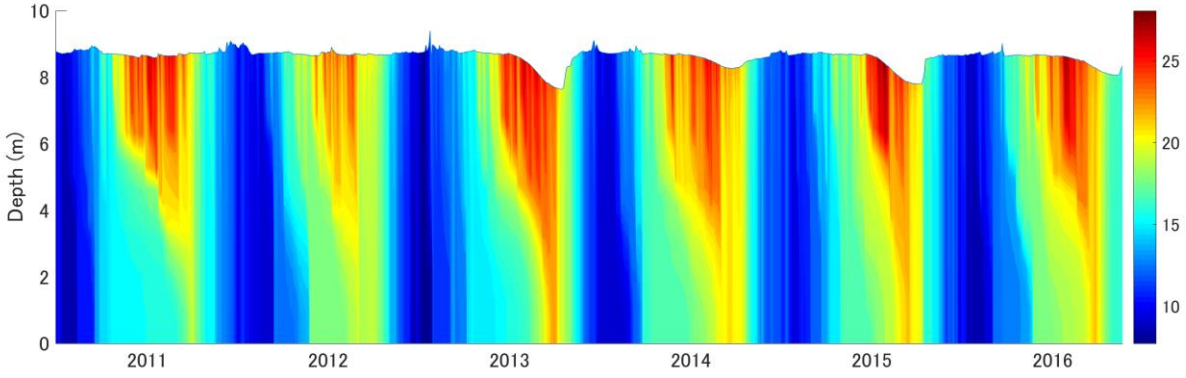

Figure 104: Temperature through the water column of Lake Rotomānuka for the five-year simulation period. Colours represent water temperature with a scale (°C) given on the right-hand side.

Figure 105: Surface (top) and (bottom) near-bottom dissolved oxygen for Lake Rotomānuka. Orange line is the simulated values and blue dots are observed values.

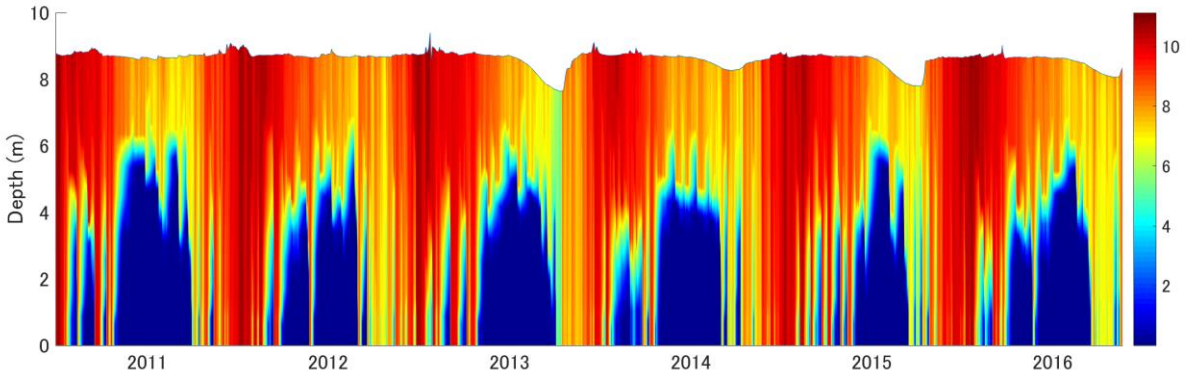

Figure 106: Dissolved oxygen through the water column of Lake Rotomānuka for the five-year simulation period. Colours represent water temperature with a scale (°C) given on the right-hand side.

Like simulations of TN for the other two shallow lakes, those for Lake Rotomānuka reproduced the approximate magnitude of concentrations but failed for some of the trends of consistent increase or decrease in TN over periods of six months or so (e.g., in the latter half of 2014) (Figure 107). The most obvious feature of the colour contour plot of TN through the water column (Figure 108) is the increase in response to anoxia and buildup of NH_4-N in the lower water column. Nitrate-N concentrations mostly represent only a small fraction of the TN so it is likely that the organic component of TN is not simulated accurately by the model. Nitrate-N showed strong seasonal fluctuations despite low peak concentrations (Figure 109). It is difficult to ascertain if the model has reproduced interannual variations in NO_3-N because these were mostly small, likely driven by the phenology of the late-winter flush of NO_3-N from the catchment. The colour contour of simulated nitrate through the water column shows a repeated pattern characterized by a winter peak when the whole water column is well oxygenated and a summer trough in the lower water column in particular, when there would be expected to be good conditions for denitrification and loss of NO_3-N, especially during alternating cycles of oxic-anoxic conditions (Figure 110). Ammonium in bottom waters in particular, but more generally through the water column, tended to vary inversely with nitrate, reflecting the alternating anoxic (NH_4-N dominant) – oxic (NO_3-N dominant) conditions (Figure 111). A prominent feature was the increase in NH_4-N in the water column during the stratified period (Figure 112). The small number of measurements of nutrients in bottom waters of Lake Rotomānuka meant it was difficult to validate the extent of nutrient buildup in this part of the water column. This applies also for total phosphorus where the time series plot for the water surface shows low concentrations (c. 0.02 g m^{-3}) (Figure 113) but concentrations in bottom waters are simulated to increase to c. 0.15 g m^{-3} (Figure 114), which is accounted for almost entirely by buildup of DRP in the lower water column as a result of releases from the sediments under anoxic conditions. Concentrations of DRP appeared to use a lower analytical detection limit than in the other two lakes and indicated very low levels of DRP (Figure 115). Higher-resolution time series measurements of nutrients at fixed depths in the water column and/or incubations to examine sediment nutrient release rates would assist greatly with developing confidence in the nutrient release rates specified as parameters in the DYRESM-CAEDYM model (Figure 116).

There is little to point about observations, model performance or variability of chlorophyll *a* (Figure 117, Figure 118), suspended solids (Figure 120, Figure 121) or Secchi depth (Figure 122). There was no particular seasonality to these state variables although chlorophyll *a* was simulated to be extremely low in the bottom waters but quite elevated in surface waters in late summer. Secchi depth was around 1.2 m with chromophoric dissolved organic matter (i.e., peat staining) likely playing a role in attenuating light with depth. Because of the limited seasonal variability, the focus of

calibration was to closely approximate the magnitude of observed values with the model, rather than the temporal variability. The result was a modest level of statistical fit in the model for these variables.

Figure 119 shows the limitation functions for cyanobacteria over the course of the simulation. For reasons discussed above, temperature and light limitation are not particularly useful but the value of that figure is in comparing periods and severity of nitrogen and phosphorus limitation. In this case phosphorus limitation was highly persistent with only brief periods for some winters when limitation was approximately balanced between nitrogen and phosphorus.

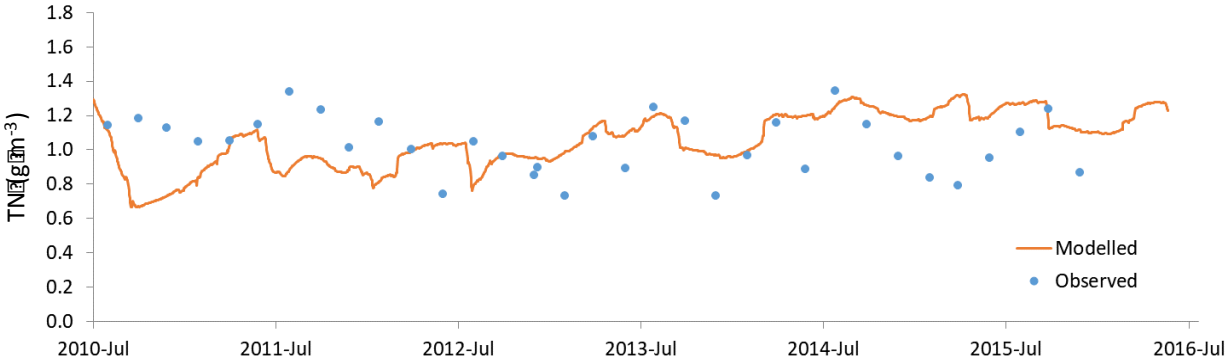

Figure 107: Total nitrogen in surface waters of Lake Rotomānuka for the five-year simulation period.

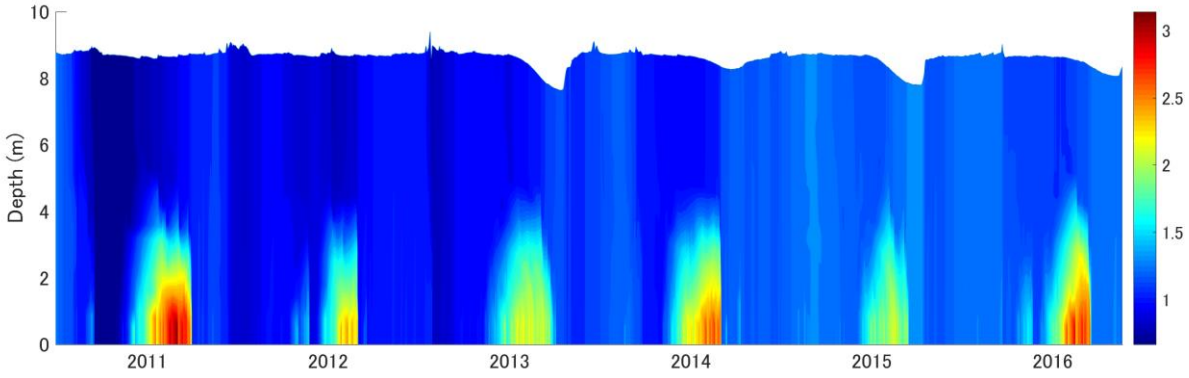

Figure 108: Total nitrogen through the water column of Lake Rotomānuka for the five-year simulation period. Colours represent total nitrogen with a scale (g m^{-3}) given on the right-hand side.

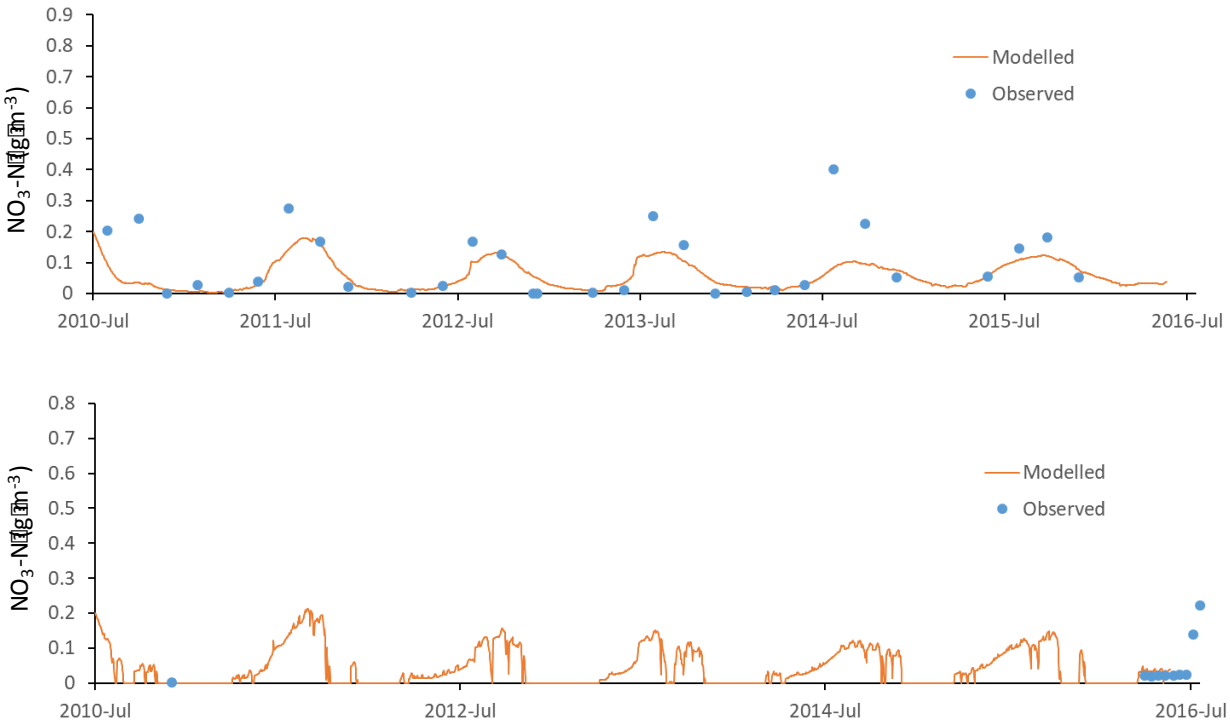

Figure 109: Surface (top) and (bottom) near-bottom nitrate concentrations for Lake Rotomānuka. Orange line is the simulated values and blue dots are observed values.

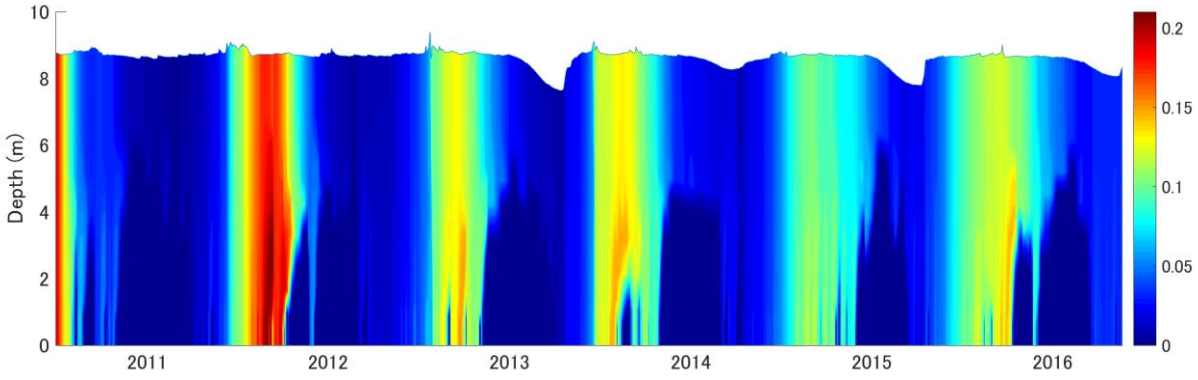

Figure 110: Nitrate (NO3-N) through the water column of Lake Rotomānuka for the five-year simulation period. Colours represent NO_3-N with a scale (g m^{-3}) given on the right-hand side.

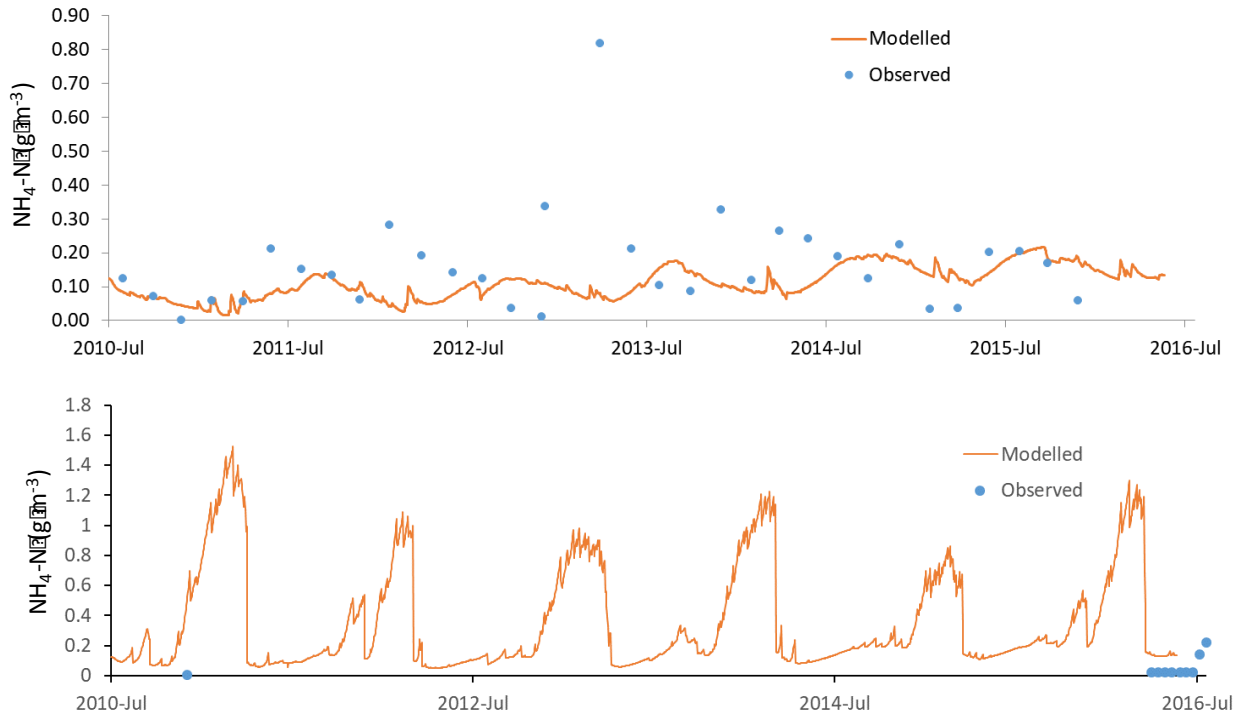

Figure 111: Surface (top) and (bottom) near-bottom ammonium (NH4-N) concentrations for Lake Rotomānuka. Orange line is the simulated values and blue dots are observed values.

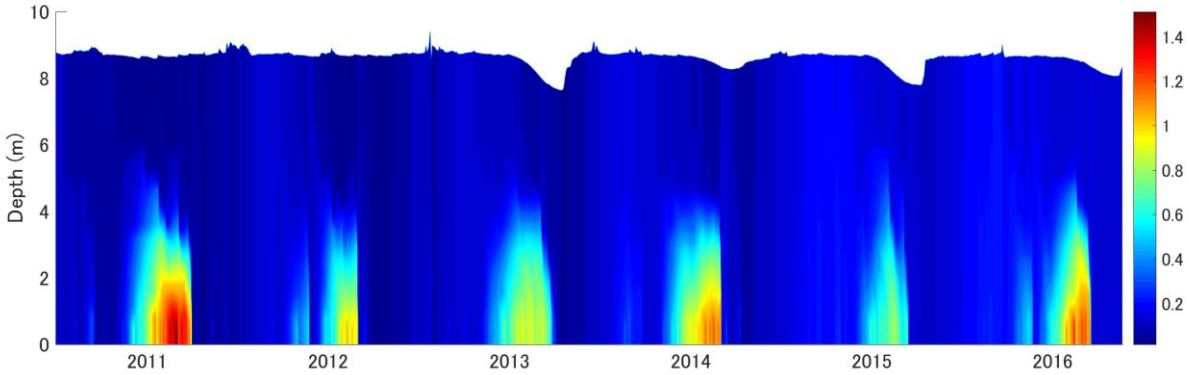

Figure 112: Ammonium (NH_4-N) concentrations through the water column of Lake Rotomānuka for the five-year simulation period. Colours represent NH_4-N with a scale (g m^{-3}) given on the right-hand side.

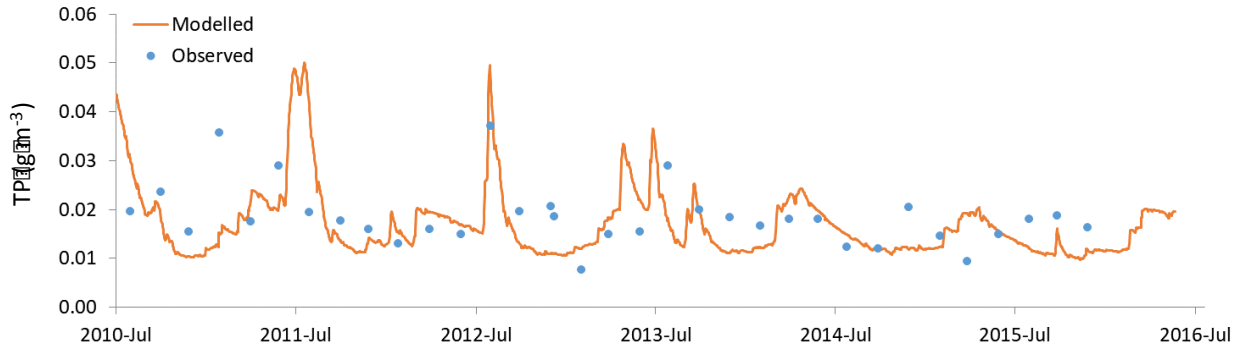

Figure 113: Observed (blue dots) and simulated (orange) total phosphorous concentration at the surface.

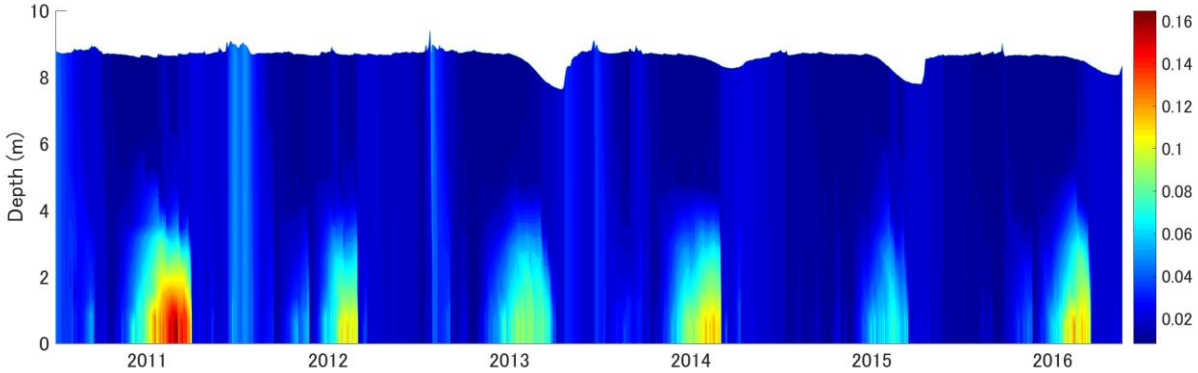

Figure 114: Total phosphorus concentrations through the water column of Lake Rotomānuka for the five-year simulation period. Colours represent TP with a scale (g m^{-3}) given on the right-hand side.

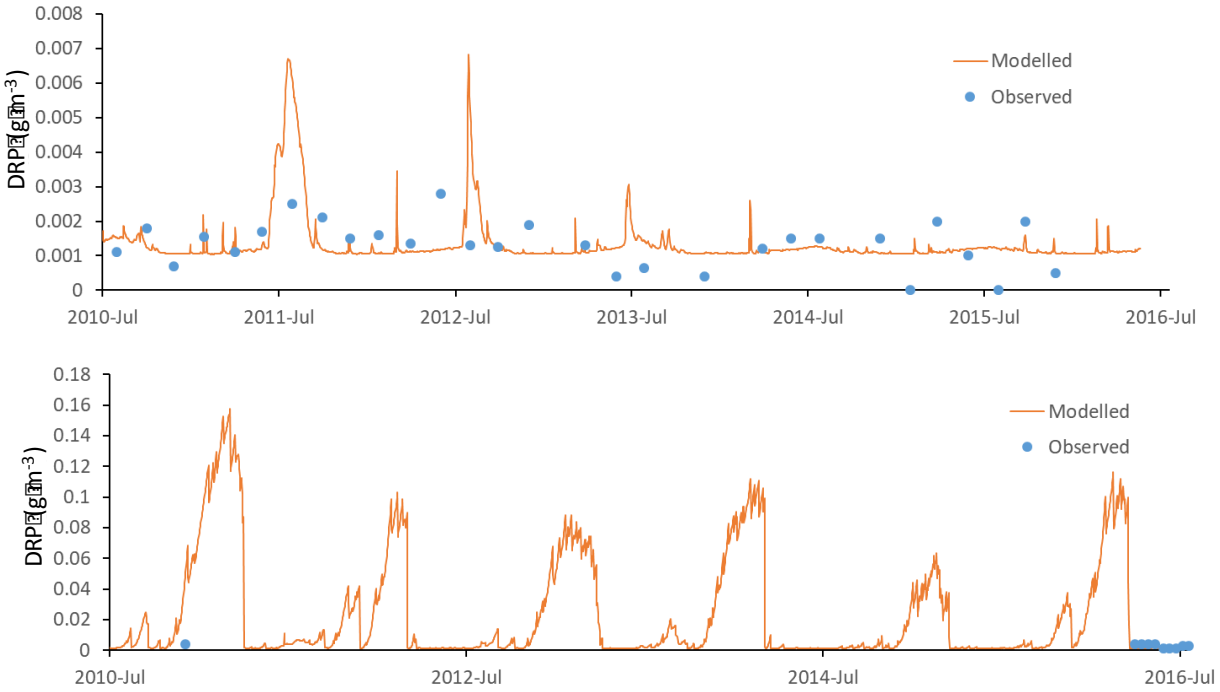

Figure 115: Surface (top) and (bottom) near-bottom dissolved reactive phosphorus (DRP) concentrations for Lake Rotomānuka. Orange line is the simulated values and blue dots are observed values.

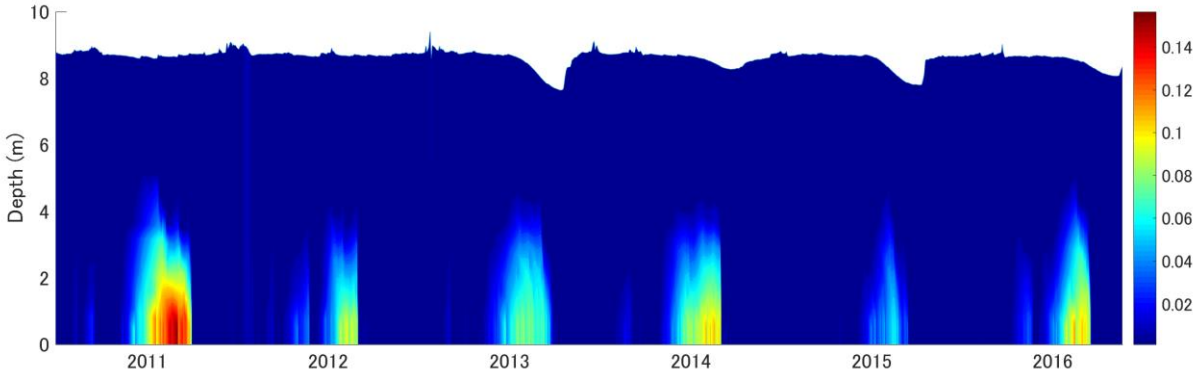

Figure 116: Dissolved reactive phosphorus (DRP) concentrations through the water column of Lake Rotomānuka for the five-year simulation period. Colours represent DRP with a scale (g m^{-3}) given on the right-hand side.

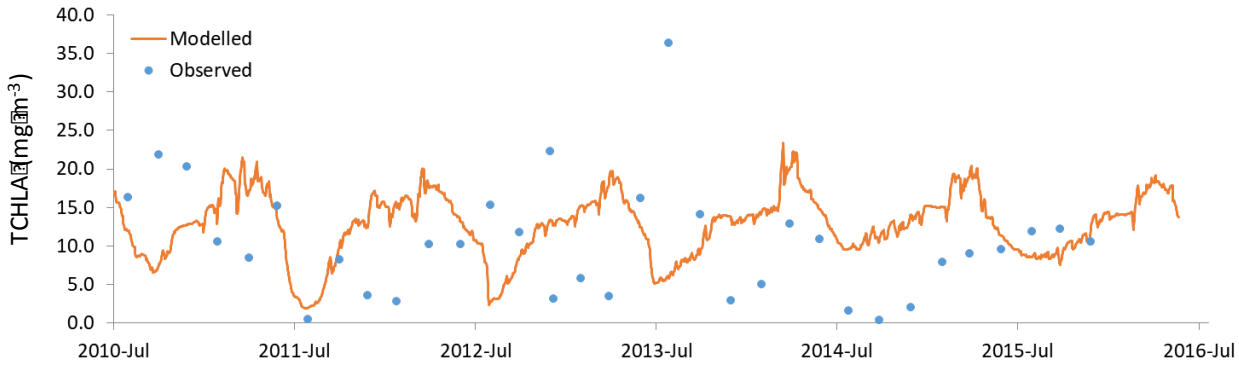

Figure 117: Surface-water total chlorophyll a concentrations for Lake Rotomānuka. Orange line is the simulation results and blue dots are observed values.

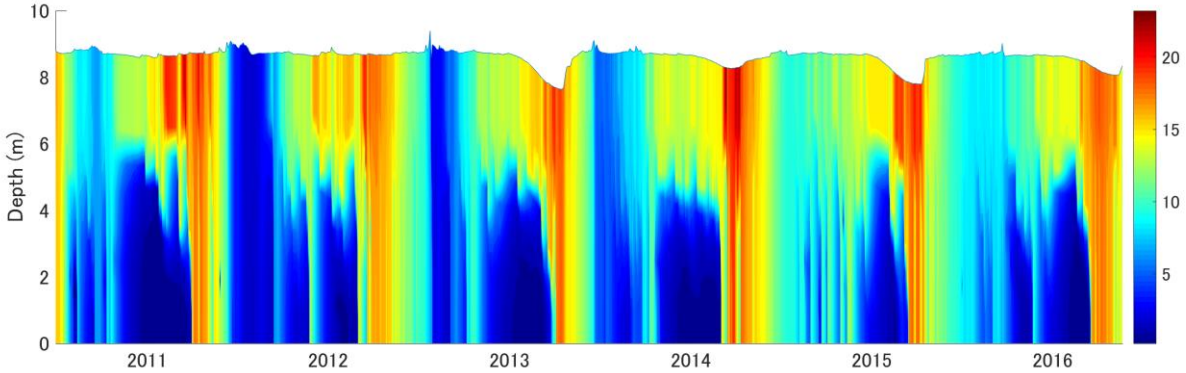

Figure 118: Concentrations of chlorophyll *a* through the water column of Lake Rotomānuka for the five-year simulation period. Colours represent TCHLA with a scale (mg m^{-3}) given on the right-hand side.

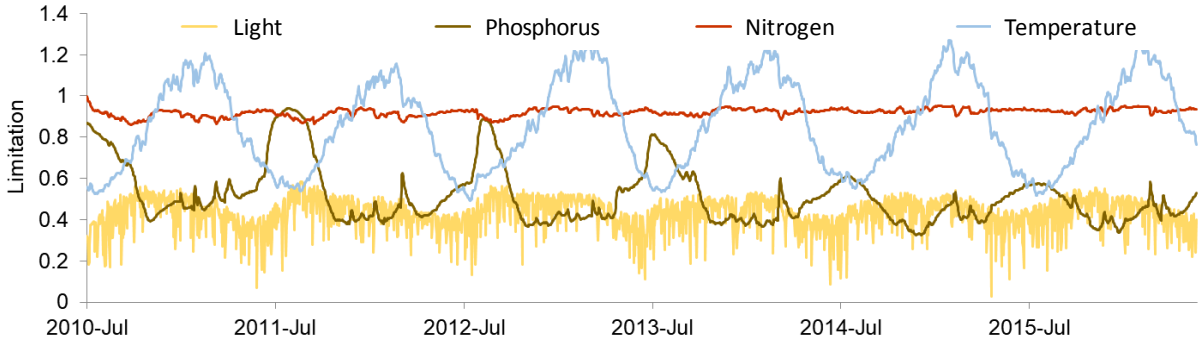

Figure 119: Time series of limitation factors for cyanobacteria in Lake Waahi. The temperature function extends above one as it is referenced as one for 20˚C); the model multiplies the temperature function by the minimum of the light, nitrogen or phosphorus functions.

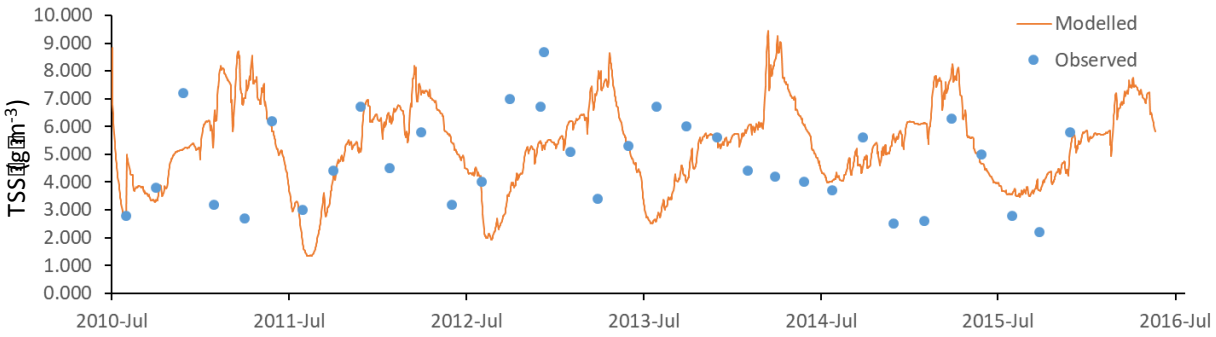

Figure 120: Surface-water suspended solids concentrations for Lake Rotomānuka. Orange line is the simulated values and blue dots are observed values.

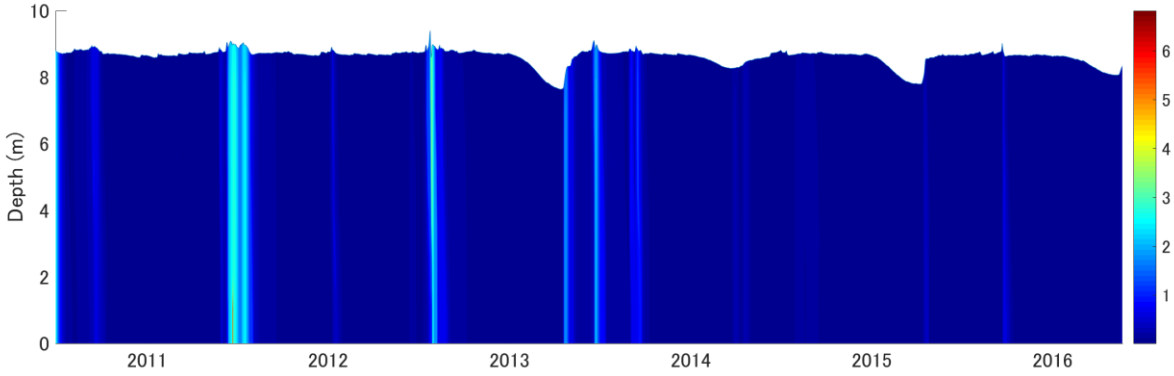

Figure 121: Suspended solids concentrations for Lake Rotomānuka for the five-year simulation period. Colours represent TCHLA with a scale (µg L^{-1}) given on the right-hand side.

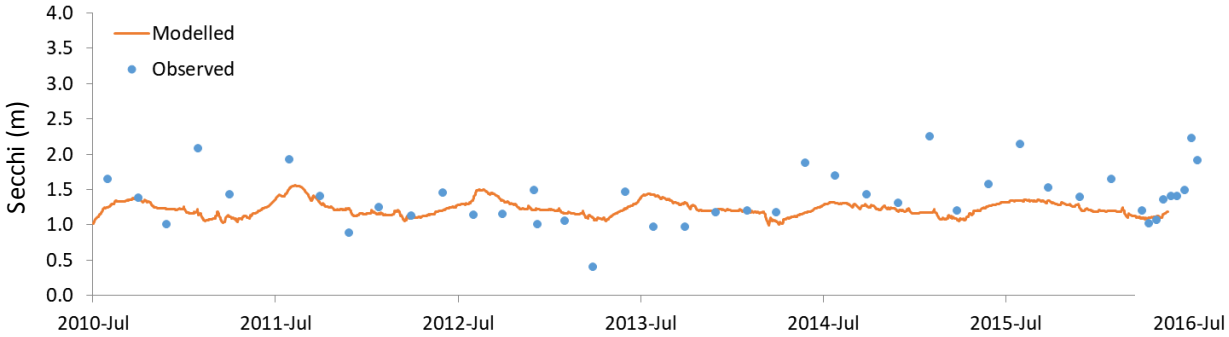

Figure 122: Secchi disk depth for Lake Rotomānuka. Orange line is the simulated values and blue dots are observed values.

Sensitivity to key parameters: uncertainty analysis

Sensitivity of the calibrated Lake Rotomānuka model was examined for 65 one-at-a-time parameter adjustments (by ±10% of their calibrated values). The 65 parameters are listed in Appendix A. Table 28 summaries show state variables which were altered by > ±10% from their value in the calibrated model.

Table 28: Summary of one-factor-at-a-time sensitivity analysis for Lake Rotomānuka DYRESM-CAEDYM model. δ%: is percent difference of simulation from the calibrated one.

TP surface		TP bottom		TN surface		TN bottom		TCHLA surface		TCHLA bottom	
Parameter	***δ%***	**Parameter**	***δ%***	**Parameter**	***δ%***	**Parameter**	***δ%***	**Parameter**	***δ%***	**Parameter**	***δ%***
Density of POM particles -	823.9	Density of POM particles -	174.8	Temperature multiplier of sediment fluxes -	17.6	Temperature multiplier of sediment fluxes -	36.5	Temperature multiplier for phytoplankton growth (FDIAT) -	69.0	Temperature multiplier for phytoplankton respiration (CYANO) +	61.3
Temperature multiplier for phytoplankton growth (FDIAT) -	48.2	Temperature multiplier of sediment fluxes -	61.2	Temperature multiplier for phytoplankton growth (FDIAT) -	16.2	Temperature multiplier for phytoplankton growth (FDIAT) -	21.3	Temperature multiplier for phytoplankton respiration (CYANO) -	43.1	Temperature multiplier for phytoplankton growth (CYANO) -	53.6
Temperature multiplier of sediment fluxes -	28.3	Temperature multiplier for phytoplankton growth (CYANO) -	52.6	Density of POM particles -	14.3	Temperature multiplier for phytoplankton respiration (CYANO) -	14.8	Temperature multiplier for phytoplankton growth (CYANO) -	40.4	Temperature multiplier for phytoplankton respiration (CYANO) -	34.3
Temperature multiplier for phytoplankton respiration (CYANO) -	17.4	Temperature multiplier for phytoplankton respiration (CYANO) -	25.2	Temperature multiplier for phytoplankton respiration (CYANO) -	11.2	Temperature multiplier of sediment fluxes +	11.7	Temperature multiplier for phytoplankton growth (CYANO) +	37.8	Temperature multiplier for phytoplankton growth (CYANO) +	30.8
Density of POM particles +	14.0	Temperature multiplier of sediment fluxes +	22.3	Temperature multiplier for phytoplankton growth (CYANO) -	11.0	Temperature multiplier for phytoplankton growth (CYANO) +	11.7	Temperature multiplier for phytoplankton respiration (CYANO) +	27.5	Temperature multiplier for phytoplankton growth (FDIAT) -	23.2
Temperature multiplier for phytoplankton growth (CYANO) +	12.9	Temperature multiplier for phytoplankton growth (CYANO) +	16.8			Temperature multiplier for phytoplankton growth (CYANO) -	11.5	Temperature multiplier of sediment fluxes -	23.7	Respiration rate coefficient (CYANO) -	18.1
Fraction of metabolic loss rate that goes to DOM (CYANO) +	12.3							Fraction of metabolic loss rate that goes to DOM (CYANO) +	14.5	Respiration rate coefficient (CYANO) +	15.3
								Respiration rate coefficient (CYANO) -	14.5	Temperature multiplier of sediment fluxes -	14.3
								Respiration rate coefficient (CYANO) +	13.3	Fraction of metabolic loss rate that goes to DOM (CYANO) +	11.4
										Maximum growth rate (CYANO) +	11.0

The most sensitive parameters related to phytoplankton growth rates (mostly the cyanobacteria group) and sediment nutrient release rates. Specifically, the temperature multipliers for phytoplankton growth and respiration, as well for sediment nutrient releases, were most sensitive. The sensitivity to temperature multipliers can probably be related to the logarithmic relationship of the parameter value to temperature (i.e., a 'Q10' function).

Scenario simulation results

Table 16 gives the nine scenarios which were compared against the base scenario, R0. The scenarios involved a sensitivity analysis of the wetland attenuation – from none at all to double the present levels (ROW1 and ROW2, respectively). The rest of the scenarios (R1-R9) with one exception (R9), involved alterations of TP, TN or both TN and TP loads, reducing the loads by 25% or 50%. The final scenario (R9) involved diversion of Rotomānuka South inflow and a 25% reduction in external TN and TP to the lake from catchment immediately around the lake (catchment D, Figure 38). In the case of total phosphorus, the effect of different management scenarios was primarily to alter the height of the peaks in concentration (Figure 123). By contrast, for total nitrogen the separation of the scenarios was less variable, at least through the middle phase of the simulation. For chlorophyll *a*, R9 deviated most from the other scenarios, mostly as a result of chlorophyll a being elevated consistently above the others through winter and spring (Figure 123).

As expected, the different management scenarios did not have a lot of effect on suspended solids concentrations, and for Secchi disk depth there was also not a lot of change amongst the scenarios (Figure 124). What was of particular significance, however, was that some scenarios indicated a change (improvement) in the NOF band. For TP, Lake Rotomānuka remained in a B band, irrespective of the scenario. For TN, scenarios R6 and R8 moved Lake Rotomānuka's simulated NOF classification out of the bottom line (D) to a C value, and for chlorophyll *a*, scenarios R6 and R7 moved the classification to the threshold of C-D bands after previously (in base case R0) clearly failing to meet the bottom line. Overall, R8 (50% reduction in external TN and TP load across the catchment) was superior to the others, but it should be kept in mind that there is a high level of uncertainty about internal loading fluxes in Lake Rotomānuka. Figure 125 shows a percentage change metric for state variables and a range of derived variables.

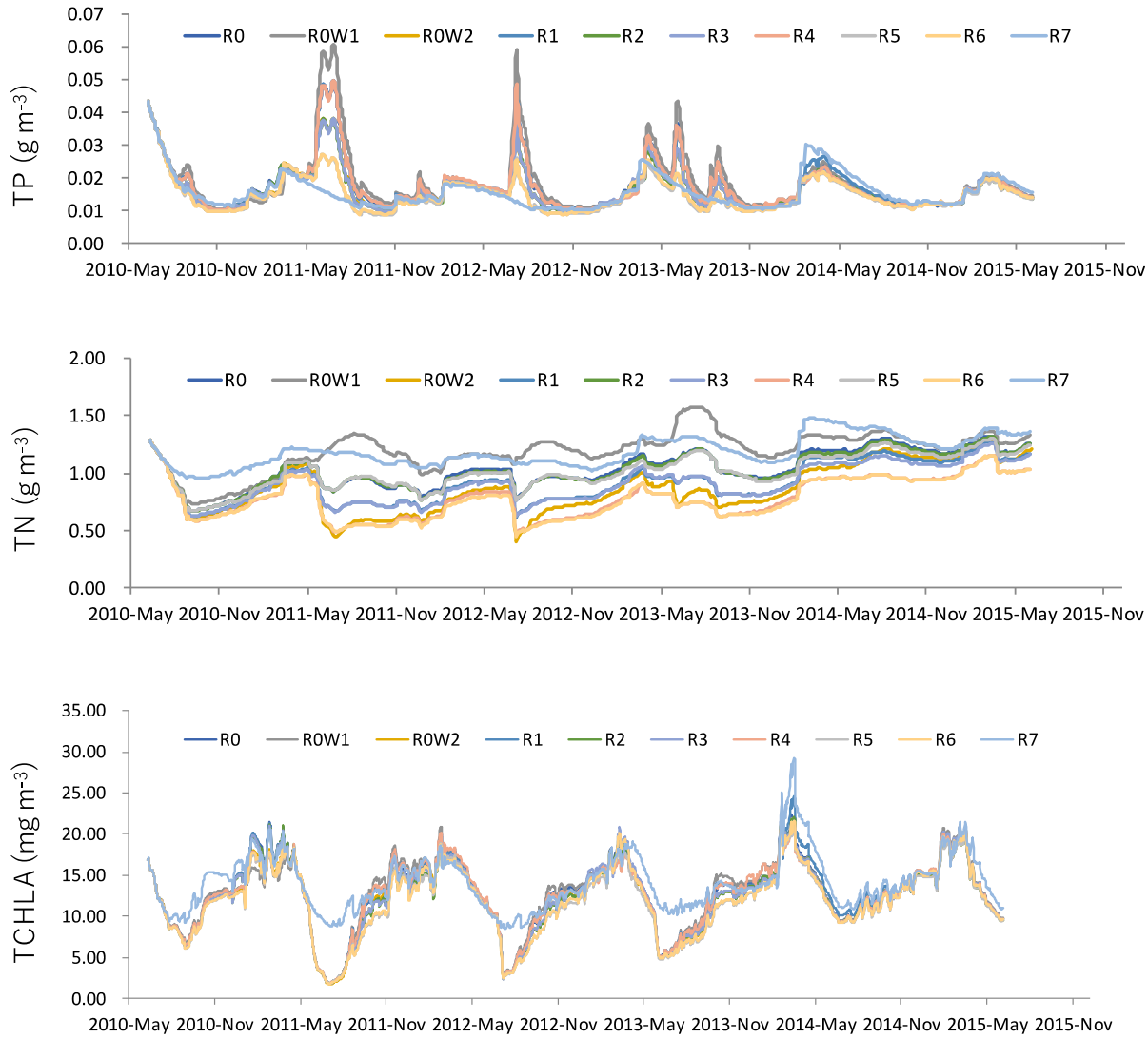

Figure 123: Simulated concentrations of total phosphorus, total nitrogen and total chlorophyll *a* concentrations at the surface for the nine management scenarios for Lake Rotomānuka (see Table 9 for a list of the scenarios).

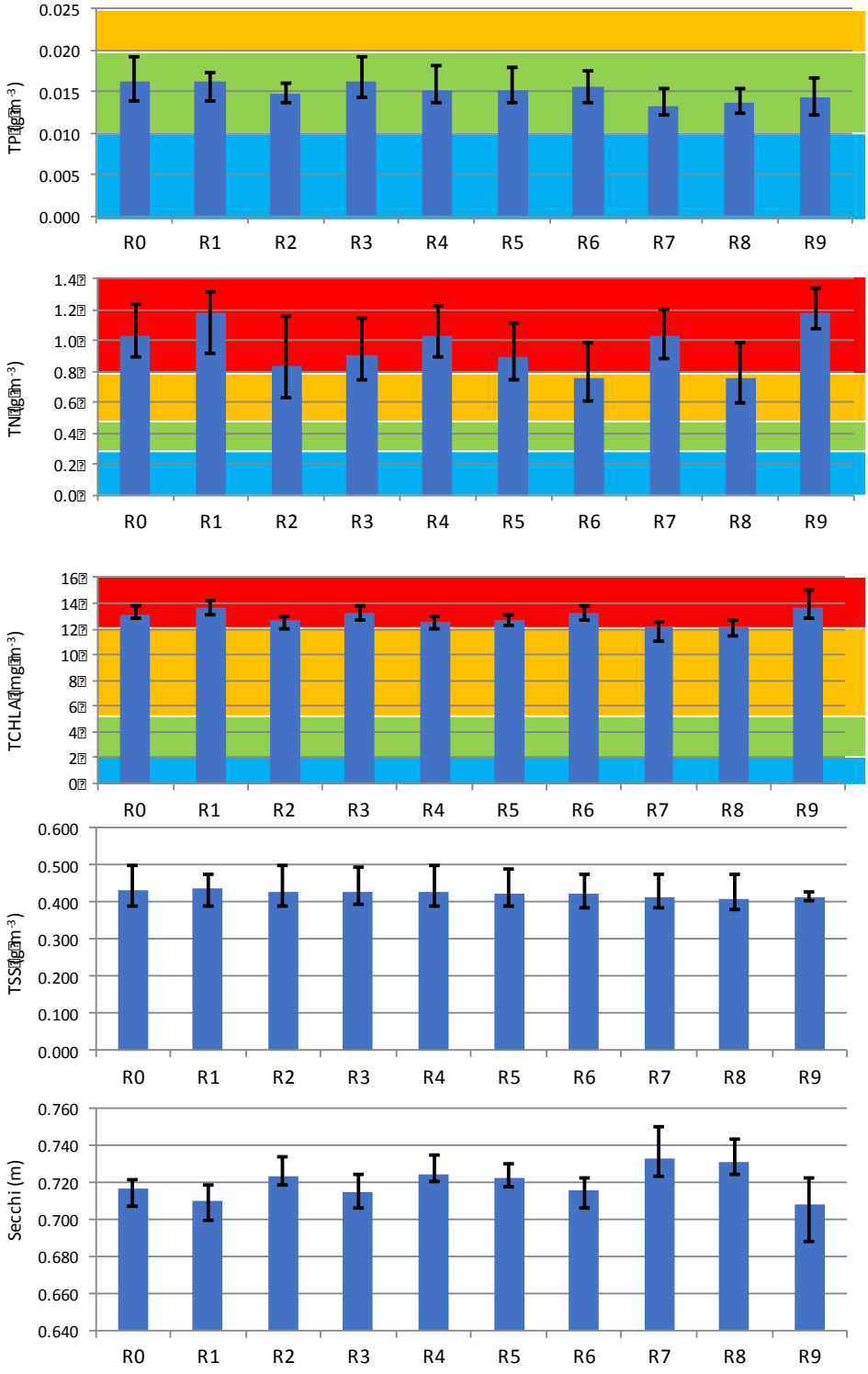

Figure 124: Bar charts of median water quality attributes for Lake Rotomānuka scenario simulations. Bar height is the average of five yearly medians, error bars are the minima and maxima of the five yearly medians. Coloured background in TP, TN and TCHLA charts indicates NOF bands (D: red, C: yellow, B: green, A: blue).

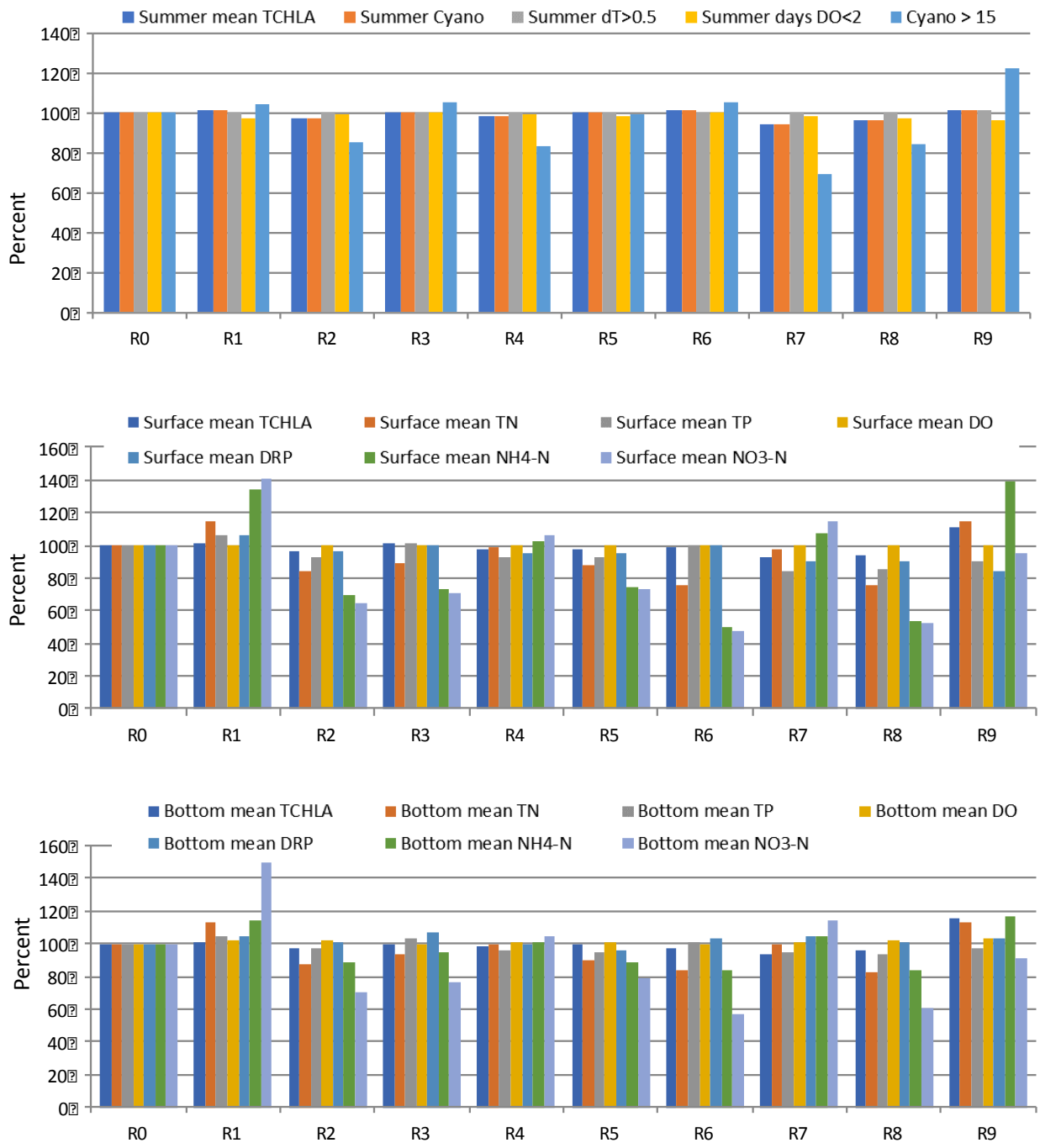

Figure 125: Bar graphs showing the percentage change of water quality attributes relative to the base simulation (N0) for Lake Rotomānuka. The water quality attributes are defined in Table **1**.

Summary

At almost 9 metres depth, Lake Rotomānuka is the deepest of the study lakes. Its physical and biogeochemical structure is strongly influenced by thermal stratification which occurs both seasonally and even ephemerally during the winter when it is aided by chromophorically stained water and the sheltering effect of surrounding hills. Field observations show fast responses of dissolved oxygen concentration to stratification events and the summertime is characterised by

extensive periods of anoxia throughout a substantial part of the water column. The lake model predicts oxygenation-driven variations of NO_3-N, NH_4-N and DRP in the deep water of the lake, but these findings can not be confirmed due to the lack of suitable observations. Despite seasonality in the physical structure, observations of chlorophyll *a*, water clarity and suspended solids show little systematic seasonality. Our model does not predict this variability very well, pointing to uncertainties in the model set-up and assumptions, such as those related to the external inputs. Therefore, the model results for Lake Rotomānuka probably have the greatest degree of uncertainty of this study and further field-based investigations are recommended prior to deciding on management actions.

Based on our assumptions of external inputs and internal biogeochemical processes, the simulation suggests that phosphorus releases from the sediment are about three-quarters of the catchment phosphorus load and sediment nitrogen releases are about one-half of external inputs (Table 29).

The fish community of Lake Rotomānuka is known only from a single netting in March 2015. However, this was a fairly intensive exercise that involved gill nets, fyke nets and trammel nets. From this netting we can safely conclude that koi carp are not present in Lake Rotomānuka and a natural barrier downstream of the lake (Rowe & Dean-Speirs 2009) should at least hinder natural introduction of the species. Common bullies are numerically the most abundant fish in Lake Rotomānuka North, but appear to be absent from smaller Lake Rotomānuka South. Shortfin eels, rudd and goldfish comprise most of the fish community in Lake Rotomānuka South. Our calculations of fish contributions to nutrient and sediment budgets contributions are based on koi carp only, because these are the only numbers available at the time. Therefore, Table 30 states that there is no effect of carp on nutrients and sediment in this lake. It would be useful to establish quantitative relationships of sediment and nutrient mobilization for other fish and to boat electrofish Lake Rotomānuka to provide a better estimate of their effect on water quality.

Some of the management scenarios tested with the Lake Rotomānuka model are projected to move the lake into a better NOF band. Overall, R8 (50% reduction in external TN and TP load across the catchment) was superior to the others. For TN, scenarios R6 (50% reduction in external TN load) and R8 (50% reduction in external TN and TP load) moved Lake Rotomānuka's simulated NOF classification out of the bottom line (D) to a C value. For chlorophyll *a*, scenarios R6 (50% reduction in external TN load) and R7 (50% reduction in external TP load) moved the classification to the threshold of C-D bands after previously (in base case R0) clearly failing to meet the bottom line.

These three scenarios are projected to establish Lake Rotomānuka at the upper end of the C-band for total nitrogen and move the median total chlorophyll *a* concentration right on the border between C and D. The effectiveness of the scenario including high attenuation of nutrients in the wetland (R2) suggests that flow-through wetlands present an opportunity to enhance water quality of the lake by attenuating nutrients. One focus area should be to protect and enhance existing wetland areas and to convert farm drains to wetlands, and, to ensure that wetland vegetation is established should water level modifications result in further inundation. It is however pointed out that the wetland scenario is associated with high levels of uncertainty, because the volume flow through the wetland and its nutrient attenuation are not based on site-specific data, but only on assumptions.

Table 29: Lake Rotomānuka annual mean total nitrogen, total phosphorus and suspended sediment (kg ha^{-1} y^{-1}) contributed from external (catchment) loads, sediment resuspension and release of dissolved nutrients from bottom sediments. Area normalisation to lake surface area derived from the hypsographic curve used for the model (15.5 ha).

		External	Resuspension	Sediment release
Phosphorus (kg ha^{-1} y^{-1})	Mean	3.4	0	2.6
	Range	0.2 – 6.2	-	2.4 – 2.8
Nitrogen (kg ha^{-1} y^{-1})	Mean	53	0	28
	Range	25 – 99	-	27 – 29
Sediments (kg ha^{-1} y^{-1})	Mean	522	0	-
	Range	149 – 843	-	-

Table 30. Proportion (% Carp) of sediment, total phosphorus and total nitrogen inputs to Lake Rotomānuka due to carp resuspension in relation to the total inputs (external + internal loads), proportion of external to total internal inputs (External/ Internal). No value is given for resuspension to sediment nutrient release ratio (Resuspension/ Sediment release) as resuspension was not simulated in the model simulations for this lake.

	% Carp	External / Internal	Resuspension / Sediment release
Phosphorus	0	1.27	-
Nitrogen	0	1.89	-
Sediments	0	0.19	-

The flow of carbon through the food web in Lake Rotomānuka based on stable isotope data was not clear as it did not conform to expected fractionation shifts. Consequently, limited conclusions can be made regarding carbon flow in that lake (Figure 137). However, in spring at least, large- and

medium-sized eels were at the top of the food chain; in summer all fish were tightly grouped. As in Lake Ngāroto, gambusia displayed high $\delta^{15}N$ values potentially reflecting (i) localised N enrichment along lake margins, or (ii) unusual dietary pathways involving live birth where developing fish consume parental carbon. Gut content analyses underway for catfish, eels, common bully and gambusia from both lakes should help resolve feeding relationships among species. At this stage, no further conclusions can be made of Lake Rotomānuka regarding the implications of lake management on food-webs based on isotopic analysis.

Extended conclusions

The modelling used in this study provides a mechanism to synthesise available data, identify shortfalls in the data and assist with prioritisation of monitoring indicators to document the effects of remediation actions. Modelling complements expert knowledge and 'best guesses' about what remediation actions may be most effective. Certainty around model predictions could be increased substantially by ancillary field and lab-based studies that focus on the most sensitive model outputs, as well as lab and field-based studies of geochemical materials which may be used to treat internal nutrient loads (e.g. by flocculation, inactivation and/or capping). The sensitive model parameters were reasonably universal across the lakes and this universality also pertains to water quality modelling studies in general. The sensitive parameters included coefficients that alter biogeochemical transformations with temperature, sediment nutrient releases and cyanobacteria growth and respiration rates (but noting high sensitivity of diatoms to these parameters also).

Overview of key processes and modelling of the study lakes

This study has revealed important similarities and differences between riverine and peat lakes. Many of the riverine lakes have enormous sediment and phosphorus legacies and high levels of internal loading but low levels of inorganic phosphorus in the water column due to adsorption onto inorganic sediments. This adsorbed P is likely stripped off during periods of high productivity. Thus, there is a dynamic exchange of phosphorus between inorganic suspended sediments and phytoplankton (the dominant flora), but there is a sufficiently large reservoir of phosphorus associated with the inorganic sediments that it maintains a semi-continuous supply to support the high levels of phytoplankton biomass. This is somewhat analogous to the findings of Abell et al. (2013) for sediments in a tributary to Lake Rotorua but with lower levels of phosphorus enrichment in that study. Peat lakes may be slightly acidic, somewhat coloured and potentially have some resilience to catchment nutrient loads, as indicated by the case of Lake Rotomānuka. These aspects have not been modelled explicitly in this study and therefore model results for Lake Rotomānuka probably have the greatest degree of uncertainty. The large depth to area ratio for Rotomānuka means it is less subject to sediment resuspension and the wetland area between the tributary from Rotomānuka South to Rotomānuka North may also be important in attenuating nutrients generally. Lake Ngāroto is shallower than Lake Rotomānuka and represents an intermediate case (i.e., somewhat riverine and peat in character). Its suspended sediments attenuate light effectively as concentrations are not especially high considering the low water clarity (i.e., the sediments would

appear to be fine-grained) and these sediments are also likely to liberate phosphorus during periods of high demand from phytoplankton.

The extent of wetland attenuation in the area between Rotomānuka North and Rotomānuka South remains largely unknown because it could not be isolated in our study given the large number of other unknowns in the phosphorus balance. Determining wetland attenuation would be useful and, if identified to be particularly important, would provide weight to actions designed to increase riparian wetland areas including blocking drains or other hydrological modifications to increase saturated soil areas that promote development of wetlands.

Annual nutrient budgets can be very useful for derivation of restoration targets and to evaluate the relative importance of different nutrient sources. For external (catchment) nutrient loads this process is well established but is much less so for loads generated by benthivorous fish or by internal loads – either from sediment resuspension or induced biochemically (e.g., mostly in association with anoxia). State variables (total nitrogen, total phosphorus, etc.) are most commonly interrogated by users following lake model simulations output but there is considerably more information available from these simulations. This information relates to the numerous fluxes that alter the state variable concentrations during a model run. We have used this information to provide fluxes for sediment resuspension and releases of dissolved nutrients at each model time step, then integrated these fluxes over each year, ultimately to provide an annual mean contribution of sediment resuspension to water column suspended sediments, total phosphorus and total nitrogen concentrations. Table 21, Table 25 and Table 29 provide a comparison of the estimated amounts of these three constituents that are contributed from external (catchment) discharge, in-lake sediment resuspension and release of dissolved nutrients from the bottom sediments for Lake Ngāroto, Lake Rotomānuka and Lake Waahi, respectively.

It should be re-emphasized that there are considerable uncertainties in these estimates as direct validation of parameters that alter internal fluxes has not been undertaken. Nevertheless there is useful information on the relative fluxes of material contributed by the three processes. In each of the lakes the external contribution of nitrogen is more important than for phosphorus and suspended sediment. This is especially so for shallow Lake Ngāroto and Lake Waahi, where resuspension of bottom sediments has a major impact on the levels of sediment and phosphorus in the water column, to an extent that contributions from sediment resuspension for phosphorus are comparable to those from the respective lake catchments, and for sediment they are several-fold higher. By contrast, sediment resuspension represents only a fraction (~ 20-35%) of the catchment

load for nitrogen, which is contained almost entirely as particulate organic nitrogen within the bottom sediments, aside from a small dissolved component. The case for Lake Rotomānuka is quite different because sediment resuspension was not modelled in this lake due to its relatively high depth to area ratio. Releases of dissolved material do not, of course, impact on suspended sediment concentrations in the water column (i.e., there is no contribution to suspended sediments in the three lakes). Like sediment resuspension, bottom-sediment nutrient releases were a major contributor to the water column concentrations of total nitrogen and total phosphorus (Table 21, Table 25 and Table 29), but in all three lakes as opposed to only the two shallow lakes for the case of sediment resuspension. The ratio of nitrogen to phosphorus in sediment releases was also considerably higher in the dissolved nutrient releases for Lake Ngāroto (Table 22) and Lake Waahi (Table 26) owing to the dominance of particulate inorganic phosphorus associated with resuspended sediments. For Lake Rotomānuka, sediment nutrient (nitrogen and phosphorus) releases represented around one-half of the catchment nutrient load (Table 30). For Ngāroto and Rotomānuka, the combined internal load of phosphorus from resuspension and dissolved releases was of the order of 50 to 100% larger for phosphorus, and 50% smaller for nitrogen, than the combined catchment contribution. In Lake Ngāroto, dissolved nutrient releases dominated over sediment resuspension as a contribution to the internal load, and vice-versa for Lake Waahi.

Benthivorous fish have the potential to make a significant contribution to suspended sediment and nutrient concentrations in lakes by resuspending bottom sediments. Several caveats need to be outlined in calculations to assess this contribution relative to other sources. First, the sediment and nutrient loads (both internal and external) with which they are compared are themselves ‘best approximations’. Second, only carp have been assessed. Third, in terms of nutrients, only excretion has been considered, while for sediment an independent (literature) value has been assumed. The values given for nutrients can therefore be expected to be conservative although particulate nutrients resuspended by carp may sediment out rapidly and have minimal ecological impact. Fourth, there is considerable uncertainty about what material actually persists in the water column as opposed to that which rapidly sinks out of the water column and has minimal persistent effect. Putting aside these caveats, carp contribute around 3% of the total (internal + external) nitrogen and phosphorus loads to Lake Ngāroto (Table 22) and Lake Waahi (Table 26), and about 16% of the total sediment load. Carp have not been found in Lake Rotomānuka so have no effect on nutrients and sediment in this lake (Table 30).

Nutrient dynamics and cyanobacterial responses

Similarities exist in all lakes in terms of seasonal variations in nitrogen concentrations. Seasonal variations in total nitrogen and ammonium are not especially evident except for the association of anoxic waters with high ammonium concentrations, but for nitrate there is a very strong seasonality across all lakes. Concentrations of nitrate peak in mid-winter. At this time there is a net gain of water in the catchment from reduced rates of evapotranspiration and winter rains. This can potentially lead to water-logging and saturation of soils in some areas of the catchment, with minimal attenuation and a relatively direct conduit for nitrate, which is readily leached, to reach the lakes.

The nitrate load to the lakes may also be expressed in high nitrate concentrations within the lake due to relatively low water temperatures and extremely poor light climate, reinforced by lower incoming solar radiation in winter, which limits phytoplankton growth and nutrient uptake. The post-winter period may be a critical one as temperatures warm, solar radiation increases and phytoplankton biomass increases rapidly in response to large pools of phosphorus and nitrogen (notably nitrate) in the water column. Nitrate concentrations decrease correspondingly with increases in phytoplankton biomass, to the point where in mid to late summer nitrate approaches the limits of detection, i.e., to levels where inorganic nitrogen may be considered to be limiting phytoplankton growth. At most other times of the year the model output indicates that phytoplankton growth is likely to be limited by availability of phosphorus, but with occasional occurrences of switching between nitrogen and phosphorus limitation.

There are two potentially interesting and opposing views on what should be done in terms of nitrogen restrictions to limit phytoplankton growth and cyanobacteria in particular. The first is that the spring-summer phytoplankton biomass is likely to be associated with the extent of the winter build-up of nitrate. Reducing nitrate loads will therefore result in a sustained reduction of phytoplankton biomass. This view seems logical but is not easily testable with the limited duration of data available in this study. The second view is that strong nitrate limitation in summer could be reinforced by large reductions in the nitrate supply in winter. This could create conditions conducive to the proliferation of nitrogen-fixing cyanobacteria (e.g., *Dolichospermum* sp., *Aphanizomenon* sp. and *Cylindrospermopsis raciborskii*), all of which are commonly found amongst the phytoplankton assemblage in the eutrophic lakes of this study, but not the non-nitrogen-fixing *Microcystis* sp. For example, low inorganic nitrogen leading to heterocyst formation in *Dolichospermum planktonica* (basionym *Anabaena planktonica*) in Lower Karori Sanctuary Reservoir was found to be a major factor in the formation of blooms by this species.

The potential impact of controlling nitrogen is controversial and strongly contested amongst workers in the field (e.g., Schindler et al. 2008; Hamilton et al. 2016; Smith et al. 2016) but a precautionary approach would dictate that phosphorus reductions should be undertaken concomitantly with nitrogen reductions in the catchment, ensuring that nitrogen to phosphorus ratios in catchment loads are not decreased through remediation actions (Hamilton 2017). Moreover, recently Søndergaard et al. (2017) emphasised the key role of nitrogen in shallow lakes. It seems unlikely that nitrogen fixation can make up for whole-lake nitrogen deficits (although this is also contested), but the paucity of measurements of nitrogen fixation across New Zealand lakes, either directly via isotopic and/or acetylene reduction techniques or indirectly from microscopic enumeration of heterocysts, is a major gap given that so much emphasis has been placed on voluntary, planning and policy mechanisms to reduce nitrogen loads; often with little attention given to phosphorus. The role of nitrogen fixation in supporting bloom-forming, N-fixing cyanobacteria, as well as providing a source of 'new' nitrogen to lakes, should be part of a dedicated core of research. This research could also be extended to modelling, as the current shallow lakes study did not include parameterization of nitrogen fixation algorithms in the cyanobacteria state variable, mostly because of lack of observed data.

Insights from parameter sensitivity analysis

Temperature coefficients tend to be very sensitive in conventional sensitivity analyses because biogeochemical responses to temperature are exponential, i.e., a 10% change in a temperature coefficient could be expected to produce at least a 10% change in the variable it directly affects. However, temperature coefficients can generally also be constrained quite tightly around a 'Q10' function where biogeochemical rates can be expected to double for each 10^{o}C increment in temperature. The exception to this is temperature coefficients for cyanobacteria, for which it is necessary to prescribe considerably higher rates of growth with temperature than is represented by a Q10 function, and diatoms, which have lower rates. The parameters in the temperature function for these groups can, however, be constrained on the basis of literature values. What this means in general is that the model outcome is sensitive to water temperature changes but at least the trajectories of the responses of the system should be predictable. Preliminary work by the modelling group at the University of Waikato, some initial simulations of increased air temperature for the shallow lakes in the current study, and quantitative and qualitative predictions across the globe, generally show common alignment. That is that climate change is likely to make it more difficult to achieve restoration goals and conformity to water quality targets. Therefore, current lake water quality targets based on trophic state for a given catchment nutrient load will be conservative and

additional vigilance will be required in the future to protect lakes from excess nutrient loads. Achieving water quality goals under a climate-warming regime may result in additional pressure to address internal loads via geochemical engineering (Spears et al. 2014). This approach is costly and has reduced probability of success, or at least reduced longevity of response, if catchment nutrient loads are not strongly attenuated. The implication of the above is that climate change has to be built into future model scenarios for the shallow lakes.

Sediment nutrient release rates have been found to be highly sensitive in almost all applications of the DYRESM-CAEDYM water quality model used in this study. The model prescription of sediment nutrient releases is simplistic, with releases governed by dissolved oxygen, pH and temperature of the water layer in contact with the sediments. The model does not maintain an explicit inventory of bottom-sediment composition that might otherwise be possible by balancing sedimentation, exchange of dissolved nutrients and sediment resuspension. Sediment nutrient releases may be appropriately calibrated for the five-year duration of the simulations carried out in this study, but not necessarily for past or future projections. For example, bottom-sediment composition and release rates respond to catchment nutrient inputs. Özkundakci et al. (2012) made a series of assumptions and calculated past lake trophic state and sediment composition in order to adjust sediment nutrient release rates in a DYRESM-CAEDYM application to Lake Rotorua. This allowed hindcasts and forecasts to be made of water quality in Lake Rotorua with greater confidence in the model output. Given that no such adjustments were made in the present study, responses to reductions in catchment nutrient loads in the scenarios may be conservative, i.e., water quality may be improved through time to a greater extent than is indicated by the model outputs.

Lag times in response to restoration

The question arises as to how long it will take for the bottom sediments of the lake to approximately equilibrate to the catchment sediment and nutrient load. Three time scales need to be considered and these will operate in both a serial and parallel time sequences.

The first time lag relates to how long it will take for the catchment loads to reach a new equilibrium in response to targeted actions in the catchment. Given the contentious nature of policy change in this area around New Zealand and a typical ecological response time for a catchment (c. 10-20 years; Hamilton et al. 2016), we estimate that the catchment response time may be of the order of 10 to 30 years. It will take longer for nitrogen than phosphorus because there is greater sub-surface (groundwater) delivery of nitrogen in the form of nitrate. Attempts to reduce nutrient loads by going part-way towards meeting the catchment loads required to shift a lake above the bottom line (i.e,

from D to C band in the National Policy Statement for Freshwater Management) may increase the length of time for meeting restoration goals. That is not to say that there may not be some worthy outcomes from catchment management actions (e.g., plantings in riparian areas and other areas in lake catchments), and these should be used as part of the objective-setting for restoration outcomes, but they will likely be aesthetic, with little tangible outcome for water quality if they are not of sufficient scale and magnitude, i.e., leading to at least a 50% reduction in nutrient loads required to shift the lakes out of the 'bottom line'.

The second time scale is that required for the internal load to respond to changes in the catchment load of sediment and nutrients. This is extremely difficult to predict but there may be clues in the literature. Rutherford et al. (1996) used a theoretical approach to estimate that large (80 km^2) Lake Rotorua might take nearly 200 years for this bottom-sediment equilibration to occur. The lakes in our study are considerably smaller and of similar size to those examined by Jeppesen et al. (2002), who found that re-oligotrophication could occur over time scales of only 10 to 20 years. We consider that the upper limit of the study by Jeppesen et al. may be more appropriate – and perhaps longer for Lake Ngāroto and Lake Waahi – given the enormous legacy of enriched sediments present in these lakes. In the case of relatively large Lake Waikare (area 43 km^2) which has become very shallow because of extremely high sediment loads, re-oligotrophication may take even longer and a 200-year horizon may be an upper limit for recovery of the bottom sediments to some pre-eutrophication condition.

The third time scale to be considered relates to the ecological response. By comparison with the catchment and bottom-sediment recovery times scales, the ecological response time scale is likely to be quite rapid from a trophic state point of view. Uncertainties in this time scale relate to any coarse fish control actions that may be undertaken in the lakes and how the food web might respond – likely beneficially – in terms of trophic state, resilience and biodiversity. Introductions of exotic species are a further confounding factor; likely inevitable, unpredictable but perhaps less likely to be impactful nowadays given that exotic species have already exploited 'unoccupied' niches in the lakes.

Considerations of model spatial scales and relationships with field programmes

The modelling undertaken in this study is one-dimensional, i.e., it resolves vertical variations in constituents but not horizontal variations. The initial concept of the one-dimensional model

(DYRESM-CAEDYM) was to use it as a box model to carry out simulations over multiple years, with little initial concern about the vertical dimension. The one-dimensional model was used in preference to developing a box model independently, given that computational speeds on desktop computers are not especially restrictive nowadays. Resolving the vertical dimension proved to be critical not only for Lake Rotomānuka, which is relatively deep and stratifies for extended periods, but also for the other shallow lakes where periods of thermal stratification of more than a day or two brought about low oxygen levels or anoxia in bottom waters. In the case of Lake Waahi, elevated water temperatures led to relatively low levels of dissolved oxygen throughout the water column (around 50% of saturation) in both model simulations and in the high-frequency sensor data. If these changes are symptomatic of what can be expected with a warming climate, then they are a call to action; these degraded shallow lakes appear to be highly vulnerable to impacts of a warming climate, with fish kills likely to be a direct impact from increased water temperatures and loss of dissolved oxygen, and further eutrophication a response to anoxia-induced releases of nutrients from bottom sediments. What is especially concerning is that there are strong hints of the sorts of changes a warming climate might induce in these degraded shallow lakes.

Improvements in the accuracy and confidence of lake model simulations could be aided greatly by a sampling programme dedicated to capturing changes in nutrients concentrations through the water over periods of stratification. High-frequency temperature and dissolved oxygen data at Lake Ngāroto and Lake Waahi could provide a foundation for such a monitoring programme designed to validate the release rates of dissolved nutrients from the lake bed.

Resilience to global environmental change

The modelling has reinforced that these lakes require substantial and sustained interventions to meet the bottom line in the NPS, especially given that global environmental change drivers (e.g., climate, invasive species and agricultural intensification), while already influencing the ecological status of the lakes to varying extents, will intensify (e.g., Trolle et al. 2011). Observations and model simulations indicate that the effect of warm summers appears to be exacerbated by the eutrophic state of the lakes. Invasive species are already having significant effects at multiple levels of the food web (e.g., phytoplankton such as the cyanobacterial species *Cylindrospermopsis raciborskii* and a whole suite of invasive fish species such as goldfish, catfish and koi carp). Moreover, the invasive macrophyte *Egeria densa*, which has previously invaded the Waikato shallow lakes, has been implicated in sudden collapses of macrophyte populations and regime shifts to turbid, phytoplankton-dominated states. Lakes Ngāroto, Waahi and Waikare are examples where such a

regime shift appears to have already occurred. While these lakes remain in a highly turbid state with no sign of a decrease in external nutrient or sediment loads, it is highly improbable that a regime shift to a clear-water state is possible. Coarse fish which have a benthivorous feeding mode will reinforce the turbid, phytoplankton-dominated state.

Given such a predicament for the shallow Waikato lakes, what is urgently required is at least one demonstration lake where it can be shown that a change to a clear-water, macrophyte-dominated state is possible (even if the macrophyte is an introduced species). In the short-term this is only like to occur where: (1) there is significant 'buy in' from land owners in the catchment to address excess sediment and nutrient loads, and a commitment to a large percentage (>50%) reduction in current sediment and nutrient loads, (2) where there is 'buy in' from land owners to raising water levels and potentially inundating production land, to go part way towards historical levels, (3) a major and ongoing programme of coarse fish removal to get the total population biomass to a level below where it is likely to have a significant impact on water quality (i.e., c. < 50 kg ha^{-1}), and (4) once all of this is achieved, use of geochemical engineering to address the enormous legacy load of nutrients and sediments in the bottom of the lake. This consideration of geochemical engineering does not take into account any cultural or economic aspects of the application of a chemical for nutrient (generally phosphorus) control. However, it is already clear in terms of water quality that three of the lakes (Waikare, Waahi and Ngāroto) have gone beyond trophic state 'tipping points'. Continued high nutrient loading means these lakes may be subject to unpredictable outcomes (e.g., Lake Waikare 'turning red' with the phytoplankton *Monoraphidium*, which temporarily displaced the dominant cyanobacteria in that lake). Persistent and severe algal blooms are symptomatic of major degradation. A carefully designed geochemical engineering progamme for at least one lake may need to be 'put on the table' to provide outcomes that may be immeasurably better than those indicated by the current trajectory of water quality indicators, whilst noting that engineered outcomes may be short-lived if they are not complimented by catchment management actions.

Geochemical engineering

In further considering geochemical engineering, it is worth noting the case of alum (aluminium sulphate) dosing for lake restoration. The effectiveness of alum is highly dependent on lake pH and buffering capacity both in terms of phosphorus binding capability and potential toxic effects. One-off bulk dosing of alum is only possible if the lake buffering capacity is sufficient to prevent substantial release of hydrogen ions following the hydrolysis reaction of aluminium sulphate to aluminium hydroxide. If the buffering capacity is insufficient, lake water may drop below pH 6, reducing

phosphorus binding capacity of aluminium hydroxide. A decrease of pH to below 4 would likely lead to toxic effects on lake biota. Effects of continuous alum dosing are comparatively poorly understood both in terms of effectiveness of phosphorus sequestration and potential toxicological effects. In the case of Lake Rotorua (North Island), there has been a remarkable transformation of community attitudes generally with respect to the state of the lake, coinciding with marked improvements in water quality in the period since alum dosing commenced in 2006 (Smith et al. 2016). The Bay of Plenty Regional Council have been duly conservative and relatively well controlled as dosing is via trickle feed in two of the inflows, rather than a widespread single direct application to the lake (Tempero et al. 2015). Risks are reduced through the continuous dosing method used for Lake Rotorua and an intensive chemical and biological monitoring programme is in place to allow for early detection of adverse impacts of terms of legacies of geochemical contaminants (e.g., aluminium) in bottom sediments and effects of fauna (e.g., bullies, smelt). A similarly careful approach will be necessary for Waikato lakes and it has to be recognised that alum dosing is a temporary measure designed to address legacy effects while land use change and improved land use practices take effect.

The assumptions made in the model about changes in internal loading in our study are hypothetical and will depend on many factors including the geochemical material used, the dose rate, the characteristics of the water to which it is being applied, the extent of the legacy of sediment and nutrients, and the method of application. Most geochemical remediation materials target phosphorus but there can be ancillary effects on nitrogen. These may occur as a result of flocculation of organic material and general reductions in the amount of organic material in the water column. In modelling of Lake Rotorua it became evident that the effects of alum were considerably greater than removing phosphorus from stream inflows alone (Hamilton et al. 2014). It was necessary to also introduce terms for increased sedimentation of phosphorus in the lake itself as well as reduced sediment oxygen demand of the bottom sediments of the lake. The modelling of Lake Rotorua has indicated that alum has directly or indirectly reduced total phosphorus concentrations in the water column by more than 50% for the dose rates used over the past 5 or so years.

Food webs and effects of coarse fish

The field studies conducted indicate that native fauna (shortfin eels, for example; a keystone species) are remarkably resilient to water quality pressures and have responded to high rates of productivity in these systems by also being quite productive. However, the introduced species (koi

carp, catfish, gambusia and goldfish) are also similarly resilient to water quality pressures. A warming climate is likely to be a major concern for the balance of native and introduced species. Effects of increased temperature may be amplified if there are subsidiary effects leading to reduced levels of dissolved oxygen, as field data suggest and modelled data reinforce in this study.

It should be emphasized that the estimates of coarse fish contributions to water column sediments (16%) and nutrients (3%) in Lake Waahi and Lake Ngāroto are conservative and there may be wide confidence limits in these values (with some of the assumptions discussed below). This percentage may appear small but if control measures are discrete and successful then they may be nearly instantaneous (as opposed to catchment planting, for example). If the contribution of coarse fish is closer to 10% of water column nutrients, then controls could make an excellent complement to other nutrient control strategies. There are other strong imperatives for managing pest fish species, however, beyond attempting to reduce or eliminate their contributions to nutrients and sediments released from bioturbation and excretion. The isotopic studies contributing to our shallow lakes' report point to the strong likelihood of overlap of food sources and habitat of shortfin eels and catfish. Gambusia may be also alter the connectivity of terrestrial-littoral-pelagic habitats and our food web study has demonstrated that organic matter from marginal vegetation is important. Controls on exotic fish must therefore be part of a targeted multi-stressor approach to restoration in much the same way as these multiple stressors effected degradation of the shallow lakes. Connectivity has not been considered in any detail as part of this study but is implicit in the isotopic and habitat considerations, and needs to be considered carefully in all aspects of fish management. Connectivity provides the critical link for native species to re-establish or enhance lake populations but it also provides new- or re-invasion opportunities for large exotic fish populations nearby habitats (e.g., the Waikato River; Daniel et al., 2011).

There were a number of assumptions, limitations, and knowledge gaps regarding the fish objective that we could not address within the scope of this study, and these deficiencies of knowledge contribute to the uncertainty of our estimates. For instance, in our calculations, we assumed that the available sampling data was representative of the fish community and that mean fish weight was an adequate proxy for the captured fish size distributions. Sediment resuspension by carp was based on equations for carp but these cannot be guaranteed to accurately reflect the actions of invasive fish in the Waikato region. For example, experiments by (Breukelaar *et al.* 1994) included perch and were conducted in small ponds. Experiments by (Badiou & Goldsborough 2010) used large common

carp (mean weight 2790 to 4350 g), which might overestimate the measured rates compared to the smaller carp in our study (mean weight about 605 g).

The major knowledge gaps identified in our study provide a basis for future targeted research on coarse fish, which could include: 1) areal fish biomass estimates and size distributions, especially for Lake Rotomānuka, 2) sediment resuspension rates for fish other than carp (for example, goldfish) as rates for bream, for instance, are 3-fold higher than for carp (Breukelaar *et al.* 1994), and 3) sediment pore water concentrations of nitrogen and phosphorus combined with understanding water volume of this pore water is disturbed and released to the water column during feeding. Addressing these deficiencies would improve our ability to model the effects of invasive fish on shallow Waikato lakes.

Achieving successful restoration

This modelling study has addressed aspects relating to the *magnitude* of change required to attain certain levels of water quality but not detail of *how* these changes may be carried out. To demonstrate the level of detail of 'how', we provide an example of water level increases. An increase in water level did not produce the expected outcome of reduced sediment resuspension in Lake Ngāroto, but this may relate to the prescription in the model of sediment resuspension rates that are generalised to the whole lake rather than being prescribed specifically for the shallower, newly inundated areas. Such areas may have lower rates of sediment resuspension, particularly if they can be engineered to have certain desirable features. These features might include: coarse sediments with low organic content (e.g., a sand capping could be considered), moveable structures (e.g., baffles) that might reduce sediment resuspension (whilst noting that these structures could create conditions conducive to cyanobacteria blooms, hence their mobility); synthetic macrophytes that could act as refugia for zooplankton and be put in place prior to inundation; plantings of submerged macrophytes on dry land immediately prior to inundation; and habitat features that could favour native fish over coarse fish (although such a habitat differentiation may not yet be well understood). Furthermore, if there was a major drawdown of a lake prior to filling to higher levels, then it could offer an opportunity to remove areas of fine sediment and to extend the area of dry land where habitat was being modified.

The hypothetical example of drawdown emphasises that innovation and planning need to be brought out with the implementation of each remediation measure, and to optimise its performance in meeting the goals for restoration. The challenges for restoration outlined in this study are immense, in dealing with some of the most eutrophied lakes in the world, and extraordinary

measures and efforts will be required to not obviate responsibility or leave a legacy for future generations to deal with.

References

Abell, J. M., & Hamilton, D. P. (2013). Bioavailability of phosphorus transported during storm flow to a eutrophic, polymictic lake. New Zealand Journal of Marine and Freshwater Research, 47(4), 481-489.

Allan, M. G. (2016). *A coupled hydrodynamic-ecologicalmodel of management options for restoration of Lake Ohinewai.* ERI report No.68. Enviromental Research Institute, University of Waikato, Hamilton. ISSN 2350-3432.

Arhonditsis, G. B., & Brett, M. T. (2005). Eutrophication model for Lake Washington (USA) Part II - model calibration and system dynamics analysis. *Ecological Modelling, 187*(2-3), 179-200.

Badiou PH, Goldsborough LG. 2010. Ecological impacts of an exotic benthivorous fish, the common carp (Cyprinus carpio L.), on water quality, sedimentation rates and submerged macrophyte biomass in small wetland mesocosms. Wetlands 30:657–667.

Barnes, G. E. (2002a). *Water quality trends in selected shallow lakes in the Waikato region, 1995 – 2001.*Environment Waikato technical report 2002/07, Hamilton. ISSN: 1172-4005.

BCD, G. (2014). *Resource consent application to construct a new outlet weir and divert an existing inlet drain at Lake Ngāroto, Te Awamutu.* Waipa District Council, Te Awamutu, New Zealand

Beaton, R., Hamilton, D., Brokbartold, M., & Özkundakci, D. (2007). *Nutrient budget and water balance for Lake Ngāroto.* CBER contract report No. 54. Centre for Biodiversity and Ecology Research, University of Waikato, Hamilton.

Breukelaar, A. W., Lammens, E. H. R. R., Breteler, J. G. P. K., & Tatrai, I. (1994). Effects of benthivorous bream (*Abramis-Brama*) and carp (*Cyprinus-Carpio*) on sediment resuspension and concentrations of nutrients and chlorophyll-A. *Freshwater Biology, 32*(1), 113-121.

Burger, D. F., Hamilton, D. P., & Pilditch, C. A. (2008). Modelling the relative importance of internal and external nutrient loads on water column nutrient concentrations and phytoplankton biomass in a shallow polymictic lake. *Ecological Modelling, 211*(3-4), 411-423.

Burns, N., Bryers, G., & Bowman, E. (2000). *Protocol for Monitoring Trophic Levels of New Zealand Lakes and Reservoirs.* Lake Consulting report 99/2 prepared for Ministry for the Environment. Lake Consulting, Pauanui, New Zealand.

Burns, N. M., Rutherford, J. C., & Clayton, J. S. (1999). A Monitoring and Classification System for New Zealand Lakes and Reservoirs. *Lake and Reservoir Management, 15*(4), 255-271.

Collier, K. J., & Grainger, N. P. J. (2015). Invasive Fish Species and Communities in New Zealand. In K. J. Collier & G. N. P. J (Eds.), *New Zealand Invasive Fish Management Handbook* (pp. 212). Hamilton, New Zealand: Lake Ecosystem Restoration New Zealand (LERNZ; The University of Waikato) and Department of Conservation.

de Winton, M., Wadhwa, S., & Taumoepeau, A. (2014). Waikato lake bathymetry. In Unpublished memo to John Gumbley. NIWA: Department of Conservation, April 23 2014.

Daniel, A. J., Hicks, B. J., Ling, N., & David, B. O. (2011). Movements of radio- and acoustic-tagged adult koi carp in the Waikato River, New Zealand. North American Journal of Fisheries Management, 31(2), 352-362.

Davies-Colley, R. J. (1988). Measuring water clarity with a black disk. Limnology and Oceanography 33:6 16-623.

Dean-Speirs, T., & Neilson, K. (2014). *Waikato region shallow lakes management plan.* Waikato Regional Council, Hamilton, New Zealand.

Dean, H. (2015). *Living Water: Collation of Baseline Environmental Data for the Lake Rotomānuka Catchment.* Kessels Ecology Report DOC.00281 prepared for Department of Conservation of Fonterra. Kessels Ecology, Hamilton, New Zealand.

Deltares *Delft3D-FLOW: Simulation of multi-dimensional hydrodynamics flows and transport phenonmena, including sediments.* Deltares, Rotterdamseweg, The Netherlands, 1-706

Edwards, T., Winton, M., & Clayton, J. S. (2010). *Assessment of the ecological condition of lakes in the Waikato region using LakeSPI*. NIWA client report HAM2010-065. Prepared for Environment Waikato, Hamilton.

Faithfull, C., Hamilton, D. P., Burger, D., & Duggan, I. (2005). *Waikato peat lakes sediment nutrient removal scoping exercise.* Centre for Biodiversity and Ecological Research, Contract Report No. 78 prepared for Waikato Regional Council, Hamilton.

Friedman, R., Ansell, C., Diamond, S., & Haimes, Y. Y. (1984). The Use of Models for Water-Resources Management, Planning, and Policy. *Water Resources Research, 20*(7), 793-802.

Gal, G., Hipsey, M. R., Parparov, A., Wagner, U., Makler, V., & Zohary, T. (2009). Implementation of ecological modeling as an effective management and investigation tool: Lake Kinneret as a case study. *Ecological Modelling, 220*(13–14), 1697-1718.

Gal, G., Imberger, J., Zohary, T., Antenucci, J., Anis, A., & Rosenberg, T. (2003). Simulating the thermal dynamics of Lake Kinneret. *Ecological Modelling, 162*(1-2), 69-86.

Hamill, K., & Lew, D. (2006). *Snapshot of Lake Water Quality in New Zealand.* Prepared for the Ministry for the Environment by Opus International Consultants, MfE number: 776. 53pp.

Hamilton, D. P., Jones, H. F. E., Özkundakci, D., McBride, C., Allan, M. G., Faber, J., & Pilditch, C. A. (2012). Waituna Lagoon Modelling: Developing quantitative assessments to assist with lagoon management. University of Waikato, Hamilton.

Hamilton, D.P., McBride C.G. and Jones H.F.E (2014). Assessing the Effects of Alum Dosing of Two Inflows to Lake Rotorua against External Nutrient Load Reductions: Model Simulations for 2001-2012. Environmental Research Institute Report 49, The University of Waikato, Hamilton, 56 pp.

Hamilton, D. P., Salmaso, N., & Paerl, H. W. (2016). Mitigating harmful cyanobacterial blooms: strategies for control of nitrogen and phosphorus loads. Aquatic Ecology 50.3: 351-366.

Hamilton, D. P., Vant, W. N., & Neilson, K. A. (2010). The Waters of the Waikato: *Ecology of New Zealand's Longest River*, 245-264.

Hamilton , D. P. (2017). Summary of evidence in cheif statement of David Philip Hamilton on behalf of the Bay of Plenty Regional Council. Lake Rotorua Nutrient Management - Proposed plan change 10 to the Bay of Plenty Regional Water and Land Plan.The Resource Management Act 1991. SEW-133911-559-787-V1

Hayes, J. W., & Rutledge, M. J. (1991). Relationship between turbidity and fish diets in Lakes Waahi and Whangape, New Zealand. *New Zealand Journal of Marine and Freshwater Research, 25*(3), 297-304.

Hicks, B.J. & Brijs, J. 2009. Boat electrofishing survey of Lake Ngaroto. Client Report prepared for Waipa District Council. CBER Contract Report No. 111. Centre for Biodiversity and Ecology Research, Department of Biological Sciences, School of Science and Engineering, The University of Waikato, Hamilton.

Hicks, B.J., Daniel, A., Ling, N., Morgan, D. & Gautier, S. (2015) *Costs and Effectiveness of Different Methods for Capturing Invasive Fish*. Section 6.3 in Collier KJ & Grainger NPJ eds. New Zealand Invasive Fish Management Handbook. Lake Ecosystem Restoration New Zealand (LERNZ; The University of Waikato) and Department of Conservation, Hamilton, New Zealand. 123–132.

Hicks, B. J., Osborne, M. W., & Ling, N. (2006) Quantitative estimates of fish abundance from boat electrofishing. *Australian Society for Fish Biology Workshop Proceedings: A guide to monitoring fish stocks and aquatic ecosystems*. Darwin, Northern Territory, Australia: Northern Territory Department of Primary Industry, Fisheries and Mines.

Hicks, B.J., G.B. Reynolds, P.M. Jamieson, J.L. Laboyrie (2001) Fish populations of Lake Ngaroto, Waikato, and fish passage at the outlet weir. CBER Contract Report Number 14, Prepared for the Waipa District Council. Unpublished report, Centre for Biodiversity and Ecology Research, University of Waikato, Hamilton.

Hicks, B.J. and G.W. Tempero (2011) Comparative boat electrofishing surveys of Lake Waahi in 2007 and 2011. CBER Contract Report No. 117. Prepared for Genesis Energy. Centre for Biodiversity and Ecology Research, Department of Biological Sciences, Faculty of Science and Engineering, The University of Waikato, Hamilton.

Jenkins, B. R., & Vant, W. N. (2007). *Potential for reducing the nutrient loads from the catchments of shallow lakes in the Waikato Region.* Enviromental Waikato technical report 2006/54.Environmental Waikato, Hamilton, New Zealand. 29pp.

Jeppesen, E., Jensen, J. P. & Søndergaard, M. (2002). "Response of phytoplankton, zooplankton, and fish to re-oligotrophication: an 11 year study of 23 Danish lakes." Aquatic Ecosystem Health & Management 5.1: 31-43.

Jin, L., Whitehead, P. G., Baulch, H. M., Dillon, P. J., Butterfield, D., Oni, S. K., Futter, M. N., Crossman, J., & O'Connor, E. M. (2013). Modelling phosphorus in Lake Simcoe and its subcatchments: scenario analysis to assess alternative management strategies. *Inland Waters, 3*(2), 207-220.

Jones, H. F. E., & Hamilton, D. P. (2014). Hydrodynamic modelling of Lake Whangape and Lake Waahi. Prepared for Waikato Regional Council. Environmental Research Institute Report No. 31, University of Waikato, Hamilton. 33 pp.

Kingett, P. D. (1984). *An environmental history: Lake Waahi.* 201pp.

Lesser, G. R., Roelvink, J. A., van Kester, J. A. T. M., & Stelling, G. S. (2004). Development and validation of a three-dimensional morphological model. *Coastal Engineering, 51*(8–9), 883-915.

MfE. (2001). *Lake Ngāroto Restoration, a case study*. Ministry for the Environment, Wellington. 16p

MfE. (2015a). *A Draft Guide to Attributes in Appendix 2 of the National Policy Statement for Freshwater Management 2014.* Ministry for the Environment, Wellington.

MfE. (2015b). *A Guide to the National Policy Statement for Freshwater Management 2014.* Ministry for the Environment, Wellington.

Mitchell, S. F., Hamilton, D. P., MacGibbon, W. S., Nayar, P. K. B., & Reynolds, R. N. (1988). Interrelations between phytoplankton, submerged macrophytes, black swans (*Cygnus atratus*) and zooplankton in a shallow New Zealand lake. Internationale Revue der gesamten Hydrobiologie 73: 145-170.

Morgan, D. K. J., & Hicks, B. J. (2013). A metabolic theory of ecology applied to temperature and mass dependence of N and P excretion by common carp. *Hydrobiologia, 705*(1), 135-145.

Morris, M. D. (1991). Factorial sampling plans for preliminary computational experiments. *Technometrics, 33*(2), 161-174.

Norberg, J., & DeAngelis, D. (1997). Temperature effects on stocks and stability of a phytoplankton-zooplankton model and the dependence on light and nutrients. *Ecological Modelling, 95*(1), 75-86.

Özkundakci D, McBride CG, Hamilton DP. (2012). Parameterisation of sediment geochemistry for simulating water quality responses to long-term catchment and climate changes in polymictic, eutrophic Lake Rotorua, New Zealand. WIT Transactions on Ecology and the Environment 164: 171-182. [11th International Conference on Water Pollution: Modelling, Monitoring and Management, New Forest, UK, 10–12 July 2012. Brebbia CA (ed), Water Pollution XI].

Özkundakci, D., Hamilton, D. P., & Trolle, D. (2011). Modelling the response of a highly eutrophic lake to reductions in external and internal nutrient loading. *New Zealand Journal of Marine and Freshwater Research, 45*(2), 165-185.

Paul, W., Özkundakci, D., & Hamilton, D. P. (2008). *Modelling of restoration scenarios for Lake Ngāroto.* CBER Contract Report No. 81, Centre for Biodiversity and Ecology Research, The University of Waikato, Hamilton.

Rankinen, K., Lepistö, A., & Granlund, K. (2002). Hydrological application of the INCA model with varying spatial resolution and nitrogen dynamics in a northern river basin. *Hydrology and Earth System Sciences Discussions, 6*(3), 339-350.

Reeves, P., Craggs, R., Stephens, S., de Winton, M., & Davies-Colley, R. (2002). Environmental changes at Lake Waikare, North Waikato. Wave climate, water quality and 'biology'. NIWA Client Report EVW02235, Prepared for Environment Waikato, Hamilton.

Romero, J. R., Antenucci, J. P., & Imberger, J. (2004). One- and three-dimensional biogeochemical simulations of two differing reservoirs. *Ecological Modelling, 174*(1–2), 143-160.

Rowe, D., & Dean-Spears, T. (2009). Design of a fish barrier to prevent exotic fish entry into the Rotopiko/Serpentine lakes: issues, options and optimal designs. Prepared for Department of Conservation, NIWA Client Report HAM2009-079.

Rutherford, J. C., S. M. Dumnov, and A. H. Ross (1996). "Predictions of phosphorus in Lake Rotorua following load reductions." New Zealand Journal of Marine and Freshwater Research 30. 3: 383-396.

Schallenberg, M., & Sorrell, B. (2009). Regime shifts between clear and turbid water in New Zealand lakes: environmental correlates and implications for management and restoration. New Zealand Journal of Marine and Freshwater Research, 43(3), 701-712.

Scheffer, M., Vandenberg, M., Breukelaar, A., Breukers, C., Coops, H., Doef, R., & Meijer, M. L. (1994). Vegetated areas with clear water in turbid shallow lakes. *Aquatic Botany, 49*(2-3), 193-196.

Schindler, D. W., Hecky, R. E., Findlay, D. L., Stainton, M. P., Parker, B. R., Paterson, M. J., ... & Kasian, S. E. M. (2008). Eutrophication of lakes cannot be controlled by reducing nitrogen input: results of a 37-year whole-ecosystem experiment. *Proceedings of the National Academy of Sciences,* 105(32), 11254-11258.

Schladow, S. G., & Hamilton, D. P. (1997). Prediction of water quality in lakes and reservoirs .2. Model calibration, sensitivity analysis and application. *Ecological Modelling, 96*(1-3), 111-123.

Schmolke, A., Thorbek, P., DeAngelis, D. L., & Grimm, V. (2010). Ecological models supporting environmental decision making: a strategy for the future. *Trends in Ecology & Evolution, 25*(8), 479-486.

Smith, D. G., & Davies-Colley, R. J. (1992). Perception of Water Clarity and Color in Terms of Suitability for Recreational Use. *Journal of Environmental Management, 36*(3), 225-235.

Smith, V. H., Wood, S. A., McBride, C. G., Atalah, J., Hamilton, D. P., Abell, J. (2016). Phosphorus and nitrogen loading restraints are essential for successful eutrophication control of Lake Rotorua, New Zealand. Inland Waters 6.2: 273-283.

Søndergaard, M., Lauridsen, T. L., Johansson, L. S., Jeppesen, E. (2017). Nitrogen or phosphorus limitation in lakes and its impact on phytoplankton biomass and submerged macrophyte cover. *Hydrobiologia* 795: 35–48.

Spears, B. M, Maberly, S. C, Pan, G., Mackay, E., Bruere, A., Corker, N., Douglas, G., Egemose, S., Hamilton, D., Hatton-Ellis, T., Huser, B., Li, W., Meis, S., Moss, B., Lürling, M., Phillips, G., Yasseri, S., Reitzel, K.. 2014. Geo-engineering in lakes: a crisis of confidence? Environmental Science & Technology 48: 9977-9979.

Speirs, D., & Barnes, G. (2002). *Fish populations of Lake Rotomānuka 2000 & 2001.* Environment Waikato technical report 2001/07. Hamilton, New Zealand.

Stockdale, D. F. (1995). Sustainable peat lake management: The critical role of hydrological modelling. A study of the Rotomanuka dn Serpentine complexes, *Ohaupo.* MSc thesis, The University of Waikato.

Tempero, G., McBride, C., Abell, J., & Hamilton, D. (2015). Anthropogenic phosphorus loads to Lake Rotorua. Environmental Research Institute Report, 66.

Tempero, G. W., & Hicks, B. J. (2017). *Responses of the fish community and biomass in Lake Ohinewai to fish removal and the koi carp exclusion barrier.* Waikato Regional Council Technical Report 2017/10, Waikato Regional Council, Hamilton.

Thompson, M. (1994). *Substrate coring around the Waipa Peat Lakes to aid in the establishment of Esplanade Reserving.* BSc (Technology) Industry Report. University of Waikato, Hamilton, New Zealand.

Trolle, D., Skovgaard, H., & Jeppesen, E. (2008). The Water Framework Directive: setting the phosphorus loading target for a deep lake in Denmark using the 1D lake ecosystem model DYRESM–CAEDYM. *Ecological Modelling, 219*(1), 138-152.

Trolle D., Hamilton D. P., Pilditch C. A., Duggan I. C., Jeppesen E. (2011). Predicting the effects of climate change on trophic status of three morphologically varying lakes: Implications for lake restoration and management. *Environmental Modelling and Software* 26: 354-370.

Trolle, D., Hamilton, D. P., Hipsey, M. R., Bolding, K., Bruggeman, J., Mooij, W. M., Janse, J. H., Nielsen, A., Jeppesen, E., Elliott, J. A., Makler-Pick, V., Petzoldt, T., Rinke, K., Flindt, M. R., Arhonditsis, G. B., Gal, G., Bjerring, R., Tominaga, K., Hoen, J. t., Downing, A. S., Marques, D. M., Fragoso, C. R., Søndergaard, M., & Hanson, P. C. (2012). A community-based framework for aquatic ecosystem models. *Hydrobiologia, 683*(1), 25-34.

Verburg, P., Hamill, K., Unwin, M., & Abell, J. (2010). Lake water quality in New Zealand 2010: Status and trends. National Institute of Water & Atmospheric Research Ltd, Hamilton.

Vink, H. (2014). *Lake Ngāroto Hydrologic Modelling.* HVC Consulting Ltd. report prepared for Waipa Regional Council.

Wade, A. J., Durand, P., V, B., Wessel, W. W., Raat, K. J., Whitehead, P. G., Butterfield, D., Rankinen, K., & Lepisto, A. (2002). A nitrogen model for European catchments: INCA, new model structure and equations. *Hydrology and Earth System Sciences, 6*(3), 559-582.

Wade, A. J., Neal, C., Butterfield, D., & Futter, M. N. (2004). Assessing nitrogen dynamics in European ecosystems, integrating measurement and modelling: conclusions. *Hydrology and Earth System Sciences, 8*(4), 846-857.

Ward, F. J., Northcote, T. G., & Chapman, M. A. (1987). The effects of recent environmental changes in Lake Waahi on two forms of the common smelt Retropinna retropinna, and other biota. *Water, Air, and Soil Pollution, 32*(3), 427-443.

Wei, W. W. S. (1979). Some Consequences of Temporal Aggregation in Seasonal Time Series Models. In A. Zellner (Ed.), *Seasonal Analysis of Economic Time Series* (pp. 443-448). NBER.

West, D. W., Roxburgh, T., & Chisnall, B. L. (2000). *Fish communities of Lake Whangape, Waikato April 2000 survey.* Conservation Advisory Science Notes 322. Department of Conservation, Wellington.

West, A. O. and Scott, J. T. (2016), Black disk visibility, turbidity, and total suspended solids in rivers: A comparative evaluation. *Limnol. Oceanogr. Methods*, 14: 658–667. doi:10.1002/lom3.10120.

Whitehead, P. G., Wilby, R. L., Battarbee, R. W., Kernan, M., & Wade, A. J. (2009). A review of the potential impacts of climate change on surface water quality. *Hydrological Sciences Journal, 54*(1), 101-123.

Whitehead, P. G., Wilson, E. J., & Butterfield, D. (1998a). A semi-distributed integrated nitrogen model for multiple source assessment in catchments (INCA): Part I - model structure and process equations. *Science of the Total Environment, 210*(1-6), 547-558.https://doi.org/10.1016/S0048-9697(98)00037-0.

Whitehead, P. G., Wilson, E. J., Butterfield, D., & Seed, K. (1998b). A semi-distributed integrated flow and nitrogen model for multiple source assessment in catchments (INCA): Part II - application to large river basins in south Wales and eastern England. *Science of the Total Environment, 210*(1-6), 559-583.https://doi.org/10.1016/S0048-9697(98)00038-2.

Zammit, C. (2015). *Lake Whangape and Waahi inflows.* NIWA client report No. CHC2015-011 prepared for Environmental Waikato, Waikato Regional Council, Hamilton.

Zimmer K. D., Hanson M. A., Herwig B. R., Konsti M. L. (2009). Thresholds and stability of alternative regimes in shallow Prairie-Parkland Lakes of Central North America. *Ecosystems 12*, 843–852.

Appendix A: DYRESM-CAEDYM parameters used

Parameter name	Description	Ngāroto	Rotomānuka	Waahi	Sensitivity test
Pmax (CYANO)	Maximum growth rate	5.70.E-01	4.75.E-01	8.55.E-01	Y
Pmax (FDIAT)	Maximum growth rate	1.05.E+00	1.62.E+00	1.05.E+00	Y
IK (CYANO)	Parameter for initial slope of P/I curve	7.13.E+01	1.43.E+02	9.50.E+01	Y
IK (FDIAT)	Parameter for initial slope of P/I curve	2.85.E+01	1.90.E+01	1.90.E+01	Y
Kep (CYANO)	Specific attenuation coefficient of phytoplankton	1.33.E-02	2.85.E-02	1.33.E-02	Y
Kep (FDIAT)	Specific attenuation coefficient of phytoplankton	1.33.E-02	2.85.E-02	1.33.E-02	Y
KP (CYANO)	Half saturation constant for phosphorus	9.50.E-04	7.60.E-03	1.90.E-04	Y
KP (FDIAT)	Half saturation constant for phosphorus	9.50.E-04	3.80.E-03	9.50.E-04	Y
KN (CYANO)	Half saturation constant for nitrogen	1.62.E-02	3.80.E-02	1.62.E-02	Y
KN (FDIAT)	Half saturation constant for nitrogen	6.18.E-02	5.70.E-02	6.18.E-02	Y
UNmax (CYANO)	Maximum rate of phytoplankton nitrogen uptake	2.85.E+00	2.38.E+00	2.85.E+00	Y
UNmax (FDIAT)	Maximum rate of phytoplankton nitrogen uptake	3.14.E+00	2.38.E+00	3.14.E+00	Y
UPmax (CYANO)	Maximum rate of phytoplankton phosphorus uptake	3.80.E-01	1.14.E+00	2.85.E-01	Y
UPmax (FDIAT)	Maximum rate of phytoplankton phosphorus uptake	2.28.E-01	1.14.E+00	2.28.E-01	Y
vT (CYANO)	Temperature multiplier for phytoplankton growth	1.03.E+00	1.01.E+00	1.03.E+00	Y
vT (FDIAT)	Temperature multiplier for phytoplankton growth	1.01.E+00	1.01.E+00	1.01.E+00	Y
Tsta (CYANO)	Standard temperature	1.90.E+01	1.90.E+01	1.90.E+01	Y
Tsta (FDIAT)	Standard temperature	1.90.E+01	1.33.E+01	1.90.E+01	Y
Topt (CYANO)	Optimum temperature	3.04.E+01	3.04.E+01	3.23.E+01	Y
Topt (FDIAT)	Optimum temperature	2.76.E+01	2.19.E+01	2.76.E+01	Y
Tmax (CYANO)	Maximum temperature	3.52.E+01	3.71.E+01	3.71.E+01	Y
Tmax (FDIAT)	Maximum temperature	3.23.E+01	2.85.E+01	3.23.E+01	Y
kr (CYANO)	Respiration rate coefficient	6.65.E-02	4.75.E-02	6.65.E-02	Y
kr (FDIAT)	Respiration rate coefficient	1.52.E-01	1.62.E-01	1.52.E-01	Y
vR (CYANO)	Temperature multiplier for phytoplankton respiration	1.01.E+00	9.98.E-01	1.01.E+00	Y
vR (FDIAT)	Temperature multiplier for phytoplankton respiration	1.05.E+00	9.79.E-01	1.05.E+00	Y

fres (CYANO)	Fraction of respiration relative to total metabolic loss rate	9.50.E-02	7.60.E-01	9.50.E-02	Y
fres (FDIAT)	Fraction of respiration relative to total metabolic loss rate	6.65.E-01	7.60.E-01	6.65.E-01	Y
fdom (CYANO)	Fraction of metabolic loss rate that goes to DOM	9.50.E-02	6.65.E-01	9.50.E-02	Y
fdom (FDIAT)	Fraction of metabolic loss rate that goes to DOM	2.85.E-01	6.65.E-01	2.85.E-01	Y
ws (CYANO)	Constant settling velocity	0.00.E+00	9.50.E-09	0.00.E+00	Y
ws (FDIAT)	Constant settling velocity	9.50.E-10	-1.90.E-06	-9.50.E-10	Y
POC1max	Max transfer of POCL-DOCL	9.50.E-03	9.50.E-03	9.50.E-03	Y
POP1max	Max transfer of POPL-DOPL	9.50.E-03	9.50.E-05	4.75.E-02	Y
PON1max	Max transfer of PONL-DONL	3.80.E-02	9.50.E-02	7.60.E-02	Y
POMDia1	Diameter of POM particles (labile)	7.60.E-06	7.60.E-06	7.60.E-07	Y
POMDensity1	Density of POM particles (labile)	1.05.E+03	1.03.E+03	9.98.E+02	Y
tcPOM1	Critical shear stress for POM (labile)	2.85.E-02	4.75.E-02	2.85.E-02	Y
KePOC1	Specific attenuation coefficient of POM (labile)	5.42.E-02	4.47.E-02	4.47.E-02	Y
DOD1max	Max mineralisaton of DOPL-PO4	2.85.E-02	1.14.E-01	4.75.E-02	Y
DON1max	Max mineralisation of DONL-NH4	1.90.E-02	7.60.E-03	7.60.E-02	Y
KeDOC1	Specific attenuation coefficient of DOC (labile)	9.50.E-03	9.50.E-03	9.50.E-03	Y
vN2	Temperature multiplier for denitrification	1.04.E+00	9.79.E-01	1.02.E+00	Y
KoN2	Denitrification rate coefficient	1.14.E-01	8.55.E-01	2.38.E-01	Y
KN2	Half sat constant for denitrification	2.66.E+00	2.38.E-01	6.18.E+00	Y
vON	Temperature multiplier for nitrification	1.02.E+00	9.79.E-01	9.79.E-01	Y
KoNH	Nitrification rate coefficient	1.14.E-01	9.50.E-03	9.50.E-02	Y
KON	Half sat constant for nitrification	1.81.E+00	2.85.E+00	2.38.E+00	Y
deSS 01	Density of suspended solid particles	1.33.E+03	2.52.E+03	5.70.E+02	Y
diaSS 01	Diameter of suspended solid particles	9.50.E-07	2.85.E-06	1.52.E-06	Y
KeSS 01	Specific attenuation coefficient of suspended solids	4.76.E-02	4.76.E-02	9.50.E-03	Y
tcSS 01	Critical shear stress of suspended solids	7.60.E-02	4.75.E-02	8.08.E-02	Y
vSed	Temperature multiplier of sediment fluxes	1.19.E+00	1.01.E+00	1.01.E+00	Y
rSOs	Static sediment exchange rate	4.28.E+00	1.43.E+00	1.43.E+00	Y

KSOs	Half sat constant for DO sediment flux	4.75.E-01	9.50.E-01	1.90.E-01	Y
SmpPO4	Release rate of PO4	2.85.E-02	2.38.E-03	1.90.E-02	Y
KOxS-PO4	Half sat constant for PO4 sediment flux	9.50.E-01	2.85.E+00	9.50.E-01	Y
SmpNH4	Release rate of NH4	1.05.E-01	1.90.E-02	9.50.E-03	Y
KDOS-NH4	Half sat constant for NH4 sediment flux	9.50.E-01	4.75.E-01	6.18.E+00	Y
SmpNO3	Release rate of NO3	0.00.E+00	-4.75.E-02	-4.75.E-02	Y
KDOS-NO3	Half sat constant for NO3 sediment flux	8.08.E+00	1.43.E+00	8.08.E+00	Y
sedOrganicFrac	Fraction of sediment that is organics	1.43.E-01	1.43.E-01	3.80.E-02	Y
SedPorosity	Sediment porosity	2.85.E-01	8.55.E-01	5.13.E-01	Y
resusRate	Composite resuspension rate	3.80.E-02	0.00.E+00	5.23.E-02	Y
resusKT	Resuspension rate half sat constant	9.50.E+07	9.50.E+07	9.50.E+07	Y

Appendix B: Parameter sensitivity results

Results of one-factor-at-a-time sensitivity analyses of lake models for lakes Ngāroto, Waahi and Rotomānuka. The table shows the relative difference (in percent) of model summary metrics (see Table 1 in main text) relative to the simulation using calibrated values. Cells with values showing deviation by less or more than 10% are highlighted in blue and red, respectively.

Ngāroto

*This column indicates whether the parameter has been adjusted by minus or plus 10%.

Parameter	Adj*	Median					Summer metrics				
		TCHLA	TN	TP	TSS	SD	Mean summer TCHLA	Mean summer CYANO	Number stratified days	Number low oxygen days	Number of CYANO bloom days
DOD1max	Minus	97.7	99.9	101.2	99.7	100.7	99.0	99.1	99.3	100.3	99.8
DOD1max	Plus	102.5	99.9	99.2	99.9	99.1	100.2	100.6	99.3	100.7	101.1
DON1max	Minus	100.4	101.8	99.9	99.4	99.9	99.4	99.6	101.0	98.6	99.8
DON1max	Plus	100.1	98.5	100.2	99.9	99.9	100.1	100.4	100.2	99.3	100.0
IK(CYANO)	Minus	99.9	99.8	99.8	100.0	100.0	100.1	100.8	101.2	99.3	101.4
IK(CYANO)	Plus	100.2	100.0	100.1	99.8	99.9	99.8	98.8	100.7	100.7	98.9
IK(FDIAT)	Minus	100.4	100.3	100.0	100.1	99.8	100.1	100.0	100.3	99.3	100.0
IK(FDIAT)	Plus	99.8	99.8	100.0	100.1	100.0	99.6	100.2	100.2	100.7	100.3
KDOS-NH4	Minus	100.1	98.9	100.0	99.6	99.8	100.4	101.8	99.7	99.0	100.2
KDOS-NH4	Plus	100.1	101.2	100.1	99.9	99.9	100.2	99.7	100.2	100.0	100.0
KDOS-NO3	Minus	99.7	102.0	100.0	100.1	100.0	100.3	99.6	100.3	99.3	100.0
KDOS-NO3	Plus	100.2	98.6	100.0	99.7	99.8	100.4	101.7	99.3	98.6	100.2
KN(CYANO)	Minus	99.8	99.9	99.9	99.9	100.1	99.7	100.0	99.7	99.3	100.0
KN(CYANO)	Plus	100.0	99.9	100.0	99.8	99.8	99.8	100.0	100.7	100.7	100.5
KN(FDIAT)	Minus	99.8	99.9	100.1	99.8	99.9	99.6	99.4	100.2	101.4	100.0
KN(FDIAT)	Plus	100.0	99.9	100.0	99.6	99.9	100.3	100.3	100.2	99.7	100.0
KN2	Minus	99.8	100.5	100.0	99.8	100.1	100.2	100.9	100.0	99.7	100.2
KN2	Plus	100.2	99.5	100.0	99.8	99.8	99.7	100.1	100.3	99.3	100.2
KON	Minus	99.9	100.1	100.0	99.7	100.0	99.9	100.0	99.8	99.0	100.0
KON	Plus	100.3	100.1	100.0	99.9	99.9	99.4	100.0	99.8	99.7	100.0
KOxS-PO4	Minus	96.4	99.9	98.8	99.3	101.4	95.9	96.0	99.5	99.3	99.7
KOxS-PO4	Plus	104.3	100.3	101.4	100.4	98.6	104.0	105.6	99.8	98.3	101.2
KP(CYANO)	Minus	99.5	99.7	99.9	100.1	100.2	100.1	103.6	99.8	99.0	102.6
KP(CYANO)	Plus	101.1	100.3	99.8	99.7	99.7	99.5	96.0	100.5	100.3	97.6
KP(FDIAT)	Minus	101.0	100.3	100.0	99.9	99.7	99.3	96.0	100.7	99.7	97.1
KP(FDIAT)	Plus	99.5	99.9	99.9	99.8	100.1	101.1	103.6	99.8	99.0	101.7
KSOs	Minus	100.5	100.3	100.1	99.9	100.0	101.7	102.7	100.0	100.0	100.0
KSOs	Plus	100.1	99.8	99.8	99.6	100.0	98.6	98.8	100.2	100.0	100.0
KeDOC1	Minus	100.1	100.1	100.1	99.8	99.8	100.4	101.3	100.3	99.3	100.2
KeDOC1	Plus	100.3	100.0	99.8	99.9	100.1	99.9	99.8	100.3	100.3	99.8
KePOC1	Minus	100.3	99.9	100.0	99.8	100.0	99.7	99.7	98.8	99.7	100.2
KePOC1	Plus	100.1	100.1	100.0	100.0	99.8	100.0	100.0	100.7	101.0	100.0
KeSS01	Minus	100.8	100.1	99.9	100.0	99.5	100.6	101.2	98.3	100.0	101.2
KeSS01	Plus	100.1	100.1	100.0	99.9	100.2	99.7	99.3	101.8	102.4	99.5
Kep(CYANO)	Minus	100.3	99.9	100.0	99.9	99.8	100.4	100.5	99.3	99.7	100.3
Kep(CYANO)	Plus	100.0	100.0	100.1	99.8	99.9	100.0	100.6	100.8	101.4	100.0
Kep(FDIAT)	Minus	100.6	100.1	100.0	99.9	99.8	100.5	101.3	98.8	98.6	100.2
Kep(FDIAT)	Plus	99.8	99.9	100.0	99.7	99.9	99.5	99.5	101.0	100.0	100.2
KoN2	Minus	100.2	100.5	100.0	100.0	99.9	99.8	99.8	100.7	99.0	100.0
KoN2	Plus	100.2	99.4	100.0	100.2	99.8	100.4	100.5	100.0	99.3	100.0
KoNH	Minus	100.0	100.0	100.0	99.5	99.7	100.0	100.1	99.0	99.7	100.0

KoNH	Plus	100.1	99.8	100.1	99.8	99.8	99.8	99.7	100.8	100.3	100.0
Original		100.0	100.0	100.0	100.0	100.0	100.0	100.0	100.0	100.0	100.0
POC1max	Minus	100.0	99.9	99.7	100.1	100.1	100.1	99.8	100.0	97.9	100.0
POC1max	Plus	100.4	100.1	100.1	99.7	99.7	100.1	99.7	99.5	100.3	100.0
POMDensity1	Minus	116.3	254.5	409.1	174.9	94.4	106.1	78.7	102.8	93.8	92.7
POMDensity1	Plus	97.3	81.1	81.1	94.0	101.5	100.0	101.3	98.2	98.6	100.6
POMDia1	Minus	101.5	107.7	107.6	101.6	99.6	100.5	100.6	100.5	100.7	100.6
POMDia1	Plus	98.9	94.0	94.0	98.6	100.3	99.7	100.0	99.7	100.3	100.0
PON1max	Minus	100.2	98.1	100.1	99.9	99.9	100.0	100.4	99.8	99.7	100.0
PON1max	Plus	99.6	102.1	99.9	99.9	100.0	100.4	100.9	99.5	98.6	100.0
POP1max	Minus	99.3	100.0	99.4	99.8	100.2	99.7	100.3	100.0	100.0	100.0
POP1max	Plus	101.1	99.9	100.5	100.0	99.5	100.4	100.2	99.7	99.7	100.2
Pmax(CYANO)	Minus	101.0	100.9	100.6	99.4	99.6	97.4	87.4	100.0	100.7	92.3
Pmax(CYANO)	Plus	99.3	99.1	99.8	100.0	100.1	103.0	107.1	100.7	98.6	109.1
Pmax(FDIAT)	Minus	95.3	99.2	100.4	99.8	101.8	100.6	104.1	98.8	100.0	103.8
Pmax(FDIAT)	Plus	104.1	100.6	99.5	100.0	98.8	99.8	94.3	101.2	101.0	96.4
SedPorosity	Minus	99.6	100.0	99.9	99.7	100.1	99.4	99.9	100.2	101.0	100.2
SedPorosity	Plus	100.0	99.9	99.9	99.9	100.0	99.4	99.5	101.0	99.3	100.0
SmpNH4	Minus	100.2	94.8	100.0	99.1	99.9	98.9	101.0	100.7	101.0	100.5
SmpNH4	Plus	100.0	105.1	99.9	100.6	100.0	100.4	99.9	100.3	99.3	100.0
SmpNO3	Minus	100.0	100.0	100.0	100.0	100.0	100.0	100.0	100.0	100.0	100.0
SmpNO3	Plus	100.0	100.0	100.0	100.0	100.0	100.0	100.0	100.0	100.0	100.0
SmpPO4	Minus	95.0	99.9	97.9	99.4	101.7	93.1	92.7	99.8	101.0	99.5
SmpPO4	Plus	104.7	100.5	101.9	100.2	98.3	107.3	109.6	100.5	101.4	102.0
Tmax(FDIAT)	Minus	100.0	100.1	99.8	99.8	100.0	100.3	100.6	99.2	99.7	100.0
Tmax(FDIAT)	Plus	100.3	100.6	99.9	99.9	99.8	98.7	88.0	99.7	100.3	96.7
Topt(FDIAT)	Minus	100.7	100.6	99.9	99.9	99.7	98.8	90.1	100.5	99.7	97.0
Topt(FDIAT)	Plus	100.2	99.9	100.0	99.9	99.8	100.8	102.4	100.7	99.7	100.3
Tsta(CYANO)	Minus	100.2	99.9	100.1	99.5	99.9	99.6	99.6	100.0	100.0	100.0
Tsta(CYANO)	Plus	100.1	99.9	99.9	99.9	100.0	99.7	100.0	98.8	101.0	100.2
Tsta(FDIAT)	Minus	98.2	99.0	100.3	100.1	100.9	101.0	106.8	100.5	98.6	104.4
Tsta(FDIAT)	Plus	100.4	100.5	100.0	99.8	99.8	98.7	88.8	100.3	99.7	97.0
UNmax(CYANO)	Minus	100.1	100.0	99.8	99.8	100.1	100.1	99.6	99.7	100.3	100.0
UNmax(CYANO)	Plus	99.8	100.1	100.0	100.0	99.9	100.2	101.2	99.0	100.0	100.2
UNmax(FDIAT)	Minus	100.3	99.7	99.9	99.7	99.8	99.6	99.7	100.2	100.7	100.0
UNmax(FDIAT)	Plus	100.2	100.2	100.1	99.6	99.9	100.0	99.8	99.8	99.7	100.2
UPmax(CYANO)	Minus	101.1	100.5	100.4	99.9	99.3	99.1	90.3	100.5	100.0	94.5
UPmax(CYANO)	Plus	98.7	99.3	99.8	99.9	100.5	100.5	104.1	99.3	99.0	103.9
UPmax(FDIAT)	Minus	97.7	99.3	100.2	99.9	100.1	100.8	104.6	99.8	99.7	105.0
UPmax(FDIAT)	Plus	101.2	100.4	99.9	99.6	99.4	98.9	90.9	100.3	102.1	94.7
deSS01	Minus	99.7	100.0	100.2	120.4	97.7	99.9	99.6	101.5	102.4	99.1
deSS01	Plus	100.5	100.1	100.2	86.4	101.7	101.3	102.6	98.0	97.9	101.7
diaSS01	Minus	99.7	100.1	99.9	110.1	98.8	99.3	99.9	100.7	101.4	99.8
diaSS01	Plus	100.4	99.9	99.8	91.3	101.1	100.5	100.5	99.8	99.0	100.8
fdom(CYANO)	Minus	100.2	99.5	99.5	99.5	100.1	99.5	99.7	100.0	99.7	99.8
fdom(CYANO)	Plus	100.2	100.7	100.4	99.9	99.8	100.3	100.6	100.3	99.7	100.2
fdom(FDIAT)	Minus	99.2	98.8	99.5	99.8	100.3	99.8	100.6	99.2	100.0	100.0
fdom(FDIAT)	Plus	100.8	101.4	100.4	100.0	99.6	100.4	100.3	100.0	99.7	100.2
fres(CYANO)	Minus	100.2	99.9	100.0	99.8	99.8	99.5	99.6	100.7	99.7	100.0
fres(CYANO)	Plus	100.2	99.8	100.0	99.6	99.8	99.8	99.8	99.8	99.3	100.0
fres(FDIAT)	Minus	99.8	99.8	99.8	99.6	100.0	99.4	99.1	100.7	100.0	100.0
fres(FDIAT)	Plus	100.0	99.9	100.3	100.1	99.9	100.7	100.8	99.7	100.7	100.2
kr(CYANO)	Minus	102.1	101.1	101.1	100.4	99.0	112.3	118.3	100.3	99.0	111.2
kr(CYANO)	Plus	99.5	99.7	99.5	99.3	100.6	90.8	79.9	100.2	102.1	90.5
kr(FDIAT)	Minus	111.4	101.9	100.4	100.1	96.8	100.8	82.9	101.2	100.3	92.3
kr(FDIAT)	Plus	91.3	98.5	99.8	99.9	103.3	100.6	105.8	100.2	99.3	106.5
rSOs	Minus	98.3	99.9	98.5	99.5	100.8	93.2	92.6	99.3	89.2	99.4
rSOs	Plus	102.5	100.4	101.9	100.3	99.2	106.5	108.9	99.5	106.3	101.7
resusKT	Minus	99.9	100.1	100.1	99.8	99.8	100.2	100.6	100.2	98.3	100.2
resusKT	Plus	100.0	100.1	99.9	100.0	100.1	99.9	100.5	100.0	98.6	100.2
resusRate	Minus	100.1	98.4	97.3	93.0	102.2	99.6	100.3	99.2	98.3	100.9
resusRate	Plus	100.3	101.6	102.3	107.0	97.9	99.6	99.0	101.3	100.3	99.4
sedOrganicFrac	Minus	99.9	100.0	100.0	99.5	99.9	99.6	100.0	100.3	99.3	100.0
sedOrganicFrac	Plus	100.1	99.9	100.0	99.9	99.9	99.9	100.1	99.8	99.3	100.0

tcPOM1	Minus	100.3	101.6	102.1	100.5	99.7	100.2	100.4	100.8	99.7	100.0
tcPOM1	Plus	100.0	98.7	98.0	99.4	100.1	99.6	99.6	100.2	99.7	100.0
tcSS01	Minus	99.4	100.1	100.1	116.1	96.6	100.2	100.0	101.7	99.0	98.9
tcSS01	Plus	100.8	100.1	100.0	86.2	103.4	100.4	101.9	97.9	98.3	101.5
vN2	Minus	100.6	97.6	100.0	99.9	99.9	100.0	100.1	100.0	98.3	100.0
vN2	Plus	99.4	101.6	100.0	100.0	100.0	100.4	100.9	100.0	99.7	99.8
vON	Minus	100.3	100.0	100.0	99.6	99.8	99.8	100.0	100.7	101.0	100.0
vON	Plus	100.1	100.2	100.1	99.9	99.8	99.8	100.5	100.2	99.7	100.0
vR(CYANO)	Minus	99.8	103.2	99.4	101.8	100.4	113.2	102.7	99.7	101.7	76.2
vR(CYANO)	Plus	103.9	92.2	101.7	98.4	99.0	83.7	89.1	101.7	100.7	176.8
vR(FDIAT)	Minus	76.5	94.4	101.3	99.0	108.8	101.4	108.5	97.9	97.9	137.7
vR(FDIAT)	Plus	137.3	101.3	101.7	100.2	88.9	101.3	99.9	103.8	102.1	90.9
vSed	Minus	118.4	93.9	101.6	96.8	94.8	75.6	71.9	101.0	98.3	101.1
vSed	Plus	93.6	110.0	103.1	105.1	103.3	136.8	139.1	99.3	104.9	100.8
vT(FDIAT)	Minus	146.8	104.6	102.7	100.4	89.3	97.2	7.3	105.4	106.6	29.1
vT(FDIAT)	Plus	77.8	94.6	101.4	99.0	108.4	101.4	108.5	96.5	98.6	138.2
ws(CYANO)	Minus	121.3	104.3	105.3	97.5	93.8	80.6	0.1	102.3	108.3	0.0
ws(CYANO)	Plus	102.0	103.0	101.8	101.1	99.0	110.8	116.3	100.3	100.7	110.6
ws(FDIAT)	Minus	100.0	100.0	100.0	100.0	100.0	100.0	100.0	100.0	100.0	100.0
ws(FDIAT)	Plus	100.0	100.0	100.0	100.0	100.0	100.0	100.0	100.0	100.0	100.0

Waahi

Parameter	Adj*	Median					Summer metrics				
		Chl-a	TN	TP	TSS	SD	Chl-a	CYANO	dT > 0.5	DO < 2	Cyano > 15
DOD1max	Minus	101.65	100.80	99.59	100.02	99.67	101.81	101.81	98.31	84.00	100.08
DOD1max	Plus	99.56	101.55	99.95	99.96	100.05	99.68	99.68	99.66	104.00	99.83
DON1max	Minus	100.33	98.93	100.23	99.98	99.48	100.78	100.78	98.65	84.00	99.92
DON1max	Plus	100.76	100.10	100.11	99.73	99.64	100.54	100.54	99.66	104.00	100.42
IK(CYANO)	Minus	99.75	99.87	100.06	99.73	100.06	99.92	99.92	100.00	104.00	99.41
IK(CYANO)	Plus	100.20	100.39	100.08	100.22	100.06	100.13	100.13	99.32	88.00	99.83
IK(FDIAT)	Minus	100.06	100.12	99.84	99.94	99.89	100.16	100.16	98.65	92.00	99.92
IK(FDIAT)	Plus	100.06	99.77	99.93	99.67	100.18	100.06	100.06	98.99	88.00	99.92
KDOS-NH4	Minus	99.92	100.20	99.75	99.97	100.28	100.23	100.23	98.65	88.00	99.92
KDOS-NH4	Plus	100.23	100.21	100.29	99.77	99.87	100.33	100.33	98.99	96.00	100.08
KDOS-NO3	Minus	100.08	99.63	99.99	99.50	100.35	100.20	100.20	98.99	84.00	100.08
KDOS-NO3	Plus	100.11	99.91	99.86	100.06	99.98	100.26	100.26	99.32	88.00	100.00
KN(CYANO)	Minus	100.00	99.98	99.72	99.52	100.22	100.13	100.13	100.00	96.00	99.92
KN(CYANO)	Plus	100.11	100.06	99.81	99.59	100.31	100.38	100.38	98.65	92.00	99.92
KN(FDIAT)	Minus	100.03	99.89	99.89	99.64	100.37	100.15	100.15	99.66	104.00	99.92
KN(FDIAT)	Plus	99.93	100.22	99.85	99.65	99.87	100.16	100.16	98.99	96.00	100.08
KN2	Minus	100.13	99.74	99.74	99.73	100.19	100.21	100.21	98.99	84.00	100.08
KN2	Plus	100.03	100.04	99.70	99.97	100.26	100.04	100.04	97.30	92.00	99.92
KON	Minus	100.08	100.09	99.69	99.90	100.29	100.12	100.12	98.99	96.00	99.92
KON	Plus	91.22	97.27	94.84	99.72	103.18	92.64	92.63	97.64	92.00	97.97
KOxS-PO4	Minus	106.95	102.73	105.48	100.33	97.82	107.05	107.06	99.32	84.00	100.76
KOxS-PO4	Plus	100.16	99.89	99.86	99.77	100.05	100.21	100.21	98.99	108.00	99.92
KP(CYANO)	Minus	100.26	100.40	100.12	99.86	99.71	100.12	100.12	100.34	104.00	100.00
KP(CYANO)	Plus	100.20	100.10	99.91	99.38	100.04	100.19	100.19	97.97	104.00	99.92
KP(FDIAT)	Minus	100.17	100.18	99.88	99.62	100.36	100.20	100.20	99.66	100.00	100.00
KP(FDIAT)	Plus	100.22	100.48	100.09	100.12	100.25	100.33	100.33	97.97	100.00	99.92
KSOs	Minus	100.13	99.93	99.70	99.29	100.26	100.16	100.16	98.99	96.00	99.92
KSOs	Plus	99.91	100.07	99.76	100.06	100.38	100.18	100.18	99.32	96.00	99.83
KeDOC1	Minus	100.02	100.28	100.01	100.35	100.20	100.45	100.45	98.65	100.00	99.92
KeDOC1	Plus	100.41	100.21	100.17	100.07	100.34	100.30	100.30	98.31	92.00	100.00
KePOC1	Minus	99.73	99.90	99.92	100.05	100.37	100.20	100.20	99.66	100.00	99.66
KePOC1	Plus	100.72	99.92	100.18	99.69	99.99	100.36	100.36	98.65	96.00	100.25
KeSS01	Minus	99.57	100.44	100.30	100.17	99.78	99.97	99.96	98.65	96.00	99.58
KeSS01	Plus	100.47	100.04	100.05	99.71	100.37	100.51	100.51	96.96	104.00	100.08
Kep(CYANO)	Minus	99.81	100.30	100.29	100.18	99.95	99.85	99.85	98.99	88.00	99.83
Kep(CYANO)	Plus	100.12	99.94	99.88	99.52	100.00	100.41	100.41	100.00	96.00	99.92
Kep(FDIAT)	Minus	100.21	99.93	100.14	100.08	100.00	100.32	100.32	99.32	96.00	100.00
Kep(FDIAT)	Plus	100.09	100.46	99.86	99.85	100.03	100.40	100.40	98.65	88.00	99.92
KoN2	Minus	100.28	99.62	99.97	99.39	100.05	100.23	100.23	98.31	88.00	100.00
KoN2	Plus	99.86	100.59	99.89	100.01	100.09	100.16	100.16	99.32	100.00	99.83

KoNH	Minus	100.10	99.85	99.86	99.90	100.08	100.10	100.10	97.64	88.00	99.83
KoNH	Plus	99.91	100.11	100.05	100.28	100.37	100.03	100.03	99.66	92.00	99.83
Original		100.00	100.00	100.00	100.00	100.00	100.00	100.00	100.00	100.00	100.00
POC1max	Minus	100.20	100.27	99.96	100.09	99.91	100.18	100.18	99.66	104.00	99.92
POC1max	Plus	100.27	100.30	100.42	99.86	99.72	100.15	100.15	99.32	92.00	100.08
POMDensity1	Minus	98.13	96.81	97.69	99.68	100.36	96.06	96.06	98.31	84.00	99.41
POMDensity1	Plus	99.95	99.91	99.89	99.71	100.39	100.14	100.14	99.66	96.00	99.83
POMDia1	Minus	100.17	100.04	100.11	99.58	100.10	99.93	99.93	98.99	76.00	100.08
POMDia1	Plus	99.72	101.45	100.37	100.04	100.29	99.63	99.63	98.99	92.00	100.08
PON1max	Minus	100.04	98.80	99.98	99.58	99.78	100.65	100.65	99.32	88.00	99.92
PON1max	Plus	98.72	99.60	100.29	100.07	100.39	98.65	98.65	98.65	96.00	99.66
POP1max	Minus	101.23	100.58	99.66	100.06	99.81	101.45	101.46	99.66	84.00	100.08
POP1max	Plus	96.13	99.31	100.61	99.98	100.35	98.49	98.48	98.31	104.00	94.58
Pmax(CYANO)	Minus	102.33	100.95	99.55	99.86	99.81	101.55	101.55	99.32	100.00	102.63
Pmax(CYANO)	Plus	100.19	100.08	99.81	99.96	99.99	100.05	100.05	98.99	100.00	100.08
Pmax(FDIAT)	Minus	100.04	100.14	99.70	99.90	100.34	100.16	100.16	98.65	88.00	100.00
Pmax(FDIAT)	Plus	100.13	100.33	99.86	99.91	100.13	100.51	100.52	100.00	96.00	100.08
SedPorosity	Minus	99.86	100.04	99.73	99.96	100.37	100.12	100.12	98.65	88.00	99.92
SedPorosity	Plus	99.96	99.60	99.95	99.12	99.99	99.95	99.95	98.99	96.00	100.08
SmpNH4	Minus	100.15	100.44	100.02	99.75	100.02	100.37	100.37	99.32	88.00	99.92
SmpNH4	Plus	100.04	100.40	99.74	99.35	100.03	100.35	100.35	98.65	88.00	100.08
SmpNO3	Minus	100.11	99.53	100.12	99.97	99.85	100.26	100.27	98.99	92.00	99.92
SmpNO3	Plus	90.05	97.08	94.47	99.86	103.08	91.41	91.40	98.99	104.00	97.63
SmpPO4	Minus	107.94	103.56	106.73	100.53	97.32	107.99	108.00	101.01	92.00	100.85
SmpPO4	Plus	100.03	99.93	99.70	99.85	100.16	100.14	100.14	100.34	88.00	100.08
Tmax(FDIAT)	Minus	99.91	100.48	100.04	100.29	100.20	100.29	100.29	98.99	96.00	100.08
Tmax(FDIAT)	Plus	100.04	99.94	99.92	99.53	99.96	100.10	100.10	98.99	108.00	99.92
Topt(FDIAT)	Minus	99.93	100.19	99.77	99.89	100.23	100.18	100.18	98.99	92.00	100.08
Topt(FDIAT)	Plus	100.09	99.93	99.85	99.59	100.14	100.15	100.15	99.32	80.00	100.08
Tsta(CYANO)	Minus	100.03	100.03	99.71	100.03	100.23	100.04	100.04	97.97	96.00	99.83
Tsta(CYANO)	Plus	100.24	99.94	99.96	99.52	100.10	100.21	100.21	99.66	84.00	100.08
Tsta(FDIAT)	Minus	100.09	100.06	99.82	99.55	99.94	100.14	100.14	97.97	88.00	99.92
Tsta(FDIAT)	Plus	98.86	99.40	99.78	99.63	100.32	99.89	99.89	99.66	108.00	97.71
UNmax(CYANO)	Minus	100.17	100.63	99.87	100.06	99.83	100.44	100.44	99.32	96.00	100.93
UNmax(CYANO)	Plus	100.04	99.87	100.05	99.52	99.85	100.25	100.25	98.65	88.00	100.08
UNmax(FDIAT)	Minus	100.18	100.23	99.63	99.63	100.21	100.15	100.14	100.00	80.00	100.08
UNmax(FDIAT)	Plus	99.94	100.07	99.83	99.51	100.07	100.15	100.15	99.32	72.00	99.92
UPmax(CYANO)	Minus	99.97	99.96	99.70	99.87	100.35	99.92	99.91	100.34	92.00	99.92
UPmax(CYANO)	Plus	100.27	99.88	100.32	99.86	100.06	100.30	100.30	98.31	88.00	99.92
UPmax(FDIAT)	Minus	100.07	100.49	99.72	99.98	100.25	100.02	100.02	97.97	84.00	100.08
UPmax(FDIAT)	Plus	95.55	98.55	101.91	103.41	99.73	96.59	96.59	99.66	72.00	98.73
deSS01	Minus	103.87	101.24	98.86	95.06	100.78	102.92	102.92	97.97	84.00	100.42
deSS01	Plus	101.75	100.55	99.27	93.74	102.25	101.39	101.39	98.65	96.00	100.25
diaSS01	Minus	98.47	99.56	101.53	105.17	98.38	98.53	98.53	98.65	88.00	98.98
diaSS01	Plus	99.71	100.02	99.72	99.74	100.39	99.75	99.75	98.99	100.00	99.92

fdom(CYANO)	Minus	100.14	99.88	99.71	99.58	100.20	100.43	100.43	98.65	92.00	100.00
fdom(CYANO)	Plus	99.93	99.88	99.80	99.62	100.33	100.06	100.06	97.97	96.00	99.92
fdom(FDIAT)	Minus	99.99	99.91	99.75	99.70	100.37	100.36	100.36	99.66	92.00	99.92
fdom(FDIAT)	Plus	99.94	99.92	99.93	100.07	100.26	100.21	100.21	99.66	68.00	99.92
fres(CYANO)	Minus	100.21	100.16	100.07	99.94	99.97	100.24	100.24	98.31	104.00	100.00
fres(CYANO)	Plus	100.17	99.88	99.81	99.52	100.10	100.19	100.19	98.99	72.00	99.92
fres(FDIAT)	Minus	100.09	100.01	99.75	99.66	100.06	100.13	100.13	99.32	88.00	100.08
fres(FDIAT)	Plus	109.11	101.20	99.65	99.45	97.47	109.10	109.11	99.32	96.00	102.54
kr(CYANO)	Minus	92.16	99.45	99.96	99.96	102.60	92.32	92.31	98.31	104.00	94.83
kr(CYANO)	Plus	100.10	100.27	99.74	99.99	100.26	100.14	100.13	99.66	92.00	99.92
kr(FDIAT)	Minus	99.92	99.85	99.76	99.80	100.32	100.18	100.18	98.65	96.00	99.92
kr(FDIAT)	Plus	98.18	99.52	98.79	99.83	100.66	98.71	98.71	99.66	64.00	99.58
rSOs	Minus	102.05	100.79	101.38	99.54	99.73	101.88	101.89	97.97	168.00	100.25
rSOs	Plus	100.22	99.96	99.64	99.28	100.14	100.12	100.12	98.65	100.00	100.00
resusKT	Minus	100.13	99.98	99.98	100.03	99.84	100.20	100.20	98.99	84.00	99.92
resusKT	Plus	101.56	96.32	99.62	91.91	103.71	100.92	100.93	97.97	104.00	100.42
resusRate	Minus	96.83	104.39	100.53	108.03	97.31	98.72	98.72	100.00	92.00	98.98
resusRate	Plus	100.10	99.96	99.85	99.45	100.15	100.24	100.24	99.32	92.00	99.92
sedOrganicFrac	Minus	100.20	100.24	100.07	100.29	99.95	100.12	100.12	98.65	92.00	99.92
sedOrganicFrac	Plus	99.83	104.67	99.81	100.41	99.85	101.34	101.35	98.99	92.00	99.75
tcPOM1	Minus	99.03	96.17	99.92	99.56	100.79	98.37	98.37	98.99	92.00	99.92
tcPOM1	Plus	91.66	97.55	101.80	120.82	92.61	94.38	94.37	99.66	96.00	98.14
tcSS01	Minus	106.81	102.46	99.30	81.23	107.66	104.84	104.84	98.31	96.00	100.85
tcSS01	Plus	100.18	97.59	99.90	99.43	100.20	100.24	100.24	99.32	88.00	99.66
vN2	Minus	99.71	103.76	99.78	100.18	100.34	100.09	100.09	98.31	88.00	99.92
vN2	Plus	99.97	99.36	99.71	99.93	100.30	100.15	100.15	99.66	96.00	100.08
vON	Minus	100.19	100.87	99.75	99.40	100.00	100.11	100.11	99.32	108.00	99.92
vON	Plus	70.02	99.55	101.48	99.88	107.86	115.84	115.86	96.96	120.00	64.24
vR(CYANO)	Minus	110.70	102.06	99.90	100.12	94.13	80.83	80.80	99.32	100.00	116.27
vR(CYANO)	Plus	100.38	99.87	99.91	99.79	99.95	100.06	100.06	99.66	100.00	100.08
vR(FDIAT)	Minus	99.83	101.10	99.83	100.22	99.82	100.08	100.08	99.32	84.00	99.49
vR(FDIAT)	Plus	130.76	108.89	136.72	101.23	88.56	96.01	96.01	104.05	192.00	100.59
vSed	Minus	85.97	97.01	93.42	98.82	106.00	105.68	105.67	95.27	120.00	78.73
vSed	Plus	98.36	102.26	99.78	99.43	100.18	100.22	100.22	98.99	84.00	92.29
vT(FDIAT)	Minus	101.08	99.43	100.15	99.26	99.95	100.06	100.07	98.31	116.00	100.25
vT(FDIAT)	Plus	99.91	100.11	100.05	100.28	100.37	100.03	100.03	99.66	92.00	99.83
ws(CYANO)	Minus	99.91	100.11	100.05	100.28	100.37	100.03	100.03	99.66	92.00	99.83
ws(CYANO)	Plus	99.91	100.11	100.05	100.28	100.37	100.03	100.03	99.66	92.00	99.83
ws(FDIAT)	Minus	99.91	100.11	100.05	100.28	100.37	100.03	100.03	99.66	92.00	99.83
ws(FDIAT)	Plus	0.00	0.00	0.00	0.00	0.00	0.00	0.00	0.00	0.00	0.00

Rotomānuka

Parameter	Adj*	Median					Summer metrics				
		Chl-a	TN	TP	TSS	SD	Chl-a	CYANO	dT > 0.5	DO < 2	Cyano > 15
DON1max	Minus	94.7	97.7	100.1	98.1	98.1	100.3	99.9	93.9	98.4	101.9
DON1max	Plus	98.0	99.9	99.7	99.6	99.6	100.4	100.3	106.4	100.8	98.8
IK(CYANO)	Minus	100.7	101.9	99.3	101.0	101.1	100.7	99.2	115.8	104.3	102.1
IK(CYANO)	Plus	99.2	99.7	100.3	100.7	100.7	99.8	98.2	102.7	98.3	99.8
IK(FDIAT)	Minus	100.0	100.4	99.9	98.4	98.1	100.7	99.2	104.5	101.0	101.3
IK(FDIAT)	Plus	95.0	99.2	100.0	99.6	99.6	100.4	98.6	103.5	98.8	99.7
KDOS-NH4	Minus	94.8	97.9	100.0	97.6	97.6	100.1	98.9	87.5	98.0	99.1
KDOS-NH4	Plus	97.1	99.9	100.0	100.3	100.3	100.2	98.0	100.6	98.8	99.8
KDOS-NO3	Minus	94.1	99.0	100.0	98.9	98.9	100.5	97.2	96.7	98.3	100.6
KDOS-NO3	Plus	98.2	100.0	99.8	99.1	98.9	100.0	99.7	99.8	99.9	99.4
KN(CYANO)	Minus	98.9	100.8	100.0	101.5	101.6	100.1	99.5	102.9	99.7	99.8
KN(CYANO)	Plus	95.5	98.5	99.8	98.3	98.3	100.4	101.7	93.8	98.9	100.0
KN(FDIAT)	Minus	100.0	100.6	99.8	100.3	100.3	100.7	99.0	108.8	101.5	101.3
KN(FDIAT)	Plus	96.5	99.2	100.0	99.8	99.8	100.4	99.2	101.4	98.5	99.4
KN2	Minus	97.6	100.2	100.0	100.4	100.2	100.1	99.1	102.9	99.2	100.4
KN2	Plus	98.3	99.5	99.9	100.0	100.0	100.6	97.8	102.1	99.6	99.5
KON	Minus	100.7	100.7	99.8	100.1	100.1	100.8	98.4	108.4	101.4	101.1
KON	Plus	98.3	99.8	99.8	98.9	98.9	100.7	99.9	104.9	101.2	101.6
KOxS-PO4	Minus	94.4	96.9	101.5	95.8	95.5	99.6	98.5	78.9	95.1	98.9
KOxS-PO4	Plus	102.7	103.8	98.4	105.3	105.3	100.5	98.0	126.4	104.7	101.6
KP(CYANO)	Minus	95.9	99.2	99.9	100.7	100.7	100.1	98.3	104.5	99.1	99.6
KP(CYANO)	Plus	99.1	100.1	100.2	99.2	99.0	100.2	97.9	100.2	99.2	99.8
KP(FDIAT)	Minus	98.4	99.8	100.4	100.1	99.9	99.8	96.4	103.1	98.3	99.5
KP(FDIAT)	Plus	97.0	98.4	99.9	99.1	99.0	100.4	97.4	98.0	98.9	99.6
KSOs	Minus	99.5	100.4	99.9	100.4	100.4	100.1	98.3	103.3	100.2	100.2
KSOs	Plus	96.2	98.6	100.2	99.6	99.6	100.2	99.0	94.1	98.2	99.3
KeDOC1	Minus	95.5	98.3	100.0	98.1	98.1	100.4	98.5	92.8	98.5	99.7
KeDOC1	Plus	97.2	99.6	100.0	99.6	99.5	100.1	99.5	100.8	99.2	99.9
KePOC1	Minus	96.7	99.2	100.1	99.1	98.9	100.1	99.1	97.7	98.8	99.7
KePOC1	Plus	99.6	100.4	99.8	99.4	99.4	100.8	99.0	105.9	101.5	101.4
KeSS01	Minus	97.7	99.3	100.1	98.9	98.7	100.4	97.8	96.9	99.0	99.8
KeSS01	Plus	97.0	100.1	100.0	100.7	100.7	100.4	98.6	105.9	99.0	99.8
Kep(CYANO)	Minus	98.4	100.3	99.7	101.5	101.5	99.5	99.4	110.0	101.1	100.3
Kep(CYANO)	Plus	97.2	98.6	100.3	98.4	98.3	100.3	98.4	92.6	97.6	99.2
Kep(FDIAT)	Minus	99.7	100.2	100.0	100.3	100.3	100.0	97.9	104.1	100.0	100.1
Kep(FDIAT)	Plus	99.8	99.9	100.1	100.2	100.2	100.1	98.3	101.0	99.6	99.9
KoN2	Minus	96.8	99.1	100.0	98.6	98.4	100.6	99.9	98.8	98.8	100.3
KoN2	Plus	97.6	99.9	99.7	99.9	99.7	100.8	100.1	104.3	100.2	100.3
KoNH	Minus	95.6	98.8	99.7	98.3	98.2	101.0	98.6	99.2	100.3	101.2
KoNH	Plus	95.1	98.7	99.9	99.0	98.9	100.5	98.5	97.7	99.1	99.5

Original		100.0	100.0	100.0	100.0	100.0	100.0	100.0	100.0	100.0	100.0
POC1max	Minus	99.3	101.3	99.9	102.2	102.2	100.1	98.2	111.1	100.3	99.9
POC1max	Plus	97.5	99.4	100.0	99.2	99.1	100.1	98.4	96.1	99.2	99.7
POMDensity1	Minus	1043.7	126.3	98.7	107.1	107.1	100.4	98.6	127.5	103.9	114.3
POMDensity1	Plus	81.2	91.3	99.9	99.3	99.2	100.3	98.9	97.7	99.4	94.2
POMDia1	Minus	105.0	102.4	100.0	100.2	100.2	100.0	99.1	104.9	100.3	101.5
POMDia1	Plus	91.2	98.2	100.0	100.1	100.0	100.3	99.3	98.4	98.7	98.1
PON1max	Minus	96.1	100.1	99.6	98.1	98.1	101.4	101.6	101.2	101.3	101.4
PON1max	Plus	99.3	99.9	99.9	101.6	101.6	100.1	98.9	110.7	99.9	100.4
POP1max	Minus	96.3	98.6	100.0	99.5	99.5	100.1	99.2	97.7	98.3	99.4
POP1max	Plus	99.5	100.1	100.0	100.3	100.3	100.0	98.7	103.5	99.8	99.8
Pmax(CYANO)	Minus	98.6	96.2	101.9	98.7	98.6	99.9	97.4	83.2	91.8	98.3
Pmax(CYANO)	Plus	98.8	103.4	98.3	102.1	102.1	101.5	99.7	125.6	108.9	103.5
Pmax(FDIAT)	Minus	95.3	99.6	99.8	100.7	100.7	100.0	99.5	104.3	99.2	99.7
Pmax(FDIAT)	Plus	97.5	98.7	100.3	98.2	98.1	100.0	98.2	94.1	98.3	99.6
SedPorosity	Minus	100.0	100.0	100.0	100.0	100.0	100.0	100.0	100.0	100.0	100.0
SedPorosity	Plus	100.0	100.0	100.0	100.0	100.0	100.0	100.0	100.0	100.0	100.0
SmpNH4	Minus	95.5	98.0	100.0	98.3	98.2	100.2	98.9	97.3	98.6	97.3
SmpNH4	Plus	96.9	99.1	100.1	98.0	98.0	100.4	99.5	92.2	98.6	101.7
SmpNO3	Minus	99.2	99.8	100.2	100.1	100.1	100.0	98.7	100.6	99.6	100.6
SmpNO3	Plus	98.9	101.0	100.1	102.3	102.3	100.0	99.1	107.6	100.0	98.9
SmpPO4	Minus	91.0	94.1	102.0	92.9	92.8	99.5	98.5	66.4	92.2	98.4
SmpPO4	Plus	103.7	105.3	98.1	108.4	108.5	100.9	99.4	134.6	105.8	100.9
Tmax(FDIAT)	Minus	95.2	97.2	100.2	96.4	96.3	100.4	99.7	83.2	98.0	99.4
Tmax(FDIAT)	Plus	99.3	101.1	99.9	102.4	102.4	99.9	98.5	110.4	100.3	99.8
Topt(FDIAT)	Minus	98.0	97.4	100.1	96.5	96.4	100.2	99.2	82.2	97.7	99.5
Topt(FDIAT)	Plus	100.1	100.8	99.6	100.4	100.4	101.2	99.9	110.0	101.8	101.4
Tsta(CYANO)	Minus	99.7	100.6	100.0	100.8	100.8	100.6	96.4	105.5	100.5	100.2
Tsta(CYANO)	Plus	100.3	101.1	99.8	100.3	100.3	100.8	99.2	110.5	102.0	101.6
Tsta(FDIAT)	Minus	100.1	99.9	99.8	100.6	100.6	100.7	99.9	105.1	100.6	100.5
Tsta(FDIAT)	Plus	95.1	98.3	99.9	98.5	98.5	100.3	97.6	96.5	98.9	99.7
UNmax(CYANO)	Minus	99.8	99.9	100.0	99.8	99.8	99.9	98.7	100.4	100.4	100.0
UNmax(CYANO)	Plus	96.4	98.7	99.9	98.2	98.2	101.0	97.4	94.1	98.9	100.1
UNmax(FDIAT)	Minus	100.4	101.0	99.8	100.9	100.9	99.6	99.3	107.8	100.7	100.3
UNmax(FDIAT)	Plus	98.5	100.3	100.1	101.1	101.1	100.2	97.8	105.9	99.3	99.5
UPmax(CYANO)	Minus	97.8	100.1	100.2	99.9	99.9	101.0	97.9	108.4	99.0	99.9
UPmax(CYANO)	Plus	99.5	100.1	99.8	100.7	100.7	99.8	99.3	105.1	100.0	99.8
UPmax(FDIAT)	Minus	96.6	98.8	99.7	100.0	100.0	100.4	98.0	97.5	98.9	99.6
UPmax(FDIAT)	Plus	95.8	98.9	100.1	98.3	98.3	100.7	98.3	97.3	99.1	100.5
deSS01	Minus	96.2	103.3	99.7	98.6	98.6	101.2	100.0	104.1	101.1	101.6
deSS01	Plus	99.5	97.7	100.0	100.3	100.3	100.1	100.6	103.5	99.6	99.8
diaSS01	Minus	97.4	104.5	100.0	100.0	100.0	100.4	99.3	103.9	99.0	99.7
diaSS01	Plus	94.7	96.5	99.9	99.7	99.6	100.5	99.2	102.1	99.5	100.0
fdom(CYANO)	Minus	87.7	93.6	103.5	85.9	85.5	99.7	99.0	52.9	90.0	97.5
fdom(CYANO)	Plus	110.0	108.7	95.5	120.3	120.4	101.3	99.4	185.7	114.5	105.1

fdom(FDIAT)	Minus	96.6	98.7	100.4	97.8	97.6	100.5	96.3	89.1	97.7	99.3
fdom(FDIAT)	Plus	100.4	101.1	99.6	102.6	102.6	100.0	99.5	111.7	100.6	100.0
fres(CYANO)	Minus	100.5	100.9	99.7	100.1	100.1	100.4	97.5	109.4	101.7	101.2
fres(CYANO)	Plus	98.6	100.1	100.1	100.4	100.3	100.1	95.7	101.4	99.6	101.0
fres(FDIAT)	Minus	97.2	98.9	100.1	98.4	98.4	99.9	99.0	96.7	98.8	99.6
fres(FDIAT)	Plus	100.1	100.9	99.7	100.9	100.8	99.9	99.0	111.1	101.8	101.2
kr(CYANO)	Minus	100.6	108.6	96.2	112.8	112.9	101.4	99.5	167.0	114.5	101.6
kr(CYANO)	Plus	95.5	91.4	103.6	90.8	90.7	99.4	97.9	41.8	86.7	98.1
kr(FDIAT)	Minus	96.4	99.0	100.5	99.1	99.0	99.9	98.6	96.5	97.6	99.3
kr(FDIAT)	Plus	96.1	99.8	99.5	99.6	99.6	100.6	98.9	101.2	99.9	100.1
rSOs	Minus	96.2	98.4	100.3	97.8	97.6	100.4	95.6	88.5	97.9	99.3
rSOs	Plus	99.6	101.1	99.3	100.2	100.1	100.2	102.6	112.5	102.1	101.8
resusKT	Minus	100.0	100.0	100.0	100.0	100.0	100.0	100.0	100.0	100.0	100.0
resusKT	Plus	100.0	100.0	100.0	100.0	100.0	100.0	100.0	100.0	100.0	100.0
resusRate	Minus	100.0	100.0	100.0	100.0	100.0	100.0	100.0	100.0	100.0	100.0
resusRate	Plus	100.0	100.0	100.0	100.0	100.0	100.0	100.0	100.0	100.0	100.0
sedOrganicFrac	Minus	100.0	100.0	100.0	100.0	100.0	100.0	100.0	100.0	100.0	100.0
sedOrganicFrac	Plus	100.0	100.0	100.0	100.0	100.0	100.0	100.0	100.0	100.0	100.0
tcPOM1	Minus	100.0	100.0	100.0	100.0	100.0	100.0	100.0	100.0	100.0	100.0
tcPOM1	Plus	100.0	100.0	100.0	100.0	100.0	100.0	100.0	100.0	100.0	100.0
tcSS01	Minus	100.0	100.0	100.0	100.0	100.0	100.0	100.0	100.0	100.0	100.0
tcSS01	Plus	100.0	100.0	100.0	100.0	100.0	100.0	100.0	100.0	100.0	100.0
vN2	Minus	97.3	99.7	99.9	100.0	99.9	100.4	98.9	103.3	99.8	98.9
vN2	Plus	96.4	99.6	100.1	99.6	99.4	100.2	97.9	98.6	98.5	100.5
vON	Minus	98.5	99.8	99.8	99.1	98.9	100.7	100.1	104.9	100.8	100.3
vON	Plus	95.3	98.3	100.1	98.3	98.3	100.4	100.0	96.3	98.6	100.3
vR(CYANO)	Minus	84.4	69.7	122.3	79.3	78.3	97.8	91.7	55.9	56.9	88.8
vR(CYANO)	Plus	103.8	121.3	93.3	84.3	84.2	101.8	99.5	204.5	127.5	104.8
vR(FDIAT)	Minus	99.7	99.6	98.7	102.1	102.0	100.3	97.1	119.7	99.8	99.7
vR(FDIAT)	Plus	92.7	95.2	103.6	88.2	88.1	100.3	98.2	65.6	92.5	95.7
vSed	Minus	131.0	119.1	93.3	119.6	119.7	102.2	122.3	195.3	123.7	117.6
vSed	Plus	95.1	101.3	103.6	107.5	107.6	100.5	78.7	112.7	98.1	96.8
vT(CYANO)	Minus	97.6	128.8	91.8	117.2	117.4	102.9	101.0	274.8	140.4	111.0
vT(CYANO)	Plus	90.7	74.0	116.4	74.2	73.4	98.8	93.2	33.8	62.2	90.0
vT(FDIAT)	Minus	37.8	47.7	127.0	22.5	1.0	96.2	86.8	0.0	31.0	83.8
vT(FDIAT)	Plus	100.3	100.3	98.4	103.9	103.9	100.3	95.9	129.9	101.3	100.1
ws(CYANO)	Minus	100.0	100.0	100.0	100.0	100.0	100.0	100.0	100.0	100.0	100.0

Appendix C: Waikare catchment model parameters and results

Table 31: Parameters for the calibrated INCA-N catchment model for Lake Waikare. Model parameters appear in the order of the .par file.

Category	Parameter	Unit	Native Forest	Exotic Forest	Scrub	Deer/drystock	Dairy	Urban
	Direct runoff initial flow	$m^3 s^{-1}$	0.00012136	0.00115	0.00058	0	0.001	0.001
	Soil water initial flow	$m^3 s^{-1}$	0.0001034	0.00029	0.00014	0	0.00024	0.001
INITIAL FLOWS	Direct runoff initial nitrate	mg N L^{-1}	0.05	0.064	1.6	0	3.6	8
	Soil water initial nitrate	mg N L^{-1}	0.5	0.64	1.6	0	5.6	6
	Direct runoff initial ammonium	mg N L^{-1}	0.46	0.08	0.2	0	0.005	0.1
	Soil water initial ammonium	mg N L^{-1}	0.46	0.08	0.2	0	0.5	0.03
	Start date		1/07/12					
	Number of timesteps		1420					
LAND N	Soil water denitrification rate	m d^{-1}	0.001	0.001	0.001	0	0.001	0
	Nitrogen fixation rate	kg ha^{-1} d^{-1}	0.001	0.00274	0.001219	0	0.0248	0
	Plant uptake rate - nitrate	m d^{-1}	0.01	0.01	0.007	0	0.02	0.08
	Maximum nitrogen uptake rate	kg ha^{-1} d^{-1}	70	70	45	0	105	20
	Nitrate addition rate	kg ha^{-1} d^{-1}	0	0	0	0	0.0001	0
	Ammonium nitrification rate	m d^{-1}	0.5	0.0001	0.01	0	0.05	0
	Ammonium mineralisation rate	kg ha^{-1} d^{-1}	0.001	0.001	0.01	0	0.2	0
	Ammonium immobilisation rate	m d^{-1}	0.0001	0.0001	0.0001	0	0.01	0
	Ammonium addition rate	kg ha^{-1} d^{-1}	0	0	0	0	0.0001	0
	Plant uptake rate - ammonium	m d^{-1}	0.002	0.002	0.002	0	0.002	0.01
PLANTS &	Plant growth start day	julian day	250	250	250	0	250	250
FERTILISER	Plant growth period	days	365	365	365	0	365	330
	Fertiliser addition start day	julian day	0	0	0	0	1	0
	Fertiliser addition period	days	0	0	0	0	90	0
	Soil moisture deficit maximum	mm	150	146	146	146	150	150
	Maximum temperature difference	°C	15	15	15	15	15	4.5
	(°C)	°C	9999	9999	9999	9999	9999	9999
SOILS &	Nitrification temperature threshold	°C	9999	9999	9999	9999	9999	9999
GROUNDWATER	Mineralisation temperature threshold	°C	9999	9999	9999	9999	9999	9999
	Immobilisation temperature threshold	°C	9999	9999	9999	9999	9999	9999

Category	Parameter	Unit	Native Forest	Exotic Forest	Scrub	Deer/drystock	Dairy	Urban
	Soil water sustainable flow	$m^3 s^{-1}$	9999	9999	9999	9999	9999	9999
	Groundwater sustainable flow	$m^3 s^{-1}$	9999	9999	9999	9999	9999	9999
	Response to a 10° change in temperature	ø	2	2	2	2	2	2
	Base temperature response	°C	30	30	30	30	30	30
	Initial snow pack depth	mm	0	0	0	0	0	0
SNOW	Degree day factor for snowmelt	$mm\ °C^{-1}\ d^{-1}$	3	3	3	3	3	3
	Water equivalent factor	Ø	0.3	0.3	0.3	0.3	0.3	0.3
	Snow depth / soil temperature factor	m^{-1}	-0.025	-0.025	-0.025	-0.025	-0.025	-0.025
	Thermal conductivity of soil	$W\ mm^{-1}\ °C^{-1}$	0.7	0.7	0.7	0.7	0.7	0.7
THERMAL	Freeze/thaw specific heat capacity	$J\ m^{-3}\ °C^{-1}$	6.6	6.6	6.6	6.6	6.6	6.6
	Growth curve offset	ø	0.66	0.66	0.66	0	0.66	0.66
	Growth curve amplitude	ø	0.34	0.34	0.34	0	0.34	0.34
	Direct runoff time constant	days	0.008	0.0008	0.005	0	0.01	2
	Soil reactive zone time constant	days	0.1	2	1	0	10	4
DISCHARGE	Ratio total to 'available' soil water		2	2	2	0	2	2
	Initial discharge volume	$m^{-3} s^{-1}$	0.01					
	Initial nitrate	$g\ m^{-3}$	0.3					
	Initial ammonium	$g\ m^{-3}$	0.03					

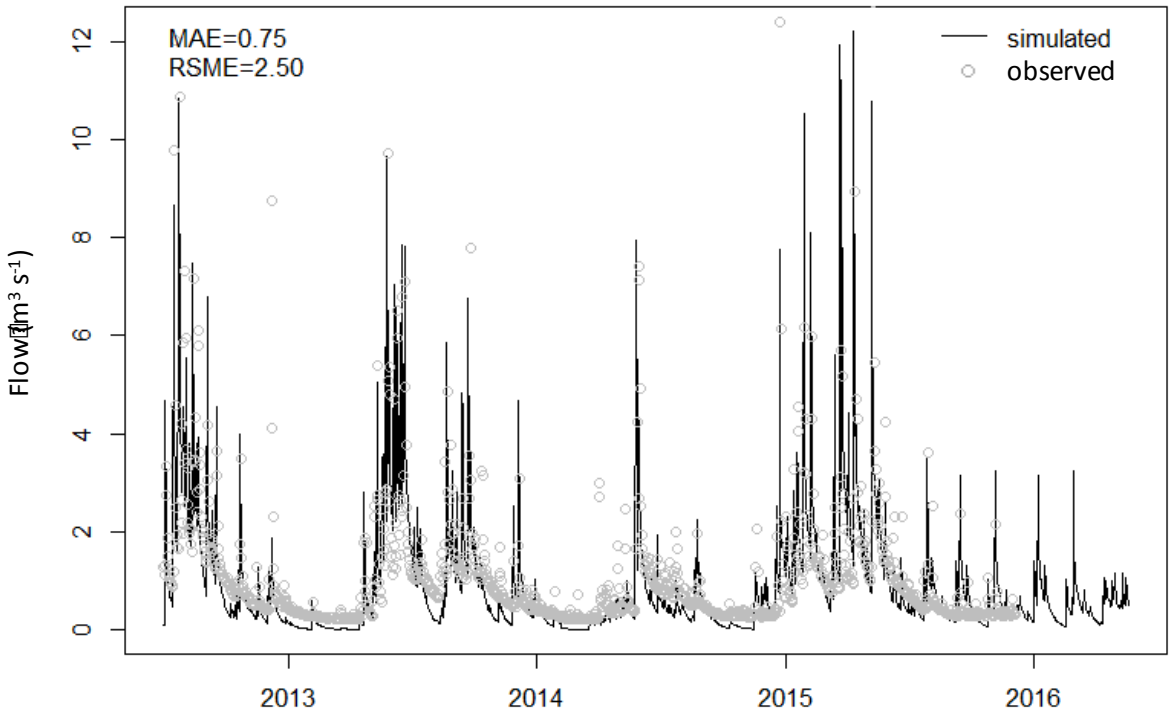

Figure 126: Matahuru Stream flow observed at Myjers Farm and modelled with INCA.

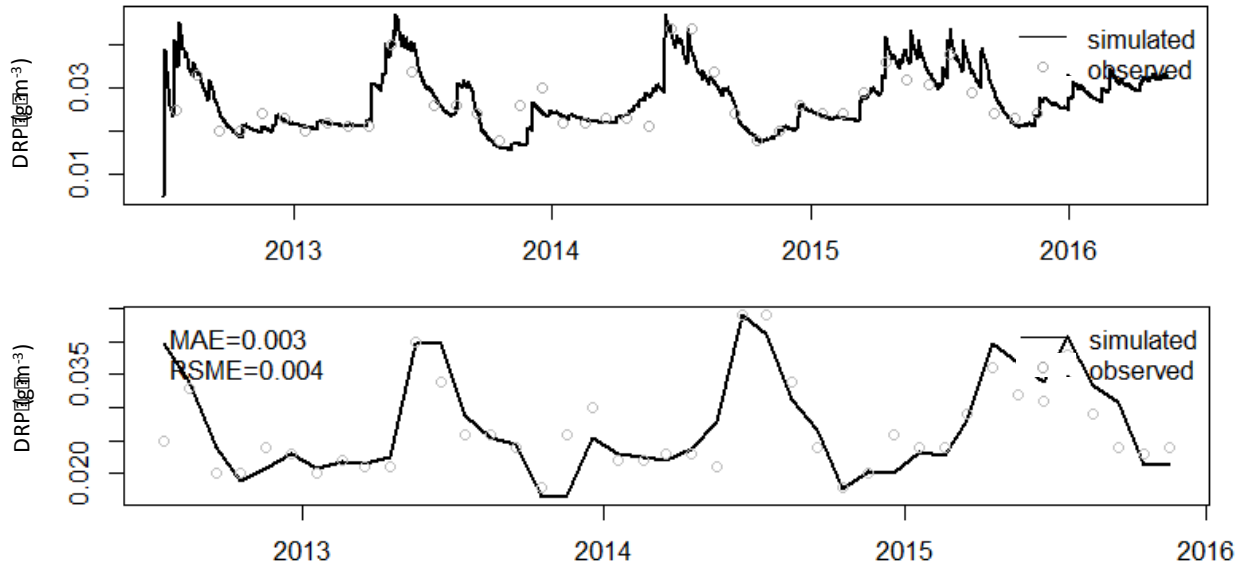

Figure 127: Observations of dissolved reactive phosphorus (DRP) in the Matahuru Stream at the Waiterimu road site and INCA-modelled DRP concentrations. Top graph shows daily model output, bottom graph shows modelled concentrations on the day of sampling which were used to calculate the root-mean-square-error (RMSE) and mean absolute error (MAE).

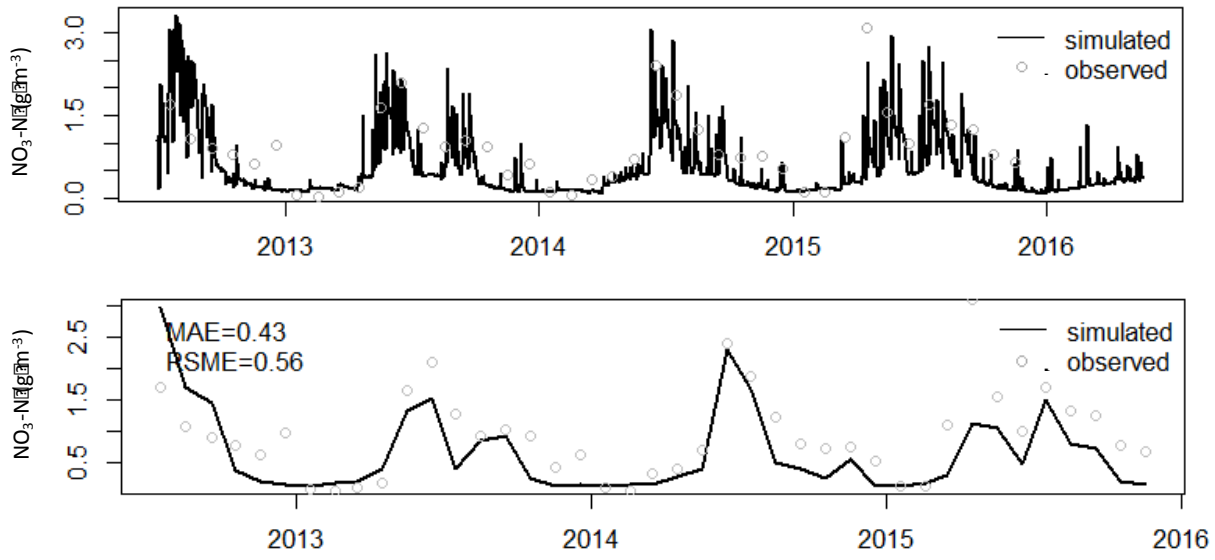

Figure 128: Observations of nitrate-N in the Matahuru Stream at the Waiterimu road site and INCA-modelled nitrate-N concentrations. Top graph shows daily model output, bottom graph shows modelled concentrations on the day of sampling which were used to calculate the root-mean-square-error (RMSE) and mean absolute error (MAE).

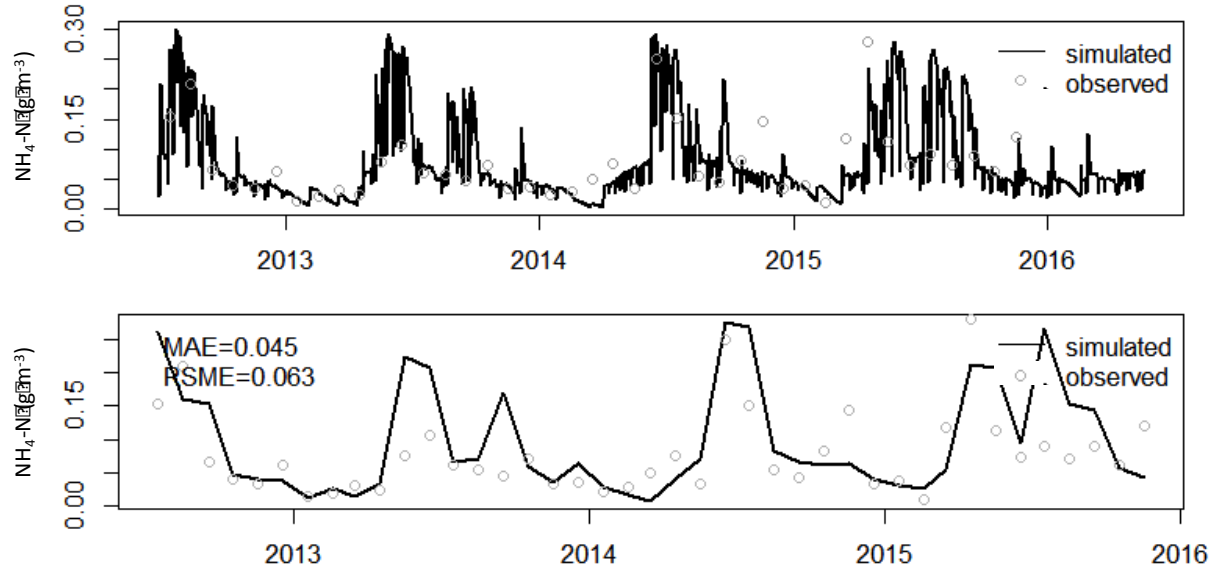

Figure 129: Observations of ammonia-N in the Matahuru Stream at the Waiterimu road site and INCA-modelled ammonia-N concentrations. Top graph shows daily model output, bottom graph shows modelled concentrations on the day of sampling which were used to calculate the root-mean-square-error (RMSE) and mean absolute error (MAE).

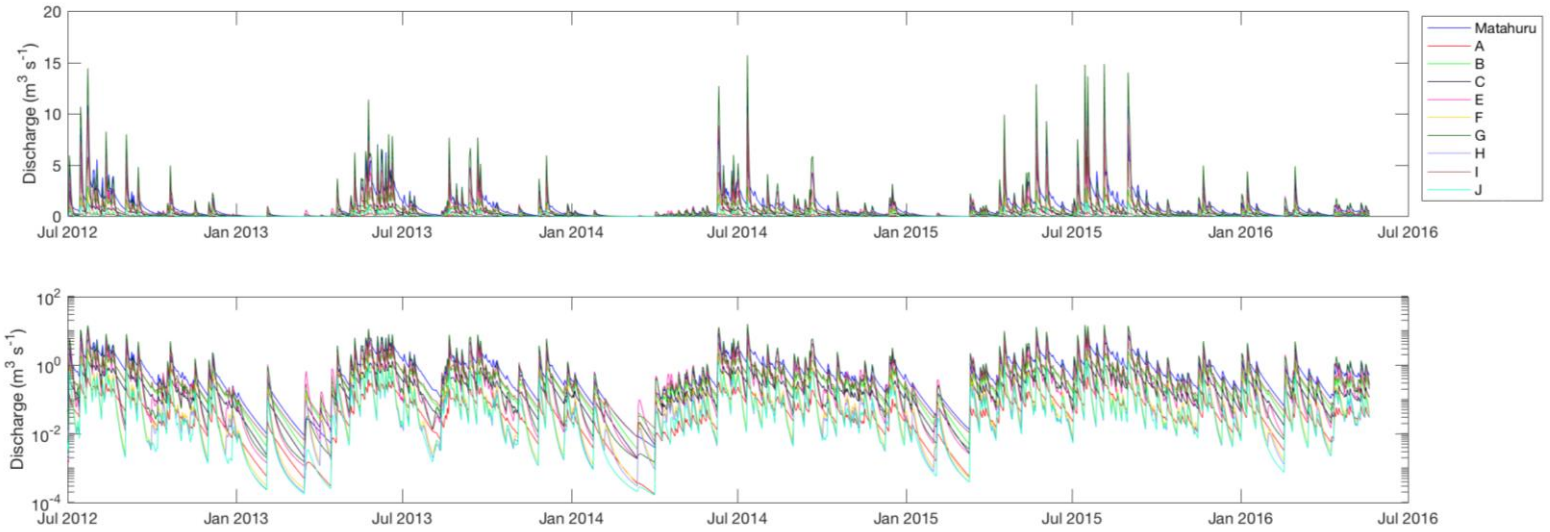

Figure 130: Discharges of the Matahuru Stream and the other aggregated inflows as modelled by INCA. The bottom graph shows the same time series as the top graph, but on a log-scaled y-axis.

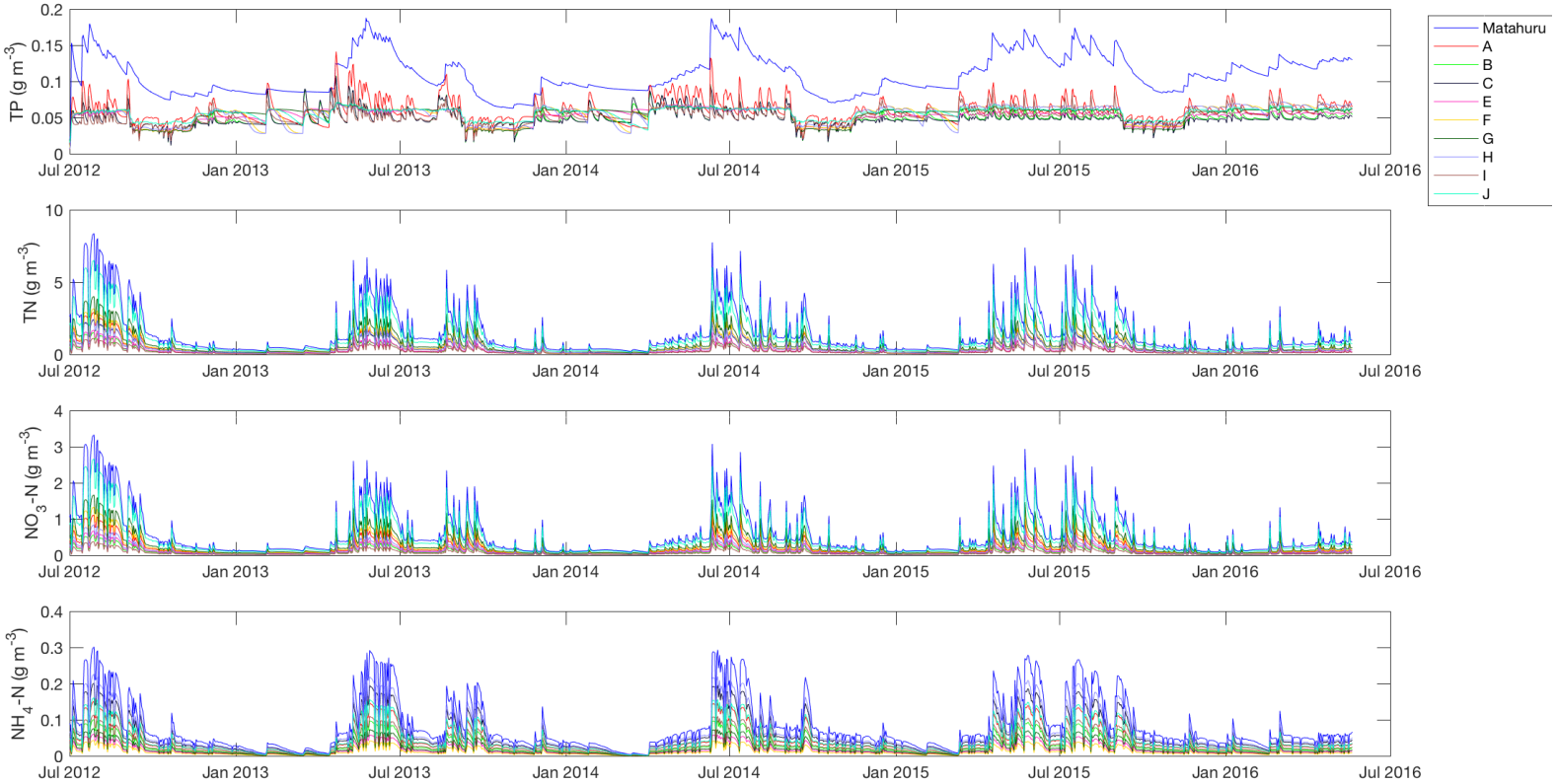

Figure 131: Nutrient concentrations in the Matahuru Stream and the other aggregated inflows as modelled by INCA.

Appendix D: Field study

Methods

Supplementary water quality monitoring of Lake Rotomānuka was conducted on a two-weekly basis from 30 March to 19 July 2016. Lake sampling was undertaken at the deepest point (8 m) of the lake (Figure 132 a) and included Secchi depth, conductivity, temperature and depth (CTD) profiles (SBE 19 plus SEACAT Profiler, Seabird Electronics Inc, USA), total suspended solids (TSS), surface (0.5 m) and bottom (7 m) nutrient concentrations (total nitrogen, total phosphorus, NO_3-N, NO_2-N, NH_4-N and PO_4-P) and surface and bottom chlorophyll *a* concentrations. Nutrient samples were retrieved using a 10-L Schindler trap. In addition, a thermistor chain logging water temperature and dissolved oxygen was deployed from 30 March to 19 July 2016. Temperature sensors (HOBO TidbiT, Onset, USA) were placed at 1 m intervals from 1 to 7 m, and dissolved oxygen sensors (D-Opto Dissolved Oxygen sensor, Zebra-tech LTD, Nelson, New Zealand) at 1 m and 7 m. Planned inflow monitoring to Lake Rotomānuka was restricted as the small catchment size resulted in only one notable inflow in the south-west corner of the lake (Figure 132 a). Further, low rainfall over the late summer and autumn period resulted in no detectable inflow until the latter half of May. Inflow samples were collected on five occasions from 27 May to 19 July 2016, and included discharge, nutrient concentrations (total nitrogen, total phosphorus, NO_3-N, NO_2-N, NH_4-N and PO_4-P) and total suspended solids (TSS).

Supplementary water quality monitoring of Lake Ngāroto was conducted on a two-weekly basis from 27 April to 19 July 2016. Lake sampling was undertaken at the University of Waikato monitoring buoy (Figure 132 b) and included Secchi depth, TSS, surface (0.5 m) and bottom (2.5 m) nutrient concentrations (total nitrogen, total phosphorus, NO_3-N, NO_2-N, NH_4-N and PO_4-P) and surface and bottom chlorophyll *a* concentrations.

Total suspended solids were determined by filtering (Advantec GC 50 filters), then drying for 12 h at 100 °C, followed by gravimetric determination. Nutrient concentrations were analysed using a Flow Injection Analyser 8500 Series II. Phosphate was analysed using LACHAT QuickChem method 31-115-01-1-H; ammonium was analysed using LACHAT QuickChem method 31-107-06-1-B and LACHAT QuickChem

Method 31-107-04-1-A was used to analyse nitrate/nitrite. Concentrations of chlorophyll *a* were determined by fluorometric analysis following maceration and extraction with 90% buffered acetone.

Figure 132: Lake Rotomānuka with supplementary in-lake sampling location (red dot) (left) and Lake Ngāroto with location of supplementary sampling and University of Waikato monitoring buoy indicated by red dot and inflow sampling site (yellow dot) indicated (right).

Results

CTD vertical profiles of temperature and dissolved oxygen indicate Lake Rotomānuka was strongly stratified when sampled on 30 March and 13 April 2016 (Figure 133a, b). However, stratification had broken down and the lake had mixed by 27 April, and there appeared to be no other notable stratification apart from possible diel stratification on 22 June (Figure 133a, b) during an extended period of calm weather. Dissolved oxygen profiles indicate hypoxia (< 0.1 mg L^{-1} detection limit) or anoxia (arbitrarily, < 2 mg L^{-1}) of the hypolimnion during periods of stratification and some evidence for oxygen decline in the bottom waters during periods of lake stability even in the winter months (Figure 134a, b).

A thermistor string with temperature and dissolved oxygen sensors logging every 15 minutes was deployed from 30 March to 19 July 2016. Although the 2-m temperature sensor failed to record any data, data from the other sensors has been plotted (Figure 133a, b). The data support the assertion that Lake Rotomānuka was stratified until 17 April followed by a sudden breakdown of stratification and mixing on 18 April 2016. Interestingly, the bottom waters of the lake appear to have become hypoxic for a short period on 7 - 8 May, with some evidence of limited stratification (Figure 134a, b) before the lake mixed again on 11 May when regular periodic sampling took place. Dissolved oxygen concentrations

through the lake water column could not be provided for 11 May due to a fault in the CTD oxygen sensor. Nutrient concentrations, Secchi depth, TSS and chlorophyll *a* concentrations for Lake Rotomānuka from 30 March to 19 July 2016 are presented in Table 32. Nutrient and chlorophyll *a* samples were taken from the surface (0.5 m depth and bottom waters (7 m depth) using a 10 L Schindler trap, TSS samples were taken from the surface water only. For the study period (30 March to 19 July 2016) mean Secchi depth was 1.45 m (± 0.13 m SE), mean TSS 3.03 g m^{-3} (± 0.39 mg L^{-1} SE) and mean chlorophyll *a* 16.7 µg L^{-1} (± 2.7 µg L^{-1} SE). Surface and bottom water chlorophyll *a* concentrations were variable, but both increased after the lake mixed in early May. Total nitrogen (mean 1.13 mg L^{-1} ± 0.4 mg L^{-1} SE) and nitrate-N (mean 0.05 ± 0.02 mg L^{-1} SE) concentrations were relatively consistent until July 2016 when large increases were observed (Table 32). In contrast, total phosphorus (mean 0.03 ± 0.002 mg L^{-1} SEM) showed a declining trend from March to June and then remained relatively consistent, while dissolved reactive phosphorus was near or below the detection limits (0.004 mg L^{-1}) for the duration of the study (Table 32). Ammonium-N concentrations (mean 0.14 ± 0.02 mg L^{-1} SEM) were greater in the bottom waters during stratification, but were more evenly distributed following lake mixing in early May 2016.

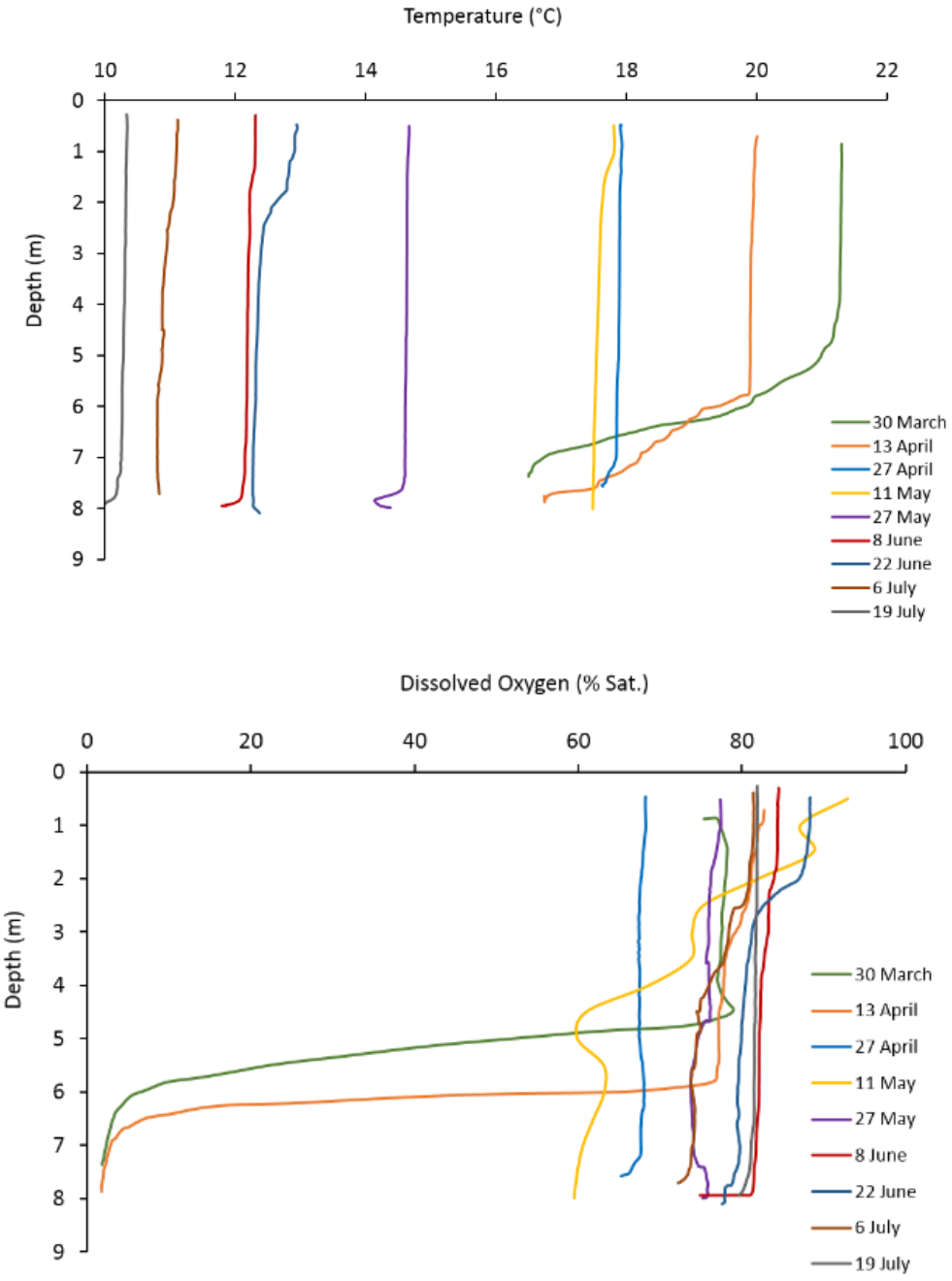

Figure 133: Vertical profiles of (a) temperature, and (b) dissolved oxygen in Lake Rotomānuka from 30 March - 19 July 2016. Note: Dissolved oxygen for 11 May has been omitted due to a fault in the oxygen sensor.

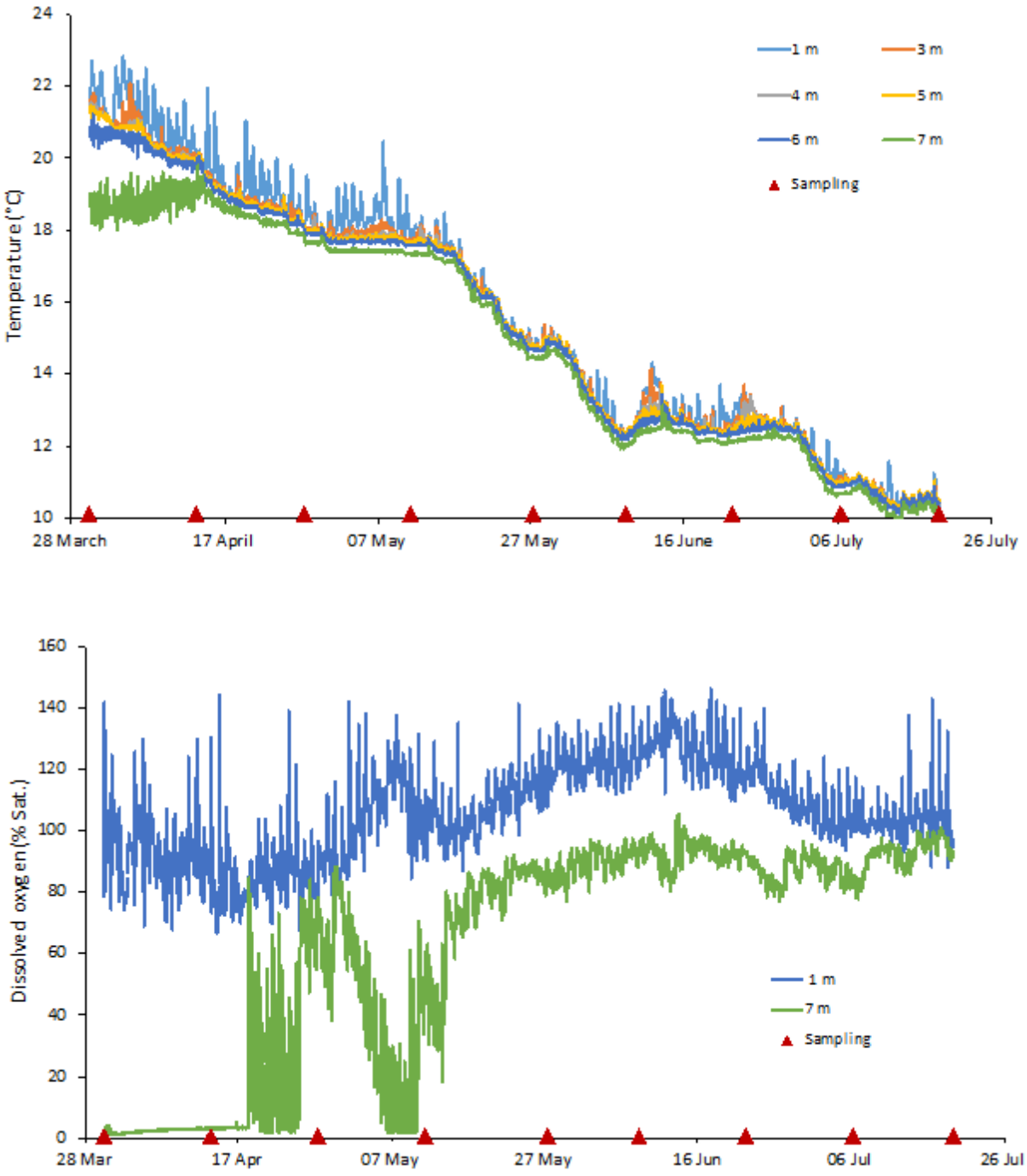

Figure 134: Lake Rotomānuka temperature (top) and dissolved oxygen (bottom) at 15 minutes intervals from 30 March to 19 July 2016. Red arrows indicate when in-lake water sampling occurred.

Table 32: Secchi depth, total suspended solids (TSS), chlorophyll *a* (TCHLA), total nitrogen (TN), nitrate (NO_3-N), nitrite (NO_2-N), ammonium (NH_4-N), total phosphorus (TP) and dissolved reactive phosphorus (PO_4-P) sampled from surface (0.5 m) and bottom (7 m) waters of Lake Rotomānuka from 30 March to 19 July 2016.

Sampling date	Depth (m)	Secchi depth (m)	TSS (g m^{-3})	Chl *a* (µg L^{-1})	TN (mg L^{-1})	NO_3 (mg L^{-1})	NO_2 (mg L^{-1})	NH_4 (mg L^{-1})	TP (mg L^{-1})	PO_4 (mg L^{-1})
30 March 2016	0.5	1.20	2.80	20.22	0.970	0.021	0.006	0.043	0.043	<0.004
	7.0			2.90	1.051	0.021	0.005	0.095	0.043	0.004
13 April 2016	0.5	1.02	2.90	7.18	0.951	0.021	0.006	0.059	0.047	0.005
	7.0			9.25	1.451	0.020	0.006	0.342	0.043	<0.004
27 April 2016	0.5	1.07	5.00	6.57	1.048	0.023	0.004	0.102	0.043	<0.004
	7.0			8.48	0.966	0.022	0.005	0.091	0.042	<0.004
11 May 2016	0.5	1.35	4.20	13.15	0.930	0.021	0.006	0.083	0.040	<0.004
	7.0			4.58	0.936	0.022	0.006	0.112	0.040	<0.004
27 May 2016	0.5	1.40	2.27	17.1	1.132	0.021	0.006	0.157	0.023	<0.004
	7.0			16.85	1.072	0.021	0.005	0.143	0.021	<0.004
8 June 2016	0.5	1.40	4.00	28.45	1.093	0.021	0.006	0.131	0.021	<0.004
	7.0			18.89	1.158	0.024	0.003	0.134	0.025	<0.004
22 June 2016	0.5	1.49	2.80	42.34	1.102	0.023	0.005	0.147	0.024	<0.004
	7.0			8.95	1.089	0.023	0.004	0.162	0.022	<0.004
6 July 2016	0.5	2.22	2.00	42.21	1.238	0.116	0.008	0.178	0.029	<0.004
	7.0			14.68	1.489	0.139	0.009	0.193	0.027	<0.004
19 July 2016	0.5	1.91	1.33	22.58	1.304	0.219	0.008	0.185	0.027	<0.004
	7.0			19.14	1.352	0.221	0.008	0.187	0.025	<0.004

Discharge, TSS and nutrient concentrations were monitored from a single inflow to Lake Rotomānuka on a two-weekly basis from 27 May to 19 July 2016 (Table 33). Prior to sampling on 27 May the inflow was dry and when the inflow had sufficient water to allow sampling the flow velocity was generally low (mean discharge was 3.2 ± 1.12 L s^{-1} SE), allowing build-up of filamentous algae and particulate matter on the submerged vegetation. Nutrient concentrations were generally higher than in-lake concentrations with nitrate (mean 0.81 ± 0.45 mg L^{-1} SE) and dissolved reactive phosphorus (mean 0.014 ± 0.001 mg L^{-1} SE) inflow concentrations notably higher than lake concentrations (Table 32 and Table 33). Total suspended solids (mean 8.96 ± 4.15 mg L^{-1} SEM) were variable and likely to be related to flow velocity prior to sampling.

Table 33: Total suspended solids (TSS), discharge, total nitrogen (TN), nitrate (NO_3-N), nitrite (NO_2-N), ammonium (NH_4-N), total phosphorus (TP) and dissolved reactive phosphorus (PO_4-P) concentrations in surface inflow to Lake Rotomānuka from 27 May to 19 July 2016.

Date	Discharge (L s^{-1})	TSS (g m^{-3})	TN (mg L^{-1})	NO_3 (mg L^{-1})	NO_2 (mg L^{-1})	NH_4 (mg L^{-1})	TP (mg L^{-1})	PO_4 (mg L^{-1})
27 May 2016	4.13	4.9	1.087	0.088	0.007	0.103	0.058	0.014
8 June 2016	1.01	23.0	0.856	0.032	0.006	0.214	0.085	0.019
22 June 2016	7.20	1.8	1.310	0.150	0.010	0.123	0.071	0.015
6 July 2016	1.31	13.7	2.423	2.152	0.014	0.109	0.050	0.008
19 July 2016	2.81	1.4	2.138	1.635	0.015	0.043	0.040	0.012

Lake Ngāroto was sampled for nutrient concentrations, Secchi depth, TSS and chlorophyll *a* concentrations from 27 April to 19 July 2016 (Table 34). Nutrient and chlorophyll *a* samples were taken from the surface (0.5 m depth) and bottom waters (3 m depth) using a 10 L Schindler trap, TSS samples were taken from the surface water only. Mean Secchi depth was 0.47 m (± 0.03 m SE), mean TSS 25.7 mg L^{-1} (±2.97 mg L^{-1} SE) and mean chlorophyll *a* 99.1 µg L^{-1} (±16.2 µg L^{-1} SE). Total nitrogen (mean 1.69 mg L^{-1} ± 0.12 mg L^{-1} SE), nitrate-N (mean 0.45 mg L^{-1} ±0.18 mg L^{-1} SE) and nitrite-N (mean 0.01 mg L^{-1} ± 0.002 mg L^{-1} SE) increased throughout the sampling period while total phosphorus concentrations (mean 0.10 mg L^{-1} ± 0.005 mg L^{-1} SE) declined (Table 34). Monitoring of inflows to Lake Ngāroto was not conducted, however it is interesting to note that total nitrogen and nitrate-N concentrations of Lake Rotomānuka, the Rotomānuka inflow and Lake Ngāroto all increased in July when runoff had increased substantially.

Table 34: Secchi depth, total suspended solids (TSS), chlorophyll *a* (Chl *a*), total nitrogen (TN), nitrate-N (NO_3), nitrite-N (NO_2), ammonium-N (NH_4) total phosphorus (TP) and dissolved reactive phosphorus (PO_4) sampled from surface (0.5 m) and bottom waters (3 m) of Lake Ngāroto from 27 April to 19 July 2016.

Sampling date	Depth (m)	Secchi depth (m)	TSS (g m^{-3})	Chl *a* (µg L^{-1})	TN (mg L^{-1})	NO_3 (mg L^{-1})	NO_2 (mg L^{-1})	NH_4 (mg L^{-1})	TP (mg L^{-1})	PO_4 (mg L^{-1})
27 April 2016	0.5 m	0.49	24.9	17.74	1.252	0.019	0.008	0.02	0.109	0.004
	3 m			9.93	1.162	0.019	0.008	0.026	0.112	<0.004
11 May 2016	0.5 m	0.38	34.0	95.89	1.657	0.019	0.009	0.023	0.146	0.004
	3 m			20.79	1.157	0.02	0.007	0.021	0.103	0.004
27 May 2016	0.5 m	0.47	29.7	93.3	1.699	0.057	0.007	0.034	0.132	0.004
	3 m			87.3	1.489	0.044	0.006	0.014	0.115	0.004
8 June 2016	0.5 m	0.42	28.9	202.76	1.764	0.085	0.011	0.01	0.116	0.005
	3 m			191.2	1.664	0.088	0.009	0.009	0.117	0.005
22 June 2016	0.5 m	0.49	16.29	93.58	1.395	0.032	0.011	0.017	0.096	0.003
	3 m			86.31	1.191	0.032	0.011	0.016	0.081	0.004
6 July 2016	0.5 m	0.62	13.71	74.2	2.405	1.501	0.024	0.07	0.095	0.006
	3 m			112.18	2.368	1.486	0.024	0.069	0.092	0.006
19 July 2016	0.5 m	0.43	32.29	123.65	2.251	1.423	0.027	0.011	0.07	0.006
	3 m			178.46	2.206	1.432	0.027	0.014	0.066	0.006

Appendix E: Food-web analyses

Analysis of the flow of energy through lake food webs can give insights into trophic inter-relationships among species and their reliance of particular food resources. Such analyses can highlight the potential for trophic interactions between native and non-indigenous species, and key energy pathways that need to be maintained to promote of productivity of aquatic species of interest. One method that has been widely used to help resolve these inter-relationships is stable isotope analysis which uses changes in the ratio of natural nitrogen ($^{15}N/^{14}N$) and carbon ($^{13}C/^{12}C$) isotopes to track (i) the utilisation of carbon from basal resources (e.g., algae, terrestrial organic matter) through to secondary and primary consumers as $\delta^{13}C$, and (ii) the trophic position of different consumers as $\delta^{15}N$.

Methods

Sampling sites

Lake Ngāroto food-web sampling was conducted at three littoral sites and one mid-lake sites in spring (September) as part of this contract, and at five littoral and one mid-lake sites in summer (March) as part of the MBIE Health and Resilience of New Zealand Lakes programme (Figure 135). Lake Rotomānuka data included here were collected from three littoral sites and one mid-lake site in spring (October) and summer (February) as part of a separate study in the predecessor to the current MBIE programme (Figure 135).

Figure 135: Isotope sampling sites in Lakes Ngāroto (left; 2016) and Rotomānuka (right; 2014-15).

Basal resources

Allochthonous and autochthonous basal isotope signatures were obtained from (i) dominant riparian plant species, (ii) filamentous green algae collected opportunistically from lake edges, and (iii) phytomicrobenthos (PMB) growing on wood and macrophyte tissue. Prior to analysis, large particles of entrained terrestrial organic matter, filamentous algae and macroinvertebrates (mainly Chironomidae) were removed from PMB. Coarse particulate organic matter (CPOM; >500 µm) was obtained from all sites in water > 1 m deep using a Ponar grab sample rinsed through a sieve bucket; representative samples were retained for isotope analysis. Seston (material suspended in the water column) was collected as (i) the residue of a 500 mL water sample filtered through a 40 µm sieve and then a MSGC filter (1.2 µm pore size; “fine” seston), and from plankton net trawls (40 µm-mesh) subsequently filtered through 40, 90 and 250 µm sieves to obtain “small”, “medium” and “large” seston fractions. Horizontal plankton tows were collected at littoral sites whereas vertical tows were obtained at mid-lake sites.

Collection of consumers

Invertebrates colonising submerged littoral vegetation and banks were collected using sweep netting (250 µm mesh net), while benthic invertebrates were picked from the Ponar samples collected at littoral and mid-lake sites. Ponar samples were picked in full (mainly Chironomidae) while representatives key

invertebrate groups were picked from sweep samples. Mussels were collected from Lake Ngāroto by wading. Fish were collected using a combination of sweep-netting (mainly gambusia) along shorelines, fyke-nets and fine-mesh mesh minnow traps (n = 1 and 3, respectively, at each littoral location). Additional large fish were caught opportunistically, including electric fishing in September on Lake Ngāroto. Fyke nets and minnow traps were deployed overnight whereas all other collections were made during the day.

Representative fish in each of three fish size classes (Table 35) were retained where possible and euthanised before being placed on ice and later frozen. Fin clips were taken from the threatened longfin eel and also from shortfin eels >500 m in length so they could be returned to the lake; a regression between fin clip and muscle tissue isotopes indicated similar $\delta^{15}N$ values but average of 1-2‰ depletion of $\delta^{15}N$ values in fins (corrected results are presented here). Whole bodies minus head and guts were used for isotope analysis of larval fish, whereas for larger fish filets or plugs of white muscle below the dorsal fin were used because it has less variable fractionation than other tissue. Scales were removed prior to removing samples from fish, and plugs and filters were examined for bones which were removed prior to analysis.

Table 35: Size classes (lengths, mm) of fish used for isotope analyses.

	Small	**Medium**	**Large**
Common carp	51-150	151-500	500+
Catfish	20-50	51-150	151+
Rudd	21-99	100-149	150+
Gambusia	6-15	16-25	26+
Long-fin eel	101-300	301-500	500+
Shortfin eel	101-300	301-500	500+*
Smelt	41-60	61-80	81+
Common bully	21-40	41-60	61+

Isotope sample analyses

All basal and consumer samples were dried at 60^{o}C before grinding using a mortar and pestle or ball grinder. Between 2-40 mg of ground material was weighed to the nearest 0.01 mg and placed in

aluminium cups for analysis of $\delta^{13}C$ and $\delta^{15}N$ on a fully automated Europa Scientific 20/20 isotope analyser at the University of Waikato's stable isotope facility. Basal samples and invertebrate consumers were pooled for each lake on each date, while fish were analysed separately, although mean isotope values only are presented here. Stable isotope ratios ($^{13}C/^{12}C$ and $^{15}N/^{14}N$) are expressed as delta (δ) and defined as parts per thousand (‰) relative to the laboratory standard leucine, calibrated relative to atmospheric nitrogen for $\delta^{15}N$ and to Vienna Pee Dee Belemnite for $\delta^{13}C$. The instrument precision was c. 0.3 ‰ for $\delta^{13}C$ and c. 0.5 ‰ for $\delta^{15}N$. Animal tissue values presented here are corrected for lipid content. Fractionation occurs as carbon is transferred across trophic levels and must be accounted for when interpreting stable isotope biplots (typically around 1‰ for carbon and 2.4‰ for nitrogen).

Results

In summary, the food web data suggest that decaying organic matter derived from terrestrial vegetation is likely to be an important source of carbon for higher trophic levels, highlighting the importance of riparian plants for supporting littoral food webs. The potential overlap in diet between catfish and eels, suggests that management outcomes targeted an increasing eel biomass may also need to control catfish numbers.

The Lake Ngāroto food-web was well resolved using isotope biplots (Figure 136). Isotope data indicate that the food base was dominated by organic matter most likely primarily of terrestrial origin although this appeared to vary seasonally with seston apparently more important in spring. Large eels (note short-fins only are presented in plots) were at the top of the food-web in both seasons with other fish/size classes generally closely grouped in biplot space. There was some suggestion of dietary overlap between catfish and small-medium sized eels in summer, confirmed by subsequent gut analyses (Collier et al. in prep.). Common carp in spring were similar to large catfish presumably reflecting a similar benthic diet.

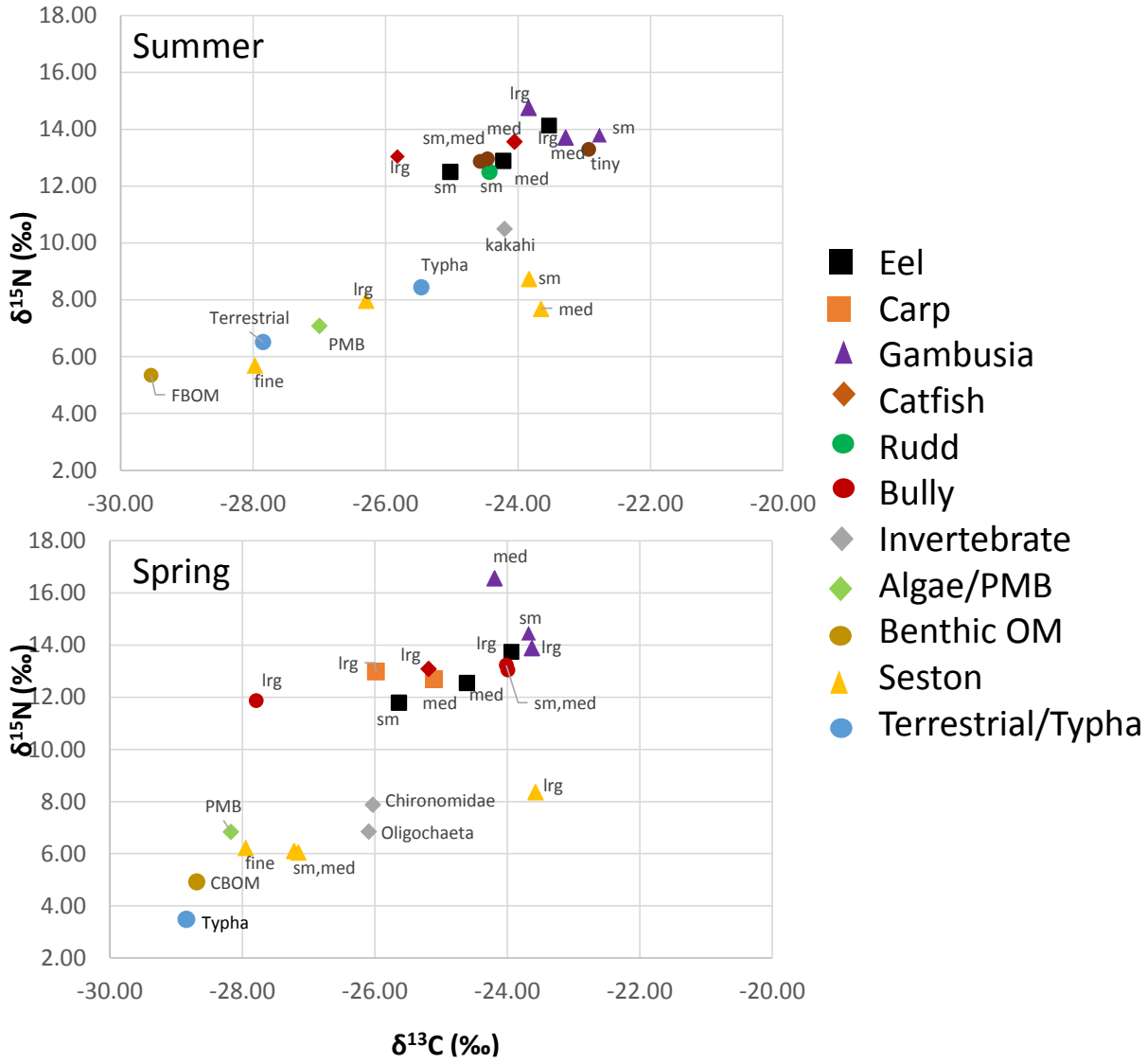

Figure 136: Stable isotope bi-plots of food-web in Lake Ngāroto (PMB=phytomicrobenthos, FBOM = fine benthic organic matter, CBOM = coarse benthic organic matter; for fish, sm=small, med=medium, lrg = large.

The flow of carbon through the food web in Lake Rotomānuka based on stable isotope data was not clear as it did not conform to expected fractionation shifts. Consequently, limited conclusions can be made regarding carbon flow in that lake (Figure 137). However, in spring at least, large- and medium-sized eels were at the top of the food chain; in summer all fish were tightly grouped. As in Lake Ngāroto, gambusia displayed high $\delta^{15}N$ values in both lakes potentially reflecting (i) localised N enrichment along lake margins, or (ii) unusual dietary pathways involving live birth where developing fish consume parental carbon. Gut content analyses underway for catfish, eels, common bully and gambusia from

both lakes should help resolve feeding relationships among species. At this stage, no further conclusions can be made of Lake Rotomānuka regarding the implications of lake management on food-webs are made at this stage based on isotopic analysis.

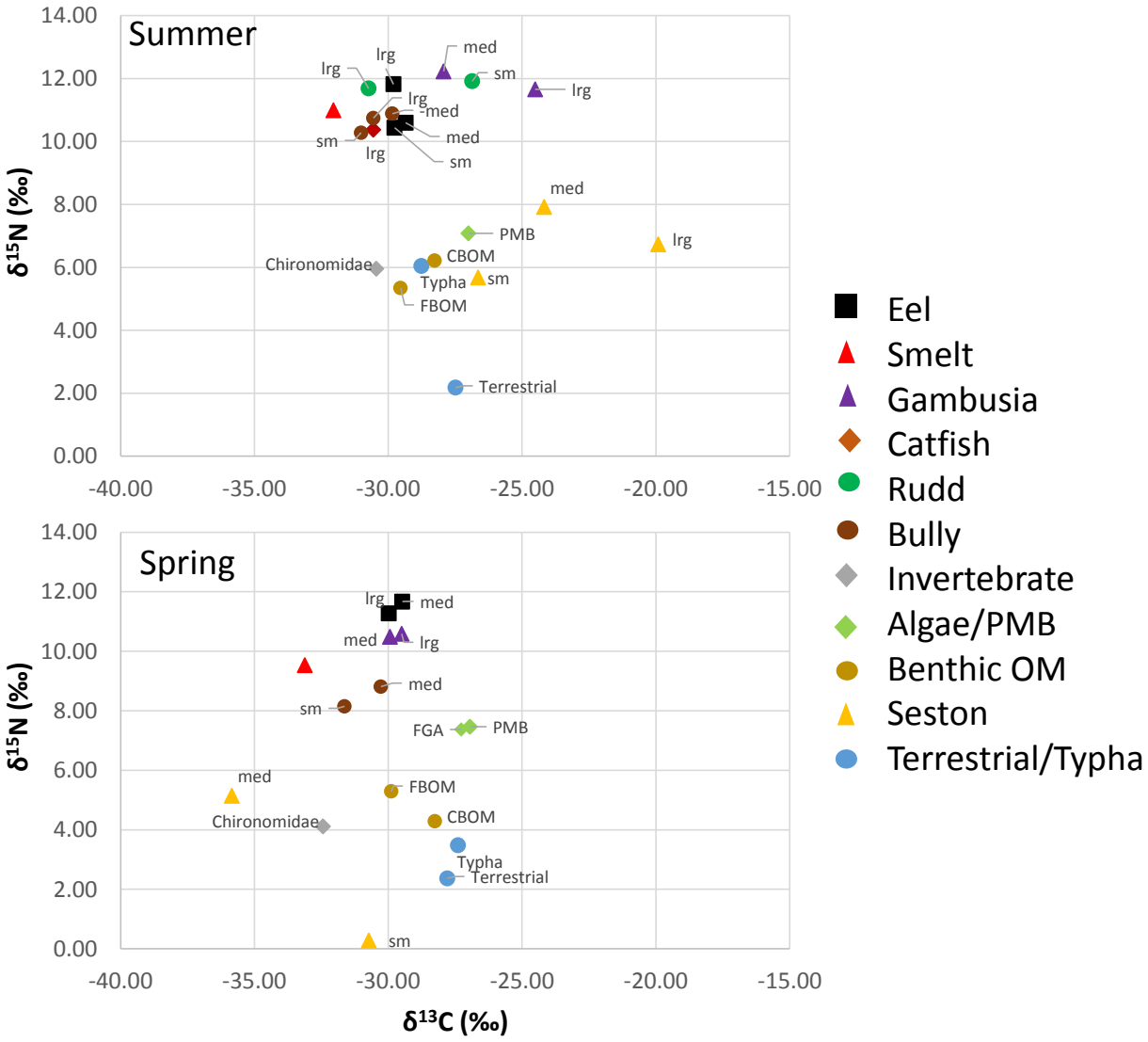

Figure 137: Stable isotope bi-plots of food-web in Lake Rotomanuka (PMB=phytomicrobenthos, FBOM = fine benthic organic matter, CBOM = coarse benthic organic matter; for fish, sm=small, med=medium, lrg = large.

Appendix F: Fish study

Introduction

The purpose of incorporating a fish component into the shallow lakes modelling was to estimate the potential for improvement of water quality that might be associated with removal of invasive fish. To do this, we aimed to predict the amount of sediment that could be resuspended by koi carp compared to other processes, e.g., wind turbulence. The fate of resuspended sediment is two-fold; the coarse sand and silt-sized fractions will rapidly resettle to the lake bed and become deposited sediment, whereas the clay-sized fractions may remain suspended for hours or days, contributing to visible water turbidity. Secondly, we aimed to predict the reduction of nutrients that might occur upon removal of carp, rudd, catfish and goldfish. We used a previously published study (Morgan and Hicks 2013) to estimate nutrient excretion by koi carp and our unpublished results to estimate nutrient excretion by eels, goldfish, and catfish (Hicks, unpubl. data). To produce estimates of nutrient release and sediment resuspension we required estimates of mass-dependent release rates of N and P, mean fish size, areal fish biomass, and water temperature.

Summary of results

Fish abundance estimates

This study relied on previous research to establish the species and biomass of fish present in each lake but did not allow for additional field work to provide revised estimates of fish biomass. One shortcoming was the lack of areal biomass fish estimates for Lake Rotomānuka, for which only catch-per-unit-effort data was available. The most cost-effective method to arrive at an areal biomass and mean fish size for the complete range of fish species present is by single-pass boat electrofishing (Hicks et al. 2006). This method, however, is biased towards koi carp and goldfish and underrepresents eels and catfish. Lake Waikare, for example, had only boat electrofishing estimates from 2003 and 2008. Despite these shortcomings, we were able to build a comprehensive comparison of relative fish abundance in the four lakes (Table 36).

From these estimates where boat electrofishing records were available, and from gill and fyke netting undertaken by DOC for Lake Rotomānuka and Waipa District Council for fyke netting in 2015, we

compiled the most current view of the fish communities (Table 36). Koi carp populations are dominated by large, highly-coloured individuals, and goldfish are generally smaller and olive-bronze (Figure 138).

Table 36: Fish capture by lake and method. [1]Number of fish estimated from total weights by species from fyke netting divided by mean weights (Table 37).

Lake	Survey type	Date	*N* fish	Fish biomass (kg)	Survey type and date	Percent species by number							
						Catfish	Goldfish	Common bully	Common smelt	Rudd	Koi	Shortfin eel	Longfin eel
Ngaroto	Gill and fyke nets	2001	3,970	4,317	Gill and fyke nets 21 Aug-29 Oct 2001	73	1	0.5	0.05	20	0.02	6	0.14
	Boat electrofishing	2009	193	32	Boat electrofishing 2 Feb 2009	4	27	11		18	12	11	
	Fyke nets[1]	2015	14,845	2,259	Fyke netting 14-23 Dec 2015	36	2		0.01	2	0.04	54	6
Rotomanuka North	Gill and fyke nets	2015	701	29	Gill and fyke nets 12 Mar 2015	1	1	72	2	9		9	0.3
Rotomanuka South	Gill and fyke nets	2015	176	45	Gill and fyke nets 12 Mar 2015	7	11			35		45	
Waahi	Boat electrofishing	2007	537	87	Boat electrofishing 7-26 Mar 2007	4	45	4	2	4	5	31	
	Boat electrofishing	2011	216	68	Boat electrofishing 23 Mar 2011	4	27		2	8	8	31	
Waikare	Boat electrofishing	2003	69	36	Boat electrofishing 11 Sep 2003		16	12	29		26	17	
	Boat electrofishing	2008	98	14	Boat electrofishing 24 Jan 2008		28	20			21	6	

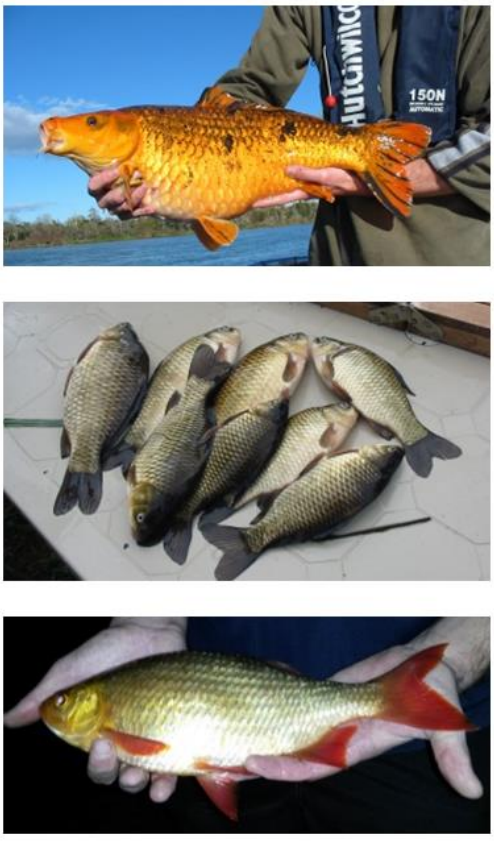

Figure 138: Fish caught in Waikato shallow lakes. From top to bottom: koi carp, goldfish, and rudd.

Estimating sediment and nutrient yields from fish

Rates of sediment resuspension are available for common carp, the same species as the koi carp race found in NZ, and are dependent on fish size and biomass. For these estimates we assumed a mean weight 605 g (*N* = 1,464), calculated from Lake Ohinewai carp population before removal in 2011 (Tempero and Hicks 2017), and a mean water temp 15°C. The biomass-dependent equations from two studies are shown in Table 37.

Table 37: Rates of sediment resuspension for common carp in relation to fish areal biomass.

Response variable	Unit of response variable	Slope *b*	*Y* intercept, *a*	r^2	*N*	*P*	Source
Suspended sediment	mg DW/L	0.07724	0	0.92	5	0.0027	Breukelaar et al. (1994)
Sedimentation rate	g DW/m^2/day	0.0281	1.705	0.995	5	0.001	Baidou and Goldsborough (2010)

The contribution of koi carp to the observed suspended sediment concentrations ranged from 7% to 20% based on the equation of Breukelaar et al. (1994). Sedimentation derived from the suctorial feeding activities of carp ranged from 2.6 to 7.8 g m^{-2} d^{-1} (Table 38). Nutrients excreted by koi carp contributed substantial amounts of nitrogen and phosphorus.

Table 38: Predicted suspended sediment concentrations, sedimentation rates, and nutrients excreted based on koi carp biomasses for 4 shallow Waikato lakes.

Lake	Date	Area	Observed mean TSS	Koi carp biomass	Suspended sediment[1]		Sedimentation rate[2]	Nutrients excreted[3]	
		(ha)	(mg/L)	(kg/ha)	(mg DW/L)	% from carp	(g/m^2/day)	(kg TN/year)	(kg TP/year)
Rotomanuka	12/03/2015	17.1	18.4	0	0.0	0	0.0	0	0
Ngaroto	2/02/2009	108	34.8	72.2	5.6	16	3.5	1,010	155
Waahi	7/03/2007	522	34.7	65.1	5.0	14	3.5	4,416	676
Waahi	23/03/2011	522	34.7	33.0	2.6	7	2.6	2,239	343
Waikare	11/09/2003	3,442	85.9	131.1	10.1	12	5.4	58,633	8,970
Waikare	24/01/2008	3,442	85.9	217.7	16.8	20	7.8	97,366	14,900

[1]Calculated from Breukelaar et al. (1994), Table 37

[2] Calculated from Badiou and Goldsborough (2010), Table 37

[3]Nutrient excretion rates (Morgan and Hicks 2013) are dependent on fish size and biomass and water-temperature, and assume a mean carp weight of 605 g and a mean annual water temp of 15°C

Detailed estimates of fish abundance in Lake Ngāroto

Fishing effort

Lake Ngāroto was fished in 2001 (fyke nets, gill nets and seine netting), 2009 (boat electrofishing) and 2015 (fyke netting). The most recent netting in December 2015 occurred when the Waipa District Council contracted the eel fisherman Mike Holmes to set 48 25-mm mesh fyke nets in Lake Ngāroto over 10 nights between 14 and 23 December 2015. All eels (1,358 kg of shortfin eels and 72 kg of longfin eels) were returned alive to the lake but a total of 729 kg of introduced fish (catfish, goldfish, rudd and, koi carp) were humanely destroyed and collected for rendering. The lake shoreline was divided into 7 littoral sites with site 8 in the middle of the lake (Figure 139). Sites 1 and 2 were fished twice during the 10 nights.

Figure 139: Approximate location of the fishing sites in December 2015 around Lake Ngāroto.

In 2009, boat electrofishing was conducted at twelve sites in 10-minute shots. Eleven sites were littoral, and one site (site 4) was in the middle of the lake (Hicks and Brijs 2009).

From 21 to 29 August 2001, ten fyke nets with 25-mm stretched mesh were set overnight with their wings extended towards the shore at each of 6 sites (Hicks et al. 2001). Three 40-m long, 2-m deep panel gill nets were set overnight offshore from the fyke nets at each site. Each panel gill net had five panels of monofilament nylon mesh joined end to end. The lengths and stretched-mesh dimensions of the panels were as follows: 6 m of 25-mm mesh, 8 m of 38-mm mesh, 8 m of 56-mm mesh, 8 m of 84-mm mesh, and 10 m of 106-mm mesh. The gill nets were set for approximately 20 h (about 1430 h to about 1030 h), and fyke nets were set at about 1500 h for approximately 24 h. Seine hauls were made during the day onto the beaches at sites 7 and 8. Three hauls were made at site 7, and 2 hauls at site 8. An additional 10 seine hauls were made at site 7 on 29 October 2001. The seine net was 5.3-m long with 5-mm mesh in the wings and a central bag of 3-mm mesh. The net height was 2 m.

Results

In 2015, a total of 2,259 kg of fish were caught in 480 net nights (Table 39). Shortfin eels comprised 60% of this biomass and longfin eels comprised 8%. Koi carp comprised just 0.3% of the total biomass, which is fairly typical of the bias against koi carp in fyke net catches. Catch per unit effort (CPUE) at the eight sites, excluding repeated fishing sites 1 and 2, gave a mean CPUE of 3.0±0.9 kg net^{-1} $night^{-1}$ for shortfin eels, 0.3±0.9 kg net^{-1} $night^{-1}$ for longfin eels, and 1.4±0.9 kg net^{-1} $night^{-1}$ for catfish (Table 40). Low numbers of koi carp were caught at three of the eight sites. By extrapolating the weight of fish caught at each site by the mean individual fish weight (Table 41) the calculated total catch was 6,967 shortfin eels, 731 longfin eels, 4,663 catfish, and 5 koi carp (Table 42). Goldfish and rudd were approximately equally abundant.

Boat electrofishing in twelve 10-minute shots in 2009, by comparison, caught 32 kg of fish (Table 43), of which 58% were koi carp and 15% were shortfin eels (Hicks et al. 2009). No fish were caught at the mid-lake site (site 4).

A combination of fyke netting, gill netting, and beach seine netting caught 4,317 fish in August and October 2001 (Table 44). In fyke netting, catfish (3,127 individuals in total) far outnumbered shortfin eels (243 individuals). Gill netting caught more rudd (374 in total) and goldfish (40 in total) than all other species. The total biomass of all species caught was 520 kg (Table 45), with catfish comprising the

greatest weight (373 kg) of this total and shortfin eels comprising only 41 kg). CPUE from fyke netting alone gave a mean CPUE of 0.80±0.50 kg net^{-1} night^{-1} for shortfin eels, 0.02±0.03 kg net^{-1} night^{-1} for longfin eels, and 7.40±4.42 kg net^{-1} night^{-1} for catfish (Table 46). Fyke netting and seine netting caught no koi carp in 2001, and gill netting caught only a single koi carp.

Conclusion

It is clear from the comparison of fyke netting in 2001 and 2015 that shortfin eels have made a dramatic recovery in Lake Ngāroto, increasing approximately fourfold from 0.8 to 3.0 kg net^{-1} night^{-1}. Though less abundant, longfin eels have made an even greater recovery, increasing tenfold from 0.03 to 0.3 kg net^{-1} night^{-1}. Over the same period, catfish reduced in abundance by 80% from 7.4 to 1.4 kg net^{-1} night^{-1}. We conclude that the reduced fishing pressure on eels has allowed their biomass to recover, with consequent equivalent reduction in catfish biomass, most likely due to the combination of increased predation and competition of eels on catfish.

Table 39: Biomass of fish caught over 10 successive nights in Lake Ngāroto in 48 fyke nets.

		Weight (kg)						
Site	Date	Shortfin eel	Longfin eel	Catfish	Goldfish	Rudd	Koi carp	Total
1	14/12/2015	225	25	180	10.0	1.0	1.0	442
2	15/12/2015	152	17	45	7.0	3.0		224
3	16/12/2015	112	2	100	19.0		1.0	234
4	17/12/2015	86	12	25	8.0	1.0		132
5	18/12/2015	200	30	39	7.0	5.1	2.0	283
6	19/12/2015	97	10	62	8.7	0.5		179
7	20/12/2015	130	29	85	1.8	3.4		249
8	21/12/2105	155	0	17	9.3	11.1		193
1	22/12/2015	157	22	35	17.1	2.7	2.3	236
2	23/12/2105	44	24	15	0.9	2.8		87
Total		1358	172	603	88.8	30.6	6.3	2259
Percent of total		60	8	27	4	1	0.28	100

Table 40: Catch per unit effort of fish caught over 8 successive nights in Lake Ngāroto in 48 fyke nets. Repeated fishing at sites 1 and 2 on 22 and 23 Dec 2015 is excluded.

		Catch per unit effort (kg net^{-1} night^{-1})						
Site	Date	Shortfin eel	Longfin eel	Catfish	Goldfish	Rudd	Koi carp	Total
1	14/12/2015	4.7	0.5	3.8	0.21	0.02	0.02	9.2
2	15/12/2015	3.2	0.4	0.9	0.15	0.06	0.00	4.7
3	16/12/2015	2.3	0.0	2.1	0.40	0.00	0.02	4.9
4	17/12/2015	1.8	0.3	0.5	0.17	0.02	0.00	2.8
5	18/12/2015	4.2	0.6	0.8	0.15	0.11	0.04	5.9
6	19/12/2015	2.0	0.2	1.3	0.18	0.01	0.00	3.7
7	20/12/2015	2.7	0.6	1.8	0.04	0.07	0.00	5.2
8	21/12/2105	3.2	0.0	0.4	0.19	0.23	0.00	4.0
Mean		3.0	0.3	1.4	0.2	0.1	0.0	5.0
95% confidence interval		0.9	0.2	0.9	0.1	0.1	0.0	1.6
Percent of total		60	6	29	4	1	0.21	100

Table 41: Mean weights of fish in Lake Ngāroto from 2001 and 2009 that were used to calculate number of fish.

Species	*N*	Mean weight (g)	Source	Total weight (kg)	Estimated *N* 2015
Catfish	3141	118.8	Hicks et al. (2001)	603	5081
Goldfish	42	281.2	Hicks et al. (2001)	89	316
Koi carp	23	799.0	Hicks and Brijs (2009)	6	8
Longfin eel	6	171.3	Hicks et al. (2001)	172	1002
Rudd	857	107.9	Hicks et al. (2001)	31	283
Shortfin eel	247	166.6	Hicks et al. (2001)	1358	8155
Total				2259	14845

Table 42: Number of fish per night in the pooled fish biomass in Lake Ngāroto from 48 fyke nets calculated from total biomass per night (Table 39) and mean fish weight (Table 41). Repeated fishing at sites 1 and 2 on 22 and 23 Dec 2015 is excluded.

	No. of individuals								
Site	Shortfin eel	Longfin eel	Catfish	Goldfish	Rudd	Koi carp	Common smelt	Kaeo	Total
1	1351	146	1516	36	9	1			3058
2	913	99	379	25	28	0			1443
3	672	12	842	68	0	1			1595
4	516	70	211	28	9	0		1	835
5	1203	175	328	25	47	2	1		1782
6	583	58	525	31	5	0		3	1202
7	781	169	717	6	31	0		1	1705
8	929	2	145	33	103	0		1	1212
Total	6947	731	4663	252	233	5	1	7	12831
Percent of	54	6	36	2	2	0.04	0.01		100

Table 43: Biomasses of fish species caught in Lake Ngāroto on 2 February 2009. Gambusia and shortfin eels were underestimated. Trail 4 was mid-lake, and all other sites were littoral.

	Fish biomass (g)								
Trail	Shortfin eel	Common bully	Rudd	Koi	Koi/goldfish hybrid	Catfish	Goldfish	Gambusia	Total
1	1276	13	150	1018	1552	0	2	2	4013
2	1320	1	171	957	0	0	134	4	2587
3	0	5	24	0	680	0	88	0	797
4	0	0	0	0	0	0	0	0	0
5	0	0	76	505	0	0	266	0	847
6	694	0	53	3595	746	73	3	1	5165
7	249	1	0	0	650	0	781	0	1681
8	0	0	0	255	0	56	126	0	437
9	538	1	198	3009	0	623	107	2	4478
10	357	0	149	3815	0	0	121	0	4442
11	418	0	257	3605	0	203	124	0	4607
12	0	0	67	1619	0	549	319	0	2554
Total	4852	21	1145	18378	3628	1504	2071	9	31608
Average	404	2	95	1532	302	125	173	1	2634

Table 44: Number of fish caught by nightly sets of ten 25-mm mesh fyke nets and three 40-m panel nets in Lake Ngāroto in 2001.

	Number of fish									
Site	Catfish	Rudd	Shortfinned eel	Longfinned eel	Goldfish	Koi carp	Common bullies	Common smelt	Mosquito fish	Total
Fykes nets										
1	645	39	42	1	0	0	0	0	0	727
2	654	103	39	0	0	0	0	0	0	796
3	916	10	90	3	0	0	0	0	0	1019
4	525	17	27	1	2	0	0	0	0	572
5	385	71	45	1	0	0	0	0	0	502
6	2	0	0	0	0	0	0	0	0	2
Total	3127	240	243	6	2	0	0	0	0	3618
Gill nets										0
1	4	65	1	0	5	0	0	0	0	75
2	0	44	0	0	0	0	0	0	0	44
3	0	54	1	0	9	1	0	0	0	65
4	4	149	0	0	13	0	0	0	0	166
5	5	23	0	0	2	0	0	0	0	30
6	1	39	0	0	11	0	0	0	0	51
Total	14	374	2	0	40	1	0	0	0	431
Beach seine netting										
7	0	243	2	0	0	0	20	2	1	268
Grand total	3141	857	247	6	42	1	20	2	1	4317

Table 45: Biomass of fish caught by nightly sets of ten 25-mm mesh fyke nets and three 40-m panel nets in Lake Ngāroto in 2001.

		Biomass of fish (kg)									
Date	Method	Catfish	Rudd	Longfin eel	Shortfin eel	Goldfish	Koi carp	Common bully	Common smelt	Moquitofish	Grand Total
21/08/2001	fyke	33	10	0	7	0	0	0	0	0	50
22/08/2001	fyke	53	7	0	7	0	0	0	0	0	68
23/08/2001	fyke	84	16	0	7	0	0	0	0	0	107
28/08/2001	fyke	127	1	1	15	0	0	0	0	0	144
29/08/2001	fyke	73	3	0	4	2	0	0	0	0	81
Total for fyke nets		370	37	1	40	2	0	0	0	0	450
22/08/2001	gill	1	3	0	0	0	0	0	0	0	4
23/08/2001	gill	1	10	0	0	1	0	0	0	0	12
24/08/2001	gill	0	6	0	0	0	0	0	0	0	6
29/08/2001	gill	0	8	0	0	2	1	0	0	0	11
30/08/2001	gill	1	21	0	0	4	0	0	0	0	26
31/08/2001	gill	0	4	0	0	2	0	0	0	0	6
Total for gill nets		3	53	0	1	10	1	0	0	0	67
27/08/2001	seine	0	0	0	0	0	0	0	0	0	0
29/10/2001	seine	0	2	0	1	0	0	0	0	0	3
Total for seine nets		0	3	0	1	0	0	0	0	0	3
Grand total		373	93	1	41	12	1	0	0	0	520

Table 46: Catch per unit effort of fish in nightly sets of ten 25-mm mesh fyke nets in Lake Ngāroto in 2001.

	Catch per unit effort (kg net^{-1} night^{-1})						
Date	Shortfin eel	Longfin eel	Catfish	Goldfish	Rudd	Koi carp	Total
21/08/2001	0.69	0.01	3.27	0.00	1.01	0.00	4.98
22/08/2001	0.74	0.01	5.32	0.00	0.67	0.00	6.75
23/08/2001	0.71	0.00	8.39	0.00	1.63	0.00	10.74
28/08/2001	1.46	0.06	12.73	0.00	0.13	0.00	14.38
29/08/2001	0.38	0.02	7.28	0.18	0.25	0.00	8.12
Mean	0.80	0.02	7.40	0.04	0.74	0.00	8.99
95% confidence interval	0.50	0.03	4.42	0.10	0.75	0.00	4.56
Percent of total	8.9	0.2	82.3	0.4	8.2	0.0	100.0

Detailed estimates of fish abundance in Lake Waahi

Fishing effort

We used a 4.5 m-long, aluminium-hulled electrofishing boat with a 5-kilowatt pulsator (GPP, model 5.0, Smith-Root Inc, Vancouver, Washington, USA) powered by a 6-kilowatt custom-wound generator. Two anode poles, each with an array of six stainless steel wire droppers, created the fishing field at the bow, with the boat hull acting as the cathode (Hicks and Tempero 2011).

Surveys were conducted on 7 and 26 March 2007 and 23 March 2011, fishing 11 sites in 2007 and 10 sites in 2011. These sites were located in the eastern half of Lake Waahi (Hicks and Tempero 2011). The sites chosen for electrofishing were chosen to represent as diverse a range of habitats as possible while attempting to maximise catch rates based on previous boat electrofishing experience. All sites were fished with the GPP set to high range (50-500 V direct current) and a frequency of 60 pulses per second. We adjusted the percent of range setting of the GPP to 30% to give an applied current of 4 amps root mean square. We assumed from past experience that an effective fishing field was developed to a depth of 2-3 m, and about 2 m either side of the centre line of the boat. We thus assumed that the boat fished a transect 4 m wide, which was generally consistent with behavioural reactions of fish at the water surface. This assumption was used to calculate the area fished from the linear distance measured with the on-board global positioning system.

All sites where fished with a consistent effort of 10 minutes. Fish collected were weighed to the nearest gram and fork length measured to the nearest millimetre. Electrical conductivity was measured with a YSI 3200 conductivity meter and horizontal water visibility was measured using a black disc (Davies-Colley 1988).

Results

Water temperatures were 24.5°C in 2007 and 20.6°C in 2011. Specific conductivity was 422.8 µS cm^{-1} in 2007 and 344.8 µS cm^{-1} in 2011. Black disc measurement was 0.2 m in both 2007 and 2011. We caught 493 fish in 2007 and 216 in 2011 in from a total of 21 sites across the two years fishing 12,652 m^2 in 2011 and 8,916 m^2 in 2007. In order of declining density, native species caught were shortfin eel, common bully, and common smelt. The introduced species were goldfish, perch, rudd, catfish, and koi carp. Gambusia and common bullies were captured in 2007 but not in 2011.

Total fish densities were notably lower in 2011 (1.78 fish 100 m^{-2}) compared to 2007 (6.31 fish 100 m^{-2}, Table 47). Catfish, goldfish, koi carp, rudd, shortfin eel and common smelt densities were all lower in 2011 compared to 2007 (Table 47). Perch were the only species found to have increased in density between 2007 and 2011. Of particular note were the 4 to 6-fold reductions in goldfish and shortfin eel densities (Table 47). Associated with the decrease in fish density was a decrease in biomass, with all species' biomass decreasing between 2007 and 2011 except for perch and rudd (Table 48). However, the mean weight for all species except perch and common smelt increased between 2007 and 2011 (Table 48), which compensated somewhat for much lower fish densities at most sites in 2011 (Table 49).

Table 47: Number of fish caught from each species and density of each species from two boat electrofishing surveys (eleven 10-min fishing tracks in 2007, ten 10-min fishing tracks in 2011) conducted in Lake Waahi.

	Number of fish		Density (fish 100 m^{-2})	
Species	2007	2011	2007	2011
Common bully	21	–	0.27	–
Catfish	23	8	0.29	0.07
Goldfish	233	58	2.98	0.51
Koi carp	21	18	0.27	0.14
Perch	9	44	0.12	0.34
Rudd	19	18	0.24	0.16
Shortfin eel	158	66	2.02	0.55
Common smelt	9	4	0.12	0.03
Mean	493	216	6.31	1.78

Table 48: Biomass and mean weight of fish species captured during boat electrofishing of Lake Waahi in March 2007 and 2011.

	Biomass (g m^{-2})		Mean weight (g)	
	2007	2011	2007	2011
Catfish	0.72	0.20	232.8	303.8
Common bully	<0.01	–	0.30	–
Gambusia	<0.01	–	0.42	–
Goldfish	4.30	2.00	160.0	387.3
Inanga	<0.01	0.00	2.50	–
Koi carp	2.91	2.00	1104.7	1466.7
Perch	0.59	0.67	555.0	188.7
Rudd	0.16	0.20	60.1	131.8
Shortfin eel	1.02	0.47	53.1	88.9
Common smelt	0.01	<0.01	4.91	4.8
Total	9.70	5.55		

Table 49: Area surveyed and density of fish caught by boat electrofishing in Lake Waahi in March 2007 and 2011.

	2007				2011			
Site	Total distance fished (m)	Total area fished (m^2)	Density (fish 100 m^{-2})	Biomass (g m^{-2})	Total distance fished (m)	Total area fished (m^2)	Density (fish 100 m^{-2})	Biomass (g m^{-2})
1	180	719	6.8	14.6	353	1,412	4.0	13.4
2	205	819	5.7	7.7	242	968	1.9	4.9
3	258	1,032	4.1	7.9	425	1,700	0.2	0.1
4	235	940	10.5	17.4	302	1,208	2.0	4.2
5	203	814	8.1	9.5	225	900	0.9	3.1
6	204	817	5.9	6.6	247	988	2.2	3.1
7	206	825	4.7	5.8	350	1,400	0.9	2.5
8	146	585	5.1	7.9	315	1,260	1.7	6.9
9	187	750	5.6	7.8	428	1,712	0.8	2.9
10	129	515	7.8	11.0	276	1,104	3.3	14.4
11	275	1,101	3.0	10.5	–	–	–	–
Total	2,229	8,916			3,163	12,652		
Mean	203	811	6.1	9.7	316	1,265	1.8	5.6

The reasons for the lower catch of fish in Lake Waahi in 2011 compared to 2007 is not clear, but could be due to successive droughts that may have reduced fish abundance, or to the windy conditions during fishing in 2011. Boat electrofishing relies on seeing fish for optimal capture, and wind disturbance of the water surface makes fish harder to see. Despite this reservation, goldfish and koi carp dominated the fish biomass in Lake Waahi in 2007 and 2011, comprising 72-74% of the total fish biomass caught.

Detailed estimates of fish abundance in Lake Rotomānuka

Fishing effort

Lake Rotomānuka was fished on 11-12 March 2015 with gill nets by the Department of Conservation. Nets were set between 0900 and 1100 h on 11 March and hauled from 0843 to 0845 h on 12 March in both Rotomānuka North and Rotomānuka South (Table 50). A total of 28 nets comprising fyke, gill, and trammel nets were set (Table 51).

Results

A total of 701 fish were caught in Rotomānuka North and 176 in Rotomānuka South (Table 52). Common bullies were numerous in Rotomānuka North but absent from Rotomānuka South. Shortfin eels were common in both lakes, but had a greater total biomass in Rotomānuka South (20.2 kg, Table 53). Rudd were equally abundant in both lakes, longfin eels were only found in Rotomānuka North. A comparison of CPUE of shortfin eels showed considerably higher mean in Rotomānuka South (1.76 kg net^{-1} $night^{-1}$) than Rotomānuka North (4.01 kg net^{-1} $night^{-1}$). The CPUE of catfish was low in both lakes (0.01 to 0.08 kg net^{-1} $night^{-1}$) (Table 54).

Table 50: Time, date, water temperature and Secchi depth in Lake Rotomānuka during netting in March 2015.

Lake	Fishing activity	Date	Time (h)	Water temperature (°C)	Secchi depth (m)	Weather
Rotomanuka North	Set nets	11-Mar-15	1100	24.5	1.40	sunny (cloudy), calm, smooth water
Rotomanuka North	Lift nets	12-Mar-15	0843	23.0		overcast, drizzly, calm, smooth water
Rotomanuka South	Set nets	11-Mar-15	0900	21.0	0.77	sunny (cloudy), calm, smooth water
Rotomanuka South	Lift nets	12-Mar-15	0845	21.5		overcast, drizzly, calm, smooth water

Table 51: Number of nets set in Lake Rotomānuka in March 2015.

	Number of nets set			Mesh size
Net type	Rotomanuka North	Rotomanuka South	Total	(mm)
Fyke	8	5	13	4
Gill	6	4	10	14, 25, 38
Trammel	3	2	5	45, 60
Total	17	11	28	

Table 52: Number of fish caught in one night's fishing in A. Rotomānuka North and B. Rotomānuka South in March 2015.

A. Rotomānuka North

		Number of fish net^{-1} night^{-1} (g)								
Net type	Net	Catfish	Common bully	Common smelt	Gambusia	Goldfish	Rudd	Shortfin eel	Longfin eel	Total
Fyke	F1		70				5	5		80
Fyke	F2		100		1		1	20		122
Fyke	F3	1	40					10		51
Fyke	F4		12		1			7		20
Fyke	F5		100	3	20		15	6	1	145
Fyke	F6		55	3	3		13	5		79
Fyke	F7		50	8			2	11		71
Fyke	F8		80					1	1	82
Gill	G1						1			3
Gill	G2	3				1	3			7
Gill	G3					5	2			8
Gill	G4					1	10			11
Gill	G5	4					7			13
Gill	G6									0
Trammel	T1	2				3	3			9
Trammel	T2									0
Trammel	T3									0
Total		10	507	14	25	10	62	65	2	701

B. Rotomānuka South

		Number of fish net^{-1} night^{-1} (g)								
Net type	Net	Catfish	Common bully	Common smelt	Gambusia	Goldfish	Rudd	Shortfin eel	Longfin eel	Total
Fyke	F1							14		14
Fyke	F2							22		22
Fyke	F3							16		16
Fyke	F4							13		13
Fyke	F5	1						14		15
Gill	G1	8				8	8			24
Gill	G2						12			16
Gill	G3	1				9	16			26
Gill	G4	1					10			11
Trammel	T1	1				2	15	1		19
Trammel	T2									0
Total		12				19	61	80		176

Table 53: Biomass of fish caught in one night's fishing in A. Rotomānuka North and B. Rotomānuka South in March 2015.

A. Rotomānuka North

		Biomass net^{-1} night^{-1} (g)								
Net type	Net	Catfish	Common bully	Common smelt	Gambusia	Goldfish	Rudd	Shortfin eel	Longfin eel	Total
Fyke	F1		57				20	638		715
Fyke	F2		82		1		2	5899		5985
Fyke	F3	84	33					1391		1508
Fyke	F4		10		1			1020		1030
Fyke	F5		82	3	20		986	1826	215	3132
Fyke	F6		45	3	3		1122	825		1998
Fyke	F7		41	7			455	2330		2833
Fyke	F8		66					141	134	340
Gill	G1						227			464
Gill	G2	477				186	682			1345
Gill	G3					790	455			1482
Gill	G4					194	3390			3584
Gill	G5	272					1592			2100
Gill	G6									
Trammel	T1	670				864	1018			2789
Trammel	T2									
Trammel	T3									
Total		1503	416	13	25	2035	9949	14070	350	29305

B. Rotomānuka South

		Biomass net^{-1} night^{-1} (g)								
Net type	Net	Catfish	Common bully	Common smelt	Gambusia	Goldfish	Rudd	Shortfin eel	Longfin eel	Total
Fyke	F1							5887		5887
Fyke	F2							3592		3592
Fyke	F3							2725		2725
Fyke	F4							2664		2664
Fyke	F5	383						5196		5579
Gill	G1	2219				2026	3014			7259
Gill	G2						2728			2965
Gill	G3	94				546	3423			4064
Gill	G4	300					2383			2683
Trammel	T1	440				797	6470	176		7883
Trammel	T2									
Total		3437				3370	18018	20239		45301

Table 54: Catch per unit effort (CPUE) in fyke netting in Rotomānuka North and Rotomānuka South in March 2015.

		Biomass CPUE (kg net^{-1} night^{-1})			
Lake	*N* nets	Catfish	Rudd	Shortfin eel	Longfin eel
Rotomanuka North	8	0.01	0.32	1.76	0.04
Rotomanuka South	5	0.08	0.00	4.01	0.00

Detailed estimates of fish abundance in Lake Waikare

Fishing effort

For a large lake, fishing in Lake Waikare (3,440 ha) has been very limited. Boat electrofishing was carried out in Lake Waikare in 2003 and 2008 (Table 55) in sites mainly at the northern end of the lake (Figure 140). While more koi carp were caught in 2008 than 2003 (Table 56), fish were considerably smaller in 2008 leading to a lower biomass (Table 57).

Table 55: Boat electrofishing sites, duration, distance and area fished in Lake Waikare in 2003 and 2008.

Site	Date	Label code	Waypoint	Time fished (min)	Latitude	Longitude	Distance fished (m)	Area fished (m^2)
17	11-Sep-03	LWAIK0903		76	-37.43989	175.2255	1000	4000
342-01	24-Jan-08	LW001	595	10	-37.4298	175.1740	202	806
342-02	24-Jan-08	LW002	598	10	-37.4293	175.1722	226	903
342-03	24-Jan-08	LW003	600	10	-37.4160	175.1896	200	799
342-04	24-Jan-08	LW004	604	10	-37.4151	175.1873	223	893
342-05	24-Jan-08	LW005	607	10	-37.4145	175.1855	249	995
342-06	24-Jan-08	LW006	614	16	-37.4063	175.2108	74	298
Total 2008				66			1173	4693

Figure 140: Locations of fishing sites in Lake Waikare. Sites correspond to those in Table 55.

Table 56: Number of fish caught by boat electrofishing in Lake Waikare in 2003 and 2008.

		Number of fish						
Site	Year	Koi	Goldfish	Common smelt	Common bully	Shortfin eel	Gambusia	Total
17	2003	18	11	20	8	12	0	69
342-01	2008	4	1	0	0	0	0	5
342-02	2008	2	5	0	1	0	0	8
342-03	2008	2	3	0	1	2	2	10
342-04	2008	3	8	0	1	0	0	12
342-05	2008	3	14	0	0	0	0	17
342-06	2008	10	1	0	20	5	10	46
342-07	2008	0	0	0	0	0	17	17
Total 2008		24	32	0	23	7	29	115

Table 57: Biomass of fish caught by boat electrofishing in Lake Waikare in 2003 and 2008.

		Fish biomass (kg)						
Site	Year	Koi	Goldfish	Common smelt	Common bully	Shortfin eel	Gambusia	Total
17	2003	32.9	2.3	-	-	-	0	35.2
342-01	2008	3.8	0.3	0	0	0	0	4.1
342-02	2008	0.2	1.3	0	0.002	0	0	1.6
342-03	2008	0.7	0.4	0	0.001	0.579	0.001	1.7
342-04	2008	0.8	1.2	0	0.002	0	0	2.0
342-05	2008	0.7	1.8	0	0	0	0	2.5
342-06	2008	0.8	0.2	0	0.026	0.878	0.004	1.9
342-07	2008	0.0	0.0	0	0	0	0.005	0.005
Total 2008		7.0	5.2	0	0.031	1.457	0.01	13.7

Discussion

Lessons from Ohinewai

Modelling suggested that removal of koi carp would reduce internal nutrient recycling by 10% of TN and 21% of TP (Allan 2016). The invasive fish removal programme and installation of a one-way gate in Lake Ohinewai to allow adult carp to leave the lake but not re-enter provided a test of the effect of this reduction on water quality. We reduced the koi carp population from the estimated original biomass of 308 kg/ha (211–466, 95% CL) to 14 kg/ha (7–27, 95% CL) in 2014. In 2016, after 2 years without fish removal, we estimated that the koi carp biomass had increased to 94 kg/ha (49–197, 95% CL).

One important question in lake restoration is the effect of biomass replacement of invasive fish by increased native fish biomass and whether nutrient excretion by invasive species will simply be replaced

by similar nutrient excretion by an increased biomass of native species. We investigated the predicted change in nutrient excretion following invasive fish biomass reduction in Lake Ohinewai, and the amounts of N and P were halved following carp removal despite the increased catfish abundance (Table 36).

Water quality indicators such as nutrient concentrations, Secchi depth and total suspended solids showed no change in the 5 years following the reduction in invasive fish biomass. In addition, phytoplankton species and abundance remained characteristic of other hypereutrophic lakes in the Waikato region. The annual mean TLI3, which excludes Secchi depth, ranged from 6.1 to 6.6 between 2006 and 2017, indicating that the lake remained hypertrophic following fish removal. We concluded that chemically-driven internal nutrient cycling and catchment nutrient inputs exceeded the gains from carp removal and maintained the hypereutrophic condition and low water clarity (Tempero and Hicks 2017).

There was an ecosystem benefit from carp removal, however. Biomass of native shortfin eels increased 5-fold following carp removal and also increased in mean fish size. However, catfish biomass increased 3-fold following invasive fish removal, which was a less desirable outcome. Isotopic evidence suggests that there is a close dietary overlap between large carp, eels, and catfish so the response of eels and catfish to a reduction in koi carp biomass was predictable considering the food resources that became available to eels and catfish when carp was greatly reduced. We can predict that the three shallow lakes with carp in this study would respond in a similar manner to carp removal, so no water quality gains would be expected. Eel biomass would respond positively, but catfish would need to be controlled to allow eels to fully utilise the resources made available by invasive fish removal.

Key discussion points from a fish perspective

There were a number of assumptions, limitations, and knowledge gaps regarding the fish objective that we could not address within the scope of this study, and these deficiencies of knowledge contribute to the uncertainty of our estimates. For instance, in our calculations, we assumed that:

- The available sampling was representative of the fish community
- Mean fish weight adequately captured fish size distributions
- Mean water temperature adequately captures seasonal variation

We also identified the following limitations:

- Extrapolated sediment resuspension was based on limited fish data
- Equations used for sediment resuspension by carp were professional judgement of the most appropriate to use and cannot be guaranteed to accurately reflect the actions of invasive fish in the Waikato region. For instance, Bruekelaar et al.'s (1994) experiments included perch and were conducted in small ponds. Badiou and Goldsborough's (2010) experiments used large common carp (mean weight 2790 to 4350 g), which might overestimate the measured rates compared to the smaller carp in our study (mean weight about 800 g).

We identified the following knowledge gaps:

- Lack of areal fish biomass estimates, especially for Lake Rotomanuka
- Sediment resuspension rates for fish other than carp (for example, goldfish) are unknown. Rates for bream, for instance, were 3x higher than for carp in Breukelaar et al. (1994).
- Current estimates of fish abundance and size distribution are required
- Pore water in bottom sediments contain N and P, and the effect of invasive fish on pore water release rates are unknown.

Addressing these deficiencies would improve our ability to model the effects of invasive fish on shallow Waikato lakes.

One clear need is application of consistent fishing methods across all lakes. Mark-recapture population estimates from Lake Kaituna demonstrate the differential capture efficiency of boat electrofishing and fyke netting for a range of species common to shallow Waikato lakes (Table F24). Boat electrofishing is most efficient for koi carp and goldfish, whereas fyke netting is more efficient for eels and catfish.

Table 58: Capture efficiencies of boat electrofishing and fyke netting in Lake Kaituna determined from mark-recapture population estimates.

	Capture efficiency (%)	
Species	Boat electrofishing	Fyke netting
Koi carp	21	0
Goldfish	12	2
Shortfin eel	6	49
Catfish	4	16
Rudd	2	13
Longfin eel	1	28

A comparison of boat electrofishing and fyke netting in nearby Lake Mangahia, a 10-ha peat lake, 10 km to the north of Lake Ngaroto, also showed a clear bias of boat electrofishing towards goldfish; fyke netting was biased towards catfish and eels (Table 59: Mean catch per unit effort in Lake Mangahia, Waikato, from fyke netting on 25 Aug 2009 (10 nets set overnight) and boat electrofishing on 4 February 2009 (ten 10-minute shots covering 3,673 m^2 in total).). Goldfish and shortfin eels were less abundant in Lake Waahi than in Lake Mangahia, but rudd were more abundant. Perch were absent from Lake Mangahia.

Table 59: Mean catch per unit effort in Lake Mangahia, Waikato, from fyke netting on 25 Aug 2009 (10 nets set overnight) and boat electrofishing on 4 February 2009 (ten 10-minute shots covering 3,673 m^2 in total).

Species	Fyke netting		Boat electrofishing	
	Fish net^{-1} $night^{-1}$	kg net^{-1} $night^{-1}$	Density (number 100 m^{-2})	Biomass (g m^{-2})
Catfish	39.8	8.4	0.82	1.76
Shortfin eel	8.2	5.2	0.67	2.49
Longfin eel	3.3	5.2	0.06	0.76
Goldfish	1.8	0.6	13.72	7.88
Rudd	0.2	0.1	0.00	0.00
Common bully	0	0.0	0.11	<0.01
Gambusia	0	0.0	0.38	<0.01
Total	53.3	19.4	15.74	12.90

Acknowledgements

We thank the Department of Conservation staff who carried out gill netting in Lake Rotomanuka and Mike Holmes for fyke netting in Lake Ngaroto under contract to the Waipa District Council through Paula Reeves.

Appendix G: Sediment core incubations for phosphorus release

Sediment core incubation studies were used to evaluate the release rate of P from the sediment under anoxic conditions in Lakes Ngaroto, Rotomanuka, Waikare and Waahi. An intact sediment core was taken from the central region of each lake. The cores were covered with 0.5 L of filtered lake water and incubated for 28 days. Cores were kept in the dark and at 12^{o}C. Nitrogen gas and sodium sulphite were added to the water to create anoxic conditions. Samples were taken daily and analysed for total phosphorus (TP). No replenishment of the 10 mL of daily sample taken for TP analysis was undertaken. Calculations have been corrected for this volume.

Figure 141 shows the total phosphorus concentration in each core from each lake over the first five days of the incubation. We chose the first five days because of a reasonably linear response of increases in the TP through this period. Regression lines were fitted to the time series of TP. The slope of the regression lines equates to a change in concentration per day. Corrections were made for the volume of water above the core sample, the area of the core sample (0.022 m^2) and the temperature (standardising from 12 to 20^{o}C) in order to derive a phosphorus release rate in mg m^{-2} day^{-1}. This release rate may be compared to the maximum sediment phosphorus release rate at 20^{o}C which is prescribed in the water quality calibration file in the input to the model for each lake (Table 60). The calculation for sediment phosphorus release rate is:

$$Sp = S \times \frac{V}{A} \times f(T)$$

Where *Sp* is the sediment phosphorus release rate (mg m^{-2} d^{-1}), *S* is the slope of the regression (g m^{-3} d^{-1}), *V* is the volume of water in the core (m^3), *A* is the area of the core (0.022 m^2) and *f*(*T*) is a temperature normalisation function (1.757) designed to adjust release rates at 12^{o}C to what would occur at 20^{o}C.

For Lake Rotomānuka the release rate in the core is more than 2-fold higher than what was prescribed in the calibrated model. For the other two lakes the release rates are comparable. We suggest that it may be useful to run a similar experiment for several cores from each lake and closely monitor

environmental conditions (e.g., dissolved oxygen and pH) before prescribing the measured release rates directly into the model inputs.

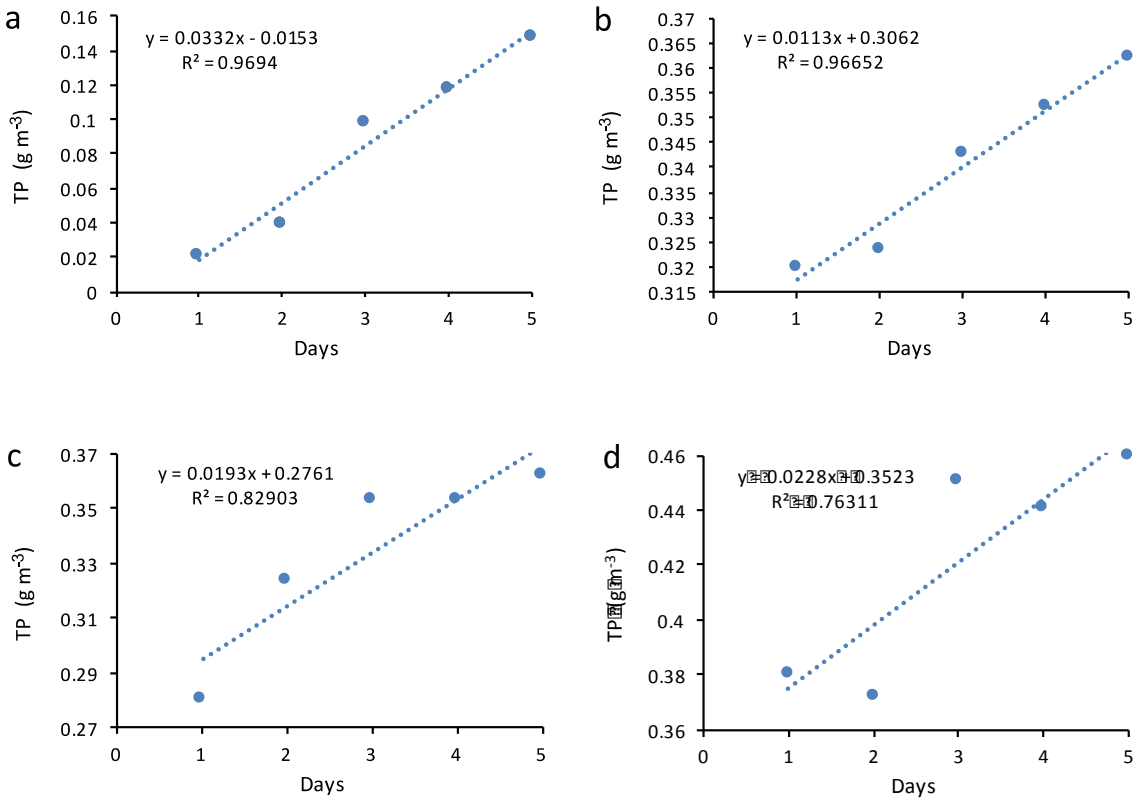

Figure 141: Change in concentrations of total phosphorus concentrations in water overlying sediment cores from Lakes (a) Rotomānuka, (b) Waahi, (c) Ngāroto and (d) Waikare for the first five days of the incubation. A linear regression fit for each lake is shown including percentage variation explained (R^2).

Table 60: Comparison of release rates derived from sediment core incubations for the four lakes and release rates prescribed in the model. All release rates are normalised to 20°C and are considered to be maximum values when anoxic water overlies the sediments. No model P release rate is given for Lake Waikare because this lake was not modelled.

Lake	Core P release rate (mg m^{-2} d^{-1})	Model P release rate (mg m^{-2} d^{-1})
Rotomānuka	1.33	2.85
Waahi	0.52	0.95
Ngāroto	0.84	0.95
Waikare	2.00	